EARLY EVENTS DURING HOST CELL - PARASITE INTERACTIONS

EDITED BY: Patricia Sampaio Tavares Veras, Albert Descoteaux, Maria Isabel Colombo and Juliana Perrone Bezerra De Menezes

PUBLISHED IN: Frontiers in Cellular and Infection Microbiology

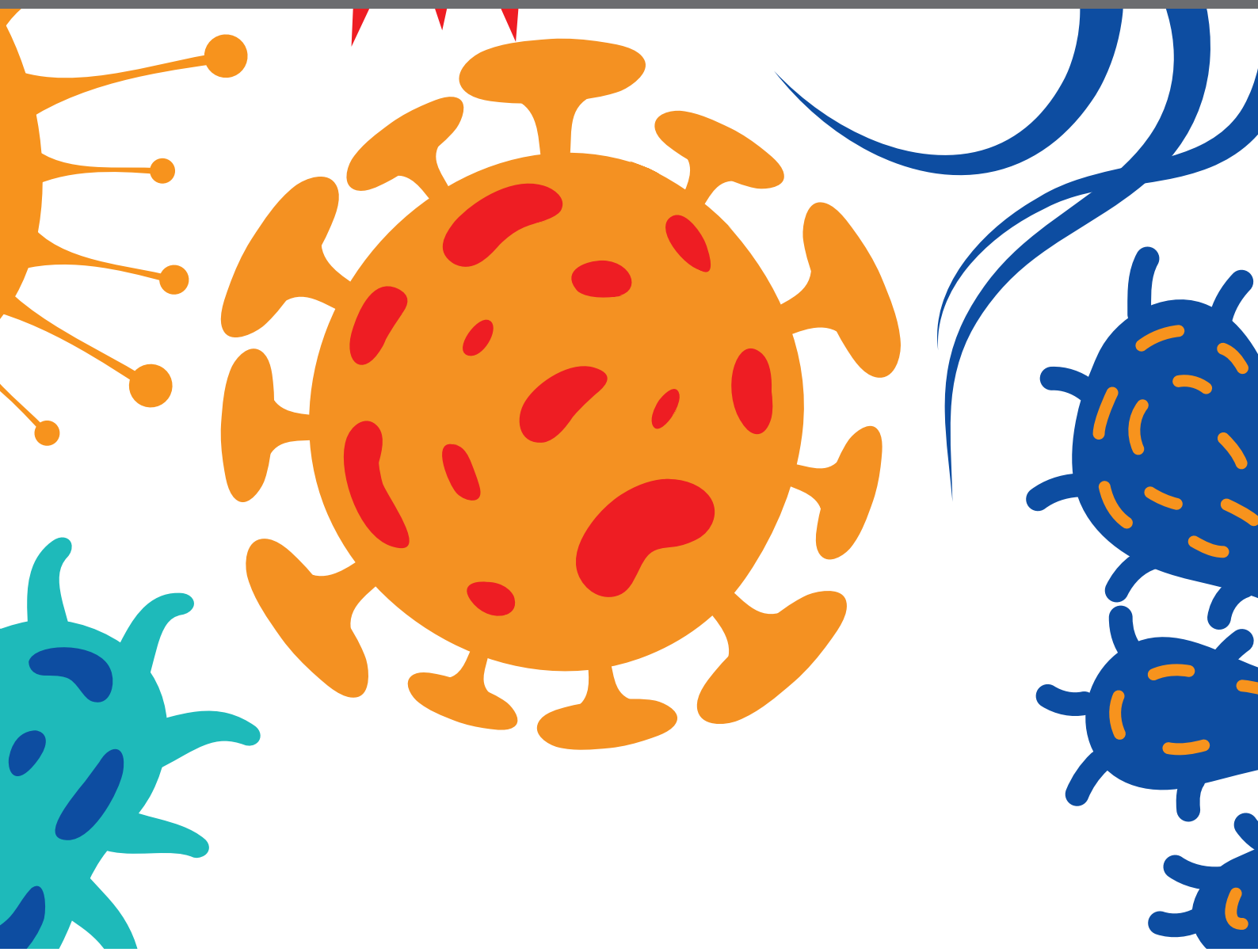

frontiers Research Topics

ISSN 1664-8714
ISBN 978-2-88971-041-6
DOI 10.3389/978-2-88971-041-6

About Frontiers

Frontiers is more than just an open-access publisher of scholarly articles: it is a pioneering approach to the world of academia, radically improving the way scholarly research is managed. The grand vision of Frontiers is a world where all people have an equal opportunity to seek, share and generate knowledge. Frontiers provides immediate and permanent online open access to all its publications, but this alone is not enough to realize our grand goals.

Frontiers Journal Series

The Frontiers Journal Series is a multi-tier and interdisciplinary set of open-access, online journals, promising a paradigm shift from the current review, selection and dissemination processes in academic publishing. All Frontiers journals are driven by researchers for researchers; therefore, they constitute a service to the scholarly community. At the same time, the Frontiers Journal Series operates on a revolutionary invention, the tiered publishing system, initially addressing specific communities of scholars, and gradually climbing up to broader public understanding, thus serving the interests of the lay society, too.

Dedication to Quality

Each Frontiers article is a landmark of the highest quality, thanks to genuinely collaborative interactions between authors and review editors, who include some of the world's best academicians. Research must be certified by peers before entering a stream of knowledge that may eventually reach the public - and shape society; therefore, Frontiers only applies the most rigorous and unbiased reviews.
Frontiers revolutionizes research publishing by freely delivering the most outstanding research, evaluated with no bias from both the academic and social point of view. By applying the most advanced information technologies, Frontiers is catapulting scholarly publishing into a new generation.

What are Frontiers Research Topics?

Frontiers Research Topics are very popular trademarks of the Frontiers Journals Series: they are collections of at least ten articles, all centered on a particular subject. With their unique mix of varied contributions from Original Research to Review Articles, Frontiers Research Topics unify the most influential researchers, the latest key findings and historical advances in a hot research area! Find out more on how to host your own Frontiers Research Topic or contribute to one as an author by contacting the Frontiers Editorial Office: frontiersin.org/about/contact

EARLY EVENTS DURING HOST CELL - PARASITE INTERACTIONS

Topic Editors:
Patricia Sampaio Tavares Veras, Gonçalo Moniz Institute (IGM), Brazil
Albert Descoteaux, Université du Québec, Canada
Maria Isabel Colombo, Universidad Nacional de Cuyo, Argentina
Juliana Perrone Bezerra De Menezes, Gonçalo Moniz Institute (IGM), Brazil

Citation: Veras, P. S. T., Descoteaux, A., Colombo, M. I., De Menezes, J. P. B., eds. (2021). Early Events During Host Cell - Parasite Interactions. Lausanne: Frontiers Media SA. doi: 10.3389/978-2-88971-041-6

Table of Contents

frontiers in Cellular and Infection Microbiology

EDITORIAL
published: 19 May 2021
doi: 10.3389/fcimb.2021.680557

Editorial: Early Events During Host Cell-Pathogen Interaction

Patrícia S. T. Veras[1*], *Albert Descoteaux*[2], *Maria Isabel Colombo*[3] *and Juliana P. B. de Menezes*[1]

[1] Laboratory of Parasite-Host Interaction and Epidemiology, Gonçalo Moniz Institute, Salvador, Brazil, [2] Centre Armand-Frappier Santé Biotechnologie, Institut National de la Recherche Scientifique (INRS), Quebec, QC, Canada, [3] Instituto de Histología y Embriología de Mendoza (IHEM), Consejo Nacional de Investigaciones Científicas y Técnicas (CONICET)-Universidad Nacional de Cuyo, Mendoza, Argentina

Keywords: early immune response, microoorganism, disease control, disease progression, immunotherapeutic interventions

Editorial on the Research Topic

Early Events During Host Cell-Pathogen Interaction

INTRODUCTION

The outcome of diseases caused by microbial pathogens (Torgerson et al., 2015) depends on the nature of the pathogen and initial host immune response (Aderem and Ulevitch, 2000; Liu and Uzonna, 2012). This Research Topic "Early Events During Host Cell-Pathogen Interaction" includes 1 review and 1 minireview, and 8 original research articles in the investigation of early events of host immune response against microbial infection.

Toxoplasma gondii, *Plasmodium* spp., *Leishmania* spp., and helminths, activate the interleukin-33 (IL-33) pathway, known as the 'alarmin' route (Tonacci et al., 2019). Nathan et al. revise the crucial role played by the IL-33 axis in host immune response to these parasites by priming the immune system toward a strong T helper type-2 (Th2) response that subsequently promotes pathogen clearance. Alternatively, IL-33 can also participate in infection exacerbation. Additionally, these authors provide insight into novel immunotherapeutic interventions by modulating early host immune response using antibodies against IL-33 pathway elements. The essential role of autoantibodies in malaria continues to be debated (Hogh et al., 1994; Guiyedi et al., 2007). Another review published in this Research Topic by Mourão et al. summarizes recent findings regarding autoimmune response in malaria. Mainly, the authors discuss controversies surrounding autoantibody response that contribute to disease pathogenesis or protection.

Among food-borne diseases, amebiasis, caused by the protozoan *Entamoeba histolytica*, affects approximately 100 million people worldwide (Haque et al., 2003; Lozano et al., 2012). The parasite life cycle involves inter-conversion between trophozoite, that colonizes the mammalian gut, and cyst, which allows disease transmission through the ingestion of contaminated food or water (Haque et al., 2003). The molecular mechanisms governing parasite life cycle remain poorly studied, and cues triggering stage conversion remain unelucidated (Aguilar-Diaz et al., 2010). Singh's group previously identified a novel *Entamoeba* transcription factor, Encystation Regulatory Motif-Binding Protein (ERM-BP), which contributes to encystation (Manna et al., 2018). Manna et al. further characterized ERM-BP by evaluating its DNA binding functions and nicotinamidase domains *in vivo*. The overexpression of ERM-BP mutants revealed that this protein is an early regulator of development and heat shock response during *Entamoeba* infection. *Clonorchis sinensis* causes

OPEN ACCESS

Edited and Reviewed by:
William Clark Gause, Rutgers, The State University of New Jersey, United States

***Correspondence:**
Patrícia S. T. Veras
patricia.veras@fiocruz.br

Specialty section:
This article was submitted to Microbes and Innate Immunity, a section of the journal Frontiers in Cellular and Infection Microbiology

Received: *14 March 2021*
Accepted: *05 May 2021*
Published: *19 May 2021*

Citation:
Veras PST, Descoteaux A, Colombo MI and P. B. de Menezes J (2021) Editorial: Early Events During Host Cell-Pathogen Interaction. Front. Cell. Infect. Microbiol. 11:680557. doi: 10.3389/fcimb.2021.680557

another zoonotic food-borne parasitic disease that can infect mammals *via* the ingestion of raw or undercooked fresh fish and shrimp, eventually resulting in host death (Tang et al., 2016). Yan et al. demonstrated that TLR4 might be involved in *C. sinensis* infection in a resistant mouse strain, C57BL/10. The absence of TLR4 in *C. sinensis*-infected mice led to severe inflammation in the liver, bile duct proliferation, and biliary and hepatocellular injury. TLR4def mice immune response exhibited M2-like macrophages, a robust Th2 and a reduced Th1 responses.

Intracellular protozoan parasites infect millions of people worldwide. These parasites can cause severe forms of diseases that may result in death. Among vector-borne diseases, Chagas disease, caused by *Trypanosoma cruzi*, and leishmaniasis by *Leishmania* spp. are considered the most important due to severity and global distribution (Tang et al., 2016; OMS. Organización Mundial de la Salud, 2019). *T. cruzi* chronicity and persistence depend on parasitic capacity to escape host control mechanisms (OMS, 2020). Gutierrez et al. compared the effect of parasite infection on immune modulation by bone marrow-derived dendritic cells (DCs) and epithelial DCs *in vitro*. These authors found that DC can facilitate infection progression depending on parasite growth phase and DC maturation. Following *T. cruzi* invasion, the formation and maturation of parasitophorous vacuoles (TcPV) occurs. Host Rab GTPases are proteins that regulate intracellular vesicular trafficking. Salassa et al. found that endocytic Rabs, including Rab22a, Rab5, and Rab21, are selectively recruited to TcPV at early times of infection, followed by Rab7 and Rab39a at later stages. However, recycling and secretory Rabs are not recruited to the TcPV membrane. The contribution of these proteins to successful *T. cruzi* infection was demonstrated using cells transfected with mutated endocytic Rab genes.

Although dogs are considered the main reservoir of visceral leishmaniasis caused by *L. infantum*, most knowledge regarding host-parasite interaction stems from murine models (Cestari et al., 2012; Teixeira-Neto et al., 2014). Nadaes et al. evaluated the potential of DH82, a canine macrophage cell line, response to *Leishmania* infection. A comparison of the responses of DH82 and RAW 264.7 mouse macrophages against *L. infantum* promastigotes revealed that both cell lines similarly supported parasite replication/survival. However, notable differences were found in cytokine production, arginase activity and the release of nitric oxide, providing a model to elucidate several aspects of host cell immune response.

Lipophosphoglycan (LPG) is an abundant *Leishmania* promastigote surface molecule that contribute to parasite phagocytosis and survival within host cells (Mosser and Rosenthal, 1993; Descoteaux and Turco, 1999). When duplication of the *LPG2* gene in the *L. infantum* genome impeded gene targeting by conventional homologous recombination, Jesus-Santos et al. used CRISPR/Cas9 technology to generate *Δlpg2* mutants that displayed impaired capacity to infect neutrophils, reinforcing the role of LPG as a virulence factor.

The apicomplexan parasite *T. gondii* causes worldwide foodborne infections in mammals following the consumption of contaminated water or raw fruits or vegetables (Guha-Niyogi et al., 2001; Flegr et al., 2014). *T. gondii* oocysts can cause infections in mice in the absence of digestive factors, differentiating into replicative tachyzoites following phagocytosis by macrophages (Shapiro et al., 2019). Ndao et al. characterized the dynamics of oocyst phagocytosis at the single-cell level. The improved development of tachyzoites in macrophages challenged with free sporocysts or sporozoites compared to whole oocysts suggests that oocyst wall disruption hampers sporozoite excystation in macrophages. Once internalized, *T. gondii* reprograms host gene expression, including the up-regulation of mTOR-dependent host mRNA translation, resulting in the establishment of infection (Al-Bajalan et al., 2017). In addition to the mTOR-4E-BP1/2 axis, MAPK-interacting kinases 1 and 2 (MNK1/2) control the activity of eIF4E, a mRNA cap-binding protein (Leroux et al., 2018). Leroux et al. showed that *T. gondii* inhibits the phosphorylation of axis downstream targets, MNK1/2 and eIF4E, in mouse macrophages. These authors also demonstrated higher *T. gondii* replication in macrophages mutated at the eIF4E phosphorylation residue *vs.* WT cells. Of note, mutant mice were more susceptible to acute toxoplasmosis and showed exacerbated levels of IFNγ. In all, these data suggest that the MNK1/2-eIF4E axis is required to control *T. gondii* infection, and that its inactivation can be exploited by parasites to promote their survival.

In sum, this Research Topic gives insight into the complexity of host early interactions with various microorganisms, providing information about recent advances on the initial immune response that triggers mechanisms, which result in diseases' control or progression and identifying targets for future interventions on parasitic infections.

AUTHOR CONTRIBUTIONS

PV wrote the first draft and AD, MC and JM edited and commented on the draft. All authors contributed to the article and approved the submitted version.

FUNDING

PV holds a grant from CNPq for productivity in research (307832/2015-5).

REFERENCES

Aderem, A., and Ulevitch, R. J. (2000). Toll-Like Receptors in the Induction of the Innate Immune Response. *Nature* 406, 782–787. doi: 10.1038/35021228

Aguilar-Diaz, H., Diaz-Gallardo, M., Laclette, J. P., and Carrero, J. C. (2010). In Vitro Induction of Entamoeba Histolytica Cyst-Like Structures From Trophozoites. *PloS Negl. Trop. Dis.* 4, e607. doi: 10.1371/journal.pntd.0000607

Al-Bajalan, M. M. M., Xia, D., Armstrong, S., Randle, N., and Wastling, J. M. (2017). Toxoplasma Gondii and Neospora Caninum Induce Different Host Cell Responses At Proteome-Wide Phosphorylation Events; a Step Forward for Uncovering the Biological Differences Between These Closely Related Parasites. *Parasitol. Res.* 116, 2707–2719. doi: 10.1007/s00436-017-5579-7

Cestari, I., Ansa-Addo, E., Deolindo, P., Inal, J. M., and Ramirez, M. I. (2012). Trypanosoma Cruzi Immune Evasion Mediated by Host Cell-Derived Microvesicles. *J. Immunol.* 188, 1942–1952. doi: 10.4049/jimmunol.1102053

Descoteaux, A., and Turco, S. J. (1999). Glycoconjugates in Leishmania Infectivity. *Biochim. Biophys. Acta* 1455, 341–352. doi: 10.1016/s0925-4439(99)00065-4

Flegr, J., Prandota, J., Sovickova, M., and Israili, Z. H. (2014). Toxoplasmosis–a Global Threat. Correlation of Latent Toxoplasmosis With Specific Disease Burden in a Set of 88 Countries. *PloS One* 9, e90203. doi: 10.1371/journal.pone.0090203

Guha-Niyogi, A., Sullivan, D. R., and Turco, S. J. (2001). Glycoconjugate Structures of Parasitic Protozoa. *Glycobiology* 11, 45R–59R. doi: 10.1093/glycob/11.4.45r

Guiyedi, V., Chanseaud, Y., Fesel, C., Snounou, G., Rousselle, J-C., Lim, P., et al. (2007). Self-Reactivities to the non-Erythroid Alpha Spectrin Correlate With Cerebral Malaria in Gabonese Children. *PloS One* 2, e389. doi: 10.1371/journal.pone.0000389

Haque, R., Huston, C. D., Hughes, M., Houpt, E., and Petri, W.A. Jr. (2003). Amebiasis. *N Engl. J. Med.* 348, 1565–1573. doi: 10.1056/NEJMra022710

Hogh, B., Petersen, E., Crandall, I., Gottschau, A., and Sherman, I. W. (1994). Immune Responses to Band 3 Neoantigens on Plasmodium Falciparum-Infected Erythrocytes in Subjects Living in an Area of Intense Malaria Transmission are Associated With Low Parasite Density and High Hematocrit Value. *Infect. Immun.* 62, 4362–4366. doi: 10.1128/IAI.62.10.4362-4366.1994

Leroux, L. P., Lorent, J., Graber, T. E., Chaparro, V., Masvidal, L., Aguirre, M., et al. (2018). The Protozoan Parasite Toxoplasma Gondii Selectively Reprograms the Host Cell Translatome. *Infect. Immun.* 86. doi: 10.1128/IAI.00244-18

Liu, D., and Uzonna, J. E. (2012). The Early Interaction of Leishmania With Macrophages and Dendritic Cells and its Influence on the Host Immune Response. *Front. Cell Infect. Microbiol.* 2, 83. doi: 10.3389/fcimb.2012.00083

Lozano, R., et al. (2012). Global and Regional Mortality From 235 Causes of Death for 20 Age Groups in 1990 and 2010: A Systematic Analysis for the Global Burden of Disease Study 2010. *Lancet* 380, 2095–2128. doi: 10.1016/S0140-6736(12)61728-0

Manna, D., Lentz, C. S., Ehrenkaufer, G. M., Suresh, S., Bhat, A., and Singh, U. (2018). An NAD(+)-dependent Novel Transcription Factor Controls Stage Conversion in Entamoeba. *Elife* 7. doi: 10.7554/eLife.37912

Mosser, D. M., and Rosenthal, L. A. (1993). Leishmania-Macrophage Interactions: Multiple Receptors, Multiple Ligands and Diverse Cellular Responses. *Semin. Cell Biol.* 4, 315–322. doi: 10.1006/scel.1993.1038

OMS (2020). *Leishmaniasis*.

OMS. Organización Mundial de la Salud (2019). *La Enfermedad De Chagas (Tripanosomiasis Americana)*.

Shapiro, K., Bahia-Oliveira, L., Dixon, B., Dumétre, A., de Wit, L. A., VanWormer, E., et al. (2019). Environmental Transmission of Toxoplasma Gondii: Oocysts in Water, Soil and Food. *Food Waterborne Parasitol.* 15, e00049. doi: 10.1016/j.fawpar.2019.e00049

Tang, Z. L., Huang, Y., and Yu, X. B. (2016). Current Status and Perspectives of Clonorchis Sinensis and Clonorchiasis: Epidemiology, Pathogenesis, Omics, Prevention and Control. *Infect. Dis. Poverty* 5, 71. doi: 10.1186/s40249-016-0166-1

Teixeira-Neto, R. G., da Silva, E. S., Nascimento, R. A., Belo, V. S., de Oliveira, C. L., Pinheiro, L. C., et al. (2014). Canine Visceral Leishmaniasis in an Urban Setting of Southeastern Brazil: An Ecological Study Involving Spatial Analysis. *Parasit. Vectors* 7, 485. doi: 10.1186/s13071-014-0485-7

Tonacci, A., Quattrocchi, P., and Gangemi, S. (2019). Il33/St2 Axis in Diabetic Kidney Disease: A Literature Review. *Med (Kaunas)* 55. doi: 10.3390/medicina55020050

Torgerson, P. R., Devleesschauwer, B., Praet, N., Speybroeck, N., Willingham, A. L., Kasuga, F., et al. (2015). World Health Organization Estimates of the Global and Regional Disease Burden of 11 Foodborne Parasitic Diseases, 2010: A Data Synthesis. *PloS Med.* 12, e1001920. doi: 10.1371/journal.pmed.1001920

Conflict of Interest: The authors declare that the research was conducted in the absence of any commercial or financial relationships that could be construed as a potential conflict of interest.

frontiers in Cellular and Infection Microbiology

BRIEF RESEARCH REPORT
published: 27 February 2020
doi: 10.3389/fcimb.2020.00020

Modulatory Effect of *Trypanosoma cruzi* Infective Stages in Different Dendritic Cell Populations *in vitro*

Brenda Celeste Gutierrez[1], *Estela Lammel*[1], *Marcel Ivan Ramirez*[2,3], *Stella Maris González-Cappa*[1,4] *and Carolina Verónica Poncini*[1,4]*

[1] *Laboratório de Inmunología Celular e Inmunopatología de Infecciones, Instituto de Investigaciones en Microbiología y Parasitología Médica (MPaM) UBA-CONICET, Buenos Aires, Argentina,* [2] *Instituto Oswaldo Cruz, FIOCRUZ, Rio de Janeiro, Brazil,* [3] *Departamento de Bioquímica, Universidade Federal Do Paraná, Curitiba, Brazil,* [4] *Departamento de Microbiología, Parasitología e Inmunología, Facultad de Medicina, Universidad de Buenos Aires, Buenos Aires, Argentina*

Trypanosoma cruzi is a protozoan parasite that infects at least 7 million persons in the world (OMS, 2019). In endemic areas, infection normally occurs by vectorial transmission; however, outside, it normally happens by blood and includes congenital transmission. The persistence of *T. cruzi* during infection suggests the presence of immune evasion mechanisms and the modulation of the anti-parasite response to a profile incapable of eradicating the parasite. Dendritic cells (DCs) are a heterogeneous population of antigen-presenting cells (APCs) that patrol tissues with a key role in mediating the interface between the innate and adaptive immune response. Previous results from our lab and other groups have demonstrated that *T. cruzi* modulates the functional properties of DCs, *in vitro* and *in vivo*. During vectorial transmission, metacyclic (m) trypomastigotes (Tps) eliminated along with the insect feces reach the mucous membranes or injured skin. When transmission occurs by the hematic route, the parasite stage involved in the infection is the circulating or blood (b) Tp. Here, we studied *in vitro* the effect of both infective mTp and bTp in two different populations of DCs, bone marrow–derived DCs (BMDCs) and XS106, a cell line derived from epidermal DCs. Results demonstrated that the interaction of both Tps imparts a different effect in the functionality of these two populations of DCs, suggesting that the stage of *T. cruzi* and DC maturation status could define the immune response from the beginning of the ingress of the parasite, conditioning the course of the infection.

Keywords: *Trypanosoma cruzi*, dendritic cells, cell activation, cytokines, T cells

OPEN ACCESS

Edited by:
Maria Isabel Colombo, Universidad Nacional de Cuyo, Argentina

Reviewed by:
Laurent Gorvel, INSERM U1068 Centre de Recherche en Cancérologie de Marseille, France
Patricia Silvia Romano, National Scientific and Technical Research Council, Argentina

***Correspondence:**
Carolina Verónica Poncini
cvponcini@gmail.com

Specialty section:
This article was submitted to Microbes and Innate Immunity, a section of the journal Frontiers in Cellular and Infection Microbiology

Received: *04 September 2019*
Accepted: *14 January 2020*
Published: *27 February 2020*

Citation:
Gutierrez BC, Lammel E, Ramirez MI, González-Cappa SM and Poncini CV (2020) Modulatory Effect of Trypanosoma cruzi Infective Stages in Different Dendritic Cell Populations in vitro. Front. Cell. Infect. Microbiol. 10:20. doi: 10.3389/fcimb.2020.00020

INTRODUCTION

Trypanosoma cruzi, the etiological agent of Chagas disease, is a protozoan parasite that affects 7 million people in the world (OMS, 2019).

The parasite life cycle includes at least three particular morphological stages. In the insect vector, there is the presence of multiplicative epimastigotes and infective metacyclic trypomastigotes (mTp), released with feces. In the mammal host, two stages are present, the intracellular multiplicative amastigotes and bloodstream trypomastigotes (bTp), involved in the parasite dissemination to tissues. While vectorial and oral transmission involves mTp entry via injured skin or mucous membranes, parasite dissemination in the mammalian host occurs by bTp, also

responsible for congenital and sanguineous transmission even in non-endemic regions (de Souza et al., 2014; OMS, 2019).

A limited number of studies compare the immune response against different *T. cruzi* infective stages.

In a comparative study between mTp and bTp, Dias et al. (2013) have demonstrated that the infection by intraperitoneal or oral inoculation of bTp is more virulent than with mTp. Specifically, animals infected with bTp presented higher parasitemia and mortality in comparison to infection with mTp (Dias et al., 2013).

Dendritic cells (DCs) are professional antigen-presenting cells (APCs) with a central role in the development of immunity against infections. In steady state, DCs patrol tissues in order to maintain immune homeostasis. Under certain conditions such as inflammation or infection, these cells can be activated after recognizing danger signals. This process includes uptake and processing of antigens for presentation in addition to DC migration to draining lymph nodes (LNs). DCs are responsible for T-cell priming, the activation of secondary immune responses, or the induction of tolerogenic programs (Merad et al., 2013).

Previous studies from our group demonstrated that bTp from the virulent strain RA (Gonzalez Cappa et al., 1981) negatively regulates bone marrow–derived DC (BMDC) activation *in vitro*. The parasite promotes the production of anti-inflammatory cytokines and diminishes the T-cell stimulatory capacity of DCs (Poncini et al., 2008). In addition, our results demonstrate that both live bTp and heat-killed Tp, but not fixed Tp, condition DCs to a tolerogenic profile, suggesting that Tp–DC surface interaction and not infection triggers the DCs polarization. In fact, we confirmed that early in time, Tp–DC interaction induces ERK phosphorylation and IL-10 upregulation via a TLR-4–dependent pathway (Poncini et al., 2010).

In a previous report, da Costa et al. (2014) have shown that Tp from strains with variable virulence differentially modulates DC activation *in vitro*. *In vivo*, it was demonstrated that during infection, splenic DCs and APCs display low expression of MHCII and/or costimulatory molecules and impaired function (Alba Soto et al., 2003; Planelles et al., 2003), and more recently, that DCs with tolerogenic properties promote Treg cell induction and parasite persistence (Poncini et al., 2015). The fact that the parasite successfully infects the mammalian host via different portals of entry and by different infective stages highlights the importance the model of infection acquires during experimentation. As a result, a detailed characterization of the interaction of the parasite with cells involved in the first line of defense during primoinfection was needed (Poncini and González-Cappa, 2017).

This work comparatively describes the effect of two different infective stages of a virulent strain of *T. cruzi* (RA) in DCs from different origins. By studying the interaction of bTp and mTp with BMDCs and XS106, a cell line derived from epidemic DCs (Mohan et al., 2005), we found an interesting approach to understand and hypothesize about the different responses that may be occurring at the parasite entry site.

MATERIALS AND METHODS

Animals

C3H/HeN, C57BL/6, and CF1 mice were maintained in the animal facilities of IMPaM UBA-CONICET, Facultad de Medicina, Universidad de Buenos Aires, and bred under a sanitary barrier in specific-pathogen-free conditions (Poncini et al., 2015).

All experiments were performed according to protocol CD N° 04/2015 approved by the University of Buenos Aires's Institutional Committee for the Care and Use of Laboratory Animals (CICUAL) in accordance with the Council for International Organizations of Medical Sciences (CIOMS) and International Council for Laboratory Animal Science (ICLAS) and the international ethical guidelines for biomedical research involving animals.

Parasites

RA *T. cruzi* bTps were maintained in CF1 mice and obtained from whole blood at the peak of parasitemia (7 days post-infection) by differential centrifugation or by density gradient, using Histopaque-1083 (Sigma-Aldrich) as previously reported (Poncini et al., 2008). Parasites were obtained from the supernatant by centrifugation (10,000 g, 30 min, and 20°C) and resuspended in fresh Iscove's modified Dulbecco's medium (IMDM, Sigma-Aldrich). Epimastigotes were cultured *in vitro* in liver infusion tryptose (LIT) medium at 27°C to the exponential phase of growth and centrifuged at 3,000 g for 15 min at 10°C. The flasks had a liquid depth not exceeding 10 mm and were incubated without agitation for different amounts of time according to the experimental schedule (Isola et al., 1986). mTps were obtained as described by Cestari et al. (2012) with some adjustments. Briefly, after *in vitro* culture of 10×10^7 epimastigotes in 10% fetal bovine serum (FBS) LIT plus Grace's insect medium (MERC) and incubation at 27°C in tightly closed culture flasks, parasites were purified in a DEAE column equilibrated with PBS-glucose (20%) at pH 8.2. Purity was analyzed by microscopic examination.

BMDCs and XS106 Cell Line Cultures

Bone marrow from C3H/HeN mice was cultured for 7 days as previously described (Poncini et al., 2008). Briefly, bone marrow was flushed from femurs and tibias by syringe and 25-gauge needles with IMDM supplemented with 10% FBS, 100 U/ml penicillin, 100 mg/ml streptomycin, and 50 μM 2-mercaptoethanol (referred to below as 10-IMDM). The tissue was mechanically disaggregated, and DCs were obtained by culturing BM cells, supplemented with 20% supernatant from a GM-CSF–expressing cell line (J558 GM-CSF) at 37°C and 5% CO2. Then, at days 2 and 5, fresh medium was added to the cultures. At day 7, cells displayed a myeloid phenotype (>95 % CD11b) and were highly enriched in DCs (>70 % CD11c).

XS106, a long-term DC line established from newborn epidermis of A/J mice, was kindly provided by Dr. Takashima (University of Toledo, MTA M2014-25). They express a mature phenotype as described by Mohan et al. (2005).

Then, cells were harvested, washed, and plated (1×10^6 cells/ml) in 24-well plates (Nunc, NY, USA) and cultured in conditioned medium (Mohan et al., 2005) with or without 10 μg/ml LPS (*Escherichia coli* O26:B6, Sigma-Aldrich), and/or b/mTp (cell-to-parasite ratio 1:1, 1:4, or 1:10, depending on the experiment) overnight (ON).

BMDCs and XS106 Cell Culture, Stimulation, and Infection

As described above, cells were cultured in 24-well plates (Nunc, NY, USA) in medium with bTp or mTp (cell-to-parasite ratio 1:1, 1:4, or 1:10, depending on the experiment) ON at 37°C and 5% CO_2. Then, cells were washed to eliminate parasites in suspension and cultured in fresh medium for 4 or 7 more days. Then, samples were processed by cytospin and cell imprints stained with Giemsa. For immunofluorescence microscopy, cells were washed and stained with anti-mouse CD11c PE-conjugated mAb (BD PharMingen), attached to positively charged glass slides (Fisherbrand, Pittsburgh, PA), fixed in methanol, and stained with anti-parasite rabbit serum or appropriate controls and FITC-conjugated secondary Ab (Sigma-Aldrich).

The percentages of infected cells at the different cell–Tp ratios were defined after microscopic examination (400 × or 1,000 × magnification) by quantifying the relative number of cells with amastigotes in 15 random fields counted per treatment per sample.

Mixed Lymphocyte Reaction

To characterize APC capacity to induce lymphoproliferation, BMDCs or XS106 cells were cocultured with lymphocytes to test alloresponse as previously reported (Poncini et al., 2008). Briefly, DCs were cultured with different stimuli (medium, LPS, bTp/mTp) for 24 h, harvested, washed, irradiated (30 Gy), and plated with single-cell suspension enriched in T cells prepared from LNs of 8-week-old male C57BL/6 mice after $CD3^+$ T-cell purification by positive selection (MiniMACS separation; Miltenyi Biotec). Briefly, T cells ($CD3^+$) were purified from LN by using anti-mouse biotin-conjugated CD3 mAb (145-2C11; BD Biosciences) and streptavidin-conjugated microbeads for magnetic positive selection (MiniMACS). Purity was checked by flow cytometry and found to be around 90% of $CD3^+$ cells, as previously reported (Poncini et al., 2015). Cells were plated at a 1:10 APC–LN cell ratio, using 1×10^5 LN cells/well, and cultured at 37°C and 5% CO2 in 10-RPMI 1640 medium (Gibco, NY, USA) supplemented with 2 mM L-glutamine, 100 U/ml penicillin, 100 mg/ml streptomycin, and 50 μM 2-mercaptoethanol. Mixed lymphocyte reaction (MLR) assay was performed in 96-well microplates (Nunc) and cultured for 3 days. Proliferation was quantified by Ki-67 (REA183, Miltenyi Biotec) detection by flow cytometry according to the manufacturer's protocol.

Flow Cytometry

Cells (1×10^6) were washed in ice-cold PBS supplemented with 1% bovine serum albumin and 0.1% NaN_3, and incubated for 30 min at 4°C with a previously optimized amount of one or more of the following anti-mouse mAbs conjugated to different fluorophores: CD11b-PE (M1/70), CD11c-PE (HL3), I-Ak-FITC (11-5.2), CD40-Biot (3/23), CD80-Biot (16-10A1), and CD86-Biot (GL-1). Finally, cells were fixed with 1% paraformaldehyde. All mAbs and second reagents were purchased from PharMingen or Miltenyi Biotec. Samples were acquired on FACSCalibur (Becton Dickinson), and data were analyzed with FlowJo 7.6.2 software.

Enzyme Linked Immuno Assay

Cell culture supernatants were collected and stored at −80°C until used. Mouse IL-10 and TNF-α were detected by enzyme linked immune assay (ELISA) (R&D Systems) according to the manufacturer's protocol.

Statistical Analysis

Two groups were compared with unpaired Student's *t*-test. ANOVA and Bonferroni's or Dunnett's multiple comparison tests were performed in order to analyze statistical significance. All analyses were carried out with GraphPad Prism 4 software for Windows. A $p < 0.05$ value was assumed as significant.

RESULTS

XS106 Cell Line Phenotypic Characterization

As previously reported by Mohan et al. (2005), the XS106 cell line presented surface expression of CD11b and CD11c integrin in accordance with DCs of myeloid origin. In contrast to BMDCs that, in steady state, display low expression of activation markers (Poncini et al., 2008), XS106 cells showed high CD40, CD86, and MHCII surface expression. We also detected the macrophage related marker F4/80 and low expression of the monocytic markers Ly6C and CD207 in XS106, resembling Langerhans cells or migratory DCs in the skin (**Figure 1A**).

Previous studies have demonstrated that at certain conditions, bTp alone does not affect the activation of BMDCs, measured as MHCII, CD40, CD80, and CD86 surface expression (Poncini et al., 2008). Analyzing here the stimulatory effect of LPS, bTp, or mTp in the XS106 cell line, we found that while these cells displayed a higher basal activation status than BMDCs, neither LPS nor the parasite alone (from 1:1 to 1:10 cell-to-Tp relation, data not shown) enhanced the expression of CD40, CD86, or MHCII. However, LPS plus bTp starting at a 1:4 cell-to-bTp ratio increased the expression of MHCII and the costimulatory molecules CD40 and CD86 (**Figure 1B**).

The parasite itself, bTp or mTp alone, did not modify the activation status of XS106 in culture (**Figure 1C**). These results were also observed at 1:10 XS106 cell–Tp relation (data not shown). All data suggest that while bTp can polarize the activation of steady-state BMDCs (Poncini et al., 2008), the parasite could not modify the status of mature DCs such as XS106.

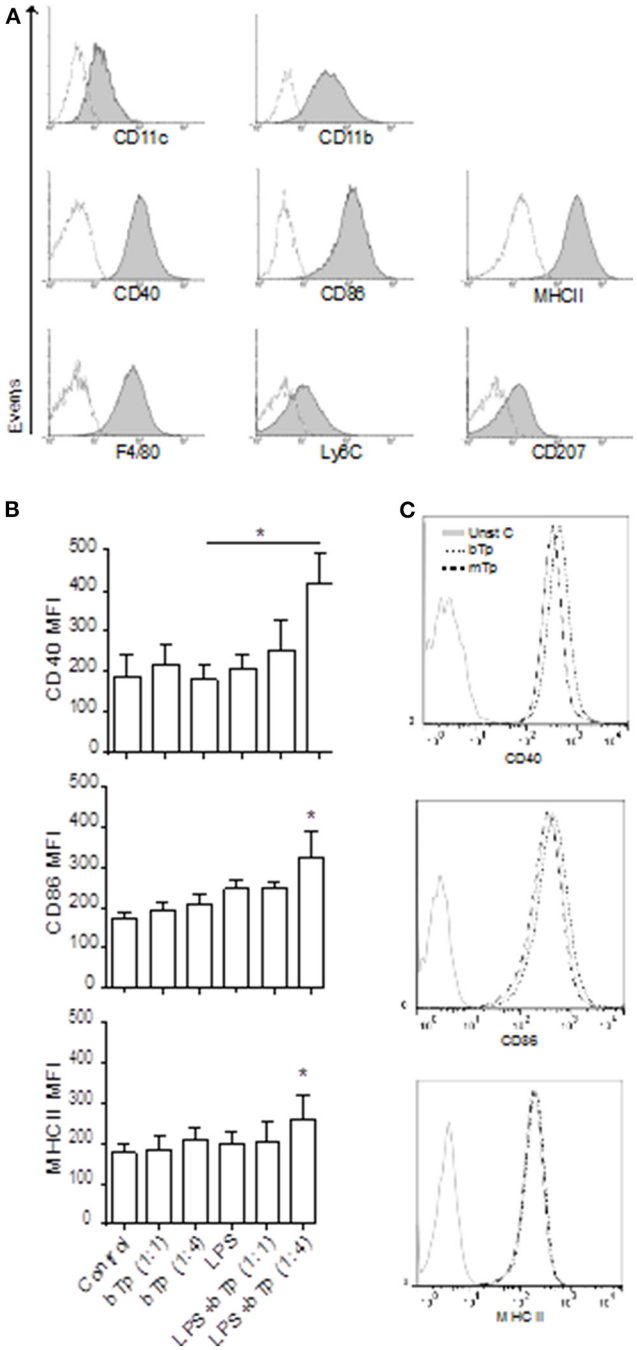

FIGURE 1 | Surface markers in XS106 cell line and comparative expression of activation markers in XS106 stimulated with bTp ± LPS or mTp. **(A)** XS106 were cultured at 1 × 10^6/well, stained with anti-mouse CD11c, CD11b, CD40, CD86, MHCII, F4/80, Ly6C, CD207 monoclonal Abs and analyzed by flow cytometry. One independent experiment of five is represented by histograms. Dotted line represents negative control for the staining. **(B,C)** 5 × 10^5 cells XS106 were incubated for 24 h with medium (control), bTp with or without LPS **(B)**, and bTp vs. mTp **(C)**. CD40, CD86, and MHCII were analyzed by flow cytometry. Bar graphic represents MFI (mean fluorescence intensity), mean ± SEM ($n = 5$), *$p < 0.05$. One-way ANOVA and Bonferroni's *post-hoc* correction.

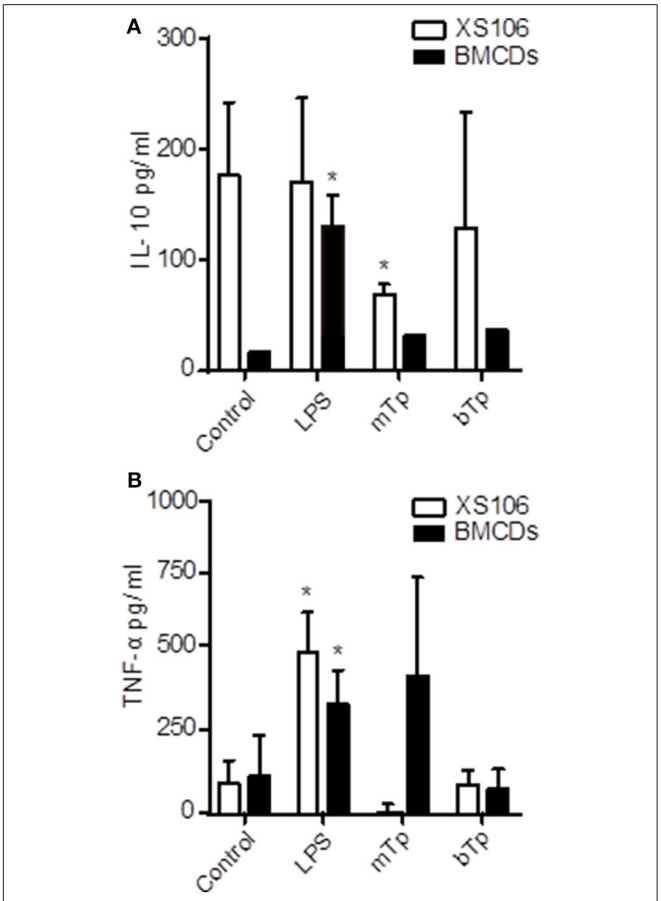

FIGURE 2 | Different IL-10 and TNF-α production patterns in XS106 cell line and BMDCs. 5 x 10^5 XS106 cells or BMDCs were incubated for 24 h in 10-IMDM (control), LPS, bTp or mTp at a parasite to cell ratio of 4. IL-10 **(A)** and TNF-α **(B)** were measured in culture supernatants by ELISA. ND, not detected. The results are presented as the mean ± SEM of seven independent experiments, *$p < 0.05$ (compared to the respective control). One-way ANOVA and Dunnett's post Test.

Comparative Production of TNF and IL-10 in BMDC and XS106 Stimulated With *T. cruzi* Infective Forms

Considering the basal activation of XS106, next we analyzed the production of TNF-α and IL-10, two cytokines with antagonistic properties in culture supernatants. XS106 and BMDCs were stimulated *in vitro* as described in *Materials and Methods*, and then, TNF-α and IL-10 were measured in culture supernatants as previously described by ELISA (Poncini et al., 2008).

XS106 showed a basal production of IL-10, which was downregulated in the presence of the parasite. The decline in the IL-10 production in XS106 was significant for mTp. As expected for BMDCs, only LPS increased IL-10 secretion (**Figure 2A**). TNF-α was upregulated by LPS but not by Tp in XS106. In contrast, in BMDCs, both LPS and mTp enlarged the production of this cytokine (**Figure 2B**), but

it was significant only for LPS, results consistent with cellular activation.

T. cruzi Infectivity in BMDC vs. XS106 Cell Line

To characterize the invasion and multiplication of the infective stages of *T. cruzi* bTp and mTp in XS106 cells and BMDCs, the parasites were cocultured with cells as described in *Materials and Methods*. Infection was determined and quantified by optic or fluorescence microscopy. Both XS106 cells and BMDCs presented intracellular amastigotes, confirming successful infection by bTp at 8 days post-infection (**Figure 3A**). However, XS106 cells were two times more infected with bTp than with mTp at the highest ratio of parasites (**Figures 3B,C**), and in comparison with BMDCs (**Figure 3C**). In BMDCs, no significant difference was detected in the percentage of infection between bTp and mTp (**Figure 3C**). These results suggest that at a high ratio of parasite to cell, bTp found a more conducive niche for multiplication in the XS106 cell line than in BMDCs.

Effect of *T. cruzi* Infective Forms on BMDC and XS106 Capacity to Induce Lymphoproliferation

Previous studies demonstrated that acute infection affects the maturation state of APCs and impairs the T-cell stimulatory capacity of splenic DCs (Alba Soto et al., 2003). In addition, *in vitro* and *in vivo*, we have demonstrated the ability of *T. cruzi* to modulate the differentiation of tolerogenic DCs (Poncini et al., 2008, 2015). *In vitro*, bTps fail to activate BMDCs, prevent the full activation by LPS, and induce high IL-10 secretion and a poor alloresponse (Poncini et al., 2008). Here we comparatively studied the antigen-presenting capacity of both XS106 cells and BMDCs after the stimulation with bTp, mTp, and LPS (positive control) in a model of alloresponse in an MLR.

As expected, LPS stimulated the antigen-presenting capacity of BMDCs. Despite not being significant, BMDCs cocultured with bTp presented less capacity to induce lymphoproliferation than mTp-treated BMDCs, which enhanced BMDCs' lymphoproliferative properties (**Figures 4A,B**). Interestingly, XS106 cells treated with bTp or mTp displayed enhanced capacity to induce T-cell proliferation compared with controls (**Figures 4A,B**). In addition, bTp-treated XS106 showed better antigen presentation than BMDCs (**Figure 4B**).

All these results demonstrate that the interaction of different *T. cruzi* infective stages with diverse APCs, but not the cell invasion and the parasite multiplication, could condition the antigen-presenting capacity of different DCs subsets early.

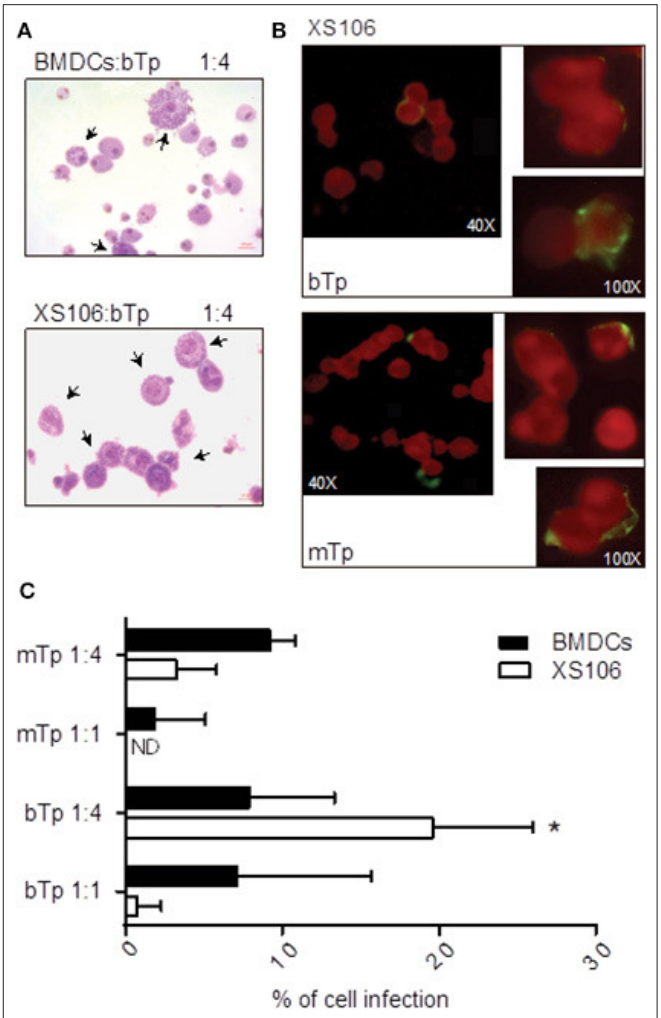

FIGURE 3 | XS106 cell line and BMDCs were differently infected by bTp and mTp. XS106 cells and BMDCs were cultured with bTp or mTp at different cell-to-Tp ratios (1:1 or 1:4). Cell infection was analyzed by optic microscopy after Giemsa staining, at 8 days post-infection **(A)**, 5 days post-infection **(C)**, or by fluorescence microscopy in XS106 cells **(B)** at 5 days post-infection, as described in materials and methods. Mean ± SEM ($n = 3$, 15 random fields counted per treatment). *$p < 0.05$; unpaired Student's *t*-test. Arrows shown cells with intracellular amastigotes. Bar size: 10 μm **(A)**.

DISCUSSION

The aim of this work was to characterize the effect of two infective stages of *T. cruzi* on APCs, particularly DCs from a different origin. Previously, our group has demonstrated that bTps promote tolerogenic BMDCs *in vitro* (Poncini et al., 2008). Here, we comparatively studied the interaction of mTp, the representative stage involved in vectorial transmission via the skin or mucous membranes (and gastric epithelium), and bTp responsible for transfusion and congenital transmission with two populations of DCs. The interaction was analyzed *in vitro* by using two different subsets of APCs that could interact with each of the stages described at different biological barriers: on one hand, XS106, a cell line obtained from skin epithelial DCs that resembles LCs (Mohan et al., 2005), and on the other, BMDCs, related to monocyte-derived (Mo)-DCs (Lutz et al., 2016).

The interest in XS106 cell–parasite interaction arises since they are similar to some of the APCs present in the skin. In fact, they presented intermediate expression of CD207 and F4/80 markers, commonly displayed in LCs, several migrating DCs, and some cells from the macrophage linage (Otsuka et al., 2018). In contrast to BMDCs, XS106 displayed

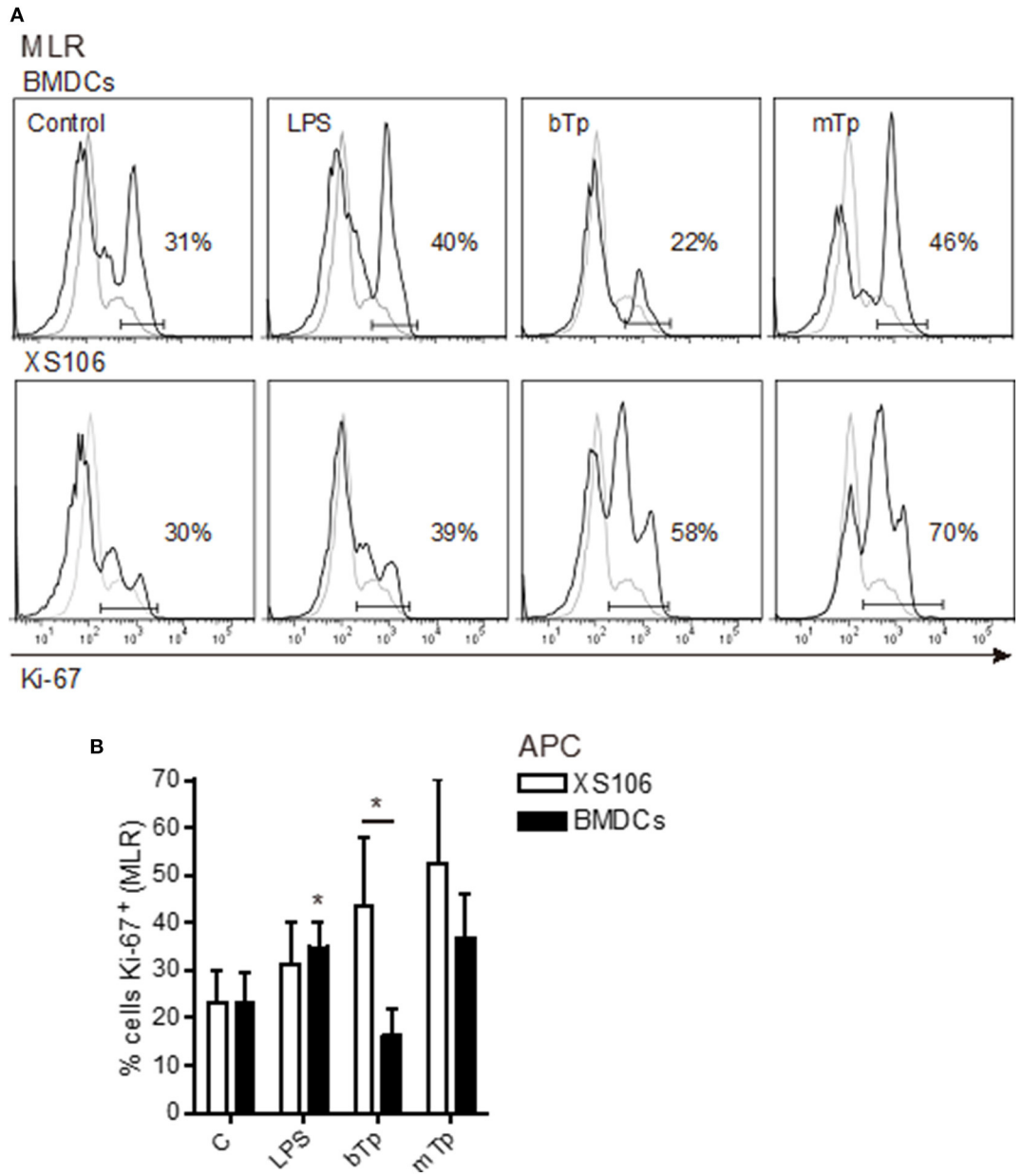

FIGURE 4 | T cell proliferation stimulated by BMDCs or XS106 cells conditioned by different infective stages of *T. cruzi.* BMDCs or XS106 cells were cultured with medium or different stimuli for 24 h. Then, cells were washed, irradiated and cocultured with LN cells enriched in T-cells at 1:10 APCs:LN cells ratio for 3 days. Cell proliferation was assessed by intracellular detection of Ki-67 in T cells obtained from LNs by FACS. One independent experiment of three is represented by histograms. Gray lines show negative controls for the staining, while black lines correspond to cells stained with specific Ab **(A)**. Cultures were set up in triplicate, and results are expressed as the mean ± SEM **(B)**. $^*p < 0.05$; two-way ANOVA and Bonferroni's *post-hoc* correction.

a mature/activated phenotype. That difference opened the possibility of exploring the effect of the parasite in DCs at different differentiation/activation statuses, showing that the XS106 cell line and BMDCs responded differently to *T. cruzi*.

mTps are transiently involved in the infection during vectorial transmission. Infection occurs via the skin, and after mTp entry into the host, the parasite suffers intracellular multiplication, as amastigotes and then bTp are present at the site of infection, interacting with resident APCs from the skin or migratory APCs. During this process, the parasite probably conditions the response triggered at the very beginning of the infection at the portal of entry. However, there are no reports yet showing skin APCs as a niche for parasite multiplication. Extended literature describes the wide range of tissues where *T. cruzi* resides in the host (Melo and Brener, 1978; Silva Pereira et al., 2019). Interestingly, a previous study in humans has demonstrated

that the parasite can persist in the skin, giving cutaneous lesions associated with the presence of multiplicative amastigotes (Hemmige et al., 2012).

In relation to APCs, it was previously demonstrated in humans that *T. cruzi* modulates the activation state of Mo-DCs *in vitro* (Van Overtvelt et al., 1999) and also during experimental infection (Chaussabel et al., 2003). Our results in the XS106 cell model propose that the basal activation phenotype displayed by mature DCs is not negatively modified by the interaction with the parasite, either mTp nor bTp. Basal IL-10 production was particularly reduced by mTp concomitantly with an enhanced antigen presentation activity, suggesting that mature epidermal DCs conserved their functional properties while interacting with the parasite (both bTp and mTp). In BMDCs, no important changes were detected in comparison to control cells, as previously reported for bTp (Poncini et al., 2008, 2010). However, we found that mTp increased TNF-α production and also antigen presentation in these cells. All results together suggest that *T. cruzi*, depending on the infective stage and the activation/maturation status of the APC, could polarize the immune response during the encounter.

Interestingly, invasion and multiplication of the parasite changed depending on the number of parasites added to cell cultures, the infective stage, and the DCs as recipient cell, demonstrating the importance of the niche the parasite finds to settle up and disseminate during infection. However, Tp invasion and the possibility of the parasite multiplying inside the cell would not be conditioning the antigen-presenting capacity in these two types of DCs, since mTp enhanced the lymphoproliferative capacity of both BMDCs and XS106 cells independently of the percentage of cell infection.

Previous reports with mTp obtained from culture or the vector and bTp from mouse infection showed differences in the immune response associated with the stage of the parasite involved. In a dog experimental model, animals presented enhanced cardiac parasitism and inflammatory response when infected with bTp, suggesting that the inoculum source affects the immunopathological aspects of Chagas disease (de Souza et al., 2014). In addition, it was also demonstrated in a mouse model of infection that bTps were more virulent than culture mTps, via both oral and peritoneal inoculation (Dias et al., 2013), concluding and remarking on the importance of the stage used, its origin, and the model of the infection in order to study the immune response.

Unpublished results from our group demonstrate that the infection with mTp displays reduced cell infiltrate and response at the site of infection (Gutierrez, manuscript under redaction) in comparison with the response described for bTp (Poncini and González-Cappa, 2017). Here, we studied functional properties of BMDCs and XS106 cells stimulated with mTp or bTp in an MLR and found that mTp improved the capacity to induce lymphoproliferation in both cells. In addition, we found that bTp did not impair the antigen-presenting property of XS106 cells, as reported for BMDCs (Poncini et al., 2008), and also that mTps enhance the immunogenicity of BMDCs. These data suggest that infective *T. cruzi* stages could interact and induce diverse effects in different APCs. One interesting conclusion emerging from these results is that apparently, mTp, in contrast to bTp, does not exert tolerogenic signals on DCs. In addition, the tolerogenic properties of bTp seem to be effective only in early differentiated DCs (BMDCs) resembling Mo-DCs in experimental models (Lutz et al., 2016). Those differences between bTp and mTp propose that parasite stages associated to the type of transmission could condition the early immune response and, in part, the outcome of the infection. When the vectorial transmission occurs, the first interaction of the innate immune system with the parasite is with mTp, a stage that, according to our results, would not affect APC immunogenicity. In contrast, when bTps are responsible for the infection (blood transfusion or congenital transmission), its interaction with steady-state DCs or Mo-DCs (in general, monocytes reach inflammatory foci, Poncini and González-Cappa, 2017) could probably impair antigen presentation by these cells, and this could make the immunity against the parasite not strong enough to control *T. cruzi* dissemination.

The importance of the study of *T. cruzi*–APCs interactions opens knowledge to better understand the strategies the parasite has developed in order to evade immunity. In addition, these are key topics on the road to developing new strategies for immunotherapy.

DATA AVAILABILITY STATEMENT

The datasets generated for this study are available on request to the corresponding author.

ETHICS STATEMENT

The animal study was reviewed and approved by CD N° 04/2015 approved by the University of Buenos Aires's Institutional Committee for the Care and Use of Laboratory Animals (CICUAL).

AUTHOR CONTRIBUTIONS

BG, MR, SG-C, and CP contributed the conception and design of the study. BG and CP performed the experiments and analyzed data. EL conducted the epimastigote cultures. BG and CP wrote sections of the manuscript. All authors contributed to manuscript revision and read and approved the submitted version.

FUNDING

This work was supported by Consejo Nacional de Investigaciones Científicas y Técnicas (CONICET), Fundación Bunge & Born, and Universidad de Buenos Aires (UBACyT 2017 20020160100117BA), Argentina.

ACKNOWLEDGMENTS

We thank Eduardo Gimenez, Ricardo Chung, and, Marianela Lewicki for technical assistance.

REFERENCES

Alba Soto, C. D., Mirkin, G. A., Solana, M. E., and González Cappa, S. M. (2003). *Trypanosoma cruzi* infection modulates *in vivo* expression of major histocompatibility complex class II molecules on antigen-presenting cells and T-cell stimulatory activity of dendritic cells in a strain-dependent manner. *Infect. Immun.* 71, 1194–1199. doi: 10.1128/IAI.71.3.1194-1199.2003

Cestari, I., Ansa Addo, E., Deolindo, P., Inal, J. M., and Ramírez, M. I. (2012). *Trypanosoma cruzi* immune evasion mediated by host cell-derived microvesicles. *J. Immunol.* 188, 1942–1952. doi: 10.4049/jimmunol.1102053

Chaussabel, D., Pajak, B., Vercruysse, V., Bisseyé, C., Garzé, V., Habib, M., et al. (2003). Alteration of migration and maturation of dendritic cells and T-cell depletion in the course of experimental *Trypanosoma cruzi* infection. *Lab. Invest.* 83, 1373–1382. doi: 10.1097/01.LAB.0000087587.93781.6F

da Costa, T. A., Silva, M. V., Mendes, M. T., Carvalho-Costa, T. M., Batista, L. R., Lages-Silva, E., et al. (2014). Immunomodulation by *Trypanosoma cruzi*: toward understanding the association of dendritic cells with infecting TcI and TcII populations. *J. Immunol. Res.* 2014:962047. doi: 10.1155/2014/962047

de Souza, S. M., Vieira, P. M., Roatt, B. M., Reis, L. E., da Silva Fonseca, K., Nogueira, N. C., et al. (2014). Dogs infected with the blood trypomastigote form of *Trypanosoma cruzi* display an increase expression of cytokines and chemokines plus an intense cardiac parasitism during acute infection. *Mol. Immunol.* 58, 92–97. doi: 10.1016/j.molimm.2013.11.007

Dias, G. B., Gruendling, A. P., Araújo, S. M., Gomes, M. L., and Toledo, M. J. (2013). Evolution of infection in mice inoculated by the oral route with different developmental forms of *Trypanosoma cruzi* I and II. *Exp. Parasitol.* 35, 511–517. doi: 10.1016/j.exppara.2013.08.013

Gonzalez Cappa, S. M., Bijovsky, A. T., Freilij, H., Muller, L. A., and Katzin, A. M. (1981). Aislamiento de una cepa de *Trypanosoma cruzi* a predominio de formas delgadas en la Argentina. *Medicina* 41, 119–120.

Hemmige, V., Tanowitz, H., and Sethi, A. (2012). *Trypanosoma cruzi* infection: a review with emphasis on cutaneous manifestations. *Int. J. Dermatol.* 51, 501–508. doi: 10.1111/j.1365-4632.2011.05380.x

Isola, E. L. D., Lammel, E. M., and González Cappa, S. M. (1986). *Trypanosoma cruzi*: differentiation after interaction of epimastigotes and *Triatoma infestans* intestinal homogenate. *Exp. Parasitol.* 62, 329–335. doi: 10.1016/0014-4894(86)90039-1

Lutz, M. B., Inaba, K., Schuler, G., and Romani, N. (2016). Still alive and kicking: *in-vitro*-generated GM-CSF dendritic cells! *Immunity* 19, 1–2. doi: 10.1016/j.immuni.2015.12.013

Melo, R. C., and Brener, Z. (1978). Tissue tropism of different *Trypanosoma cruzi* strains. *J. Parasitol.* 64, 475–482. doi: 10.2307/3279787

Merad, M., Sathe, P., Helft, J., Miller, J., and Mortha, A. (2013). The dendritic cell lineage: Ontogeny and function of dendritic cells and their subsets in the steady state and the inflamed setting. *Annu. Rev. Immunol.* 31, 563–604. doi: 10.1146/annurev-immunol-020711-074950

Mohan, J., Hopkins, J., and Mabbott, N. A. (2005). Skin-derived dendritic cells acquire and degrade the scrapie agent following *in vitro* exposure. *Inmunology* 116, 122–133. doi: 10.1111/j.1365-2567.2005.02207.x

OMS (2019). *Organización Mundial de la Salud. La Enfermedad de Chagas (Tripanosomiasis Americana).* Available online at: http://www.who.int/mediacentre/factsheets/fs340/es/

Otsuka, M., Egawa, G., and Kabashima, K. (2018). Uncovering the mysteries of langerhans, cells, inflammatory dendritic epidermal, cells, and monocyte-derived langerhans cell-like cells in the epidermis. *Front. Immunol.* 30:1768. doi: 10.3389/fimmu.2018.01768

Planelles, L., Thomas, M. C., Marañón, C., Morell, M., and López, M. C. (2003). Differential CD86 and CD40 co-stimulatory molecules and cytokine expression pattern induced by *Trypanosoma cruzi* in APCs from resistant or susceptible mice. *Clin. Exp. Immunol.* 131, 41–47. doi: 10.1046/j.1365-2249.2003.02022.x

Poncini, C. V., Alba Soto, C., Batalla, E., Solana, M. E., and González Cappa, S. M. (2008). *Trypanosoma cruzi* induces regulatory dendritic cells *in vitro*. *Infect. Immun.* 76, 2633–2641. doi: 10.1128/IAI.01298-07

Poncini, C. V., Giménez, G., Pontillo, C. A., Alba-Soto, C. D., de Isola, E. L., Piazzón, I., et al. (2010). Central role of extracellular signal-regulated kinase and Toll-like receptor 4 in IL-10 production in regulatory dendritic cells induced by *Trypanosoma cruzi*. *Mol. Immunol.* 47, 1981–1988. doi: 10.1016/j.molimm.2010.04.016

Poncini, C. V., and González-Cappa, S. M. (2017). Dual role of monocyte-derived dendritic cell in *Trypanosoma cruzi* infection. *Eur. J. Immunol.* 47, 1936–1948. doi: 10.1002/eji.201646830

Poncini, C. V., Illarregui, J. M., Batalla, E. I., Engels, S., Cerliani, J. P., Cucher, M. A. van Kooyk, Y., et al. (2015). *Trypanosoma cruzi* infection imparts a regulatory program in dendritic cells and T cells via galectin-1-dependent mechanisms. *J. Immunol.* 195, 3311–3324. doi: 10.4049/jimmunol.1403019

Silva Pereira, S., Trindade, S., De Niz, M., and Figueiredo, L. M., (2019). Tissue tropism in parasitic diseases. *Open Biol.* 31:190036.doi: 10.1098/rsob.190124

Van Overtvelt, L., Vanderheyde, N., Verhasselt, V., Ismaili, J., De Vos, L., Goldman, M., et al. (1999). *Trypanosoma cruzi* infects human dendritic cells and prevents their maturation: inhibition of cytokines, HLA-DR, and costimulatory molecules. *Infect. Immun.* 67, 4033–4040. doi: 10.1128/IAI.67.8.4033-4040.1999

Conflict of Interest: The authors declare that the research was conducted in the absence of any commercial or financial relationships that could be construed as a potential conflict of interest.

frontiers in Cellular and Infection Microbiology

REVIEW
published: 17 April 2020
doi: 10.3389/fcimb.2020.00153

The IL-33/ST2 Axis in Immune Responses Against Parasitic Disease: Potential Therapeutic Applications

Nathan Ryan[1,2], *Kelvin Anderson*[1], *Greta Volpedo*[1,3], *Sanjay Varikuti*[1], *Monika Satoskar*[4], *Sanika Satoskar*[4] *and Steve Oghumu*[1]*

[1] Department of Pathology, The Ohio State University Wexner Medical Center, Columbus, OH, United States, [2] Division of Anatomy, The Ohio State University Wexner Medical Center, Columbus, OH, United States, [3] Department of Microbiology, The Ohio State University, Columbus, OH, United States, [4] Northeast Ohio Medical University, Rootstown, OH, United States

Parasitic infections pose a wide and varying threat globally, impacting over 25% of the global population with many more at risk of infection. These infections are comprised of, but not limited to, toxoplasmosis, malaria, leishmaniasis and any one of a wide variety of helminthic infections. While a great deal is understood about the adaptive immune response to each of these parasites, there remains a need to further elucidate the early innate immune response. Interleukin-33 is being revealed as one of the earliest players in the cytokine milieu responding to parasitic invasion, and as such has been given the name "alarmin." A nuclear cytokine, interleukin-33 is housed primarily within epithelial and fibroblastic tissues and is released upon cellular damage or death. Evidence has shown that interleukin-33 seems to play a crucial role in priming the immune system toward a strong T helper type 2 immune response, necessary in the clearance of some parasites, while disease exacerbating in the context of others. With the possibility of being a double-edged sword, a great deal remains to be seen in how interleukin-33 and its receptor ST2 are involved in the immune response different parasites elicit, and how those parasites may manipulate or evade this host mechanism. In this review article we compile the current cutting-edge research into the interleukin-33 response to toxoplasmosis, malaria, leishmania, and helminthic infection. Furthermore, we provide insight into directions interleukin-33 research may take in the future, potential immunotherapeutic applications of interleukin-33 modulation and how a better clarity of early innate immune system responses involving interleukin-33/ST2 signaling may be applied in development of much needed treatment options against parasitic invaders.

Keywords: IL-33, ST2, parasite, innate, immunity

OPEN ACCESS

Edited by:
Patricia Sampaio Tavares Veras, Gonçalo Moniz Institute (IGM), Brazil

Reviewed by:
Gaurav Gupta, NIIT University, India
Vasco Rodrigues, Institut Curie, France
Diego Luis Costa, University of São Paulo, Brazil

***Correspondence:**
Steve Oghumu
oghumu.1@osu.edu

Specialty section:
This article was submitted to Microbes and Innate Immunity, a section of the journal Frontiers in Cellular and Infection Microbiology

Received: *13 January 2020*
Accepted: *23 March 2020*
Published: *17 April 2020*

Citation:
Ryan N, Anderson K, Volpedo G, Varikuti S, Satoskar M, Satoskar S and Oghumu S (2020) The IL-33/ST2 Axis in Immune Responses Against Parasitic Disease: Potential Therapeutic Applications. Front. Cell. Infect. Microbiol. 10:153. doi: 10.3389/fcimb.2020.00153

INTRODUCTION

Interleukin-33 (IL-33) is a member of the IL-1 cytokine superfamily, and plays an important role in innate immunity, inflammatory and autoimmune diseases (Tonacci et al., 2019). Previously it has been presumed that IL-33, through its association with chromatin in the nucleus, acts as a repressor of transcription (Carriere et al., 2007). More recent studies have further elaborated on

IL-33 as being a transcriptional regulator of nuclear factor NF-κB where it has demonstrated involvement in the pathogenesis of esophageal squamous cell carcinoma and atherosclerosis, as well as in the activation of endothelial cells (Choi et al., 2012; Buckley et al., 2019; Yue et al., 2019). However, it has been shown in a 2018 study by Travers et al. that IL-33 may have less of a transcriptional regulatory role than was previously thought, and that the role IL-33 plays with chromatin may be post-translational and more involved in controlling the release of nuclear IL-33 (Travers et al., 2018). Additionally, IL-33 has the distinct characteristic of being subject to post-translational modifications that dramatically affect its ability to bind to its receptor, suppression of tumorigenicity 2 (ST2). For example, its affinity to ST2 becomes null after subjection to apoptosis-induced caspases (Cayrol and Girard, 2009; Luthi et al., 2009), while its affinity increases greatly after encountering neutrophil and mast cell-derived serine proteases (Lefrançais et al., 2012, 2014). IL-33 displays high basal expression in endothelial cells and the epithelial cells of many tissues including those of the central nervous system, respiratory, excretory, circulatory, integumentary, and reproductive systems (Yasuoka et al., 2011; Pichery et al., 2012; Cao et al., 2018). It has also been shown that dendritic cells, macrophages, and microglia can produce IL-33 under certain conditions (Pichery et al., 2012; Tjota et al., 2013; Cao et al., 2018). The lack of a secretory sequence and well-defined mechanism for its secretion outside of cell death have led to the designation of IL-33 as an "alarmin," though some studies suggest it may be released independent of cell death through mechanisms involving mechanical stress, extracellular ATP or active release by macrophages (Molofsky et al., 2015).

IL-33 primarily functions through its receptor ST2 (Liew et al., 2010; Liu et al., 2019). ST2 is a member of the IL-1 receptor superfamily and is found in two spliced isoforms: one soluble and one membrane-bound. The soluble form, sST2, sequesters circulating IL-33, dampening IL-33 signaling. ST2 is the membrane-bound form that participates in signal transduction through myeloid differentiation primary response 88 (MyD88) and nuclear factor NF-κB after binding to its ligand IL-33 (Griesenauer and Paczesny, 2017; Pusceddu et al., 2019). In the innate immune system, ST2 has been shown to be expressed on macrophages, dendritic cells, basophils, eosinophils, mast cells, type 2 innate lymphoid cells (ILC2s), endothelial cells, and neutrophils (Griesenauer and Paczesny, 2017). ST2 signaling has been shown to have pleiotropic effects on these cells including promotion of dendritic cell-mediated activation of $ST2^+$ regulatory T cells (Tregs) (Matta et al., 2014), enhancement of lipopolysaccharide response by macrophages (Espinassous et al., 2009), activation of ILC2s (Riedel et al., 2017), promotion of lymphangiogenesis by lymphatic endothelial cells (Han et al., 2017) and induction of eosinophilic chemotaxis, survival and degranulation (Cherry et al., 2008). In the adaptive immune system, ST2 has been shown to be preferentially expressed by Th2 cells, where IL-33 stimulation has been shown to induce the production of IL-4, IL-5 and IL-13 (Schmitz et al., 2005; Paul and Zhu, 2010). IL-33 has also been shown to suppress T helper type 1 (Th1) responses (Rostan et al., 2013; Stier et al., 2019), though some studies have shown that it may potentiate Th1 responses as well in an IL-12 dependent manner (Smithgall et al., 2008; Komai-Koma et al., 2016). A compiled meta-analysis study of the IL-33/ST2 axis has revealed the enormous extent of the complexity and involvement of this signaling pathway, revealing just how much remains to be understood (Pinto et al., 2018).

Interestingly, IL-33/ST2 signaling has been demonstrated to play both pathological and protective roles in various pathologies by exerting pro-inflammatory and anti-inflammatory effects in a context-dependent manner. For example, in the context of obesity, IL-33 was shown to reduce chronic adipose tissue inflammation by promoting the activity of Th2 and alternatively activated macrophage (M2) populations (Miller et al., 2010). However, in the context of cancer, IL-33 aids in tumor immune evasion by upregulating the activity, survival and expansion of myeloid derived suppressor cells via ST2 signaling, which was reduced in $ST2^{-/-}$ mice (Xiao et al., 2016). Recent discoveries have further suggested that IL-33 can induce the proliferation, survival, and metastasis of cancer cells (Allegra et al., 2019; Gorbacheva and Mitkin, 2019). IL-33 is also known to exacerbate asthmatic and allergic inflammation in the skin, GI tract and lungs through the ST2-mediated activation of basophils, eosinophils, mast cells, dendritic cells, macrophages and ILC2s by promoting the chemo-attraction of Th2 cells and the production of Th2-associated cytokines by various cell types (Louten et al., 2011; Bartemes et al., 2012; Sjoberg et al., 2017; Chan et al., 2019). In the context of infectious disease, many studies have further shown that IL-33/ST2 activity displays context-dependent protection and exacerbation of infection dependent on multiple factors, including the infectious agent, cellular microenvironment, and affected organs. IL-33 has been demonstrated in viral infection to promote a protective immune response through enhanced $CD8^+$ T cell responses (Bonilla et al., 2012). Interestingly, viral infection within lung tissue has shown a necessity for $ST2^+$ ILC accumulation in influenza recovery (Monticelli et al., 2011). However, contrary to this point, it has been observed that over-expression of IL-33 may be associated with COPD (Byers et al., 2013). IL-33/ST2 signaling has further been demonstrated to be of positive benefit in innate immunity at the site of the skin, where its expression activates downstream production of antimicrobial reactive oxygen and nitrogen species (Li et al., 2014). Pathologies associated with bacterial infections including pediatric asthma and *Staphylococcus aureus* induced septic arthritis, however, have been found to respond negatively with expression of IL-33 or ST2 (Hentschke et al., 2017; Staurengo-Ferrari et al., 2018). IL-33 involved mechanisms have also been demonstrated to show divergent roles in the resistance to different fungal infections, where it has been noted to be protective in the context of candidiasis but hinders clearance of *Aspergillus fumigatus* infection (Park et al., 2016; Garth et al., 2017). Within this review, we will be focusing on IL-33/ST2 signaling within the context specifically of parasitic infection.

Parasitic diseases affect a significant percentage of the world's populations, with billions being infected or at risk of infection (Hay et al., 2004; Torgerson et al., 2015; Short et al., 2017; Jourdan et al., 2018), with more and more becoming susceptible due to factors such as climate change, increasing population density, loss of biodiversity, habitat restriction and overall ecological

remodeling (Cable et al., 2017; Short et al., 2017). Despite recent improvements in the infection and mortality rates of parasitic diseases like malaria (WHO, 2019), issues such as drug resistance by both parasites and vectors pose a significant threat (Sibley and Hunt, 2003; Vanaerschot et al., 2014; Bushman et al., 2016; Alout et al., 2017). Host-directed approaches toward therapies displays significant promise, though further research is needed to make their application viable (Varikuti et al., 2018). Research investigating IL-33/ST2's role in parasitic infection shows that its modulation may demonstrate a viable treatment strategy, though due to the varying nature in IL-33/ST2 signaling in the host immune response, there is a need for further research on the topic. While the IL-33/ST2 signaling axis has been researched in the context of many systems and diseases, the roles of such findings in the context of parasitic disease have not been exhaustively compiled. In this review, we explore IL-33/ST2 signaling of the innate immune system's response and provide insight into its role during parasitic infections caused by *Toxoplasma*, *Plasmodium*, *Leishmania*, and helminths.

TOXOPLASMA

Toxoplasma gondii, the causative agent of the neglected parasitic disease toxoplasmosis, is an obligate intracellular protozoan capable of infecting most types of mammalian cells. Toxoplasmosis affects 25–30% of humans worldwide and is usually asymptomatic in immunocompetent individuals, but can become a life threatening condition in immunocompromised patients as well as in developing fetuses (Delgado Betancourt et al., 2019; Lima and Lodoen, 2019). Toxoplasmosis can be transmitted via consumption of contaminated food, zoonotically or congenitally (Delgado Betancourt et al., 2019). Oocysts are excreted in the feces of infected animals and can be consumed by other animals. In the new host, oocysts release sporozoites, which can then differentiate into bradyzoites and tachyzoites. Tachyzoites can form cysts in various organs, which predator animals may consume. After ingestion, cysts release bradyzoites, which can then convert back into the fast growing tachyzoites and infect the surrounding tissue (Delgado Betancourt et al., 2019). Once an individual becomes infected, the parasite can disseminate through the bloodstream and establish a chronic infection in different organs. The three canonical types of toxoplasmosis are cerebral, lymphatic and ocular (Lima and Lodoen, 2019). After the entry of infected tachyzoids into the host intestine, a rapid recruitment of neutrophils occurs, followed by the action of other immune cells such as macrophages and dendritic cells. These cells elicit a strong inflammatory response characterized by the production of IL-12 and interferon-gamma (IFN-γ), inducers of a protective Th1-type immunity (Khan et al., 2019; Ryffel et al., 2019). This T cell-mediated immunity is crucial for resolving acute infection and controlling chronic disease. *Toxoplasma gondii* is also able to inhibit apoptotic pathways in infected mammalian cells (Lima and Lodoen, 2019).

While a pro-inflammatory response is important for controlling the parasites, a Th2 response is necessary to prevent pathology and tissue damage caused by over-active Th1 responses. A balance between Th1 and Th2 responses is crucial for controlling toxoplasmosis. The Th2 response can be amplified by several cytokines, including IL-33. IL-33 signaling through T1/ST2 was shown to be required for controlling *Toxoplasma* infection in the brain and preventing the development of encephalitis. T1/ST2$^{-/-}$ BALB/c mice infected with *Toxoplasma* showed increased pathology and parasitic burdens and had higher levels of *Nos2, Ifng* and *Tnf* mRNA transcripts in their brains compared to T1/ST2$^{+/+}$ mice (Jones et al., 2010).

In the eye, an immune-privileged site, the immune response to toxoplasmosis is different compared to other organs. Immune-mediated inflammation is reduced in the eye, but the preservation of immune privilege is dependent upon immune-suppressive responses (Tong and Lu, 2015). Ocular toxoplasmosis can cause vision-threatening complications depending on the levels of inflammation. The action of IL-33 is important to control inflammation and pathology in the eye (Zhang et al., 2019). Kunming mice infected intraocularly with *Toxoplasma* showed increased numbers of IL-33 positive cells as well as higher levels of IL-33 and ST2 mRNA transcripts in the eyes and cervical lymph nodes. Additionally, there was a significant correlation between the levels of IL-13 and ST2 and also the levels of IL-4 and ST2, suggesting that IL-33 signaling may be involved in the immunopathology of ocular toxoplasmosis (Tong and Lu, 2015). Higher levels of *Il33* mRNA transcripts were also found in the eyes of *Toxoplasma*-infected susceptible C57BL/6 mice compared to resistant BALB/c mice; however, it was not clear whether this or other cytokines were responsible for the ocular pathology seen in C57BL/6 mice (Zhang et al., 2019).

In an oral model of *Toxoplasma* infection, absence of IL-33 receptor/ST2 attenuated neutrophilic inflammation and ileitis in susceptible C57BL/6 mice and enhanced their survival. These effects are mediated by the increased expression of IL-22, a protective cytokine of the IL-10 family released mainly by dendritic cells and Th17 cells. Blockade of ST2 via neutralizing anti-ST2 antibodies conferred partial protection, while blockade of IL-22 abrogated this protection. These findings show that IL-33 plays a dual role in inflammation (Ryffel et al., 2019).

A delicate balance between the pro and anti-inflammatory response is crucial for controlling toxoplasmosis. While inflammation is needed to eliminate the parasite and the infected cells, an anti-inflammatory response is necessary to limit tissue damage. IL-33 signaling through the ST2 receptor has been shown to play a dual role in inflammation and can therefore have different effects on toxoplasmosis depending on the tissue. For instance, in the brain and eye IL-33 controls immunopathology and is instrumental for disease resolution, while in an oral model of toxoplasmosis, the action of this cytokine is detrimental to murine survival. More studies are needed to fully determine the complex role of IL-33/ST2 in different infected tissues and stages of toxoplasmosis. A better understanding of this signaling pathway could aid the discovery of novel immunomodulatory therapies against toxoplasmosis.

PLASMODIUM

Malaria is widely known as the parasitic disease with the most damaging global impact, with an estimated 228 million cases occurring in 2018, and to which ∼405,000 deaths can be directly attributed, most of whom are children under 5 in Sub-Saharan

Africa. While these numbers are an improvement from recent years, they remain dangerously high (WHO, 2019). Malaria is a mosquito-borne illness spread by *Anopheles* mosquitoes that is known to be caused by six species of protozoans from the genus *Plasmodium*, though the most virulent and prevalent is *Plasmodium falciparum* (Milner, 2018; WHO, 2019). Upon entry to the host through mosquito saliva, *Plasmodium* sporozoites enter the bloodstream and invade hepatocytes, where they germinate via schizogony into merozoites in what is known as the liver stage of infection. The subsequent blood stage of infection is initiated when the merozoites release from the hepatocytes into the bloodstream to invade erythrocytes, where they feed as trophozoites and further replicate via schizogony before liberating from the erythrocytes, continuing the blood stage of infection (Miller et al., 2002). Malaria leads to system-wide symptoms, the most severe of which occur in the form of hypoglycemic acidosis, anemia, renal failure, respiratory failure and cerebral malaria, which have been implicated to occur in the blood stage as a result of the sequestration of infected erythrocytes in microvasculature, the rupture of erythrocytes, and the systemic burden of circulating parasites (Miller et al., 2002, 2013; Bartoloni and Zammarchi, 2012). Interestingly, evidence has mounted to implicate the immune system in playing both protective and pathological roles in malaria symptomology, with context-dependent inflammatory responses helping the host by reducing parasitemia on one hand, but hurting the host by contributing to severe symptomology and sequelae on the other (Miller et al., 2002; Gowda and Wu, 2018; Pais and Penha-Goncalves, 2018).

Emerging evidence has implicated IL-33 and ST2 as having significant influence on the severity of symptoms in malarial infection. The role of IL-33/ST2 axis in early onset infection remains unclear. Previously, a study using intradermal injection of *Plasmodium berghei* sporozoites into C57BL/6 mice showed no differences in IL-33 expression via RTqPCR within the draining lymph nodes compared to uninfected controls 1.5 h after infection (Mac-Daniel et al., 2014). However, it should be noted that IL-33 is constitutively expressed and maintained at high basal levels in endothelial and epithelial cells, and can be released when these cells are damaged (Moussion et al., 2008). Thus IL-33 may not need to be further induced to be biologically active in early malarial infection, though any role it may play at this stage is yet to be elucidated. Moreover, IL-33 is known to play a role in the activity of tissue-resident immune cells, including mast cells and ILC2s. Specifically, IL-33 has been shown to potentiate mast cell activity (Komai-Koma et al., 2012; Joulia et al., 2017), while mast cell degranulation has been separately shown to correlate with *P. falciparum* severity (Wilainam et al., 2015); though it also has been demonstrated to promote the expansion of $ST2^+$ ILC2s in the skin (Salimi et al., 2013), a cell type whose systemic expansion is shown to correlate with improved protection against cerebral malaria (Besnard et al., 2015). Ultimately, IL-33's importance in these processes remains speculative and associative in the context of malaria, providing rationale to further explore and identify the mechanisms and activities of IL-33 during the initial malarial infection.

Interestingly, IL-33 has been associated with severe respiratory symptoms during malaria infection. A study analyzing histological samples taken from the lungs of Southeast Asian patients who had died from severe *P. falciparum* infection showed a significant accumulation of IL-33 in their bronchioles, which correlated with severity of pathological pulmonary remodeling and inflammatory lymphocyte, monocyte, and neutrophil recruitment into the lungs (Ampawong et al., 2015). Likewise, a study using a *P. berghei* ANKA (PbA) model of infection on C57BL/6 mice showed that malaria-induced acute respiratory distress was alleviated by dexamethasone treatment, which coincided with decreased levels of serum IL-33 (dos Santos Ortolan et al., 2018). These findings are especially significant considering the tendency for IL-33 transgenic mice to develop spontaneous pulmonary inflammation (Zhiguang et al., 2010), though further research is needed to elucidate the mechanisms by which IL-33 contributes to *Plasmodium*-induced pulmonary distress.

Further evidence for a role of IL-33 in malarial infection was demonstrated in a study by Ayimba et al. assessing pediatric patients under the age of 5 in central Togo, which found that IL-33 was significantly elevated in the plasma of patients with severe *P. falciparum* infection (classified by a parasite load of 250,000/μL and/or a hemoglobin concentration of 5g/dL) compared to infection-free controls, with the authors calling for further exploration of IL-33's role in cerebral malaria (Ayimba et al., 2011). Cerebral malaria is a severe complication of *P. falciparum* infection marked by coma, seizures, and neurological abnormalities. Furthermore, survivors of cerebral malaria typically demonstrate debilitating sequelae manifesting from neurological damage including cognitive, motor and behavioral deficits (Idro et al., 2005, 2010). Currently, the underlying mechanism of cerebral malaria is poorly understood, though inflammatory cytokines appear to play a major role (Armah et al., 2005; Idro et al., 2010). The logic behind Ayimba et al.'s call for investigation into IL-33 was due in part to constitutive expression of IL-33 in the central nervous system by endothelial cells and astrocytes, and the observation that $ST2^+$ microglia demonstrate pro-inflammatory effects via upregulation of inflammatory cytokines and chemokines, nitric oxide and microglial phagocytosis (Yasuoka et al., 2011; Fairlie-Clarke et al., 2018).

Per the suggestion of Ayimba et al. the roles of IL-33 and its receptor ST2 have been investigated mechanistically, and the results of these studies have implicated them as major players in cerebral malaria. Surprisingly, IL-33/ST2 was shown to have potential therapeutic properties via direct administration of IL-33 as well as serving as an etiological component of cerebral malaria pathogenesis. One study using a blood-stage PbA model of infection on C57BL/6 mice found that administration of IL-33 attenuated the development of experimental cerebral malaria, with its therapeutic effect being attributed to induction of M2 polarization, reduction of inflammatory mediators and expansion of $CD45^+ST2^+ICOS^+$ ILC2s and Tregs (Besnard et al., 2015). Specifically, this study found that IL-33 induced ILC2s in promoting M2 activity *in vitro* and *in vivo*, which could promote Treg expansion *in vitro*. This group demonstrated using

PbA-infected Treg-depleted mice receiving IL-33 or no treatment displayed significant cerebral malaria compared to mice receiving IL-33 with normal Treg function. This downregulated Treg activity resulted in with increases in serum levels of IL-12, IFN-γ as well as IFN-γ and granzyme b expression by $CD8^+$ cells compared to IL-33 treated Treg competent mice. Taken together, this demonstrates that IL-33 mediated Treg function is important in preventing cerebral malaria, though the exact mechanisms of which remains to be elucidated. Another study using the same model of infection corroborated these findings, showing that IL-33 was downregulated in experimental cerebral malaria and that administration improved the efficacy of the anti-malarial drugs artesunate and chloroquine, though no therapeutic effect was elicited by IL-33 alone when administered in the context of experimental cerebral malaria. Mechanistically, this study found that IL-33 administration in concomitance with artesunate and chloroquine led to decreased IL-1β production and NLRP3 inflammasome formation in the brain compared to mice treated with the anti-malarial drugs alone (Strangward et al., 2018). This finding is particularly significant when taking into account the NLRP3 inflammasome's etiological role in neuroinflammatory diseases (Song et al., 2017) and IL-1β's association with fatal cerebral malaria (Maneerat et al., 1999).

Paradoxically, another study using the PbA model of malaria showed antithetical results, with ST2-deficient mice showing significantly reduced experimental cerebral malaria symptoms. Specifically, this study found reduced cerebral inflammation and decreased pathological migration of T-cells to the brain in ST2-deficient mice via downregulation of ICAM-1 correlating with a reduction in LT-α, though no differences were observed in systemic and pulmonary inflammation (Palomo et al., 2015). Interestingly, this lack of neural T cell infiltration in $ST2^{-/-}$ mice occurred independently of the CXCR3-associated chemokines CXCL9/10 expression and did not correlate with any changes in expression of granzyme b, IFN-γ, or TNF-α in lysates of the whole brain (Palomo et al., 2015). This same group in a later study demonstrated that $ST2^{-/-}$ mice showed resistance to cognitive defects resulting from PbA infection and improved survival compared to WT mice. The improved prognosis observed in $ST2^{-/-}$ mice was attributed to preservation of neurogenesis pathways and reduced inflammatory cytokine production by hippocampal glial cells, including IL-1β, which they found in turn to stimulate IL-33 production by oligodendrocytes (Reverchon et al., 2017). IL-33 produced by oligodendrocytes could further induce IL-1β and inflammatory activity in glial cells, creating a pathological feedback contributing to cerebral malaria. Surprisingly, within the hippocampus, they found increased levels of CXCL9 and CXCL10 as well as IFN-γ, IL-6 and TNF-α, contrary to previous showing no difference in these chemokines in the whole brain (Reverchon et al., 2017). Additionally supporting a pathological role of IL-33 in malaria, a study utilizing a *Plasmodium chaubadi* model of infection on BALB/c mice showed that deficiency of ST2 reduced mortality, hepatocyte damage and inflammatory cytokine production (Seki et al., 2018). Further complicating the matter, another group found that IL-33 was not upregulated in the brain following PbA infection and that $IL\text{-}33^{-/-}$ showed a similar survival and parasitemia to wild-type mice; though IL-33 was found to be decreased in the liver and increased in both the lungs and spleen in wild-type mice after infection (Shibui et al., 2016).

Given the pleiotropic nature of IL-33, these findings when taken together could suggest that IL-33 activity on $ST2^+$ cells may contribute to the development of severe cerebral malaria, while IL-33 activity may induce a therapeutic effect outside of the IL-33/ST2 axis. Another school of thought is that cell-specific ST2 activity may play a contributory role in the pathogenesis of cerebral malaria in a differentially IL-33 dependent or IL-33 independent manner. Nonetheless, these ostensibly diametric findings demonstrate a gap in our understanding of the role of IL-33 in malarial infection, thus highlighting the need for more research to bolster our understanding of this complicated cytokine in the context of cerebral malaria. The effects of IL-33 in the context of cerebral malaria is summarized in **Figure 1**.

LEISHMANIA

Leishmaniasis is the second-largest neglected tropical disease and recent estimates by the CDC approximate that upwards of 1.2 million new cases will be diagnosed this year (https://www.cdc.gov/parasites/leishmaniasis/epi.html). Leishmaniasis is caused by more than 20 different species of protozoan parasite belonging to the genus *Leishmania* (http://www.who.int/leishmaniasis/en/). *Leishmania* is more prevalent in countries of tropical and subtropical regions, especially in areas of lower socioeconomic position. This disease is classified into three types based upon the type of parasite infection and disease outcome. The most common form is cutaneous leishmaniasis (CL), which causes painless localized skin lesions leading to severe tissue damage and disfigurement without treatment (Varikuti et al., 2017). CL is caused by *L. major*, *L. tropica* and *L. aethiopica* in the old world (Asia and Africa) and *L. mexicana* and *L. braziliensis* in the New World (Central and South America) (Oghumu et al., 2015). The most severe form of the disease is Visceral Leishmaniasis (VL) which is mainly caused by *L. donovani*, *L. chagasi* and *L. infantum* (McGwire and Satoskar, 2014). VL is characterized by the quick progression of parasites into the liver, spleen and bone marrow resulting in anemia, weight loss and hepatosplenomegaly and ultimately leading to the death of the host if left untreated (de Freitas et al., 2016).

The protective host immunity toward leishmaniasis primarily depends on the type of infection. Generation of an appropriate Th1 immune response, such as the production of IFN-γ and activation of phagocytic cells, is critical to host immunity against both CL and VL, as they lead to the production of reactive nitrogen species which directly cause the death of intracellular parasites (Oghumu et al., 2015; Terrazas et al., 2017; Varikuti et al., 2019). On the other hand, Th2 responses characterized by the production of IL-4 and IL-10 are known to exacerbate CL (Oghumu et al., 2010). In contrast to CL, the Th2-associated cytokines IL-4 and IL-13 are shown to play a protective role in VL by inducing the formation of

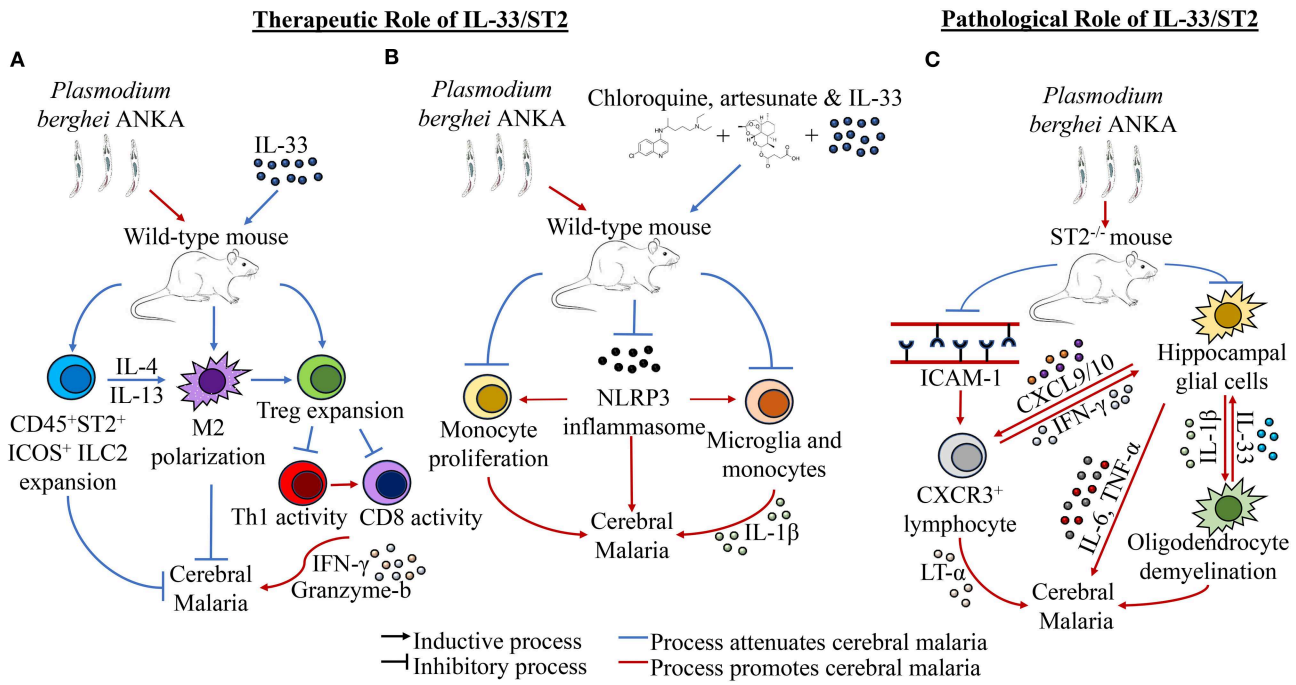

FIGURE 1 | Effects of IL-33 in the context of cerebral malaria. **(A)** IL-33 treatment in the context of *Plasmodium berghei* ANKA (PbA) has been shown to induce the expansion of CD45$^+$ ST2$^+$ICOS$^+$ ILC2s and Tregs, as well as induce M2 polarization. Specifically, ILC2s elicit M2 expansion, while M2s can promote Treg activity. Tregs themselves reduce cerebral malaria by downregulating the activity of Th1 and CD8$^+$ cells, which induce neurological inflammation and cerebral malaria through effectors such as IFN-γ and granzyme b. **(B)** IL-33 in concomitance with the antimalarial drugs artesunate and chloroquine has been shown to improve the outcome of PbA infection by reducing cerebral malaria. It has been observed specifically that addition of IL-33 to these therapies resulted in decreased NLRP3 inflammasome formation, monocyte expansion, and IL-1β production by monocytes and microglia. **(C)** ST2$^{-/-}$ mice have been shown to have reduced cerebral malarial cognitive function and improved survival in PbA infection. This reduction has been attributed to reductions in ICAM-1 expression and CXCR3$^+$ lymphocyte populations in the brain, which corresponded with lower LT-α levels in the brain, though other inflammatory cytokines expression has not been shown to be significantly affected. Separately, it has been shown that hippocampal glial cells are stimulated to produce IL-1β, which in turn stimulates oligodendrocytes to increase IL-33 expression. Upregulated IL-33 in turn induces more inflammatory activity in hippocampal glial cells, which creates a positive feedback loop that leads to hippocampal demyelination and increased inflammation, resulting in cerebral malaria morbidity and cognitive dysfunction. Additionally, increased levels of CXCL9 and CXCL10 found in the hippocampus could recruit Th1 cells to the site, further exacerbating cerebral malaria through inflammatory induction of microglia through IFN-γ.

mature hepatic granulomas and clearance of the parasites (Stäger et al., 2003; McFarlane et al., 2011). Since IL-33 is involved in the activation of Th2 cells, as well as Th1 and CD8$^+$ cells, a rationale exists for exploring its role in both VL and CL.

Recent studies have detected significantly elevated levels of IL-33 in the serum of both VL patients and mice infected with VL caused by *L. donovani*. In addition, higher proportions of IL-33$^+$ cells were also detected in liver biopsy specimens from VL patients who competed in the healthy tissues (Rostan et al., 2013). It has been also shown that ST2 deficient mice can control hepatic parasitic burdens and have reduced hepatomegaly and splenomegaly resulting in protection against experimental VL caused by *L. Infantum* (Khalid et al., 2017). Additionally, lack of ST2 also resulted in increased IFN-γ expression by both CD4$^+$ T and CD8$^+$ T cells suggesting depletion of ST2 possibly leads to a shift of immune responses toward Th1-polarization. A recent study has shown that increased levels of IL-33 were detected in malnourished human patients suffering from VL, suggesting that this may also impact Th1 immune responses and contribution of inflammation (Takele et al., 2016).

Our current understanding of the involvement of IL-33 and ST2 signaling in *Leishmania* infection suggest an upregulation of these signaling molecules results in deficient Th1 cellular immune responses. IL-33 activation of a Th2 cellular immune response would be detrimental in patients suffering from leishmaniasis, and inhibition of this signaling has been demonstrated to abrogate infection within the liver of VL. While it is presently understood that IL-33 is modulated during *Leishmania* infection, the research available is scarce and a great deal remains to be elucidated.

HELMINTHS

Helminth infections in humans are the result of infestation by a wide variety of nematodes, cestodes, trematodes and acanthocephalans (Mathison and Pritt, 2018), the most common of which are the soil-transmitted helminths *Ascaris lumbricoides*, *Trichuris trichuria*, *Necator americanus* and *Ancylostoma duodenale* as well as members of the genus *Schistosoma*, the causative agent of schistosomiasis. According to most recent estimates by the World Health Organization and other

epidemiological studies about 1.5 billion or 24% of the global population and another 207 million are infected with either soil-transmitted helminths or *Schistosoma,* respectively (Hajissa et al., 2018; Jourdan et al., 2018). With such widespread transmission any development in the treatment or prevention of helminth infection would have significant global impact, and a better understanding of the initial response of the host to helminth infection will guide research toward these critical developments.

While helminths are known to rarely infect ectopic niches in the human host, they are typically found harbored within the intestines. Expulsion of helminths from the host is understood to require a strong type-2 immune response utilizing host ILC2s, M2s, mast cells, eosinophils and ultimately $CD4^+$ Th2 cells (Grencis, 2015). Additionally, due to their location within the gut, helminths elicit a cytokine response from intestinal epithelial cells as well, including epithelial tuft cells which have been shown to respond to the presence of helminths by expanding and releasing the Th2 regulatory cytokine IL-25 (Gerbe et al., 2016). It is the end goal of the immune response to helminth parasites to induce goblet cell hyperplasia and increased mucin production which will result in the removal of the resident parasites (Marillier et al., 2008).

IL-33 is constitutively expressed by epithelial barrier cells, especially those lining the intestine, and is released upon cellular damage or death caused by helminth activity. Andronicos et al. demonstrated this showing increased IL-33 mRNA expression in epithelial cells using an *in vitro* human epithelial cell-helminth co-culture system (Andronicos et al., 2012). Once released, Il-33 is free to interact with its receptor, ST2, or to be cleaved into a more active, mature form, by local neutrophils or mast cells prior to interacting with its ligand (Lefrançais et al., 2012, 2014). ST2, originally found to be expressed exclusively by Th2 cells, has since been found to be expressed by a variety of other leukocytes including Tregs, ILC2s, M2s, mast cells, eosinophils, basophils and natural killer cells (Moritz et al., 1998; Xu et al., 1998; Brett Cherry et al., 2008; Smithgall et al., 2008; Suzukawa et al., 2008; Price et al., 2010; Schiering et al., 2014). As an alarmin, IL-33 proceeds to function to promote an early shift toward a type 2 immune response, protective in the context of helminth infection. Upon interaction with its ligands, especially those expressed by ILC2s and mast cells, activated cells respond by considerably enhancing production of type 2 cytokines IL-5 and IL-13 (Henry et al., 2017). While not its only target, IL-33 is known to interact especially well with those ILC2s (Gorbacheva and Mitkin, 2019). These cytokines are critical in the expulsion of intestinal helminths, as they cause the increased production of mucin in the intestine as well as induce goblet cell hyperplasia, inhibiting the ability of the worms to adhere to the gut lumen and allowing the host to rid themselves of the invading parasites (Hasnain et al., 2011).

Beginning with the damage of epithelial cells and their subsequent IL-33 release in response to helminth infection, cells of the host immune system respond in a type-2 manner which has been shown to be necessary in a number of recent human studies and animal models. A 2018 study using a *Hymenolepis diminuta* mouse model of helminth infection demonstrated that mast cell deficient mice required a longer time frame to completely expel infecting parasites (González et al., 2018). Parasites which remained and were unable to be expelled were also found to be larger in size than those removed from mice possessing mast cells. Furthermore, they found decreased expression of TSLP, IL-25 and IL-33 in mice lacking mast cells. Inhibition of mast cell function *in vivo* has also been linked to an overall reduction in IL-33, as well as IL-25 and TSLP both in the context of helminth infection as well as without (Hepworth et al., 2012). Utilizing mice deficient in IL-33, Yasuda et al. has further shown that IL-33 plays an important role in sufficient activation and recruitment of mast cells (Yasuda et al., 2012). Ultimately, mice with ineffective mast cells are unable to prime an effective type 2 immune response regulated by IL-33, IL-25 and TSLP in response to helminth infection and are unable to clear the parasites.

Eosinophils, largely associated with the response to helminth infection and allergies, have also been proven to possess strong anti-helminthic effects mediated by IL-33. In a model in which mice are pre-sensitized to an allergen, Gazzinelli-Guimaraes et al. show that subsequent infection with *Ascaris lumbricoides* presents with abrogated effect. This helminth preventive effect was associated with significantly increased IL-4, IL-13, and IL-33 in only those mice pre-sensitized with the allergen (Gazzinelli-Guimaraes et al., 2019). Detectable levels of eosinophil peroxidase as well as IL-5 and IL-13 are suggestive of the presence of an activated cohort of eosinophils in sensitized mice. Interestingly, eosinophil deficient ΔdblGATA mice lose the protective ability to thwart a helminth infestation post-sensitization, demonstrating the necessity of these innate immune cells in combatting helminth infection. Using IL-$33^{-/-}$ mice, Yasuda et al. demonstrated a critical role for IL-33 in eosinophil recruitment and associated goblet cell hyperplasia (Yasuda et al., 2012). Looking at mRNA transcripts for eosinophilic recruitment and activation cytokine IL-5, IL-13, and CCL11 in IL-$33^{-/-}$ mice they found significantly decreased quantities of each cytokine, suggesting a possible involvement of IL-33 in the production of these eosinophil associated cytokines.

Finally, it has been shown that, in association with enhanced eosinophilia, IL-33 is also required for the appropriate accumulation of helminth-protective ILC2s (Yasuda et al., 2012, 2018). Using mice deficient in IL-33 this group shows that without IL-33 ILC2s are unable to effectively accumulate, resulting in increased parasite burden associated with a decrease in mRNA transcripts for Th2 cytokines. Interestingly, it was also demonstrated that the innate immune system independent of adaptive immunity is sufficient to induce goblet cell hyperplasia, as RAG-$2^{-/-}$ mice deficient in T and B-cells still exhibit hyperplastic goblet cells when provided with exogenous IL-33 (Kondo et al., 2008). Taken together, these results paint a clear picture of the critical role the innate immune system plays in response to helminth infection that is, at least in part, mediated through IL-33 released at first contact by invading parasites.

While great attention is being paid to host innate immune cell specific mechanisms of subduing helminths, it is also being uncovered that helminths have evolved such that they possess a number of ways to modulate or evade the host immune system in an IL-33/ST2 dependent manner. The mouse pathogenic helminth *Heligmosomoides polygyrus* was recently found to

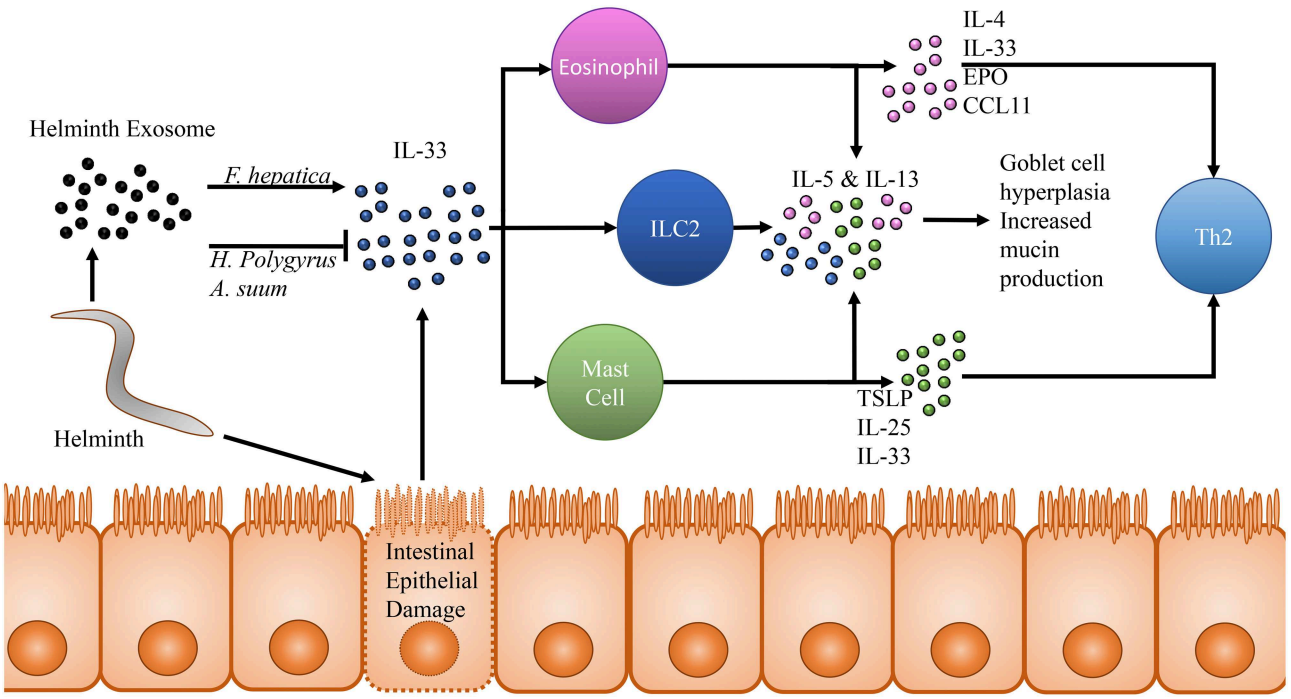

FIGURE 2 | Effects of IL-33 in the context of helminth infection. Movement and other activity by helminths within the intestinal lumen cause damage and lysis of intestinal epithelial cells. These epithelial cell in turn release pre-formed IL-33, which acts upon many cells of the innate immune system through its receptor ST2. Notably among these cells populations are eosinophils, type 2 innate lymphoid cells and mast cells. All three of these cell populations release IL-5 and IL-13 in response to IL-33 stimulation, resulting in goblet cell hyperplasia and increased mucin production. This effector response has been shown to be capable of clearing helminth infection even in RAG$^{-/-}$ mice who are incapable of generating a Th2 adaptive immune response. In addition to IL-5 and IL-13, studies focusing on eosinophils and IL-33 in response to helminth infection have also detected increased IL-4, IL-33, eosinophil peroxidase and CCL11 suggesting increased eosinophil accumulation and activity in response to IL-33 as well as a shift toward a Th2 immune response. Mast cells have been demonstrated to release thymic stromal lymphopoietin, IL-25 and IL-33 in response to IL-33 promoting a shift toward a protective Th2 immune response. In response to this defense, two species of helminth, *Heligmosomoides polygyrus* and *Ascaris suum* have been observed to release an exosome capable of inhibiting IL-33 in the host and dampening the subsequent helminth protective immune response. Interestingly, one helminth, *Fasciola hepatica*, possesses an exosome which has been observed to seemingly counter-intuitively upregulate IL-33 by the host, presenting just one example of the different physiological responses each helminth may induce and further expounding upon the importance of studying each helminth as an individual which cannot be easily generalized based on other helminth research.

secrete vesicles in the intestinal lumen of mice that are rich in inhibitory miRNAs homologous with mammalian exosome proteins (Buck et al., 2014). RT-qPCR analysis of mice treated with *H. polygyrus* derived exosomes found a downregulation in transcripts for *Il33r* coding for the ST2 protein. Interestingly, this same group previously showed that excretory products taken from *H. polygyrus* inhibits initial release of IL-33 *in vivo* with a subsequent inability for ILC2s and eosinophils to aggregate with an associated down regulation in IL-4, IL-5, and IL-13 (McSorley et al., 2014). Additionally, *H. polygyrus* vesicles have been demonstrated to be taken up by host macrophages, resulting in a downregulation of ST2, inhibiting their ability to function effectively as protective M2s (Coakley et al., 2017). Extracellular vesicles released by the porcine helminth *Ascaris suum* have also been identified as possessing numerous miRNA transcripts which likely target IL-13, IL-25 and IL-33 (Hansen et al., 2019). However, it is important to note that in the context of helminth infection, host-parasite interactions may vary widely dependent upon the specific helminth. Mice treated with *Fasciola hepatica* vesicles demonstrate an upregulation in IL-5 and IL-33 expression, highlighting the variety in immunomodulatory strategies of different helminths (Finlay et al., 2016). Despite mounting evidence of the importance IL-33 plays in clearance of helminth infection, there remains a great deal to be uncovered, as this species specificity necessitates work across the broad body of organisms that exist. The effects of IL-33 on helminth infection is summarized in **Figure 2**.

POTENTIAL IMMUNOTHERAPY

Parasitic diseases are responsible for an extensive morbidity and mortality burden across many countries and are caused by wildly different organisms ranging from unicellular protozoans to multicellular arthropods and worms (https://www.cdc.gov/parasites/about.html). There is currently no vaccine approved for human use for any parasitic disease, although the GlaxoSmithKline Biologicals' RTS,S vaccine against malaria has now successfully completed phase III clinical trials (https://www.cdc.gov/malaria/malaria_worldwide/reduction/vaccine.html). Lack of effective preventive measures,

TABLE 1 | Summary of the role of IL-33 in parasitic infections.

Parasite	Role of IL-33	References
Toxoplasma gondii	T1/ST2$^{-/-}$ BALB/c mice showed increased parasite burden in the brain	Jones et al., 2010
	Susceptible C57BL/6 mice showed increased IL-33 expression correlating with Th2 cytokines in an ocular model of toxoplasmosis	Tong and Lu, 2015; Zhang et al., 2019
	ST2 deficient C57BL/6 mice showed increased survivability in an oral model of toxoplasmosis	Ryffel et al., 2019
Plasmodium spp.	C57BL/6 mice show no difference in IL-33 expression 1.5 hours after *P. berghei* infection	Mac-Daniel et al., 2014
	Patients who died from *P. falciparum* infection showed significant IL-33 lung accumulation	Ampawong et al., 2015
	C57BL/6 mice in a *P. bergei* ANKA model demonstrated decreased IL-33 after dexamethasone treatment associated with decreased respiratory distress	dos Santos Ortolan et al., 2018
	IL-33 is significantly elevated in patients under 5 infected by *P. falciparum*	Ayimba et al., 2011
	IL-33 administration to C57/BL6 mice in a *P. berghei* ANKA model demonstrate attenuated cerebral malaria	Besnard et al., 2015
	IL-33 administration increased efficacy of anti-malarial drugs artesunate and chloroquine in a murine model of cerebral malaria	Strangward et al., 2018
	ST2 deficient mice infected with *P. berghei* show reduced cerebral malaria	Palomo et al., 2015
	Reduced inflammatory cytokine expression induced by ST2 deficiency is correlated with improved survival in *P. berghei* mice	Reverchon et al., 2017
	ST2 deficient BALB/c mice demonstrate reduced mortality and hepatocyte damage in a *P. chaubadi* model	Seki et al., 2018
	P. bergei infected IL33 deficient mice demonstrate survival and parasitemia similar to wild type mice	Shibui et al., 2016
Leishmania spp.	Increased IL-33 is detected in serum from *L. donovani* patients	Rostan et al., 2013; Takele et al., 2016
	ST2 deficient mice demonstrate an ability to control parasite burden and reduced hepatomegaly and splenomegaly in an *L. infantum* model	Khalid et al., 2017
Helminth Infection	Helminth activity causes an increase in IL-33 mRNA expression	Andronicos et al., 2012
	Hymenolupis diminuta infection of mice deficient in mast cells have reduced IL-33 associated with increased parasite burden	Hepworth et al., 2012; González et al., 2018
	Mice pre-sensitized to an allergen prior to *Ascaris lumbricoides* infection demonstrate singificantly enhanced IL-33 expression and decreased parasite burden	Gazzinelli-Guimaraes et al., 2019
	IL-33 deficient mice cannot effectively recruit eosinophils or induce goblet cell hyperplasia	Yasuda et al., 2012
	IL-33 deficient mice cannot effectively recruit ILC2 cells resulting in increased parasite burden	Yasuda et al., 2012, 2018
	Heligmosomoides polygyrus exosomes inhibit IL-33/ST2 and M2 differentiation	Buck et al., 2014; McSorley et al., 2014; Coakley et al., 2017
	Ascaris suum exosomes likely inhibit IL-33	Hansen et al., 2019
	Fasciola hepatica exosomes demonstrate an upregulation of IL-33	Finlay et al., 2016

combined with poor disease management practices, drug toxicity and a rise in parasitic resistance, have resulted in the high incidence and prevalence of parasitic infections seen in both developing and developed countries alike (Singh et al., 2019). For many years the scientific community has been working on developing novel strategies to prevent, contain and combat parasitic diseases. Investigating the early immune responses to parasitic infections could provide an insight on novel therapeutic targets and approaches (**Table 1**).

As one of the earliest responses to damage or infection, IL-33 finds itself within a unique niche in host immunity to parasitic infection, where it plays a role in priming and modulating the adaptive immune response. IL-33 has been shown to induce both Th1 or Th2 differentiation depending on the stimuli, and more recently, IL-33 is shown to also influence the behavior and physiology of Th17 and Tregs (Alvarez et al., 2019). Potentially having an impact on such a variety of T cells, this pleiotropic role makes IL-33 an interesting target for pharmaceutical immune-modulation. For example, IL-33 was shown to induce a protective Th2-polarized response during helminth diseases. Th2 cytokines such as IL-5 and IL-13 play a protective role in intestinal helminth infections by inhibiting the adhesion of these parasites to the intestinal lumen (Hasnain et al., 2011). IL-33 signaling was also required for controlling *toxoplasma* infection in the brain and preventing the development of encephalitis (Jones et al., 2010), while absence of IL-33 receptor/ST2 attenuated neutrophilic inflammation and ileitis in an oral model of toxoplasmosis (Ryffel et al., 2019). Additionally, IL-33 was shown to have pro-inflammatory properties during malaria, leading to an exacerbated pathology both in the respiratory and central nervous system (Yasuoka et al., 2011; Fairlie-Clarke et al., 2018). Because of its dual properties, IL-33 could serve as an immune-modulatory target for the early or prophylactic therapies against parasitic infections, where controlled intervention could possibly allow for a more dictated adaptive immune response by the physician.

Interestingly, one application of IL-33 immunomodulation currently being explored is that of helminth therapy: the intentional ingestion of helminth ova or their larvae to induce infection. While not presently widely administered,

there are several ongoing and recruiting clinical trials exploring such therapies (NCT02754609, NCT01940757, NCT03565939) with several more having been already completed. Each of these current studies possesses the common theme in that they are investigating how helminth infection is capable of suppressing inflammatory disorders. However, there is a wealth of information suggesting the possibility that helminth therapy could have success as an agent against allergies. A recent study has uncovered that patients infected with *Schistosoma mansoni* present with suppressed immune responses against dust mite allergen. This finding was further associated with increased IL-10, but an inverse correlation with IL-33 (Resende et al., 2018). While it is unrealistic to expect a patient to willingly harbor a helminthic infection to combat a chronic infection such as allergy, there are groups investigating the therapeutic potential of the helminth exosome. Already evidence is suggesting that certain helminth extracellular vesicles are capable of modulating the IL-33/ST2 signaling pathway, which has the capability of suppressing ILC2 accumulation and eosinophilia resulting in an abrogated allergic response (McSorley et al., 2014; Ball et al., 2018). Recent research has even uncovered a specific helminth exosome protein, HpARI, whose immunomodulatory role results in suppression of IL-33 (Osbourn et al., 2017). Moreover, there exists data suggesting that some of these parasite origin vesicles have the capacity to effectively function in potential vaccines (Coakley et al., 2017). Provided these protein isolates can be proven to be both safe and efficacious in human patients, helminth derived products may prove to be powerful immunotherapeutic agents. Already a body of evidence exists indicating that those helminth products which have been tested in human patients are likely to be both safe and effective, while generating a primarily Th2 immune response as would be anticipated (Williams et al., 2017; Capron et al., 2019). However, with such a wide variety of helminth species and exosomes to explore, it is imperative to keep in mind that not all helminths behave the same, and that while those helminths currently studied show promise, it is possible, and even likely, that better helminth therapy candidates exist that are yet to be explored (Sobotková et al., 2019).

Not only does IL-33 play a role in parasitic disease, but implications for IL-33 have also been found in the context of cancer. Previous studies have shown that this cytokine is released by fibroblasts, endothelial and epithelial cells in response to damage or cell death and can aid tumor growth by acting directly on the tumor cells to enhance proliferation and survival and by promoting angiogenesis in the tumor microenvironment. Blood vessel generation facilitates the infiltration of cancer exacerbating cells, including but not limited to, myeloid derived suppressor cells and M2s, upon which IL-33 is able to further exert effect (Afferni et al., 2018). On the other hand, IL-33 also stimulates infiltration of $CD8^+$ T cells as well as natural killer cells, crucial for tumor elimination (Gorbacheva and Mitkin, 2019). A better understanding of this differential recruitment of either pro- or anti-inflammatory immune cells in cancer models may help to explain the variable responses seen thus far in IL-33/ST2 malaria research. Additionally, recruitment of such varying immune cell populations is likely to play an important role in *Toxoplasma* infection and clearance, where a balance must be struck between pro-and anti-inflammatory responses to control infection. The net effect of IL-33 on cancer and its progression depends on the type of tumor and its microenvironment. In general, IL-33 as well as ST2 have been implicated in enhanced pathology and progression of colorectal, lung, breast and gastric cancer, as well as melanoma, head and neck squamous cell carcinoma and cholangiocarcinoma (Gorbacheva and Mitkin, 2019; Hong et al., 2019). In terms of hematological malignancies, the effects of IL-33 are controversial as a negative role has been identified for Chronic myelogenous leukemia (CML), while a positive role was shown for Acute myeloid leukemia (AML) (Allegra et al., 2019). A very recent paper by Yue et al. showed that IL-33 stimulates the recruitment of Tregs through the NF-kB/CCL2 pathway, thereby enhancing tumor growth and metastasis in esophageal squamous cell carcinoma (Yue et al., 2019). Another study showed that IL-33 serves a pivotal role in the functional stability of suppressive Tregs in the tumor microenvironment. IL-33 deficient Tregs show attenuated suppressive activity which led to augmented tumor regression (Hatzioannou et al., 2000). A similar positive correlation between IL-33 and Tregs has also been identified in head and neck squamous cell carcinoma, which is further associated with a poor prognosis. ST2 blockade was shown to abrogate the ability for IL-33 to promote Treg activity *in vitro*, however this function has yet to be clarified *in vivo* (Wen et al., 2019). This same ST2 blockade may present itself as an interesting avenue of exploration in the context of leishmaniasis treatment, where down regulation of the T regulatory response and an associated heightened inflammatory immune response has the potential to promote parasite clearance. The involvement of IL-33 in Treg regulation should be further explored in the context of cancer as well as parasitic diseases, as IL-33 immunotherapy is presenting itself as a potential therapeutic option.

Despite IL-33 being one of the earliest responders during infection involved in priming the host immune system toward a Th2 response, its involvement in many parasitic diseases is widely unexplored. A literature search will yield few results for the pathogens mentioned in this review and no results for other parasites notably including trypanosomas, amoebas, trichomonas or ectoparasites. Better understood, this largely unexplored cytokine and its signaling pathways could aid the development of new therapeutics against parasitic, and other conditions.

AUTHOR CONTRIBUTIONS

SO contributed to the conception and design of the study. NR, KA, GV, SV, MS, SS and SO wrote sections of the manuscript. All authors contributed to manuscript revision, read and approved the submitted version.

FUNDING

This research was supported by Award Number K01CA207599 from the National Cancer Institute (NIH/NCI), awarded to SO. The content is solely the responsibility of the authors and does not necessarily represent the official views of the National Institute of Health.

REFERENCES

Afferni, C., Buccione, C., Andreone, S., Galdiero, M. R., Varricchi, G., Marone, G., et al. (2018). The pleiotropic immunomodulatory functions of IL-33 and its implications in tumor immunity. *Front. Immunol.* 9:2601. doi: 10.3389/fimmu.2018.02601

Allegra, A., Innao, V., Tartarisco, G., Pioggia, G., Casciaro, M., Musolino, C., et al. (2019). The ST2/interleukin-33 axis in hematologic malignancies: the IL-33 paradox. *Int. J. Mol. Sci.* 20:5226. doi: 10.3390/ijms20205226

Alout, H., Roche, B., Dabire, R. K., and Cohuet, A. (2017). Consequences of insecticide resistance on malaria transmission. *PLoS Pathog* 13:e1006499. doi: 10.1371/journal.ppat.1006499

Alvarez, F., Fritz, J. H., and Piccirillo, C. A. (2019). Pleiotropic effects of IL-33 on $CD4^+$ T cell differentiation and effector functions. *Front. Immunol.* 10:522. doi: 10.3389/fimmu.2019.00522

Ampawong, S., Chaisri, U., Viriyavejakul, P., Prapansilp, P., Grau, G. E., Turner, G. D., et al. (2015). A potential role for interleukin-33 and γ-epithelium sodium channel in the pathogenesis of human malaria associated lung injury. *Malar. J.* 14:389. doi: 10.1186/s12936-015-0922-x

Andronicos, N. M., McNally, J., Kotze, A. C., Hunt, P. W., and Ingham, A. (2012). Trichostrongylus colubriformis larvae induce necrosis and release of IL33 from intestinal epithelial cells *in vitro*: implications for gastrointestinal nematode vaccine design. *Int. J. Parasitol.* 42, 295–304. doi: 10.1016/j.ijpara.2012.01.007

Armah, H., Dodoo, A. K., Wiredu, E. K., Stiles, J. K., Adjei, A. A., Gyasi, R. K., et al. (2005). High-level cerebellar expression of cytokines and adhesion molecules in fatal, paediatric, cerebral malaria. *Ann. Trop. Med. Parasitol.* 99, 629–647. doi: 10.1179/136485905X51508

Ayimba, E., Hegewald, J., Segbena, A. Y., Gantin, R. G., Lechner, C. J., Agosssou, A., et al. (2011). Proinflammatory and regulatory cytokines and chemokines in infants with uncomplicated and severe *Plasmodium falciparum* malaria. *Clin. Exp. Immunol.* 166, 218–226. doi: 10.1111/j.1365-2249.2011.04474.x

Ball, D. H., Al-Riyami, L., Harnett, W., and Harnett, M. M. (2018). IL-33/ST2 signalling and crosstalk with FcεRI and TLR4 is targeted by the parasitic worm product, ES-62. *Sci. Rep.* 8:4497. doi: 10.1038/s41598-018-22716-9

Bartemes, K. R., Iijima, K., Kobayashi, T., Kephart, G. M., McKenzie, A. N., and Kita, H. (2012). IL-33-responsive lineage- CD25+ CD44(hi) lymphoid cells mediate innate type 2 immunity and allergic inflammation in the lungs. *J. Immunol.* 188, 1503–1513. doi: 10.4049/jimmunol.1102832

Bartoloni, A., and Zammarchi, L. (2012). Clinical aspects of uncomplicated and severe malaria. *Mediterr. J. Hematol. Infect. Dis.* 4:e2012026. doi: 10.4084/mjhid.2012.026

Besnard, A. G., Guabiraba, R., Niedbala, W., Palomo, J., Reverchon, F., Shaw, T. N., et al. (2015). IL-33-mediated protection against experimental cerebral malaria is linked to induction of type 2 innate lymphoid cells, M2 macrophages and regulatory T cells. *PLoS Pathog.* 11:e1004607. doi: 10.1371/journal.ppat.1004607

Bonilla, W. V., Fröhlich, A., Senn, K., Kallert, S., Fernandez, M., Johnson, S., et al. (2012). The alarmin interleukin-33 drives protective antiviral CD8? T cell responses. *Science* 335, 984–989. doi: 10.1126/science.1215418

Buck, A. H., Coakley, G., Simbari, F., McSorley, H. J., Quintana, J. F., Le Bihan, T., et al. (2014). Exosomes secreted by nematode parasites transfer small RNAs to mammalian cells and modulate innate immunity. *Nat. commun.* 5, 5488–5488. doi: 10.1038/ncomms6488

Buckley, M. L., Williams, J. O., Chan, Y. H., Laubertová, L., Gallagher, H., Moss, J. W. E., et al. (2019). The interleukin-33-mediated inhibition of expression of two key genes implicated in atherosclerosis in human macrophages requires MAP kinase, phosphoinositide 3-kinase and nuclear factor-κB signaling pathways. *Sci. Rep.* 9:11317. doi: 10.1038/s41598-019-47620-8

Bushman, M., Morton, L., Duah, N., Quashie, N., Abuaku, B., Koram, K. A., et al. (2016). Within-host competition and drug resistance in the human malaria parasite *Plasmodium falciparum*. *Proc. Biol. Sci.* 283:20153038. doi: 10.1098/rspb.2015.3038

Byers, D. E., Alexander-Brett, J., Patel, A. C., Agapov, E., Dang-Vu, G., Jin, X., et al. (2013). Long-term IL-33-producing epithelial progenitor cells in chronic obstructive lung disease. *J. Clin. Invest.* 123, 3967–3982. doi: 10.1172/JCI65570

Cable, J., Barber, I., Boag, B., Ellison, A. R., Morgan, E. R., Murray, K., et al. (2017). Global change, parasite transmission and disease control: lessons from ecology. *Philos. Trans. R. Soc. Lond. B Biol. Sci.* 372:20160088. doi: 10.1098/rstb.2016.0088

Cao, K., Liao, X., Lu, J., Yao, S., Wu, F., Zhu, X., et al. (2018). IL-33/ST2 plays a critical role in endothelial cell activation and microglia-mediated neuroinflammation modulation. *J. Neuroinflammation* 15:136. doi: 10.1186/s12974-018-1169-6

Capron, M., Béghin, L., Leclercq, C., Labreuche, J., Dendooven, A., Standaert, A., et al. (2019). Safety of P28GST, a protein derived from a schistosome helminth parasite, in patients with crohn's disease: a pilot study (ACROHNEM). *J. Clin. Med.* 9:E41. doi: 10.3390/jcm9010041

Carriere, V., Roussel, L., Ortega, N., Lacorre, D. A., Americh, L., Aguilar, L., et al. (2007). IL-33, the IL-1-like cytokine ligand for ST2 receptor, is a chromatin-associated nuclear factor *in vivo*. *Proc. Natl. Acad. Sci. U.S.A.* 104, 282–287. doi: 10.1073/pnas.0606854104

Cayrol, C., and Girard, J. P. (2009). The IL-1-like cytokine IL-33 is inactivated after maturation by caspase-1. *Proc. Natl. Acad. Sci. U.S.A.* 106, 9021–9026. doi: 10.1073/pnas.0812690106

Chan, B. C. L., Lam, C. W. K., Tam, L. S., and Wong, C. K. (2019). IL33: roles in allergic inflammation and therapeutic perspectives. *Front. Immunol.* 10:364. doi: 10.3389/fimmu.2019.00364

Cherry, W. B., Yoon, J., Bartemes, K. R., Iijima, K., and Kita, H. (2008). A novel IL-1 family cytokine, IL-33, potently activates human eosinophils. *J. Allergy Clin. Immunol.* 121, 1484–1490. doi: 10.1016/j.jaci.2008.04.005

Choi, Y. S., Park, J. A., Kim, J., Rho, S. S., Park, H., Kim, Y. M., et al. (2012). Nuclear IL-33 is a transcriptional regulator of NF-κB p65 and induces endothelial cell activation. *Biochem. Biophys. Res. Commun.* 421, 305–311. doi: 10.1016/j.bbrc.2012.04.005

Coakley, G., McCaskill, J. L., Borger, J. G., Simbari, F., Robertson, E., Millar, M., et al. (2017). Extracellular vesicles from a helminth parasite suppress macrophage activation and constitute an effective vaccine for protective immunity. *Cell Rep.* 19, 1545–1557. doi: 10.1016/j.celrep.2017.05.001

de Freitas, E. O., Leoratti, F. M., Freire-de-Lima, C. G., Morrot, A., and Feijó, D. F. (2016). The contribution of immune evasive mechanisms to parasite persistence in visceral leishmaniasis. *Front. Immunol.* 7:153. doi: 10.3389/fimmu.2016.00153

Delgado Betancourt, E., Hamid, B., Fabian, B. T., Klotz, C., Hartmann, S., and Seeber, F. (2019). From entry to early dissemination-toxoplasma gondii's initial encounter with its host. *Front. Cell. Infect. Microbiol.* 9, 46–46. doi: 10.3389/fcimb.2019.00046

dos Santos Ortolan, L., Sercundes, M. K., Moura, G. C., de Castro Quirino, T., Debone, D., et al. (2018). Critical contribution of endothelial protein C receptor in experimental malaria-associated acute respiratory distress syndrome. *bioRxiv 348318*. doi: 10.1101/348318

Espinassous, Q., Garcia-de-Paco, E., Garcia-Verdugo, I., Synguelakis, M., von Aulock, S., Sallenave, J. M., et al. (2009). IL-33 enhances lipopolysaccharide-induced inflammatory cytokine production from mouse macrophages by regulating lipopolysaccharide receptor complex. *J. Immunol.* 183, 1446–1455. doi: 10.4049/jimmunol.0803067

Fairlie-Clarke, K., Barbour, M., Wilson, C., Hridi, S. U., Allan, D., and Jiang, H. R. (2018). Expression and function of IL-33/ST2 axis in the central nervous system under normal and diseased conditions. *Front. Immunol.* 9:2596. doi: 10.3389/fimmu.2018.02596

Finlay, C. M., Stefanska, A. M., Walsh, K. P., Kelly, P. J., Boon, L., Lavelle, E. C., et al. (2016). Helminth products protect against autoimmunity via innate type 2 cytokines IL-5 and IL-33, which promote eosinophilia. *J. Immunol.* 196, 703–714. doi: 10.4049/jimmunol.1501820

Garth, J. M., Reeder, K. M., Godwin, M. S., Mackel, J. J., Dunaway, C. W., Blackburn, J. P., et al. (2017). IL-33 signaling regulates innate IL-17A and IL-22 production via suppression of prostaglandin E. *J. Immunol.* 199, 2140–2148. doi: 10.4049/jimmunol.1602186

Gazzinelli-Guimaraes, P. H., de Queiroz Prado, R., Ricciardi, A., Bonne-Année, S., Sciurba, J., Karmele, E. P., et al. (2019). Allergen presensitization drives an eosinophil-dependent arrest in lung-specific helminth development. *J. Clin. Invest.* 130, 3686–3701. doi: 10.1172/JCI127963

Gerbe, F., Sidot, E., Smyth, D. J., Ohmoto, M., Matsumoto, I., Dardalhon, V., et al. (2016). Intestinal epithelial tuft cells initiate type 2 mucosal immunity to helminth parasites. *Nature* 529, 226–230. doi: 10.1038/nature16527

González, M. I., Lopes, F., McKay, D. M., and Reyes, J. L. (2018). Mast cell deficiency in mice results in biomass overgrowth and delayed expulsion of the rat tapeworm Hymenolepis diminuta. *Biosci. Rep.* 38:BSR20180687. doi: 10.1042/BSR20180687

Gorbacheva, A. M., and Mitkin, N. A. (2019). [Interleukin-33: Friend or Enemy in the Fight against Tumors?]. *Mol. Biol. (Mosk).* 53, 774–789. doi: 10.1134/S0026893319050066

Gowda, D. C., and Wu, X. (2018). Parasite recognition and signaling mechanisms in innate immune responses to malaria. *Front. Immunol.* 9:3006. doi: 10.3389/fimmu.2018.03006

Grencis, R. K. (2015). Immunity to helminths: resistance, regulation, and susceptibility to gastrointestinal nematodes. *Ann. Rev. Immunol.* 33, 201–225. doi: 10.1146/annurev-immunol-032713-120218

Griesenauer, B., and Paczesny, S. (2017). The ST2/IL-33 axis in immune cells during inflammatory diseases. *Front. Immunol.* 8:475. doi: 10.3389/fimmu.2017.00475

Hajissa, K., Muhajir, A. E. M. A., Eshag, H. A., Alfadel, A., Nahied, E., Dahab, R., et al. (2018). Prevalence of schistosomiasis and associated risk factors among school children in um-asher area, Khartoum, Sudan. *BMC Res. Notes* 11, 779–779. doi: 10.1186/s13104-018-3871-y

Han, L., Zhang, M., Liang, X., Jia, X., Jia, J., Zhao, M., et al. (2017). Interleukin-33 promotes inflammation-induced lymphangiogenesis via ST2/TRAF6-mediated Akt/eNOS/NO signalling pathway. *Sci. Rep.* 7:10602. doi: 10.1038/s41598-017-10894-x

Hansen, E. P., Fromm, B., Andersen, S. D., Marcilla, A., Andersen, K. L., Borup, A., et al. (2019). Exploration of extracellular vesicles from ascaris suum provides evidence of parasite-host cross talk. *J. Extracell. Vesicles* 8, 1578116–1578116. doi: 10.1080/20013078.2019.1578116

Hasnain, S. Z., Evans, C. M., Roy, M., Gallagher, A. L., Kindrachuk, K. N., Barron, L., et al. (2011). Muc5ac: a critical component mediating the rejection of enteric nematodes. *J. Exp. Med.* 208, 893–900. doi: 10.1084/jem.20102057

Hatzioannou, A., Banos, A., Sakelaropoulos, T., Fedonidis, C., Vidali, M. S., Köhne, M., et al. (2000). An intrinsic role of IL-33 in T. *Nat. Immunol.* 21, 75–85. doi: 10.1038/s41590-019-0555-2

Hay, S. I., Guerra, C. A., Tatem, A. J., Noor, A. M., and Snow, R. W. (2004). The global distribution and population at risk of malaria: past, present, and future. *Lancet Infect. Dis.* 4, 327–336. doi: 10.1016/S1473-3099(04)01043-6

Henry, E. K., Inclan-Rico, J. M., and Siracusa, M. C. (2017). Type 2 cytokine responses: regulating immunity to helminth parasites and allergic inflammation. *Curr. Pharmacol. Rep.* 3, 346–359. doi: 10.1007/s40495-017-0114-1

Hentschke, I., Graser, A., Melichar, V. O., Kiefer, A., Zimmermann, T., Kroß, B., et al. (2017). Corrigendum: IL-33/ST2 immune responses to respiratory bacteria in pediatric asthma. *Sci. Rep.* 7:46897. doi: 10.1038/srep46897

Hepworth, M. R., Daniłowicz-Luebert, E., Rausch, S., Metz, M., Klotz, C., Maurer, M., et al. (2012). Mast cells orchestrate type 2 immunity to helminths through regulation of tissue-derived cytokines. *Proc. Natl. Acad. Sci. U.S.A.* 109, 6644–6649. doi: 10.1073/pnas.1112268109

Hong, J., Kim, S., and Lin, P. C. (2019). Interleukin-33 and ST2 signaling in tumor microenvironment. *J. Interferon Cytokine Res.* 39, 61–71. doi: 10.1089/jir.2018.0044

Idro, R., Jenkins, N. E., and Newton, C. R. (2005). Pathogenesis, clinical features, and neurological outcome of cerebral malaria. *Lancet Neurol.* 4, 827–840. doi: 10.1016/S1474-4422(05)70247-7

Idro, R., Marsh, K., John, C. C., and Newton, C. R. (2010). Cerebral malaria: mechanisms of brain injury and strategies for improved neurocognitive outcome. *Pediatr. Res.* 68, 267–274. doi: 10.1203/PDR.0b013e3181eee738

Jones, L. A., Roberts, F., Nickdel, M. B., Brombacher, F., McKenzie, A. N. J., Henriquez, F. L., et al. (2010). IL-33 receptor (T1/ST2) signalling is necessary to prevent the development of encephalitis in mice infected with *Toxoplasma gondii*. *Eur. J. Immunol.* 40, 426–436. doi: 10.1002/eji.200939705

Joulia, R., L'Faqihi, F. E., Valitutti, S., and Espinosa, E. (2017). IL-33 fine tunes mast cell degranulation and chemokine production at the single-cell level. *J. Allergy Clin. Immunol. 140*, 497–509.e410. doi: 10.1016/j.jaci.2016.09.049

Jourdan, P. M., Lamberton, P. H. L., Fenwick, A., and Addiss, D. G. (2018). Soil-transmitted helminth infections. *Lancet* 391, 252–265. doi: 10.1016/S0140-6736(17)31930-X

Khalid, K. E., Nascimento, M. S. L., Sacramento, L. A., Costa, D. L., Lima-Júnior, D. S., Carregaro, V., et al. (2017). T1/ST2 deficient mice display protection against leishmania infantum experimental infection. *Acta Trop.* 172, 1–6. doi: 10.1016/j.actatropica.2017.04.011

Khan, I. A., Hwang, S., and Moretto, M. (2019). CD8 T cells cry for CD4 help. *Front. Cell Infect. Microbiol.* 9:136. doi: 10.3389/fcimb.2019.00136

Komai-Koma, M., Brombacher, F., Pushparaj, P. N., Arendse, B., McSharry, C., Alexander, J., et al. (2012). Interleukin-33 amplifies IgE synthesis and triggers mast cell degranulation via interleukin-4 in naïve mice. *Allergy* 67, 1118–1126. doi: 10.1111/j.1398-9995.2012.02859.x

Komai-Koma, M., Wang, E., Kurowska-Stolarska, M., Li, D., McSharry, C., and Xu, D. (2016). Interleukin-33 promoting Th1 lymphocyte differentiation dependents on IL-12. *Immunobiology* 221, 412–417. doi: 10.1016/j.imbio.2015.11.013

Kondo, Y., Yoshimoto, T., Yasuda, K., Futatsugi-Yumikura, S., Morimoto, M., Hayashi, N., et al. (2008). Administration of IL-33 induces airway hyperresponsiveness and goblet cell hyperplasia in the lungs in the absence of adaptive immune system. *Int. Immunol.* 20, 791–800. doi: 10.1093/intimm/dxn037

Lefrançais, E., Duval, A., Mirey, E., Roga, S., Espinosa, E., Cayrol, C., et al. (2014). Central domain of IL-33 is cleaved by mast cell proteases for potent activation of group-2 innate lymphoid cells. *Proc. Natl. Acad. Sci. U.S.A.* 111, 15502–15507. doi: 10.1073/pnas.1410700111

Lefrançais, E., Roga, S., Gautier, V., Gonzalez-de-Peredo, A., Monsarrat, B., Girard, J-P., et al. (2012). IL-33 is processed into mature bioactive forms by neutrophil elastase and cathepsin G. *Proc. Natl. Acad. Sci. U.S.A.* 109, 1673–1678. doi: 10.1073/pnas.1115884109

Li, C., Li, H., Jiang, Z., Zhang, T., Wang, Y., Li, Z., et al. (2014). Interleukin-33 increases antibacterial defense by activation of inducible nitric oxide synthase in skin. *PLoS Pathog.* 10:e1003918. doi: 10.1371/journal.ppat.1003918

Liew, F. Y., Pitman, N. I., and McInnes, I. B. (2010). Disease-associated functions of IL-33: the new kid in the IL-1 family. *Nat. Rev. Immunol.* 10, 103–110. doi: 10.1038/nri2692

Lima, T. S., and Lodoen, M. B. (2019). Mechanisms of human innate immune evasion by *Toxoplasma gondii*. *Front. Cell. Infect. Microbiol.* 9, 103–103. doi: 10.3389/fcimb.2019.00103

Liu, X., Xiao, Y., Pan, Y., Li, H., Zheng, S. G., and Su, W. (2019). The role of the IL-33/ST2 axis in autoimmune disorders: friend or foe? *Cytokine Growth Factor Rev.* 50, 60–74. doi: 10.1016/j.cytogfr.2019.04.004

Louten, J., Rankin, A. L., Li, Y., Murphy, E. E., Beaumont, M., Moon, C., et al. (2011). Endogenous IL-33 enhances Th2 cytokine production and T-cell responses during allergic airway inflammation. *Int. Immunol.* 23, 307–315. doi: 10.1093/intimm/dxr006

Luthi, A. U., Cullen, S. P., McNeela, E. A., Duriez, P. J., Afonina, I. S., Sheridan, C., et al. (2009). Suppression of interleukin-33 bioactivity through proteolysis by apoptotic caspases. *Immunity* 31, 84–98. doi: 10.1016/j.immuni.2009.05.007

Mac-Daniel, L., Buckwalter, M. R., Berthet, M., Virk, Y., Yui, K., Albert, M. L., et al. (2014). Local immune response to injection of plasmodium sporozoites into the skin. *J. Immunol.* 193, 1246–1257. doi: 10.4049/jimmunol.1302669

Maneerat, Y., Pongponratn, E., Viriyavejakul, P., Punpoowong, B., Looareesuwan, S., and Udomsangpetch, R. (1999). Cytokines associated with pathology in the brain tissue of fatal malaria. *Southeast Asian J. Trop. Med. Public Health* 30, 643–649.

Marillier, R. G., Michels, C., Smith, E. M., Fick, L. C., Leeto, M., Dewals, B., et al. (2008). IL-4/IL-13 independent goblet cell hyperplasia in experimental helminth infections. *BMC Immunol.* 9:11. doi: 10.1186/1471-2172-9-11

Mathison, B. A., and Pritt, B. S. (2018). A systematic overview of zoonotic helminth infections in North America. *Lab. Med.* 49, e61–e93. doi: 10.1093/labmed/lmy029

Matta, B. M., Lott, J. M., Mathews, L. R., Liu, Q., Rosborough, B. R., Blazar, B. R., et al. (2014). IL-33 is an unconventional alarmin that stimulates IL-2 secretion by dendritic cells to selectively expand IL-33R/ST2+ regulatory T cells. *J. Immunol.* 193, 4010–4020. doi: 10.4049/jimmunol.1400481

McFarlane, E., Carter, K. C., McKenzie, A. N., Kaye, P. M., Brombacher, F., and Alexander, J. (2011). Endogenous IL-13 plays a crucial role in liver granuloma maturation during *Leishmania donovani* infection, independent of IL-4Rα-responsive macrophages and neutrophils. *J. Infect. Dis.* 204, 36–43. doi: 10.1093/infdis/jir080

McGwire, B. S., and Satoskar, A. R. (2014). Leishmaniasis: clinical syndromes and treatment. *QJM* 107, 7–14. doi: 10.1093/qjmed/hct116

McSorley, H. J., Blair, N. F., Smith, K. A., McKenzie, A. N. J., and Maizels, R. M. (2014). Blockade of IL-33 release and suppression of type 2 innate lymphoid cell responses by helminth secreted products in airway allergy. *Mucosal Immunol.* 7, 1068–1078. doi: 10.1038/mi.2013.123

Miller, A. M., Asquith, D. L., Hueber, A. J., Anderson, L. A., Holmes, W. M., McKenzie, A. N., et al. (2010). Interleukin-33 induces protective effects in adipose tissue inflammation during obesity in mice. *Circ. Res.* 107, 650–658. doi: 10.1161/CIRCRESAHA.110.218867

Miller, L. H., Ackerman, H. C., Su, X. Z., and Wellems, T. E. (2013). Malaria biology and disease pathogenesis: insights for new treatments. *Nat. Med.* 19, 156–167. doi: 10.1038/nm.3073

Miller, L. H., Baruch, D. I., Marsh, K., and Doumbo, O. K. (2002). The pathogenic basis of malaria. *Nature* 415, 673–679. doi: 10.1038/415673a

Milner, D. A. Jr. (2018). Malaria pathogenesis. *Cold Spring Harb. Perspect. Med.* 8:a025569. doi: 10.1101/cshperspect.a025569

Molofsky, A. B., Savage, A. K., and Locksley, R. M. (2015). Interleukin-33 in tissue homeostasis, injury, and inflammation. *Immunity* 42, 1005–1019. doi: 10.1016/j.immuni.2015.06.006

Monticelli, L. A., Sonnenberg, G. F., Abt, M. C., Alenghat, T., Ziegler, C. G., Doering, T. A., et al. (2011). Innate lymphoid cells promote lung-tissue homeostasis after infection with influenza virus. *Nat. Immunol.* 12, 1045–1054. doi: 10.1038/ni.2131

Moritz, D. R., Rodewald, H-R., Gheyselinck, J., and Klemenz, R. (1998). The IL-1 receptor-related T1 antigen is expressed on immature and mature mast cells and on fetal blood mast cell progenitors. *J. Immunol.* 161:4866.

Moussion, C., Ortega, N., and Girard, J. P. (2008). The IL-1-like cytokine IL-33 is constitutively expressed in the nucleus of endothelial cells and epithelial cells *in vivo*: a novel 'alarmin'? *PLoS ONE* 3:e3331. doi: 10.1371/journal.pone.0003331

Oghumu, S., Lezama-Davila, C. M., Isaac-Marquez, A. P., and Satoskar, A. R. (2010). Role of chemokines in regulation of immunity against leishmaniasis. *Exp. Parasitol.* 126, 389–396. doi: 10.1016/j.exppara.2010.02.010

Oghumu, S., Stock, J. C., Varikuti, S., Dong, R., Terrazas, C., Edwards, J. A., et al. (2015). Transgenic expression of CXCR3 on T cells enhances susceptibility to cutaneous *Leishmania major* infection by inhibiting monocyte maturation and promoting a Th2 response. *Infect. Immun.* 83, 67–76. doi: 10.1128/IAI.02540-14

Osbourn, M., Soares, D. C., Vacca, F., Cohen, E. S., Scott, I. C., Gregory, W. F., et al. (2017). HpARI protein secreted by a helminth parasite suppresses interleukin-33. *Immunity 47*, 739–751.e735. doi: 10.1016/j.immuni.2017.09.015

Pais, T. F., and Penha-Goncalves, C. (2018). Brain endothelium: the "Innate immunity response hypothesis" in cerebral malaria pathogenesis. *Front. Immunol.* 9:3100. doi: 10.3389/fimmu.2018.03100

Palomo, J., Reverchon, F., Piotet, J., Besnard, A. G., Couturier-Maillard, A., Maillet, I., et al. (2015). Critical role of IL-33 receptor ST2 in experimental cerebral malaria development. *Eur. J. Immunol.* 45, 1354–1365. doi: 10.1002/eji.201445206

Park, S. J., Cho, H. R., and Kwon, B. (2016). Roles of IL-33 in resistance and tolerance to systemic candida albicans infections. *Immune Netw.* 16, 159–164. doi: 10.4110/in.2016.16.3.159

Paul, W. E., and Zhu, J. (2010). How are TH2-type immune responses initiated and amplified? *Nat. Rev. Immunol.* 10, 225–235. doi: 10.1038/nri2735

Pichery, M., Mirey, E., Mercier, P., Lefrancais, E., Dujardin, A., Ortega, N., et al. (2012). Endogenous IL-33 is highly expressed in mouse epithelial barrier tissues, lymphoid organs, brain, embryos, and inflamed tissues: *in situ* analysis using a novel Il-33-LacZ gene trap reporter strain. *J. Immunol.* 188, 3488–3495. doi: 10.4049/jimmunol.1101977

Pinto, S. M., Subbannayya, Y., Rex, D. A. B., Raju, R., Chatterjee, O., Advani, J., et al. (2018). A network map of IL-33 signaling pathway. *J. Cell Commun. Signal* 12, 615–624. doi: 10.1007/s12079-018-0464-4

Price, A. E., Liang, H-E., Sullivan, B. M., Reinhardt, R. L., Eisley, C. J., Erle, D. J., et al. (2010). Systemically dispersed innate IL-13-expressing cells in type 2 immunity. *Proc. Natl. Acad. Sci. U.S.A.* 107, 11489–11494. doi: 10.1073/pnas.1003988107

Pusceddu, I., Dieplinger, B., and Mueller, T. (2019). ST2 and the ST2/IL-33 signalling pathway–biochemistry and pathophysiology in animal models and humans. *Clin. Chim. Acta* 495, 493–500. doi: 10.1016/j.cca.2019.05.023

Resende, S. D., Magalhães, F. C., Rodrigues-Oliveira, J. L., Castro, V. N., Souza, C. S. A., Oliveira, E. J., et al. (2018). Modulation of allergic reactivity in humans is dependent on. *Front. Immunol.* 9:3158. doi: 10.3389/fimmu.2018.03158

Reverchon, F., Mortaud, S., Sivoyon, M., Maillet, I., Laugeray, A., Palomo, J., et al. (2017). IL-33 receptor ST2 regulates the cognitive impairments associated with experimental cerebral malaria. *PLoS Pathog.* 13:e1006322. doi: 10.1371/journal.ppat.1006322

Riedel, J. H., Becker, M., Kopp, K., Duster, M., Brix, S. R., Meyer-Schwesinger, C., et al. (2017). IL-33-mediated expansion of type 2 innate lymphoid cells protects from progressive glomerulosclerosis. *J. Am. Soc. Nephrol.* 28, 2068–2080. doi: 10.1681/ASN.2016080877

Rostan, O., Gangneux, J. P., Piquet-Pellorce, C., Manuel, C., McKenzie, A. N., Guiguen, C., et al. (2013). The IL-33/ST2 axis is associated with human visceral leishmaniasis and suppresses Th1 responses in the livers of BALB/c mice infected with *Leishmania donovani*. *mBio* 4, e00383–e00313. doi: 10.1128/mBio.00383-13

Ryffel, B., Huang, F., Robinet, P., Panek, C., Couillin, I., Erard, F., et al. (2019). Blockade of IL-33R/ST2 signaling attenuates *Toxoplasma gondii* ileitis depending on IL-22 expression. *Front. Immunol.* 10, 702–702. doi: 10.3389/fimmu.2019.00702

Salimi, M., Barlow, J. L., Saunders, S. P., Xue, L., Gutowska-Owsiak, D., Wang, X., et al. (2013). A role for IL-25 and IL-33-driven type-2 innate lymphoid cells in atopic dermatitis. *J. Exp. Med.* 210, 2939–2950. doi: 10.1084/jem.20130351

Schiering, C., Krausgruber, T., Chomka, A., Fröhlich, A., Adelmann, K., Wohlfert, E. A., et al. (2014). The alarmin IL-33 promotes regulatory T-cell function in the intestine. *Nature* 513, 564–568. doi: 10.1038/nature13577

Schmitz, J., Owyang, A., Oldham, E., Song, Y., Murphy, E., McClanahan, T. K., et al. (2005). IL-33, an interleukin-1-like cytokine that signals via the IL-1 receptor-related protein ST2 and induces T helper type 2-associated cytokines. *Immunity* 23, 479–490. doi: 10.1016/j.immuni.2005.09.015

Seki, T., Obata-Ninomiya, K., Shimogawara-Furushima, R., Arai, T., Akao, N., Hoshino, T., et al. (2018). IL-33/ST2 contributes to severe symptoms in plasmodium chabaudi-infected BALB/c mice. *Parasitol. Int.* 67, 64–69. doi: 10.1016/j.parint.2017.03.008

Shibui, A., Takamori, A., Tolba, M. E. M., Nambu, A., Shimura, E., Yamaguchi, S., et al. (2016). IL-25, IL-33 and TSLP receptor are not critical for development of experimental murine malaria. *Biochem. Biophys. Rep.* 5, 191–195. doi: 10.1016/j.bbrep.2015.12.007

Short, E. E., Caminade, C., and Thomas, B. N. (2017). Climate change contribution to the emergence or re-emergence of parasitic diseases. *Infect. Dis. (Auckl).* 10:1178633617732296. doi: 10.1177/1178633617732296

Sibley, C. H., and Hunt, S. Y. (2003). Drug resistance in parasites: can we stay ahead of the evolutionary curve? *Trends Parasitol.* 19, 532–537. doi: 10.1016/j.pt.2003.09.009

Singh, B., Varikuti, S., Halsey, G., Volpedo, G., Hamza, O. M., and Satoskar, A. R. (2019). Host-directed therapies for parasitic diseases. *Future Med. Chem.* 11, 1999–2018. doi: 10.4155/fmc-2018-0439

Sjoberg, L. C., Nilsson, A. Z., Lei, Y., Gregory, J. A., Adner, M., and Nilsson, G. P. (2017). Interleukin 33 exacerbates antigen driven airway hyperresponsiveness, inflammation and remodeling in a mouse model of asthma. *Sci. Rep.* 7:4219. doi: 10.1038/s41598-017-03674-0

Smithgall, M. D., Comeau, M. R., Park Yoon, B-R., Kaufman, D., Armitage, R., and Smith, D. E. (2008). IL-33 amplifies both Th1- and Th2-type responses through its activity on human basophils, allergen-reactive Th2 cells, iNKT and NK Cells. *Int. Immunol.* 20, 1019–1030. doi: 10.1093/intimm/dxn060

Sobotková, K., Parker, W., Levá, J., RuŽková, J., Lukeš, J., and Jirku Pomajbíková, K. (2019). Helminth therapy - from the parasite perspective. *Trends Parasitol.* 35, 501–515. doi: 10.1016/j.pt.2019.04.009

Song, L., Pei, L., Yao, S., Wu, Y., and Shang, Y. (2017). NLRP3 inflammasome in neurological diseases, from functions to therapies. *Front. Cell Neurosci.* 11:63. doi: 10.3389/fncel.2017.00063

Stäger, S., Alexander, J., Carter, K. C., Brombacher, F., and Kaye, P. M. (2003). Both interleukin-4 (IL-4) and IL-4 receptor α signaling contribute to the development of hepatic granulomas with optimal antileishmanial activity. *Infect. Immun.* 71, 4804–4807. doi: 10.1128/IAI.71.8.4804-4807.2003

Staurengo-Ferrari, L., Trevelin, S. C., Fattori, V., Nascimento, D. C., de Lima, K. A., Pelayo, J. S., et al. (2018). Interleukin-33 receptor (ST2) deficiency improves

the outcome of *Staphylococcus aureus*-induced septic arthritis. *Front. Immunol.* 9:962. doi: 10.3389/fimmu.2018.00962

Stier, M. T., Mitra, R., Nyhoff, L. E., Goleniewska, K., Zhang, J., Puccetti, M. V., et al. (2019). IL-33 is a cell-intrinsic regulator of fitness during early B cell development. *J. Immunol.* 203, 1457–1467. doi: 10.4049/jimmunol.1900408

Strangward, P., Haley, M. J., Albornoz, M. G., Barrington, J., Shaw, T., Dookie, R., et al. (2018). Targeting the IL33-NLRP3 axis improves therapy for experimental cerebral malaria. *Proc Natl Acad Sci U.S.A.* 115, 7404–7409. doi: 10.1073/pnas.1801737115

Suzukawa, M., Iikura, M., Koketsu, R., Nagase, H., Tamura, C., Komiya, A., et al. (2008). An IL-1 cytokine member, IL-33, induces human basophil activation via its ST2 receptor. *J. Immunol.* 181, 5981–5989. doi: 10.4049/jimmunol.181.9.5981

Takele, Y., Adem, E., Getahun, M., Tajebe, F., Kiflie, A., Hailu, A., et al. (2016). Malnutrition in healthy individuals results in increased mixed cytokine profiles, altered neutrophil subsets and function. *PLoS ONE* 11:e0157919. doi: 10.1371/journal.pone.0157919

Terrazas, C., Varikuti, S., Oghumu, S., Steinkamp, H. M., Ardic, N., Kimble, J., et al. (2017). Ly6C^{hi} inflammatory monocytes promote susceptibility to *Leishmania donovani* infection. *Sci. Rep.* 7:14693. doi: 10.1038/s41598-017-14935-3

Tjota, M. Y., Williams, J. W., Lu, T., Clay, B. S., Byrd, T., Hrusch, C. L., et al. (2013). IL-33-dependent induction of allergic lung inflammation by FcgammaRIII signaling. *J. Clin. Invest.* 123, 2287–2297. doi: 10.1172/JCI63802

Tonacci, A., Quattrocchi, P., and Gangemi, S. (2019). IL33/ST2 axis in diabetic kidney disease: a literature review. *Medicina (Kaunas)* 55:E50. doi: 10.3390/medicina55020050

Tong, X., and Lu, F. (2015). IL-33/ST2 involves the immunopathology of ocular toxoplasmosis in murine model. *Parasitol. Res.* 114, 1897–1905. doi: 10.1007/s00436-015-4377-3

Torgerson, P. R., Devleesschauwer, B., Praet, N., Speybroeck, N., Willingham, A. L., Kasuga, F., et al. (2015). World Health Organization estimates of the global and regional disease burden of 11 foodborne parasitic diseases, 2010: a data synthesis. *PLoS Med.* 12:e1001920. doi: 10.1371/journal.pmed.1001920

Travers, J., Rochman, M., Miracle, C. E., Habel, J. E., Brusilovsky, M., Caldwell, J. M., et al. (2018). Chromatin regulates IL-33 release and extracellular cytokine activity. *Nat. Commun.* 9:3244. doi: 10.1038/s41467-018-05485-x

Vanaerschot, M., Huijben, S., Van den Broeck, F., and Dujardin, J. C. (2014). Drug resistance in vectorborne parasites: multiple actors and scenarios for an evolutionary arms race. *FEMS Microbiol. Rev.* 38, 41–55. doi: 10.1111/1574-6976.12032

Varikuti, S., Jha, B. K., Volpedo, G., Ryan, N. M., Halsey, G., Hamza, O. M., et al. (2018). Host-directed drug therapies for neglected tropical diseases caused by protozoan parasites. *Front. Microbiol.* 9:2655. doi: 10.3389/fmicb.2018.02655

Varikuti, S., Oghumu, S., Saljoughian, N., Pioso, M. S., Sedmak, B. E., Khamesipour, A., et al. (2017). Topical treatment with nanoliposomal Amphotericin B reduces early lesion growth but fails to induce cure in an experimental model of cutaneous leishmaniasis caused by *Leishmania mexicana*. *Acta Trop.* 173, 102–108. doi: 10.1016/j.actatropica.2017.06.004

Varikuti, S., Volpedo, G., Saljoughian, N., Hamza, O. M., Halsey, G., Ryan, N. M., et al. (2019). The potent ITK/BTK inhibitor ibrutinib is effective for the treatment of experimental visceral leishmaniasis caused by *Leishmania donovani*. *J. Infect. Dis.* 219, 599–608. doi: 10.1093/infdis/jiy552

Wen, Y. H., Lin, H. Q., Li, H., Zhao, Y., Lui, V. W. Y., Chen, L., et al. (2019). Stromal interleukin-33 promotes regulatory T cell-mediated immunosuppression in head and neck squamous cell carcinoma and correlates with poor prognosis. *Cancer Immunol. Immunother.* 68, 221–232. doi: 10.1007/s00262-018-2265-2

WHO (2019). *World Malaria Report 2019*. Geneva: World Health Organization.

Wilainam, P., Nintasen, R., and Viriyavejakul, P. (2015). Mast cell activation in the skin of *Plasmodium falciparum* malaria patients. *Malar. J.* 14:67. doi: 10.1186/s12936-015-0568-8

Williams, A. R., Dige, A., Rasmussen, T. K., Hvas, C. L., Dahlerup, J. F., Iversen, L., et al. (2017). Immune responses and parasitological observations induced during probiotic treatment with medicinal Trichuris suis ova in a healthy volunteer. *Immunol. Lett.* 188, 32–37. doi: 10.1016/j.imlet.2017.06.002

Xiao, P., Wan, X., Cui, B., Liu, Y., Qiu, C., Rong, J., et al. (2016). Interleukin 33 in tumor microenvironment is crucial for the accumulation and function of myeloid-derived suppressor cells. *Oncoimmunology* 5:e1063772. doi: 10.1080/2162402X.2015.1063772

Xu, D., Chan, W. L., Leung, B. P., Huang, F., p., Wheeler, R., et al. (1998). Selective expression of a stable cell surface molecule on type 2 but not type 1 helper T cells. *J. Exp. Med.* 187, 787–794. doi: 10.1084/jem.187.5.787

Yasuda, K., Adachi, T., Koida, A., and Nakanishi, K. (2018). Nematode-infected mice acquire resistance to subsequent infection with unrelated nematode by inducing highly responsive group 2 innate lymphoid cells in the lung. *Front. Immunol.* 9:2132. doi: 10.3389/fimmu.2018.02132

Yasuda, K., Muto, T., Kawagoe, T., Matsumoto, M., Sasaki, Y., Matsushita, K., et al. (2012). Contribution of IL-33-activated type II innate lymphoid cells to pulmonary eosinophilia in intestinal nematode-infected mice. *Proc Natl Acad Sci U.S.A.* 109, 3451–3456. doi: 10.1073/pnas.1201042109

Yasuoka, S., Kawanokuchi, J., Parajuli, B., Jin, S., Doi, Y., Noda, M., et al. (2011). Production and functions of IL-33 in the central nervous system. *Brain Res.* 1385, 8–17. doi: 10.1016/j.brainres.2011.02.045

Yue, Y., Lian, J., Wang, T., Luo, C., Yuan, Y., Qin, G., et al. (2019). IL-33- nuclear factor -kB-CCL2 signaling pathway promotes the progression of esophageal squamous cell carcinoma by directing regulatory T cells. *Cancer Sci.* 111, 795–806. doi: 10.1111/cas.14293

Zhang, Y., He, J., Zheng, H., Huang, S., and Lu, F. (2019). Association of TREM-1, IL-1β, IL-33/ST2, and TLR expressions with the pathogenesis of ocular toxoplasmosis in mouse models on different genetic backgrounds. *Front. Microbiol.* 10:2264. doi: 10.3389/fmicb.2019.02264

Zhiguang, X., Wei, C., Steven, R., Wei, D., Wei, Z., Rong, M., et al. (2010). Over-expression of IL-33 leads to spontaneous pulmonary inflammation in mIL-33 transgenic mice. *Immunol. Lett.* 131, 159–165. doi: 10.1016/j.imlet.2010.04.005

Conflict of Interest: The authors declare that the research was conducted in the absence of any commercial or financial relationships that could be construed as a potential conflict of interest.

frontiers in Cellular and Infection Microbiology

BRIEF RESEARCH REPORT
published: 19 May 2020
doi: 10.3389/fcimb.2020.00207

Dynamics of *Toxoplasma gondii* Oocyst Phagocytosis by Macrophages

Omar Ndao[1,2†], *Pierre-Henri Puech*[3,4,5], *Camille Bérard*[1,2‡], *Laurent Limozin*[3,4,5], *Sameh Rabhi*[1,2], *Nadine Azas*[1,2], *Jitender P. Dubey*[6] *and Aurélien Dumètre*[1,2*]

[1] Aix Marseille Univ, IRD, AP-HM, SSA, VITROME, Marseille, France, [2] IHU-Méditerranée Infection, Marseille, France, [3] Aix Marseille Univ, LAI UM 61, Marseille, France, [4] Inserm, UMR_S 1067, Marseille, France, [5] CNRS, UMR 7333, Marseille, France, [6] Animal Parasitic Diseases Laboratory, Beltsville Agricultural Research Center, United States Department of Agriculture, Agricultural Research Service, Beltsville, MD, United States

OPEN ACCESS

Edited by:
Juliana Perrone Bezerra De Menezes, Gonçalo Moniz Institute (IGM), Brazil

Reviewed by:
Simon Andrew Johnston, University of Sheffield, United Kingdom
Marcia Attias, Federal University of Rio de Janeiro, Brazil
Erica dos Santos Martins Duarte, Federal University of Minas Gerais, Brazil

***Correspondence:**
Aurélien Dumètre
aurelien.dumetre@univ-amu.fr

†Present address:
Omar Ndao, Institut de Biologie Intégrative de la Cellule (i2BC), Gif-sur-Yvette, France

‡Deceased 01/14/2017

Specialty section:
This article was submitted to Microbes and Innate Immunity, a section of the journal Frontiers in Cellular and Infection Microbiology

Received: 11 January 2020
Accepted: 16 April 2020
Published: 19 May 2020

Citation:
Ndao O, Puech P-H, Bérard C, Limozin L, Rabhi S, Azas N, Dubey JP and Dumètre A (2020) Dynamics of Toxoplasma gondii Oocyst Phagocytosis by Macrophages. Front. Cell. Infect. Microbiol. 10:207. doi: 10.3389/fcimb.2020.00207

Oocysts are the environmentally resistant stage of the protozoan parasite *Toxoplasma gondii*. They are responsible for foodborne infections in humans and animals worldwide. Infectious oocysts contain sporozoites that have to exit the sporocyst and oocyst walls to initiate replication of the parasite within the host tissues. Given their robustness and resistance to chemical degradation, it is still unclear how the oocyst and sporocyst walls release the sporozoites. This process called excystation is thought to occur in the small intestine as a result of the combined action of digestive agents, yet to be identified. By using an oocyst-macrophage co-culture platform, we previously demonstrated *in vitro* that the excystation of sporozoites and their differentiation into replicative tachyzoites could occur in absence of digestive factors, following phagocytosis by macrophages. Here, we further characterize the dynamics of the oocyst phagocytosis at the single-cell level by using optical tweezers and micropipette aspiration techniques. Our results show that the oocyst internalization kinetics can vary among a given population of macrophages, but similar processes and dynamics could be observed. Most of the cells manipulate oocysts for ∼15 min before internalizing them in typically 30 min. This process mainly involves the actin cytoskeleton of the macrophages. Liberated sporozoites within macrophages then differentiate into tachyzoites within 4–6 h following oocyst-macrophage contact. Tachyzoites appear to develop better in macrophages challenged with free sporocysts or sporozoites than with whole oocysts, suggesting that opening of the oocyst wall is one of the most limiting steps for sporozoite excystation completion.

Keywords: *Toxoplasma gondii*, oocysts, sporozoites, excystation, macrophages, phagocytosis, optical tweezers, micropipette aspiration techniques

INTRODUCTION

The apicomplexan parasite *Toxoplasma gondii* can persist throughout the environment as a robust infectious stage called the oocyst (Shapiro et al., 2019). Oocysts are excreted in cat feces and become infectious following a 1–2 week sporulation process. Sporulated oocysts measure ∼13 × 11 μm and contain two sporocysts, each with four potential infective sporozoites that are protected from harsh environmental conditions by the sporocyst and oocyst walls (Freppel et al., 2019). Oocysts can infect many avian and mammal species worldwide, including humans, through the

consumption of water or raw vegetables and fruits contaminated with cat feces (Shapiro et al., 2019). Following ingestion, sporozoites excyst from the sporocyst and oocyst walls, invade host enterocytes, and lamina propria macrophages and dendritic cells prior to differentiation into tachyzoites (Delgado Betancourt et al., 2019). Tachyzoites can replicate within these phagocytic cells, and use them as Trojan horses to disseminate throughout the body (Drewry et al., 2019). Infection results in the development and persistence of the parasite as tissue cysts, mainly in the brain and muscles. In turn, tissue cysts in undercooked meat can be a source of human contamination. Irrespective of the ingested stage, most infections are asymptomatic except in congenitally infected children and immunocompromised people, who may suffer severe ocular, cerebral, or multivisceral complications (Robert-Gangneux and Dardé, 2012).

The *T. gondii* oocyst and sporocyst walls are bilayered structures, mainly composed of proteins (Freppel et al., 2019). The outer oocyst wall layer contains cysteine- and tyrosine-rich proteins that form extensive disulphide bridges and dityrosine cross-links, respectively, and triglycerides that are similar to mycobacterial mycolic acids. The inner oocyst wall layer consists of cross-linked Tyr-rich proteins and scaffolds of beta-1,3-glucan. The outer sporocyst wall layer is similar to the outer oocyst wall layer in structure while its inner layer is made of four curved plates held together by thick sutures. The sporocyst wall resembles the oocyst wall in molecular composition, except that it lacks cysteine-rich proteins and beta-1,3-glucan. Both walls are naturally blue fluorescent under UV excitation, presumably due to their dityrosine cross-links. Due to their structure and molecular composition, the oocyst and sporocyst walls appear very resistant to mechanical constraints and enzymatic digestion, and almost impermeable to water-soluble substances including common chlorinated disinfectants (Dumètre et al., 2013).

Given their robustness and resistance to chemical degradation, it is still unclear how the oocyst walls open to allow the sporozoites to invade the host cells. Ingested oocysts release their sporozoites in the small intestine, however the digestive agents that trigger the opening of the oocyst walls are not identified. Interestingly, oocysts can cause parenteral infections, at least in laboratory mice, suggesting a possible excystation of sporozoites in absence of digestive factors (Dubey and Frenkel, 1973). From these observations, we developed *in vitro* oocyst-macrophage co-cultures to investigate whether phagocytic cells could mediate sporozoite excystation following oocyst phagocytosis (Freppel et al., 2016). Previous *in vitro* experiments showed that naïve RAW 264.7 macrophagic cells could ingest oocysts, open their walls in or near acidic compartments, and host the differentiation of the sporozoites into replicative tachyzoites. In the present study, we extend the use of this oocyst-macrophage co-culture platform to further characterize the dynamics of the oocyst internalization at the single-cell level and the fate of the sporozoites within macrophages. We used optical tweezers and micropipettes to present oocysts to living macrophages, either adherent or not, at different incubation temperatures. Our results show that most of cells manipulate oocysts for ∼15 min before internalizing them in ∼30 min, by remodeling their actin cytoskeleton. Liberated sporozoites within macrophages then differentiate into tachyzoites within 4–6 h following oocyst-macrophage contact. Tachyzoites appear to develop better in macrophages challenged with free sporocysts or sporozoites than with whole oocysts suggesting that opening of the oocyst wall is one of the most limiting steps for sporozoite excystation completion in macrophages.

MATERIALS AND METHODS

Macrophage Cell Culture Conditions

Mouse macrophage-like cell line RAW 264.7 was purchased from European Collection of Authenticated Cell Cultures (ECACC, Salisbury, United-Kingdom). Cells were cultured at 37°C and 5% CO_2 in plastic 75-cm^2 flasks containing RPMI 1640 medium (Life Technologies, Saint-Aubin, France) supplemented with 2 mM L-glutamine, 100 U/ml penicillin, 100 µg/ml streptomycin (Life Technologies), and 10% heat-inactivated fetal bovine serum (FBS) (Life Technologies). Cells reaching ∼80% confluency were detached with a cell scraper and subcultured following a 10-fold dilution in fresh culture medium. Before parasite internalization assays, cells were detached as described, centrifuged at 400 g for 10 min, counted on Kova® slides and their concentration was adjusted in fresh culture medium.

Oocyst Production and Purification

Oocysts of the reference genotypes II Me49 or III VEG strains of *T. gondii* were used throughout this study and were manipulated in biosafety level 2 facilities. Available bioinformatics data indicate that oocysts of both genotypes have very similar predicted transcriptome and proteome (http://toxodb.org/toxo/). Oocysts were harvested from feces of cats 3–10 days after feeding infected mouse tissues to *T. gondii* free cats as described previously (Dumètre et al., 2013). This procedure was carried out in accordance with relevant guidelines and regulations following a protocol approved by the Institutional Animal Care and Use Committee, United States Department of Agriculture, Beltsville, MD, USA. Oocysts were collected by flotation at 4°C from cat feces on a 1.15 density sucrose solution, washed in distilled water and then resuspended in an aqueous solution containing 2% H_2SO_4. Oocysts were allowed to sporulate at room temperature (RT, 20–22°C) for 5 days under adequate aeration and gentle continuous shaking. For real-time internalization assays by using optical tweezers and micropipette aspiration, oocysts were further purified on a cesium chloride gradient to remove most of fecal debris (Dumètre and Dardé, 2004). Oocysts were stored in a 2% H_2SO_4 aqueous solution at 4°C until used. Prior experiments, oocysts were washed three times in sterile distilled water at 10,000 g for 2 min and once in cell culture medium. Oocyst concentration was adjusted by counting the parasites on Kova® slides under bright field on an Olympus BX51 equipped with a 40x objective.

Trapping Oocysts With Optical Tweezers for Internalization Assay Using Adherent Macrophages at 37°C

We used optical tweezers coupled to real-time imaging to characterize the dynamics of the oocyst internalization by adherent macrophages at 37°C. The experiments were carried out on the NanoTracker™ 2 (JPK instruments) platform, which includes an inverted microscope (Carl Zeiss, Axio Observer) equipped with a motorized plate, CCD camera, and an infrared laser source (wavelength 1,064 nm). The microscope is equipped with a motorized piezoelectric stage that allows the sample to be observed in all three directions (x, y, z). The movements, laser, and detection are controlled under GNU/Linux using NanoTrackerTM JPK Instrument software, which contains JUnicam frame grabber for image capture. A thermoregulator (JPK Petri Dish holder) allows the temperature of the sample to be maintained at 37°C during the measurement.

Petri dishes with 35 mm in diameter and 0.17 mm thick glass bottom (FluoroDish®, WPI) were used as observation chambers. A volume of 10 µl of macrophage cells (i.e. $\sim 1.5.10^5$ cells) in 2 ml fresh culture medium was placed in the dish in order to obtain a homogeneous dispersion of the cells. Macrophages were incubated overnight at 37° C and 5% CO_2 to allow them to adhere. After two successive washes in PBS, 2 ml of pre-warmed culture medium were deposited onto the cells. Oocysts in 10 µl culture medium were added at ratio 1:1 and let for sedimentation for about 5 min before performing the experiments.

An observation area containing several adhered macrophages was first chosen. An oocyst was then trapped with the laser and moved to the defined area to make slight contact with a macrophage (**Supplementary Movie 1**). After 10 sec of oocyst-macrophage contact, the laser was switched off to release the oocyst. An image was taken just after releasing the oocyst ($t = 0$, see an example in **Figure 1D**). The same process was repeated until a free oocyst was presented to each of the macrophages present in the defined area. A second zone was then selected and so on in order to have enough oocyst-macrophage pairs for statistical analyses. Then, oocyst-cell interactions were monitored, zone-by-zone, over a minimum duration of 70 min and up to 4 h, with a time step of 5 min sufficient to find the desired zone and perform a multiple acquisitions in z using the piezo stage to assess that oocysts were within the macrophage cells.

Images were analyzed using the Fiji/ImageJ software (https://fiji.sc/) to quantify the beginning and end of oocyst internalization for each oocyst-macrophage pair. We defined the beginning of oocyst internalization when macrophages started producing cellular extensions stretching toward oocysts and the end at the complete engulfment of the parasite as assessed by z scan map acquisition. Oocyst internalization was also quantified by recording the positions of the macrophage and the oocysts by elliptical/oval overlays and measuring the distance between the center of the macrophage and the center of the oocyst as a function of time (**Figure 1D**).

Micropipette Aspiration for Internalization of Oocysts by Non-adherent Macrophages at Room Temperature

We used the micropipette aspiration technique described by Freppel et al. (2016). Briefly, a glass capillary (internal diameter 0.58 mm/outer diameter 1 mm) was heated using a micropipette puller (David Kopf Instruments, Model 700C) until melting, and separated in half to obtain two closed microneedles. The tips of the two microneedles were forged as micropipettes under microscope (Microforge, Alcatel) until the desired shape and size of the opening were obtained (∼2–3 µm). The micropipettes were then bent with a 30°-angle using a second microforge (Microforge MF-830, Narishige). Both micropipettes were filled carefully with PBS/1% BSA medium to passivate their inner walls. The observation chamber consisted in a Petri dish with 35 mm in diameter and 0.17 mm thick glass bottom (FluoroDish®, WPI) filled with 2 ml of culture medium (RPMI 1640 + 10% FBS). The micropipettes were introduced in the chamber to passivate their outer wall 5–10 min before the experiment. They were mounted on x,y,z micromanipulators (one Narishige hydraulic system, one Sutter Instruments MP285 electronic one), facing each other on an inverted microscope Olympus IMT2, equipped with a Prosilica GE680 CCD camera for fast acquisitions under bright field at 40x magnification.

Aspiration of cells in suspension was performed after exchange of the buffer with culture medium at RT, introduction of diluted cells and parasites and their sedimentation. Then, a non-adherent macrophage and one oocyst were selected and aspirated with each micropipette using a homemade aspiration system based on interconnected vessels. The aspiration pressure was monitored using pressure sensors (typically $-2/-3$ cm H_2O for the macrophage, and $-2/-10$ cm H_2O for the oocyst). The oocyst was presented and gently pressed to the macrophage for 1 min. Aspiration was then quickly released on the oocyst, and the holding pipette removed while the oocyst/macrophage pair was observed over time for 60 min maximum. Images were acquired using a homemade software programmed in Python 3.6 or using proprietary acquisition Vimba from Allied Vision (https://www.alliedvision.com/en/products/software.html), and analyzed using Fiji/ImageJ software. Multiple acquisitions in z were performed by changing lens focus to assess that the oocyst was internalized by the macrophage. The culture medium, micropipettes and oocyst/macrophage suspensions were changed every hour. Experiments were run at RT.

Inhibition of Oocyst Internalization

Macrophages were plated in triplicate at the density of $1.5.10^5$ cells in 1 ml culture on 12 mm-glass coverslips (0.13–0.17 mm thick) precoated with 0.01% poly-L-lysine solution placed at the bottom of 24-well sterile plates as described previously (Freppel et al., 2016). After incubation for 24 h at 37°C, cells were pre-treated for 30 min with 1 µM of the actin polymerization inhibitor latrunculin A (LatA, Sigma-Aldrich, Saint-Quentin-Fallavier, France) or 50 µM of the myosin-II inhibitor blebbistatin (Blebb, Sigma-Aldrich). Oocysts were

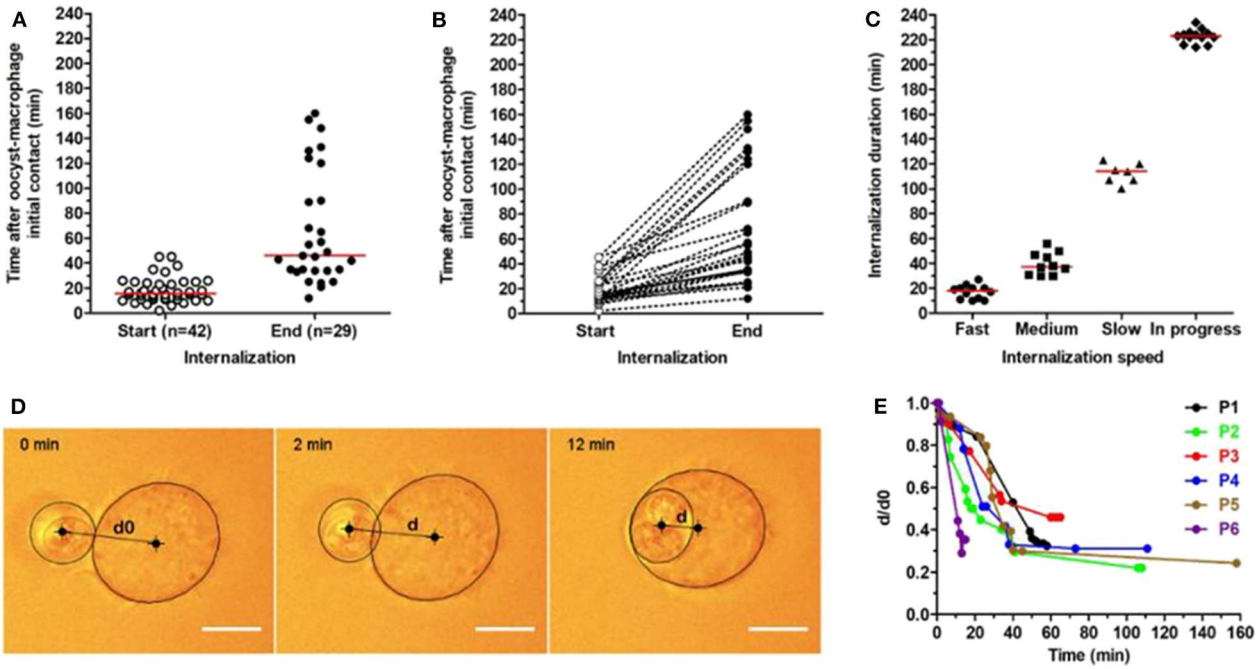

FIGURE 1 | Kinetics of *T. gondii* oocyst internalization by RAW macrophages measured using optical tweezers. Oocysts were trapped by optical tweezers and individually presented to macrophages. Each oocyst-macrophage pair was then followed for oocyst internalization by real-time imaging at 37°C for a maximum 240-min period. **(A)** Start and end of oocyst internalization after oocyst-macrophage initial contact (t0). The numbers of oocyst-macrophage pairs for which oocyst internalization started ($n = 42$) and ended ($n = 29$) within the 240-min period are indicated. Each dot represents an oocyst-macrophage pair. The red line represents the median of data distribution. **(B)** Distribution of oocyst-macrophage pairs ($n = 29$) that completed oocyst internalization during the period and **(C)** the internalization speed. Speed was arbitrarily classified as fast (full internalization in 0–29 min), medium (30–59 min), slow (≥60 min), and still in progress at the end of the experiments. Each symbol represents an oocyst-macrophage pair. The red line represents the median of data distribution. **(D,E)** Oocyst internalization dynamics was further characterized in 6 oocyst-macrophage pairs (P1 to P6) by quantifying d/d0 up to 160 min following contact, with d0 the apparent distance measured between the oocyst and macrophage centers at t0 (initial contact) and d the apparent oocyst-macrophage distance at $t > 0$. A zoom on the 0–60 min period is available in the **Supplementary Figure 1**. Scale bar = 10 μm.

added at ratio 1:1 and incubated with macrophages at 37°C for 1 h in continuous presence of 1 μM LatA or 50 μM Blebb. Cells incubated with 0.1% DMSO served as carrier control. After that, coverslips were washed three times with PBS, fixed in 4% (w/v) paraformaldehyde (PFA) in PBS for 15 min at 4°C, rinsed three times with PBS, and then permeabilized with 0.1% TritonX-100 in PBS for 15 min at RT. After three washes in PBS, coverslips were incubated for 40 min at RT on a drop of rhodamine-conjugated phalloidin (Life Technologies) diluted at 1:40 in PBS for observation of actin filaments. After three washes in PBS, coverslips were air-dried and mounted with SlowFade® Gold Antifade DAPI mounting medium (Life Technologies). Bright field and epifluorescence images of fixed cells were collected on an Olympus BX51 equipped with a XC30 CCD camera, 40x and 100x objectives, and epifluorescence filters for DAPI and rhodamine. Images were acquired using the imaging system CellA (Olympus) and were further analyzed using the Fiji/ImageJ software. Macrophages with oocysts attached at their surface, or partially or fully internalized were counted manually over randomly selected 20–40 fields (∼150–200 macrophages) per coverslip and condition.

Detection of the Sporozoites and Tachyzoites in Oocyst-Macrophage Co-cultures

Macrophages were plated on coverslips as described above and co-incubated with oocysts at ratio 1:1 for 4, 6, or 24 h at 37°C. After that, preparations were fixed in absolute cold methanol for 10 min and rinsed three times in PBS. They were then incubated at 37°C for 1 h with a human antiserum reacting with both *T. gondii* sporozoites and tachyzoites at 1:200 dilution in PBS and a rabbit polyclonal sporozoite-specific anti-AMA4 antibody at 1:1000 dilution in PBS. After three washes in PBS, cells were then incubated at 37°C for 1 h with a FITC-conjugated secondary anti-human antibody at 1:100 dilution in PBS and an Alexa546-conjugated secondary anti-rabbit antibody at 1:50 dilution in PBS. After three washes in PBS, coverslips were air-dried, mounted with SlowFade® Gold Antifade DAPI mounting medium, and observed for sporozoite and tachyzoite detection using the Olympus BX51 set-up. The respective number of sporozoites and tachyzoites was determined by manually counting the parasites over ∼200 macrophages per coverslip.

Monitoring the Development of Tachyzoites in Macrophages Challenged With Oocysts, Free Sporocysts, or Sporozoites

To investigate whether removal of the oocyst and sporocyst walls modifies the development of tachyzoites from sporozoites over time, macrophages were challenged either with oocysts, free sporocysts or sporozoites. Sporocysts and sporozoites were obtained following oocyst sonication and further incubation in an excystation medium as detailed by Freppel et al. (2016). Macrophages ($1.5.10^5$ cells) were plated on coverslips as described above and challenged with oocysts (ratio 1:1), freshly released sporocysts or freshly excysted sporozoites in cell culture medium. Sporocysts were added at ratio 2:1 assuming that one fully sporulated oocyst contained two sporocysts. Sporozoites were added at a quantity equivalent to 1.5×10^5 oocysts, i.e., $\sim 1.2 \times 10^6$ sporozoites assuming that one fully sporulated oocyst contained eight sporozoites. Macrophages and parasites were co-cultured for 24 h at 37°C to allow the development of tachyzoites. After that, coverslips were processed as described above for tachyzoite detection by fluorescence microscopy. The percent of macrophages containing tachyzoites was determined by manually counting ∼200 macrophages per coverslip and condition.

Statistical Analyses

All data were analyzed by using GraphPad Prism 5.03 software. Statistical significance between the data sets was evaluated by one-way ANOVA tests followed by the Tukey's multiple comparison test. *P*-values < 0.05 were considered significant: ***, **, and * indicate $p < 0.001$, $p < 0.01$, and $p < 0.05$, respectively. Unless stated, data were expressed as mean ± standard deviation (S.D.) of four independent experiments.

RESULTS

Oocysts Are Internalized by Macrophages at Different Speeds

To study the dynamics of oocyst internalization at the single-cell level, we used optical tweezers for trapping oocysts and presenting them individually to macrophages (see an example in **Supplementary Movie 1**). Following a 10-sec oocyst-macrophage contact, the laser was cut off and each oocyst-macrophage pair ($n = 46$) was followed for 240 min at 37°C. Oocyst internalization started in 42 (91.3%) out of 46 pairs between 2 and 45 min (median 15.5 min) after initial contact (**Figure 1A**). It ended in 29 (69.0%) out of these 42 pairs between 12 and 160 min (median 46.0 min) after initial contact (**Figure 1A**). Internalization kinetics varies greatly among oocyst-macrophage pairs (**Figures 1B,C**). Full internalization was classified as fast (0–29 min, median 18 min, $n = 12$ pairs), medium (30–59 min, median 37.5 min, $n = 10$), and slow (≥60 min, median 114 min, $n = 7$). Several macrophages ($n = 13$) were still internalizing their oocyst at the end of experiments (i.e., at $t = 240$ min after the oocyst-macrophage initial contact) (denoted as 'in progress' in **Figure 1C**). Oocyst internalization kinetics was further characterized in 6 oocyst-macrophage pairs by measuring the distance between the oocyst center and the macrophage center at $t = 0$ (d0) and then over time (d) (**Figures 1D,E**). The ratio d/d0 decreased rapidly by 15 min following contact and did not vary after 40–45 min (**Figure 1E** and **Supplementary Figure 1**). Micropipette aspiration experiments showed that oocyst internalization could occur at RT, as at 37°C, in a very few oocyst-macrophage pairs (**Supplementary Movie 2**, **Supplementary Figures 2, 3**).

The Complete Internalization of Oocysts Requires Actin Polymerisation of the Macrophage Cell Cytoskeleton

After 1 h incubation, in control conditions (DMSO 0.1%), 8.5% of macrophages had at least one oocyst attached to their membrane, 16.2% formed pseudopods around oocysts, and 20.9% contained oocysts (**Figure 2B**). In contrast, treating macrophages by the actin inhibitor LatA (1 μM, 1 h) completely abolished the formation of pseudopods (**Figures 2A,B**) and thus prevented the internalization of oocysts that remained stuck to the surface of macrophages (**Figure 2A**). Treating cells with myosin-II inhibitor Blebb (50 μM, 1 h) had no significant effect neither on the pseudopod formation nor on the complete internalization of the oocysts compared to control conditions (**Figures 2A,B**).

Differentiation of Sporozoites Into Tachyzoites and Dissemination of Tachyzoites

After 4, 6, or 24 h of oocyst-macrophage co-incubation, sporozoites and tachyzoites were detected by immunofluorescence using a *T. gondii* positive human serum and a sporozoite-specific AMA4 polyclonal antibody (**Figure 3A**). Tachyzoite number increased as sporozoite number decreased over time (**Figure 3B**). Most of tachyzoites appeared to develop from sporozoites within 4 to 6 h after the oocyst-macrophage contact. Irrespective of the time, tachyzoites were almost exclusively observed as single parasites in macrophages whether hosting an oocyst (**Figure 3A**, panel 1) or not (**Figure 3A**, panel 2).

Tachyzoites Develop Better in Macrophages Challenged With Free Sporocysts or Excysted Sporozoites Rather Than Oocysts

To investigate whether removal of the oocyst and sporocyst walls modifies the development of tachyzoites from sporozoites over time, macrophages were challenged either with whole oocysts, free sporocysts or sporozoites. After 24 h of co-incubation, immunolabelling was performed with antitoxoplasmic positive serum to determine the percentage of macrophages infected with tachyzoites (it was considered that at 24 h the proportion of sporozoites was negligible, see **Figure 3B**). Following incubation with whole oocysts, 6.8% of macrophages were infected vs. 17.2% with free sporocysts and 14.6% with free sporozoites (**Figure 4**).

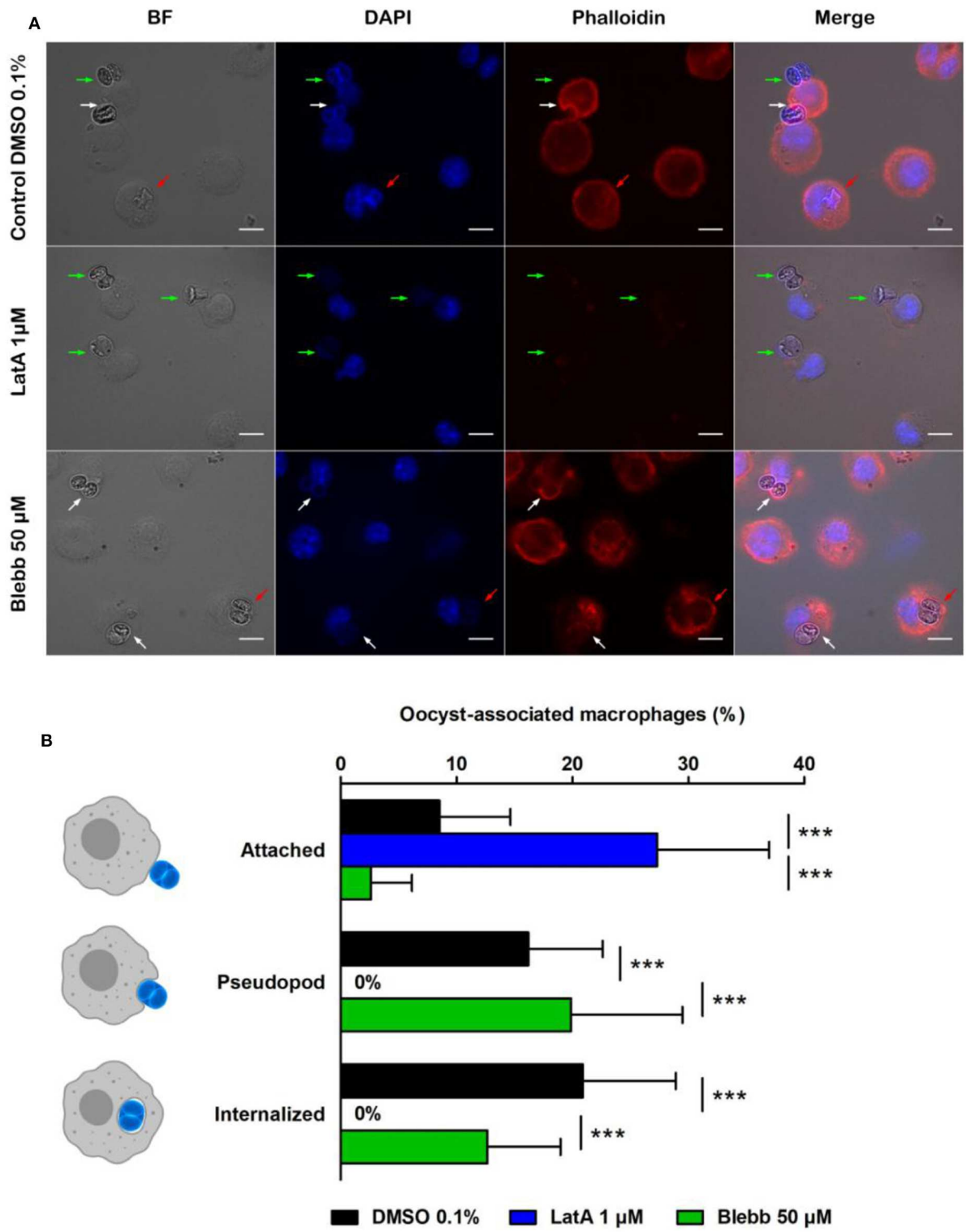

FIGURE 2 | Interactions of *Toxoplasma gondii* oocysts with RAW macrophages in the presence of inhibitors of actin polymerization (latrunculin A, LatA) or myosin II (blebbistatin, Blebb). **(A)** Microscopic monitoring showing macrophages with oocysts attached to their membrane (green arrow), engulfing the parasite (white arrow) or having internalized it (red arrow). BF, bright field; DAPI channel, natural fluorescence of oocysts and macrophage nucleus; phalloidin, macrophage actin cytoskeleton. Scale = 10 µm. **(B)** Percentage of macrophages with an oocyst attached to their membrane, engulfing the parasite (pseudopod stage), or having completely internalized it after 1 h of treatment with 1 µM LatA, 50 µM Blebb, or 0.1% DMSO (control). The values correspond to the mean ± standard deviation of 4 independent experiments. One-way ANOVA and Tukey's post-test, ***$p < 0.001$.

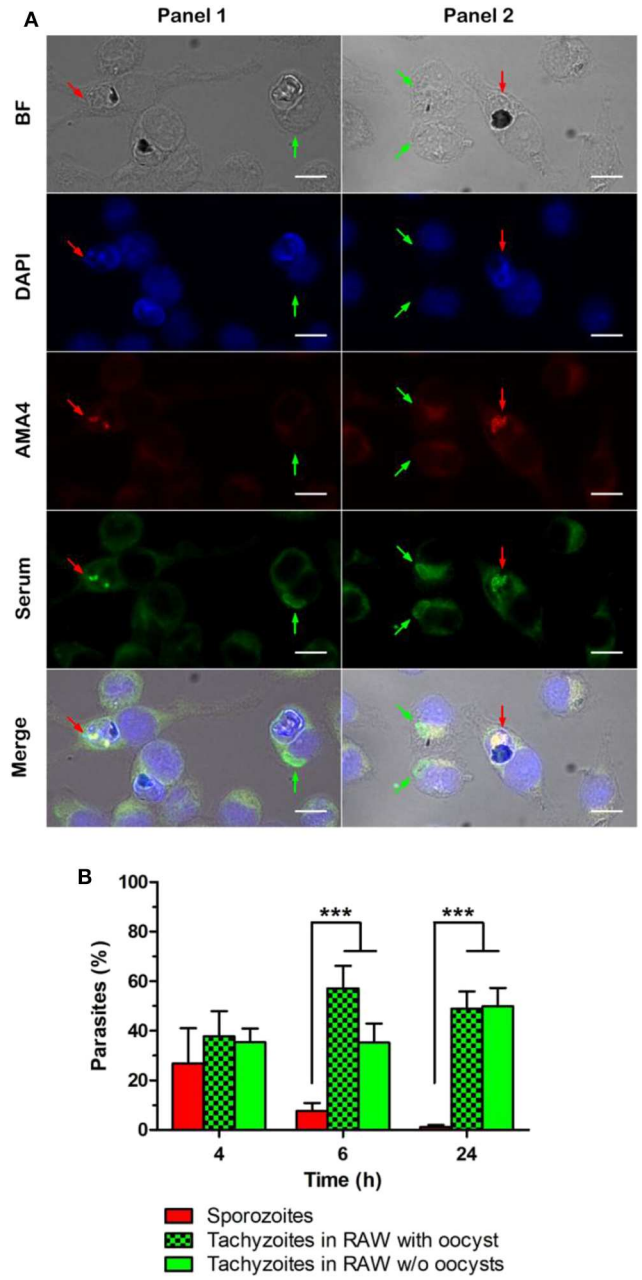

FIGURE 3 | Detection of sporozoites and tachyzoites of *Toxoplasma gondii* after 4, 6, and 24 h of oocyst-RAW macrophage co-incubation**. (A)** Representative example of the immunolabelling of sporozoites (red arrow) and tachyzoites (green arrow) whether present in macrophages with oocyst remnants (Panel 1) or in macrophages without visible oocyst remnants (Panel 2) after 4 h of oocyst-macrophage co-incubation. DAPI, macrophage nucleus and natural fluorescence of oocysts; AMA4, sporozoites; serum, sporozoites and tachyzoites. Scale = 10 μm. **(B)** Percentage of sporozoites (red bar) and tachyzoites [whether present in macrophages with visible oocyst remnants (green and black checker) or in macrophages without oocysts (green)]. Mean ± standard deviation of 3 independent experiments. One-way ANOVA and Tukey's post-test, ***$p < 0.001$.

Tachyzoites developed better in macrophage cultures challenged with free sporocysts or sporozoites than with whole oocysts ($p < 0.001$) (**Figure 4**).

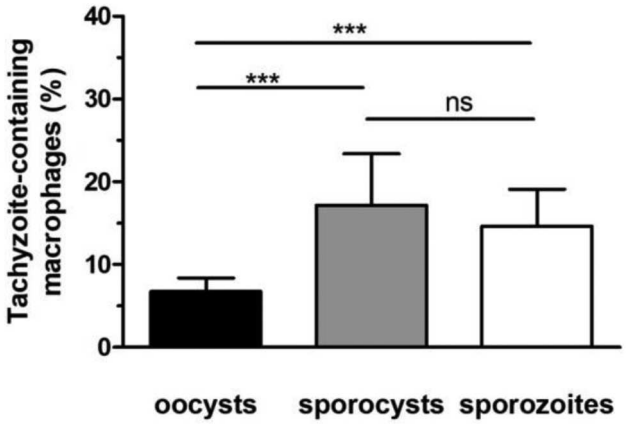

FIGURE 4 | Development of tachyzoites in RAW macrophages challenged with oocysts, free sporocysts, or sporozoites. Following parasite-macrophage incubation for 24 h, the percentage of tachyzoite-containing macrophages was determined by immunofluorescence assay as described in materials and methods. Mean ± standard deviation of 4 independent experiments. One-way ANOVA and Tukey's post-test, ***$p < 0.001$.

DISCUSSION

How *T. gondii* sporozoites excyst from the oocyst to infect host tissues remains poorly characterized. In particular, host and parasite factors that trigger the opening of the oocyst and sporocyst wall are currently unknown. Oocysts entering the host gut face various digestive agents such as pepsin, trypsin and biliary salts, however none of them (alone or in combination) significantly affect the integrity of the robust oocyst wall (Freppel et al., 2019). Digestive factors even seem unnecessary to the excystation process as *T. gondii* oocysts can cause, in rare conditions, infection following parenteral exposure (Dubey and Frenkel, 1973; Dubey, 2006). We recently hypothesized that, in absence of digestive factors, phagocytic cells could facilitate excystation of the sporozoites *in vitro* following oocyst phagocytosis (Freppel et al., 2016). In the present study, we further characterized the dynamics of the early interactions between oocysts and RAW264.7 macrophages and analyzed the fate of excysted sporozoites in oocyst-macrophage co-cultures.

Micropipette aspiration and optical tweezers allowed us to investigate early interactions between oocysts and non-adherent or adherent macrophages at different temperatures (RT vs. 37°C, respectively) and timeframes (from 1 min to few hours following the parasite-cell contact). By using optical tweezers at 37°C, most of the macrophages manipulated oocysts for ∼15 min before internalizing them in ∼30 min. Variations in internalization kinetics could rely on the way the oocysts were presented to macrophages (their length or width first), as reported for non-biological particles of different geometries (Champion and Mitragotri, 2006). Micropipette aspiration experiments at RT did not provide a robust characterization of the early events of the oocyst phagocytosis by non-adherent macrophages due to the very low number of usable data. Indeed, though oocysts adhered tightly to the macrophage

cell membrane following a forced contact, macrophages did not totally internalize oocysts, except few that completed the process as observed at 37°C by using optical tweezers. These results and previous observations (Freppel et al., 2016) indicate that both adherent and non-adherent macrophages are able to internalize oocysts even at a non-physiological temperature. We are currently extending the use of micropipette technique to investigate whether the macrophage senses the oocyst before to capture it as described for a variety of other microbial particles (Heinrich, 2015).

Macrophages treated with latrunculin A (LatA), a depolymerization agent of actin filaments (Fujiwara et al., 2018), were unable to form pseudopods around the oocysts, which remained attached to the macrophage cell membrane. Aside actin, we were further interested in myosin II. It promotes contraction of actin filaments to ensure closure of the phagocytic cup (Barger et al., 2019), and can be enriched in macrophages internalizing rigid particles (Freeman and Grinstein, 2020). As *T. gondii* oocysts are very rigid compared to other biological particles (Dumètre et al., 2013), we investigated whether myosin-II contributed to the internalization of oocysts by treating macrophages with the myosin-II inhibitor blebbistatin (Blebb) (Shu et al., 2005). Blebb-treated macrophages exhibited a fuzzy pattern of their actin cytoskeleton following phalloidin staining, however they internalized oocysts as control ones did. Collectively, our data and previous observations using other inhibitors of the macrophage cytoskeleton (Freppel et al., 2016) suggest a key role of actin polymerization in the formation of the pseudopods and phagocytic cup enclosing the oocysts, and their internalization, as described in classical phagocytosis of beads or biological particles (Rougerie et al., 2013).

Oocyst phagocytosis by RAW macrophages led to the excystation of sporozoites and their differentiation into tachyzoites within 4–6 h following oocyst-macrophage contact, as reported in mice fed with oocysts (Dubey et al., 1997). Interestingly, tachyzoites developed better in macrophages when the oocyst wall was eliminated prior to the internalization assay, either from free sporozoites or free sporocysts. The robust and hermetic oocyst wall is hard to break down by chemical or physical means (Dumètre et al., 2013). In contrast, the sporocyst wall appears more fragile, probably due to the structure of its inner sporocyst wall layer, which is formed of four curved plates held together by thick sutures. If previous studies suggested that the sporocyst wall opens in presence of bile salts at 37°C (Freppel et al., 2019), further investigations are required to characterize its mechanical properties following exposure to various chemical agents.

In conclusion, oocyst phagocytosis by macrophages appears to share common features with classical models of phagocytosis of microbeads. The oocyst wall seems to be the main oocyst substructure that limits the excystation of the sporozoites and therefore their differentiation into tachyzoites. Our oocyst-macrophage *in vitro* platform could further help to address the physical (e.g., contraction of the macrophage cytoskeleton at the phagocytic synapse) and/or chemical factors (e.g., exposure to phagolysosome content) that trigger the opening of the oocyst and the sporocyst walls. *In vivo*, the involvement of phagocytic cells in processing the oocyst walls is uncertain. Such cell types are rare in the intestinal lumen and epithelium, and the presence of mucus could prevent any oocyst-host cell interactions. Only inhalation of oocysts contained in aerosols or dust could involve macrophages at the alveolar level. Such a scenario was suspected following cases of toxoplasmosis by airborne contamination (Teutsch et al., 1979; Lass et al., 2017), but to our knowledge it has never been demonstrated *in vivo*.

DATA AVAILABILITY STATEMENT

The datasets generated for this study are available on request to the corresponding author.

ETHICS STATEMENT

The animal study was reviewed and approved by Beltsville Area Animal Care and Use Committee (BAACUC), United States Department of Agriculture, Beltsville, MD, USA.

AUTHOR CONTRIBUTIONS

P-HP and AD conceived the work. ON, P-HP, CB, LL, SR, JD, and AD carried out the experiments. ON, P-HP, CB, LL, SR, and AD analyzed the data. P-HP, LL, SR, and AD drafted the manuscript. ON, P-HP, LL, SR, NA, JD, and AD reviewed the manuscript.

FUNDING

This work was supported by the Institut Hospitalo-Universitaire (IHU), the National Research Agency grants 10-IAHU-03 and 17-CE21-0005-07, the Région Provence Alpes Côte d'Azur and European funding FEDER PRIMI. The optical tweezer setup was partially funded by Labex Inform (ANR-11-LABX-0054).

ACKNOWLEDGMENTS

We gratefully thank Maryse Lebrun (UMR CNRS 5235, Montpellier, France) for providing anti-AMA4 antibody. P-HP thanks JPK Instruments (Berlin, Germany) now part of Bruker for continuous support.

SUPPLEMENTARY MATERIAL

The Supplementary Material for this article can be found online at: https://www.frontiersin.org/articles/10.3389/fcimb.2020.00207/full#supplementary-material

REFERENCES

Barger, S. R., Gauthier, N. C., and Krendel, M. (2019). Squeezing in a meal: myosin functions in phagocytosis. *Trends Cell Biol.* 30, 157–167. doi: 10.1016/j.tcb.2019.11.002

Champion, J. A., and Mitragotri, S. (2006). Role of target geometry in phagocytosis. *Proc. Natl. Acad. Sci. U.S.A.* 103, 4930–4934. doi: 10.1073/pnas.0600997103

Delgado Betancourt, E., Hamid, B., Fabian, B. T., Klotz, C., Hartmann, S., and Seeber, F. (2019). From entry to early dissemination-*Toxoplasma gondii*'s initial encounter with its host. *Front. Cell Infect. Microbiol.* 9:46. doi: 10.3389/fcimb.2019.00046

Drewry, L. L., Jones, N. G., Wang, Q., Onken, M. D., Miller, M. J., and Sibley, L. D. (2019). The secreted kinase ROP17 promotes *Toxoplasma gondii* dissemination by hijacking monocyte tissue migration. *Nat. Microbiol.* 4, 1951–1963. doi: 10.1038/s41564-019-0504-8

Dubey, J. P. (2006). Comparative infectivity of oocysts and bradyzoites of *Toxoplasma gondii* for intermediate (mice) and definitive (cats) hosts. *Vet. Parasitol.* 140, 69–75. doi: 10.1016/j.vetpar.2006.03.018

Dubey, J. P., and Frenkel, J. K. (1973). Experimental toxoplasma infection in mice with strains producing oocysts. *J. Parasitol.* 59, 505–512.

Dubey, J. P., Speer, C. A., Shen, S. K., Kwok, O. C., and Blixt, J. A. (1997). Oocyst-induced murine toxoplasmosis: life cycle, pathogenicity, and stage conversion in mice fed *Toxoplasma gondii* oocysts. *J. Parasitol.* 83, 870–882.

Dumètre, A., and Dardé, M.-L. (2004). Purification of *Toxoplasma gondii* oocysts by cesium chloride gradient. *J. Microbiol. Methods* 56, 427–430. doi: 10.1016/j.mimet.2003.11.020

Dumètre, A., Dubey, J. P., Ferguson, D. J. P., Bongrand, P., Azas, N., and Puech, P.-H. (2013). Mechanics of the *Toxoplasma gondii* oocyst wall. *Proc. Natl. Acad. Sci. U.S.A.* 110, 11535–11540. doi: 10.1073/pnas.1308425110

Freeman, S. A., and Grinstein, S. (2020). Phagocytosis: mechanosensing, traction forces, and a molecular clutch. *Curr. Biol.* 30, R24–R26. doi: 10.1016/j.cub.2019.11.047

Freppel, W., Ferguson, D. J. P., Shapiro, K., Dubey, J. P., Puech, P.-H., and Dumètre, A. (2019). Structure, composition, and roles of the *Toxoplasma gondii* oocyst and sporocyst walls. *Cell Surface* 5:100016. doi: 10.1016/j.tcsw.2018.100016

Freppel, W., Puech, P.-H., Ferguson, D. J. P., Azas, N., Dubey, J. P., and Dumètre, A. (2016). Macrophages facilitate the excystation and differentiation of *Toxoplasma gondii* sporozoites into tachyzoites following oocyst internalisation. *Sci. Rep.* 6:33654. doi: 10.1038/srep33654

Fujiwara, I., Zweifel, M. E., Courtemanche, N., and Pollard, T. D. (2018). Latrunculin A accelerates actin filament depolymerization in addition to sequestering actin monomers. *Curr. Biol.* 28, 3183-3192.e2. doi: 10.1016/j.cub.2018.07.082

Heinrich, V. (2015). Controlled one-on-one encounters between immune cells and microbes reveal mechanisms of phagocytosis. *Biophys. J.* 109, 469–476. doi: 10.1016/j.bpj.2015.06.042

Lass, A., Szostakowska, B., Korzeniewski, K., and Karanis, P. (2017). The first detection of *Toxoplasma gondii* DNA in environmental air samples using gelatine filters, real-time PCR and loop-mediated isothermal (LAMP) assays: qualitative and quantitative analysis. *Parasitology* 144, 1791–1801. doi: 10.1017/S0031182017001172

Robert-Gangneux, F., and Dardé, M.-L. (2012). Epidemiology of and diagnostic strategies for toxoplasmosis. *Clin. Microbiol. Rev.* 25, 264–296. doi: 10.1128/CMR.05013-11

Rougerie, P., Miskolci, V., and Cox, D. (2013). Generation of membrane structures during phagocytosis and chemotaxis of macrophages: role and regulation of the actin cytoskeleton. *Immunol. Rev.* 256, 222–239. doi: 10.1111/imr.12118

Shapiro, K., Bahia-Oliveira, L., Dixon, B., Dumètre, A., de Wit, L. A., VanWormer, E. (2019). Environmental transmission of *Toxoplasma gondii*: oocysts in water, soil and food. *Food Waterborne Parasitol.* 15:e00049. doi: 10.1016/j.fawpar.2019.e00049

Shu, S., Liu, X., and Korn, E. D. (2005). Blebbistatin and blebbistatin-inactivated myosin II inhibit myosin II-independent processes in Dictyostelium. *Proc. Natl. Acad. Sci. U.S.A.* 102, 1472–1477. doi: 10.1073/pnas.0409528102

Teutsch, S. M., Juranek, D. D., Sulzer, A., Dubey, J. P., and Sikes, R. K. (1979). Epidemic toxoplasmosis associated with infected cats. *N. Engl. J. Med.* 300, 695–699.

Conflict of Interest: The authors declare that the research was conducted in the absence of any commercial or financial relationships that could be construed as a potential conflict of interest.

frontiers in Cellular and Infection Microbiology

MINI REVIEW
published: 11 June 2020
doi: 10.3389/fcimb.2020.00262

Autoantibodies and Malaria: Where We Stand? Insights Into Pathogenesis and Protection

*Luiza Carvalho Mourão, Gustavo Pereira Cardoso-Oliveira and Érika Martins Braga**

Departamento de Parasitologia, Instituto de Ciências Biológicas, Universidade Federal de Minas Gerais, Belo Horizonte, Brazil

Autoantibodies are frequently reported in patients with malaria, but whether they contribute to protection or to pathology is an issue of debate. A large body of evidence indicates that antibodies against host-self components are associated to malaria clinical outcomes such as cerebral malaria, renal dysfunction and anemia. Nonetheless, self-reactive immunoglobulins induced during an infection can also mediate protection. In light of these controversies, we summarize here the latest findings in our understanding of autoimmune responses in malaria, focusing on *Plasmodium falciparum* and *Plasmodium vivax*. We review the main targets of self-antibody responses in malaria as well as the current, but still limited, knowledge of their role in disease pathogenesis or protection.

Keywords: malaria, autoantibodies, anemia, cerebral malaria, renal dysfunction

OPEN ACCESS

Edited by:
Patricia Sampaio Tavares Veras, Gonçalo Moniz Institute (IGM), Brazil

Reviewed by:
Kai Yang, Indiana University School of Medicine—Lafayette, United States
Surya Prakash Pandey, University of Pittsburgh, United States
Ann M. Moormann, University of Massachusetts Medical School, United States

****Correspondence:***
Érika Martins Braga
embraga@icb.ufmg.br

Specialty section:
This article was submitted to Microbes and Innate Immunity, a section of the journal Frontiers in Cellular and Infection Microbiology

Received: *03 January 2020*
Accepted: *04 May 2020*
Published: *11 June 2020*

Citation:
Mourão LC, Cardoso-Oliveira GP and Braga ÉM (2020) Autoantibodies and Malaria: Where We Stand? Insights Into Pathogenesis and Protection. Front. Cell. Infect. Microbiol. 10:262. doi: 10.3389/fcimb.2020.00262

INTRODUCTION

Despite substantial progress in control efforts over the past decades, malaria still accounts for significant morbidity and mortality, mainly in underdeveloped countries. In 2018, an estimated 228 million cases of malaria occurred worldwide with 405,000 deaths, largely in Africa (WHO | World Malaria Report, 2019). Five species are known to cause malaria in humans, *Plasmodium falciparum*, *Plasmodium vivax*, *Plasmodium knowlesi*, *Plasmodium ovale,* and *Plasmodium malariae*. Since research emphasis has been placed on *P. falciparum* and *P. vivax*, parasites that are responsible for most of malaria cases, here we will focus in these two species.

Symptomatic disease occurs during the erythrocytic phase when the presence of asexual blood-stage parasites triggers a robust innate immune response. This response if properly regulated may clear infection, contributing to the development of a protective immunity. By the other hand, if not counterbalanced by anti-inflammatory responses, the exacerbated activation of the immune system may play a key role in the pathogenesis (reviewed by Antonelli et al., 2019), leading to complications such as cerebral malaria, anemia, acute kidney injury and respiratory distress syndrome (Moxon et al., 2019).

During infection, high levels of antibodies with a broad range of specificities are elicited. Although their functional activity is far from over, it is known that such molecules can have diverse effects. Antibodies are critical for the control of the disease by acting alone or in cooperation with host immune cells (For further details see Teo et al., 2016). But in some cases, antibodies that recognize host's own components may also promote pathology (Ludwig et al., 2017).

The presence of autoantibodies that recognize the host's own molecules has also been extensively reported in patients with malaria (Rosenberg et al., 1973; Berzins et al., 1983; Daniel-Ribeiro et al., 1983; Wozencraft et al., 1990; Jakobsen et al., 1993; Lacerda et al., 2011; Fernandez-Arias et al., 2016; Mourão et al., 2016, 2018; Rivera-Correa et al., 2019a). The mechanisms by which autoimmune responses could be triggered during an infection remains unclear but it is generally

accepted that they may include: molecular mimicry (Damian, 1964; Greenwood, 1974), bystander activation (Fujinami et al., 2006; Münz et al., 2009), epitope spreading (Vanderlugt and Miller, 2002; Münz et al., 2009), persistent infection and B cells polyclonal activation (Freeman and Parish, 1978; Rosenberg, 1978; Daniel-Ribeiro et al., 1983; Minoprio, 2001).

Molecular mimicry is the sharing of structurally similar antigens between parasite and host components (Damian, 1964). In malaria, molecular mimicry occurs between *P. falciparum* translationally controlled tumor protein (PfTCTP) and human histamine-releasing factor (HRF) (MaCDonald et al., 2001). Another plasmodial protein that share motifs with host's components is *P. falciparum* erythrocyte membrane protein 1 (PfEMP1), which exhibits homology with human vitronectin (Ludin et al., 2011). An *in silico* analysis comparing *P. vivax* entire proteome and human RBC proteome also revealed that 23 *P. vivax* proteins shared similarity to human RBC proteins such as ankyrin, actin, and spectrin (Mourão et al., 2018). These structural similarities can activate cross-reactive autoreactive lymphocytes, consequently disordering the immune system. So, when T- or B- cells receptors recognize a parasite epitope that is similar enough to a self-protein, an autoimmune response is elicited, leading to cell or tissue destruction in addition to activation of other branches of the immune system (Fujinami et al., 2006; Münz et al., 2009).

Bystander activation is an antigen-independent phenomenon whereby parasitized cells, either through direct cell contact or paracrine signals, alert or instruct neighboring non-infected cells to produce inflammatory mediators (Holmgren et al., 2017). The inflammatory milieu evoked by the infection promotes the activation and expansion of autoreactive T or B cells, which can initiate an autoimmune response that damage host's cells or tissues, leading to the release of self-reactive antigens (Fujinami et al., 2006; Münz et al., 2009). Evidences of bystander activation in malaria came from *in vitro* studies investigating the pathways driving inflammation in infection. These studies have demonstrated that extracellular vesicles derived from plasma of mice infected with *Plasmodium berghei* or from *P. falciparum*-infected erythrocytes were able to activate naïve host cells (Couper et al., 2010; Mantel et al., 2013).

It is widely known that in early immune responses, epitopes of the initial antigens are recognized by the acquired immune system, but during infection, epitopes other than the dominant ones may also become immunogenic and be targets of T and B cells. This reactivity to newer endogenous epitopes is termed "epitope spreading" and may be induced against other epitopes in the same autoantigen (intramolecular epitope spreading) or against epitopes in other self-antigens (intermolecular epitope spreading) that are released after T- or B-cell-mediated bystander (Münz et al., 2009). Although epitope spreading is more commonly reported in autoimmune diseases, it may also occur in persistent infections, as it has been suggested by Flanagan et al. (2006) in a study conducted with adults naturally exposed to malaria in Kenya. These authors have investigated cellular immunity to the thrombospondin-related adhesive protein of *P. falciparum* (PfTRAP) and showed that the immunodominant response stimulated in the primary exposure to this protein has progressed to encompass lesser epitopes with repeated and prolonged exposure.

In vitro experiments with *P. falciparum*-infected RBCs revealed that culture supernatant containing parasite-derived products was able to induce polyclonal B-cell activation and non-specific immunoglobulin synthesis, suggesting that B-cell's proliferation and differentiation into antibody-secreting cells triggered by pathogen's molecules can also lead to autoimmune responses (Freeman and Parish, 1978; Minoprio, 2001). One of the molecules that has been incriminated as a potential activator of B-cells in malaria is the cysteine-rich interdomain region 1 (CIDR1) of *P. falciparum* erythrocyte membrane protein 1 (PfEMP-1). Evidence in this line has been provided by a study with B cells from non-immune donors stimulated with a recombinant version of CIDR1. The recombinant protein was able to promote *in vitro* proliferation, increase in B-cell size, and expression of immunoglobulins and cytokines in those cells (Donati et al., 2004). However, just a small proportion of antibodies secreted by them was specific for parasite antigens; the greater part was non-specific and could react with different host's components, leading to cell and tissue damage.

Self-reactive antibodies recognize different self-antigens such as erythrocyte proteins (Rosenberg et al., 1973; Fontaine et al., 2010; Mourão et al., 2016, 2018; Ventura et al., 2018), brain molecules (Bansal et al., 2009; Gitau et al., 2013), phospholipids (Adebajo et al., 1993; Jakobsen et al., 1993; Facer and Agiostratidou, 1994; Fernandez-Arias et al., 2016; Barber et al., 2019; Rivera-Correa et al., 2019a,b), and nucleic acids (Adu et al., 1982; Adebajo et al., 1993; Rivera-Correa et al., 2019b). Although the literature reporting the detection of autoantibodies in plasmodial infections is vast, the role of such molecules in malaria is still a controversial issue. Some authors have associated such autoimmune responses to pathology while others to protection. In this review, we summarize the latest breakthroughs regarding autoantibody responses in malaria, emphasizing what is new on the pathogenesis front, mainly with respect to cerebral malaria, kidney injury and anemia **(Figure 1)**.

CEREBRAL MALARIA

Cerebral malaria (CM) is a clinical syndrome of severe falciparum malaria characterized by impaired consciousness assessed by Blantyre Coma Score $\leq$ 2 in children (Molyneux et al., 1989) or Glasgow Coma Score $\leq$ 11 in adults (Teasdale and Jennett, 1974), with no other cause of encephalitis (Taylor et al., 2004). Although this neurological syndrome only develops in a small percentage of *P. falciparum*-infected patients, it is responsible for more than 90% of malaria-related deaths. The treatment with anti-malarial drugs decreases mortality due to CM, but nearly 20% of treated patients still succumb and up to one-third of survivors frequently exhibit long-term neurological sequelae such as cognition and speech disorders, physical disability and cortical blindness (Birbeck et al., 2010).

Although the mechanisms leading to CM pathogenesis are not yet clearly defined, it is known that both parasite and host factors play a role in the clinical outcome of this syndrome (Idro

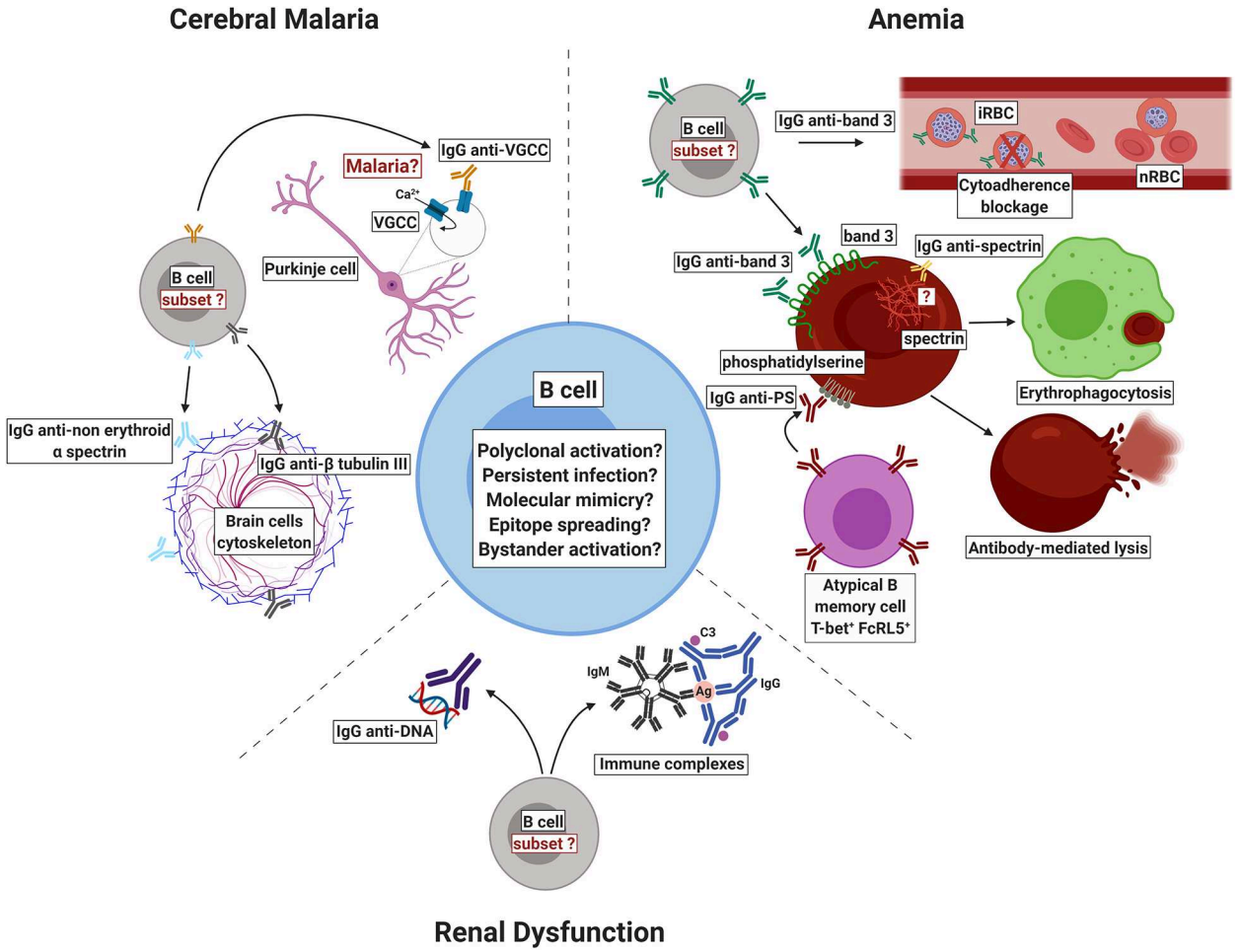

FIGURE 1 | Schematic representation of self-reactive antibodies and their proposed role in the pathogenesis or protection against malaria. Autoantibodies that recognize host's own molecules have been reported in patients with malaria but the mechanisms by which such autoimmune response is induced are still to be completely elucidated. In infections due to *P. falciparum*, self-reactive immunoglobulins against voltage-gated calcium channel (VGCC), non-erythroid alpha spectrin, and beta tubulin III have been associated to cerebral malaria. In *P. falciparum* and *P. vivax* infections, anti-phosphatidylserine antibodies (IgG anti-PS) have been shown to recognize non-infected red blood cells (nRBCs) exposing phosphatidylserine, mediating their clearance and contributing to malaria-associated anemia. During *P. vivax* malaria, autoimmune responses to anion exchanger 1 (band 3 protein) have been implicated in the removal of nRBCs by decreasing their deformability and enhancing their uptake by THP-1 cells. On the other hand, in *P. falciparum* malaria, anti-band 3 self-reactive antibodies have been associated to protection through the blockage of cytoadherence. Antibodies to erythrocytic spectrin are elicited during *P. vivax* malaria but it remains unclear how they bind to cytoplasmic proteins. It has been hypothesized that the inflammation triggered by infection may damage brain cells, leading to the exposure of spectrin, which may activate the complement, amplifying neuronal damage. Finally, anti-DNA autoantibodies and immune complexes containing self-immunoglobulins have been suggested to play a role in renal dysfunction by depositing in renal tissues. iRBC: infected red blood cell. Ag: antigen. C3: complement component 3. Figure created with BioRender.

et al., 2010). Among host components, B cells and antibodies are critical for the immune response against malaria. Large amounts of antibodies are produced in response to plasmodial infection, including those that recognize self-components such as host brain antigens (Guiyedi et al., 2007; Bansal et al., 2009; Duarte et al., 2012). However, whether such self-reactive immunoglobulins are a consequence of cerebral malaria or a factor that aggravates the disease is little explored. This could be, in part, due to the difficult in accessing human brain tissues because of the small proportion of *P. falciparum*-infected patients that develop CM. Moreover, the existence of ethical issues limits the study of CM to peripheral blood and *post-mortem* samples.

Although understudied, some research groups have associated a marked increase in specific anti-brain autoantibodies levels with disease severity in *P. falciparum* malaria. This is the case of self-reactive antibodies against the voltage-gated calcium channels (VGCCs), whose levels were shown to be higher in Kenyan children with CM than in those with uncomplicated disease or uninfected (Lang et al., 2005). Autoantibodies to VGCCs have been shown to downregulate calcium flow in Purkinje neurons and granule cells through a complement-independent process in autoimmune diseases such as limbic encephalitis and cerebellar ataxia (Pinto et al., 1998; Irani and Lang, 2008), thereby providing insight into the pathogenic role of such self-reactive molecules in malaria.

Furthermore, it has been reported that serum from Gabonese children with severe *P. falciparum* infection recognize a higher diversity of brain antigens in comparison to non-infected ones. Some of those autoantibodies display reactivity to the non-erythroid alpha spectrin (Guiyedi et al., 2007), a structural protein that is found in the cytoplasm of a variety of brain cells and is responsible for membrane structure and integrity. Since inflammation induced by malaria can damage brain cells exposing non-erythroid alpha spectrin, it is possible that this protein activates the complement system, amplifying the neuronal damage. In primary Sjögren's syndrome, an important autoimmune disease, non-erythroid spectrin undergoes proteolysis by caspase 3 and calpain, producing a fragment that acts as autoantigen (Nath et al., 1996; Haneji et al., 1997).

Other cytoskeletal protein that has also been described as a target of autoimmune responses in CM and which is considered as a disease-specific marker is beta tubulin III (TBB3) (Bansal et al., 2009), a protein that is abundant in cells from nervous system and in neoplastic cells of neural tumors (Katsetos et al., 2003). TBB3 is involved in axon guidance, thus mutations in this protein are associated with different nervous system disorders (Tischfield et al., 2010). In living cells and *in vitro* models, polyclonal antibodies with high affinity for beta tubulin have been shown to disrupt cytoplasmic microtubules, leading to their fragmentation into smaller units (Füchtbauer et al., 1985).

In addition to the self-reactive proteins mentioned above, the dendritic tree of Purkinje cell is another host component that has been considered a target of autoimmune responses in CM. In a cohort of Thai individuals, it has been demonstrated that levels of autoantibodies against dendrites are higher in *P. falciparum*-infected patients with CM than in those with uncomplicated malaria (Gallien et al., 2011). The pathogenic role of such autoantibodies was attributed to their ability in inhibiting *in vitro* development of Purkinje cells (Calvet et al., 1993). However, it is important to emphasize that these results were obtained from studies conducted with cat brain biopsies and thus, should be interpreted with caution.

On the other hand, a possible role in protection against severe *P. falciparum* malaria has already been suggested for self-reactive antibodies induced during plasmodial infection. This is the case of IgE autoantibodies to 14-3-3 ε brain protein, which induce *in vitro* mastocyte degranulation (Duarte et al., 2012). The 14-3-3 ε brain protein belongs to a family of adaptor proteins that interact with a multitude of binding partners that contain PSer/PThr motifs. Through this interaction, 14-3-3 ε protein affects the activity and localization of various substrate proteins, regulating signal cascades of a wide range of biological activities, including cell cycle and apoptosis (Cornell and Toyo-Oka, 2017). Therefore, 14-3-3 ε protein has been implicated in different neurodegenerative and neuropsychiatric diseases by mechanisms that vary from apoptosis to protein stabilization and aggregation (For further details see Foote and Zhou, 2012 and Cornell and Toyo-Oka, 2017). In Parkinson's disease, for example, the interaction of 14-3-3 ε protein with Bad and Bax proteins prevents neurons apoptosis. Neurodegeneration is avoided by interaction between 14-3-3 ε protein and phosphorylated tyrosine hydroxylase in parallel with the binding between α-synuclein to unphosphorylated tyrosine hydroxylase. An imbalance in those interactions leads to neurodegeneration in this nervous system disorder (Shimada et al., 2013). Thus, it is not surprising that an antibody response against 14-3-3 ε brain protein exert neuroprotective properties, as it has already been demonstrated in glaucoma, using a neuro-retinal cell line of mouse origin. In this case, cell viability and reduced reactive oxygen species levels were considered predictors of protection (Bell et al., 2015).

As highlighted herein, the repertoire of brain antigens that are targets of autoimmune responses during CM is vast and depends on a complex interplay of host, parasite and environmental factors. However, whether such autoantibodies have a pathogenic relevance, can be considered biomarkers of neuropathology or are merely innocent by-standers remains a focus of debate. More studies are needed in order to elucidate this, as well as to determine the epitopes, function and origin of such self-reactive immunoglobulins. Even though it is known that a breach in the blood brain barrier's (BBB) integrity is necessary to allow antibody influx into the brain (Huerta et al., 2006), studies conducted with *post mortem* brain tissues from Malawian children with fatal cerebral malaria revealed that, although BBB breakdown occurs in vessels containing cytoadherent parasitized RBCs, no gross leakage of plasma proteins occurs (Brown et al., 2001). Thus, the mechanisms by which immunoglobulins gain access to brain tissue are another issue that is still to be elucidated. Do they cross the BBB independently or do plasma cells secrete them? Further studies are necessary to understand in more details how BBB breakdown occurs in malaria. Understanding how this happens may provide new opportunities to find agents that are able to open the BBB, allowing the delivery of different molecules and shedding light on the effects of antibodies in the brain tissue. This knowledge may pave the way for the development of future interventions for malaria and other neurological diseases.

RENAL DYSFUNCTION

Acute renal failure is most reported in *P. falciparum* infections (Frutakul et al., 1974; Burchard et al., 2003; von Seidlein et al., 2012; Conroy et al., 2016; Sypniewska et al., 2017; Rivera-Correa et al., 2019b), but this complication can occasionally occurs in infection due to *P. malariae* (Neri et al., 2008; Badiane et al., 2016). Renal failure is considered a clinical manifestation with high prognostic value to severe malaria (von Seidlein et al., 2012; Sypniewska et al., 2017). In *P. malariae* infection, renal failure affects most children and is presented as steroid-resistant nephrotic syndrome. The pathogenesis is possibly mediated through immune-complex deposition containing IgM, IgG, C3, and malarial antigens in mesangiocapillary, glomerular, proximal tubules and subendothelial kidney tissues, with rarely IgA deposition (Ward and Kibuka-Musoke, 1969; Houba et al., 1971; van Velthuysen and Florquin, 2000; Das, 2008). Chronic glomerular disease due to *P. malariae* infection is usually not reversible even after treatment, raising the hypothesis that genetic and environmental factors are also involved (Houba, 1979). Although it is well-known that *P. malariae*-associated

renal impairment is caused mainly because of immune complex deposits, there are no studies investigating if autoantibodies are involved in this process.

In *P. falciparum* malaria, acute renal failure is a common and serious complication in non-immune adults and adolescents and is more frequent in patients from non-endemic regions (Barsoum, 2000; Elsheikha and Sheashaa, 2007; Nguansangiam et al., 2007), but it can also occur in pediatric severe malaria (Olowu and Adelusola, 2004; von Seidlein et al., 2012; Conroy et al., 2016; Sypniewska et al., 2017; Rivera-Correa et al., 2019b). Although it is an important clinical manifestation associated with mortality and morbidity, the pathogenesis of renal failure in *P. falciparum* malaria is not well understood. However, unlikely *P. malariae*-associated renal failure, acute kidney injury in *P. falciparum* infection is usually transient and disappears after treatment (van Velthuysen and Florquin, 2000), suggesting that the parasite does not have a great role in the pathogenesis that is most likely to be caused by host's immune response. Several hypothesis on the pathogenesis of malarial renal failure have been proposed, including mechanical obstruction of glomerular and tubulointerstitial capillaries by infected erythrocytes (Seydel et al., 2006; Nguansangiam et al., 2007), possibly leading to renal ischemia (Conroy et al., 2016); immune complex deposits leading to renal impairment (Frutakul et al., 1974); and autoantibodies against nucleic acids (Wozencraft et al., 1990; Rivera-Correa et al., 2019b).

In a children population from Uganda, Rivera-Correa et al. (2019b) demonstrated that infants with severe *P. falciparum* malaria manifesting acute kidney injury have autoantibodies against nucleic acid and lipids. Additionally, they found a correlation between those autoantibodies and creatinine and blood urea nitrogen levels, two indicators of kidney health, suggesting that such immunoglobulins may play a role in kidney injury. It was also shown that anti-DNA autoantibodies were elevated in children with acute kidney injury, a result that is in accordance with Wozencraft et al. (1990), who obtained similar data, however, in mouse malaria. It is important to mention that no difference was found in levels of antibodies against parasite antigen, indicating that systemic changes in IgG metabolism and immune-mediated pathways may contribute to malaria-associated renal failure. This result corroborates the findings from Frutakul et al. (1974), who reported an absence of antibodies against parasite antigens in immune complexes deposited in glomeruli capillary walls from a Thai child's kidney. All these data demonstrate that renal dysfunction due to autoantibodies may be relevant in severe *P. falciparum*-associated renal failure. Future investigations should be conducted to further understand the role of those autoantibodies, their involvement in renal pathogenesis, as well as their use as disease biomarkers.

ANEMIA

Anemia is the most common feature and a major concern in malaria, mainly in young children and pregnant women (Accrombessi et al., 2015; Kenangalem et al., 2016; White, 2018). Despite its relevance, the pathogenesis of malaria-associated anemia is complex, and still incompletely understood. Malaria-induced anemia is thought to arise from the rupture of infected and non-infected red blood cells (nRBCs), as well as inappropriate erythropoiesis in the erythroid germinal centers (Douglas et al., 2012; White, 2018). But the greater loss is due to the clearance of nRBCs, which persist long after infection has resolved (Looareesuwan et al., 1987; Ritter et al., 1993; Collins et al., 2003; Douglas et al., 2012). An autoimmune component has been suggested to explain this removal, although the mechanisms underlying autoimmunity in malarial anemia have not been thoroughly explored (White, 2018; Rivera-Correa and Rodriguez, 2019). Self-reactive antibodies that recognize RBCs have been documented in plasmodial infections since 1970s, when host-serum components associated with the surface of nRBCs were detected in patients with malaria using different methodologies (Rosenberg et al., 1973; Facer et al., 1979; Berzins et al., 1983; Fernandez-Arias et al., 2016; Mourão et al., 2016). However, their roles in the pathophysiology of anemia have not been thoroughly explored. Evidence in this line is given by studies that have shown a reduction in RBC life span following the clearance of *P. falciparum* (Looareesuwan et al., 1987). This reduction in RBC survival time has been observed mainly in anemic patients and is associated with the deposition of complement containing immune complexes on RBCs surface (Rosenberg et al., 1973). Furthermore, it has been demonstrated that autoantibodies against triosephosphate isomerase purified from patients with *P. falciparum* malaria can bind to RBCs, promoting their lysis and activating complement cascade thereby, contributing to anemia (Ritter et al., 1993).

Since these early findings, autoantibodies with other specificities have already been identified and associated to anemia in malaria. This is the case of anti-phosphatidylserine (PS) antibodies, which were found to tag nRBCs exposing phosphatidylserine (Fernandez-Arias et al., 2016; Barber et al., 2019; Rivera-Correa et al., 2019a). These self-reactive immunoglobulins have been shown to increase *in vitro* phagocytosis and *in vivo* clearance of nRBCs, contributing to malarial anemia in a murine model (Fernandez-Arias et al., 2016). Moreover, a negative correlation between the magnitude of anti-PS antibodies and hemoglobin levels has been reported for patients infected with *P. falciparum* and *P. vivax* (Barber et al., 2019; Rivera-Correa et al., 2019a,b). In addition, it has been demonstrated that a population of atypical B cells, which is characterized by the expression of CD11c and T-bet, secretes anti-PS antibodies. The activation of these cells has been shown to be dependent of parasite DNA and different receptors have been suggested to be involved such as interferon-γ receptor (IFN-γR), B-cell receptor (BCR) and Toll-like receptor 9 (TLR9) (Rivera-Correa et al., 2017). However, the role of such atypical cells in human malaria was still unknown until a recent evidence has emerged from a study conducted with *P. falciparum*-infected returned travelers (Rivera-Correa et al., 2019a). In this study, it has been shown that $FcRL5^{+}T\text{-}bet^{+}$ B-cells are expanded in acute malaria. Additionally, it has been observed that naïve human peripheral blood mononuclear cells are able to produce anti-PS antibodies when stimulated with lysates of *P. falciparum*-infected

TABLE 1 | Autoantibodies against self-antigens and their implications in *P. falciparum* and *P. vivax* malaria.

Self antigen	Possible functional activity of self-reactive antibody	Clinical outcome	References
14-3-3 ε brain protein	Degranulation of mast cells, basophils, eosinophils and/or monocytes/macrophages	Protection against severe *Plasmodium falciparum* malaria	Duarte et al., 2012
Beta tubulin III (TBB3)	Cytoplasm microtubule disruption	Cerebral malaria associated to *P. falciparum*	Füchtbauer et al., 1985; Bansal et al., 2009
Dendritic tree of Purkinje cell	*In vitro* inhibition of Purkinje cells development	Cerebral malaria associated to *P. falciparum*	Calvet et al., 1993; Gallien et al., 2011
Erythrocyte band 3 protein	Rigidity increase and *in vitro* clearance of non-parasitized RBCs	Anemia associated to *Plasmodium vivax*	Mourão et al., 2016, 2018
	In vitro P. falciparum cythoadherence blockage and *in vivo* adherence of RBCs; parasite growth inhibition	Protection against *P. falciparum* malaria	Hogh et al., 1994 ; Brahimi et al., 2011
Lipids	Kidney injury through immune complex deposition	Renal failure associated to *P. falciparum* malaria	Frutakul et al., 1974; Rivera-Correa et al., 2019b
Non-erythroid alpha spectrin	Disruption of brain cells cytoskeleton; complement activation and amplification of neuronal damage	Cerebral malaria associated to *P. falciparum*	Guiyedi et al., 2007
Nucleic acids	Kidney injury through immune complex deposition	Renal failure associated to *P. falciparum* malaria	Frutakul et al., 1974; Rivera-Correa et al., 2019b
Phosphatidylserine	Phagocytosis (*in vitro*) and clearance of non-parasitized RBCs	Anemia associated to *P. falciparum* and *P. vivax*	Fernandez-Arias et al., 2016; Barber et al., 2019; Rivera-Correa et al., 2019a
Spectrin	Disruption of RBCs cytoskeleton; amplification of RBCs damage	Anemia associated to *P. vivax*	Mourão et al., 2018
Triose-phosphate isomerase	*In vitro* lysis of RBC and activation of complement	Anemia associated to *P. falciparum*	Ritter et al., 1993
Voltage-gated calcium channels (VGCC)	Complement-independent downregulation of calcium flow in Purkinge and granule cells	Cerebral malaria associated to *P. falciparum*	Lang et al., 2005

RBCs, highlighting such atypical subset of memory B cells as a major promoter of autoimmune anemia in malaria. Besides anti-PS antibodies, self-reactive immunoglobulins triggered by other host cell targets are also involved in RBCs lysis, as it has been evidenced in a complement lysis assay using annexin V to block the binding of anti-PS antibodies to phosphatidylserine. After the binding of annexin to PS, RBC lysis could be partially inhibited by plasma from *P. falciparum*-infected patients (Rivera-Correa et al., 2019a).

Autoantibodies against RBCs have also been described for *P. vivax* infections (Mourão et al., 2016, 2018; Ventura et al., 2018; Barber et al., 2019). However, since this parasite has unique biological features that restricts its invasion to reticulocytes, lower densities of peripheral parasitemia are generally expected for infections due to *P. vivax* in comparison to *P. falciparum*. But despite this, *P. vivax* causes a greater loss of nRBCs. Thus, it is possible that the mechanisms leading to nRBCs removal in *P. vivax* malaria are distinct from those observed from *P. falciparum*. More work is needed to elucidate this.

Different erythrocytic antigens have been shown to be recognized by self-reactive immunoglobullins from anemic *P. vivax*-infected patients such as band 3 (Mourão et al., 2018), an anion exchanger protein which mediates the change of intracellular bicarbonate (HCO_3^-) to extracellular chloride (Cl^-) (Cordat and Reithmeier, 2014). Since IgGs purified from the same patients can bind to the surface of non-parasitized RBCs, increasing their rigidity and enhancing their clearance by THP-1 phagocytes (Mourão et al., 2018), it is also possible that anti-RBCs antibodies mediate malarial anemia through erythrophagocytosis or through decreasing RBC deformability (Mourão et al., 2016). Other possibility is the withdrawn from circulation by mechanisms like those tagging senescent RBCs for clearance (Lutz and Bogdanova, 2013), a hypothesis that should be better investigated.

Other RBC protein that has also been considered a target for autoimmune responses during *P. vivax* malaria is spectrin, although it is still unclear how anti-spectrin antibodies bind to an inner component of RBC membrane. Since *in silico* analysis revealed that human spectrin primary structure shares homology with a *P. vivax* hypothetical protein, it is possible that molecular mimicry drives autoimmune response against human spectrin (Mourão et al., 2018), a hypothesis that needs to be experimentally validated.

On the other hand, no association between anti-RBCs antibodies and anemia has been observed in a study conducted with *P. vivax*-infected children and adolescents from Pará, a State located in Brazilian Amazon (Ventura et al., 2018). A similar result was also found by (Fernandes et al., 2008), who evaluated the frequency of malarial anemia, as well as cytokines and autoantibodies levels, in an area in which *P. vivax* and *P. falciparum* coexists. It is important to mention that despite no significant association has been found in both studies,

BOX 1 | Outstanding questions in autoimmunity-mediated pathology in malaria:

- Which mechanisms are behind the generation of self-reactive antibodies in malaria?
- What are the self-antigens that trigger auto-immune responses in *P. falciparum* and *P. vivax* malaria?
- How self-reactive antibodies penetrate the blood-brain barrier, a high selective barrier that protects the central nervous system from invaders? Do they cross independently or do plasma cells secrete them?
- Do self-reactive antibody responses change with anti-malarial therapy?
- Is there any association between autoantibodies that persist after parasite clearance and long-term complications?
- What is the prevalence and the magnitude of autoantibody responses in different epidemiological settings?
- Can anti-self-antibody blockage prevent pathology?

higher frequency of anti-RBCs antibodies has been reported in patients with malaria (Fernandes et al., 2008; Ventura et al., 2018).

In other reports, a beneficial role has been attributed to anti-RBCs antibodies. This is the case of a study carried out in an area of intense transmission of malaria in Liberia, where it has been shown that immune responses to band 3 neoantigens are correlated with lower *P. falciparum* parasitemia and can block *in vitro* and *in vivo* RBCs' cytoadherence (Hogh et al., 1994). Moreover, an anti-plasmodial activity has been proposed to autoantibodies from patients with autoimmune diseases, which were able to inhibit parasite growth, suggesting a protective role for those molecules, although the authors have not ruled out the involvement of other serum components (Brahimi et al., 2011). Since the pathways involved in autoantibody-induced pathology differ among infections due to different parasites, it is possible that self-reactive antibodies exert diverse effects in infections by *P. vivax* and *P. falciparum*, an issue that should be target of future investigation.

As can be noted by the findings mentioned above, the literature concerning self-reactive antibodies against RBCs suggest a dual role for these immunoglobulins in malaria-associated anemia. But crucial gaps remain to be addressed **(Box 1)**.

These scientific breakthroughs will allow the use of autoantibodies as signatures to predict disease severity or protection, as well as provide insights toward the best vaccination strategies. Furthermore, they will open new therapeutic possibilities to treat malarial anemia.

CONCLUDING REMARKS

Studies regarding autoantibodies and plasmodial infections have indicated that those molecules may play a dual role in malaria (**Figure 1** and **Table 1**). However, it is not clear if self-reactive antibodies lead to pathogenesis or are just a consequence of plasmodial infection. Although different self-reactive antibodies have been identified in distinct populations and associated with clinical complications, their epitopes as well as their origin and functional role remains to be elucidated. This information will be essential to the search and identification of epitopes and other molecules that can hijacks pathogenic autoantibodies from circulation, minimizing or inhibiting their pathogenic effects in host cells. This is an interesting field of work that should be focus of future investigation using *in vitro* and *in vivo* models. Since few reports have associated autoantibodies to protection, this is an issue that should also be better investigated. Additionally, it would be of interest to determine the prevalence and the magnitude of self-reactive responses in cohorts from different epidemiological settings, an analysis that should be extended including prospective studies. The role of self-immunoglobulins isotypes and IgG subclasses is another gap that should also be addressed. A better knowledge of all these points (**Box 1**) may allow the use of autoantibodies as signatures to predict malaria clinical outcome. Furthermore, it may open new therapeutic possibilities to treat malaria-associated complications besides have implications for other autoimmune diseases.

AUTHOR CONTRIBUTIONS

LM, GC-O, and EB conceptualized and wrote the manuscript.

FUNDING

Funding for preparation of this review: CNPq (404365/2016-7 and 154378/2018-6), CAPES (88887.472593/2019-00), FAPEMIG (APQ-00361-16).

REFERENCES

Accrombessi, M., Ouédraogo, S., Agbota, G. C., Gonzalez, R., Massougbodji, A., Menéndez, C., et al. (2015). Malaria in pregnancy is a predictor of infant haemoglobin concentrations during the first year of life in Benin, West Africa. *PLoS ONE* 10:e0129510. doi: 10.1371/journal.pone.0129510

Adebajo, A. O., Charles, P., Maini, R. N., and Hazleman, B. L. (1993). Autoantibodies in malaria, tuberculosis and hepatitis B in a west African population. *Clin. Exp. Immunol.* 92, 73–76. doi: 10.1111/j.1365-2249.1993.tb05950.x

Adu, D., Williams, D. G., Quakyi, I. A., Voller, A., Anim-Addo, Y., Bruce-Tagoe, A. A., et al. (1982). Anti-ssDNA and antinuclear antibodies in human malaria. *Clin. Exp. Immunol.* 49, 310–316

Antonelli, L. R., Junqueira, C., Vinetz, J. M., Golenbock, D. T., Ferreira, M. U., and Gazzinelli, R. T. (2019). The immunology of *Plasmodium vivax* malaria. *Immunol. Rev.* 293, 163–189. doi: 10.1111/imr.12816

Badiane, A. S., Diongue, K., Diallo, S., Ndongo, A. A., Diedhiou, C. K., Deme, A. B., et al. (2016). Acute kidney injury associated with *Plasmodium malariae* infection. *Malar. J.* 13:226. doi: 10.1186/1475-2875-13-226

Bansal, D., Herbert, F., Lim, P., Deshpande, P., Bécavin, C., Guiyedi, V., et al. (2009). IgG autoantibody to brain beta tubulin III associated with cytokine

cluster-II driscriminate cerebral malaria in central India. *PLoS ONE* 4:e8245. doi: 10.1371/journal.pone.0008245

Barber, B. E., Grigg, M. J., Piera, K., Amante, F. H., William, T., Boyle, M. J., et al. (2019). Antiphosphatidylserine immunoglobulin M and immunoglobulin G antibodies are higher in vivax than falciparum malaria, and associated with early anemia in both species. *J. Infect. Dis.* 220, 1435–1443. doi: 10.1093/infdis/jiz334

Barsoum, R. S. (2000). Malarial acute renal failure. *J. Am. Soc. Nephrol.* 11, 2147–2154. doi: 10.46-6673/1111-2147

Bell, K., Wilding, C., Funke, S., Pfeiffer, N., and Grus, F. H. (2015). Protective effect of 14-3-3 antibodies on stressed neuroretinal cells via the mitochondrial apoptosis pathway. *BMC Ophthalmol.* 15:64. doi: 10.1186/s12886-015-0044-9

Berzins, K., Wahlgren, M., and Perlmann, P. (1983). Studies on the specificity on anti-erythrocyte antibodies in the serum of patients with malaria. *Clin. Exp. Immunol.* 54, 313–318.

Birbeck, G. L., Molyneux, M. E., Kaplan, P. W., Seydel, K. B., Chimalizeni, Y. F., Kawaza, K., et al. (2010). Blantyre malaria project epilepsy study (BMPES) of neurological outcomes in retinopathy-positive paediatric cerebral malaria survivors: a prospective cohort study. *Lancet* 9, 1173–1181. doi: 10.1016/S1474-4422(10)70270-2

Brahimi, K., Martins, Y. C., Zanini, G. M., Ferreira-da-Cruz, M. F., and Daniel-Ribeiro, C. T. (2011). Monoclonal auto-antibodies and sera of autoimmune patients react with *Plasmodium falciparum* and inhibit its *in vitro* growth. *Mem. Inst. Oswaldo Cruz* 106, 44–51. doi: 10.1590/s0074-02762011000900006

Brown, H., Rogerson, S., Taylor, T., Tembo, M., Mwenechanya, J., Molyneux, M., et al. (2001). Blood-brain barrier function in cerebral malaria in Malawian children. *Am. J. Trop. Med. Hyg.* 64, 207–213. doi: 10.4269/ajtmh.2001.64.207

Burchard, G. D., Ehrhardt, S., Mockenhaupt, F. P., Mathieu, A., Agana-Nsiire, P., Anemana, S. D., et al. (2003). Renal dysfunction in children with uncomplicated *Plasmodium falciparum* malaria in Tamale, Ghana. *Ann. Trop. Med. Parasit.* 97, 345–350. doi: 10.1179/000349803235002281

Calvet, M. C., Druilhe, P., Camacho-Garcia, R., and Calvet, J. (1993). Culture model for the study of cerebral malaria: antibodies from *Plasmodium falciparum*-infected comatose patients inhibit the dendritic development of Purkinje cells. *J. Neurosci. Res.* 36, 235–240. doi: 10.1002/jnr.490360214

Collins, W. E., Jeffery, G. M., and Roberts, J. M. (2003). A retrospective examination of anemia during infection of humans with *Plasmodium vivax*. *Am. J. Trop. Med.* 68, 410–412.

Conroy, A. L., Hawkes, M., Elphinstone, R. E., Morgan, C., Hermann, L., Barker, K. R., et al. (2016). Acute kidney injury is common in pediatric severe malaria and is associated with increased mortality. *Open Forum Infect. Dis.* 3:ofw046. doi: 10.1093/ofid/ofw046

Cordat, E., and Reithmeier, R. A. (2014). Structure, function, and trafficking of SLC4 and SLC26 anion transporters. *Curr. Top. Membr.* 73, 1–67. doi: 10.1016/B978-0-12-800223-0.00001-3

Cornell, B., and Toyo-Oka, K. (2017). 14-3-3 proteins in brain development: neurogenesis, neuronal migration and neuromorphogenesis. *Front. Mol. Neurosci.* 10:318. doi: 10.3389/fnmol.2017.00318

Couper, K. N., Barnes, T., Hafalla, J. C. R., Combes, V., Ryffel, B., Secher, T., et al. (2010). Parasite-derived plasma microparticles contribute significantly to malaria infection-induced inflammation through potent macrophage stimulation. *PLoS Pathog.* 6:e1000744. doi: 10.1371/journal.ppat.1000744

Damian, R. T. (1964). Molecular mimicry: antigen sharing by parasite and host and its consequences. *Am. Nat.* 98, 129–149.

Daniel-Ribeiro, C., Druilhe, P., Monjour, L., Homberg, J. C., and Gentilini, M. (1983). Specificity of auto-antibodies in malaria and the role of polyclonal activation. *Trans. R. Soc. Trop. Med. Hyg.* 77, 185–188. doi: 10.1016/0035-9203(83)90064-0

Das, B. S. (2008). Renal failure in malaria. *J. Vector Borne Dis.* 45, 83–97.

Donati, D., Zhang, L. P., Chêne, A., Chen, Q., Flick, K., Nyström, M., et al. (2004). Identification of a polyclonal B-cell activator in *Plasmodium falciparum*. *Infect. Immun.* 72, 5412–5418. doi: 10.1128/IAI.72.9.5412-5418.2004

Douglas, N. M., Anstey, N. M., Buffet, P. A., Poespoprodjo, J. R., Yeo, T. W., White, N. J., et al. (2012). The anaemia of *Plasmodium vivax* malaria. *Malar. J.* 11:135. doi: 10.1186/1475-2875-11-135

Duarte, J., Herbert, F., Guiyedi, V., Franetich, J. F., Roland, J., Cazenave, P. A., et al. (2012). High levels of immunoglobulin E autoantibody to 14-3-3 epsilon protein correlate with protection against severe *Plasmodium falciparum* malaria. *J. Infect. Dis.* 206, 1781–1789. doi: 10.1093/infdis/jis595

Elsheikha, H. M., and Sheashaa, H. A. (2007). Epidemiology, pathophysiology, management and outcome of renal dysfunction associated with plasmodia infection. *Parasitol. Res.* 101, 1183–1190. doi: 10.1007/s00436-007-0650-4

Facer, C. A., and Agiostratidou, G. (1994). High levels of anti-phospholipid antibodies in uncomplicated and severe *Plasmodium falciparum* and *P. vivax malaria. Clin. Exp. Immunol.* 95, 304–309. doi: 10.1111/j.1365-2249.1994.tb06528.x

Facer, C. A., Bray, R. S., and Brown, J. (1979). Direct Coombs antiglobulin reactions in Gambian children with *Plasmodium falciparum* malaria. I. incidence and class specificity. *Clin. Exp. Immunol.* 35, 119–127.

Fernandes, A. A., Carvalho, L. J., Zanini, G. M., Ventura, A. M., Souza, J. M., Cotias, P. M., et al. (2008). Similar cytokine responses and degress of anemia in patients with *Plasmodium falciparum* and *Plasmodium vivax* infections in the Brazilian Amazon region. *Clin. Vaccine Immunol.* 15, 650–658. doi: 10.1128/CVI.00475-07

Fernandez-Arias, C., Rivera-Correa, J., Gallego-Delgado, J., Rudlaff, R., Fernandez, C., Roussel, C., et al. (2016). Anti-self-phosphatidylserine antibodies recognize uninfected erythrocytes promoting malarial anemia. *Cell Host Microbe.* 19, 194–203: doi: 10.1016/j.chom.2016.01.009

Flanagan, K. L., Plebanski, M., Odhiambo, K., Sheu, E., Mwangi, T., Gelder, C., et al. (2006). Cellular reactivity to the *P. falciparum* protein TRAP in adult kenyans: novel epitopes, complex cytokine patterns, and yhe impact of natural antigenic variation. *Am. J. Trop. Med. Hyg.* 74, 367–375.

Fontaine, A., Pophillat, M., Bourdon, S., Villard, C., Belghazi, M., Fourget, P., et al. (2010). Specific antibody responses against membrane proteins of erythrocytes infected by *Plasmodium falciparum* of individuals briefly exposed to malaria. *Malar. J.* 9:276. doi: 10.1186/1475-2875-9-276

Foote, M., and Zhou, Y. (2012). 14-3-3 proteins in neurological disorders. *Int. J. Biochem. Mol. Biol.* 3, 152–164.

Freeman, R. R., and Parish, C. R. (1978). Polyclonal B-cell activation during rodent malarial infections. *Clin. Exp. Immunol.* 32, 41–45

Frutakul, P., Boonpucknavig, V., Boonpucknavig, S., Mitrakul, C., and Bhamarapravati, N. (1974). Acute glomerulonephritis complicating *Plasmodium falciparum* infection. *Clin. Pediatr.* 13, 281–283. doi: 10.1177/000992287401300315

Füchtbauer, A., Herrmann, M., Mandelkowl, E., and Jockusch, M. (1985). Disruption of microtubules in living cells and cell models by high affinity antibodies to beta-tubulin. *EMBO.* 4, 2807–2814.

Fujinami, R. S., von Herrath, M. G., Christen, U., and Whitton, J. L. (2006). Molecular mimicry, bystander activation, por viral persistence: infections and autoimmune disease. *Clin. Microbiol. Rev.* 19, 80–94. doi: 10.1128/CMR.19.1.80-94.2006

Gallien, S., Roussilhon, C., Blanc, C., Pérignon, J. L., and Druilhe, P. (2011). Autoantibody against dendrite in *Plasmodium falciparum* infection: a singular auto-immune phenomenon preferentially in cerebral malaria. *Acta Trop.* 118, 67–70. doi: 10.1016/j.actatropica.2011.01.005

Gitau, E. N., Kokwaro, G. O., Karanja, H., Newton, C. R., and Ward, S. A. (2013). Plasma and cerebrospinal proteomes from children with cerebral malaria differ from those of children with other encephalopathies. *J. Infect. Dis.* 208, 1494–1503. doi: 10.1093/infdis/jit334

Greenwood, B. M. (1974). Possible role of a B-cell mitogen in hypergammaglobulinaemia in malaria and trypanosomiasis. *Lancet* 1, 435–436. doi: 10.1016/s0140-6736(74)92386-1

Guiyedi, V., Chanseaud, Y., Fesel, C., Snounou, G., Rousselle, J. C., Lim, P., et al. (2007). Self-reactivities to the non-erythroid alpha spectrin correlate with cerebral malaria in Gabonese children. *PLoS ONE* 2:e389. doi: 10.1371/journal.pone.0000389

Haneji, N. T., Nakamura, K., Takio, K., Yanagi, H., and Higashiyama, I. (1997). Identification of alpha-fodrin as a candidate autoantigen in primary Sjogren's syndrome. *Science*, 276, 604–607. doi: 10.1126/Science.276.5312.604

Hogh, B., Petersen, E., Crandall, I., Gottschau, A., and Sherman, I. W. (1994). Immune responses to band 3 neoantigens on *Plasmodium falciparum*-infected erythrocytes in subjects living in an area of intense malaria transmission are associated with low parasite density and high hematocrit value. *Infect. Immunol.* 62, 4362–4366.

Holmgren, A. M., McConkey, C. A., and Shin, S. (2017). Outrunning the red queen: bystander activation as a means of outpacing innate immune subversion by intracellular pathogens. *Cell. Mol. Immmunol.* 14, 14–21.

Houba, V. (1979). Immunologic aspects of renal lesions associated with malaria. *Kidney Int.* 16, 3–8. doi: 10.1038/ki.1979.96

Houba, V., Allison, A. C., Adeniyi, A., and Houba, J. E. (1971). Immunoglobulin classes and complement biopsies of Nigerian children with the nephrotic syndrome. *Clin. Exp. Immunol.* 8, 761–774.

Huerta, P. T., Kowal, C., DeGiorgio, L. A., Volpe, B. T., Diamond, B. (2006). Immunity and behavior: antibodies alter emotion. *Proc. Natl. Acad. Sci. U.S.A.* 103, 678–683. doi: 10.1073/pnas.0510055103

Idro, R., Marsh, K., John, C. C., Newton, C. R. (2010). Cerebral malaria: mechanisms of brain injury and strategies for improved neurocognitive outcome. *Pediatr. Res.* 68, 267–274. doi: 10.1203/00006450-201011001-00524

Irani, S., and Lang, B. (2008). Autoantibody-mediated disorders of the central nervous system. *Autoimmunity* 41, 55–65. doi: 10.1080/08916930701619490

Jakobsen, P. H., Morris-Jones, S. D., Hviid, L., Theander, T. G., Høier-Madsen, M., Bayoumi, R. A., et al. (1993). Anti-phospholipid antibodies in patients with *Plasmodium falciparum* malaria. *Immunology* 79, 653–657.

Katsetos, G. D., Herman, M. M., and Mörk, S. J. (2003). Class III β-tubullin in human development and cancer. *Cell Motil. Cytoskeleton* 55, 77–96. doi: 10.1002/cm.10116

Kenangalem, E., Karyana, M., Burdarm, L., Yeung, S., Simpson, J. A., Tjitra, E., et al. (2016). *Plasmodium vivax* infection: a major determinant of severe anaema in infancy. *Malar. J.* 15:321. doi: 10.1186/s12936-016-1373-8

Lacerda, M. V., Mourão, M. P., Coelho, H. C., and Santos, J. B. (2011). Thrombocytopenia in malaria: who cares? *Mem. Inst. Oswaldo Cruz*. 106(Suppl. 1), 52–63. doi: 10.1590/s0074-02762011000900007

Lang, B., Newbold, C. I., Williams, G., Peshu, N., Marsh, K., and Newton, C. R. (2005). Antibodies to voltage-gated calcium channels in children with falciparum malaria. *J. Infect. Dis.* 191, 117–121. doi: 10.1086/426512

Looareesuwan, S., Merry, A. H., Phillips, R. E., Pleehachinda, R., Wattanagoon, Y., Ho, M., et al. (1987). Reduced erythrocyte survival following clearance of malarial parasitaemia in Thai patients. *Br. J. Haematol.* 67, 473–478. doi: 10.1111/j.1365-2141.1987.tb06171.x

Ludin, P., Nilsson, D., and Maser, P. (2011). Genome-wide identification of molecular mimicry candidates in parasites. *PLoS One* 6:e17546. doi: 10.1371/journal.pone.0017546

Ludwig, R. J., Vanhoorelbeke, K., Leypoldt, F., Kaya, Z., Bieber, K., McLachlan, S. M., et al. (2017). Mechanisms of autoantibody-induced pathology. *Front. Immunol.* 8:603. doi: 10.3389/fimmu.2017.00603

Lutz, H. U., and Bogdanova, A. (2013). Mechanisms tagging senescent red blood cells for clearance in healthy humans. *Front. Physiol.* 4:387. doi: 10.3389/fphys.2013.00387

MaCDonald, S. M., Bhisutthiban, J., Shapiro, T. A., Rogerson, S. J., Taylor, T. E., Tembo, M., et al. (2001). Immune mimicry in malaria: *Plasmodium falciparum* secretes a functional histamine-releasing factor honmolog *in vitro* and *in vivo*. *Proc. Natl. Acad. Sci. U.S.A.* 98, 10829–10832. doi: 10.1073/pnas.201191498

Mantel, P., Hoang, A.n., Goldowitz, I., Potashnikova, D., Hamza, B., Vorobjev, I., et al. (2013). Malaria-infected erythrocyte-derived microvesicles mediate cellular communication within the parasite population and with the host immune system. *Cell Host Microbe.* 13, 521–534. doi: 10.1016/j.chom.2013.04.009

Minoprio, P. (2001). Parasite polyclonal activators: new targets for vaccination approaches? *Int. J. Parasitol.* 31, 583–591. doi: 10.1016/S0020-7519(01)00171-0

Molyneux, M. E., Taylor, T. E., Wirima, J. J., and Borgstein, A. (1989). Clinical features and prognostic indicators in paediatric cerebral malaria: a study of 131 comatose Malawian children. *Q. J. Med.* 71, 441–459.

Mourão, L. C., Baptista, R. P., Almeida, Z. B., Grynberg, P., Pucci, M. M., Castro-Gomes, T., et al. (2018). Anti-band 3 and anti-spectrin antibodies are increased in *Plasmodium vivax* infection and are associated with anemia. *Sci. Rep.* 6:8762. doi: 10.1038/s41598-018-27109-6

Mourão, L. C., Roma, P. M., Sultane-Aboobacar, J. S., Medeiros, C. M., de Almeida, Z. B., Fontes, C. J., et al. (2016). Anti-erythrocyte antibodies may contribute to anaemia in *Plasmodium vivax* malaria by decreasing red blood cell deformability and increasing erythrophagocytosis. *Malar. J.* 15:397. doi: 10.1186/s12936-016-1449-5

Moxon, C. A., Gibbins, M. P., McGuinness, D., Milner, D. A., and Marti, M. (2019). New insights into malaria pathogenesis. *Annu. Rev. Pathol.* 15. doi: 10.1146/annurev-pathmechdis-012419-032640

Münz, C., Lünemann, J. D., Getts, M. T., and Miller, S. D. (2009). Antiviral immune responses: triggers of or triggered by autoimmunity? *Nat. Rev. Immunol.* 9, 246–258. doi: 10.1038/nri2527

Nath, R., Raser, K. J., Stafford, D. (1996). Non-erythroid alpha-spectrin breakdown by calpain and interleukin I beta-converting-enzyme-like protease(s) in apoptotic cells: contributory roles of both protease families in neuronal apoptosis. *Biochem. J.* 319, 683–690. doi: 10.1042/bj3190683

Neri, S., Pulvirenti, D., Patamia, I., Zoccolo, A., and Castellino, P. (2008). Acute renal failure in *Plasmodium malariae* infection. *Neth. J. Med.* 66, 166–168.

Nguansangiam, S., Day, N. P. J., Hien, T. T., Mai, N. T. H., Chaisri, U., Riganti, M., et al. (2007). A quantitative ultrastructural study of renal pathology in fatal *Plasmodium falciparum* malaria. *Trop. Med. Int. Health.* 12, 1037–1050. doi: 10.1111/j.1365-3156.2007.01881.x

Olowu, W. A., and Adelusola, K. A. (2004). Pediatric acute renal failure in southwestern Nigeria. *Kidney Int.* 66, 1541–1548. doi: 10.1111/j.1523-1755.2004.00918.x

Pinto, A., Gillard, S., Moss, F., Whyte, K., Brust, P., Williams, M., et al. (1998). Human autoantibodies specific for the alpha1A calcium channel subunit reduce both P-type and Q-type calcium currents in cerebellar neurons. *Proc. Natl. Acad. Sci. U.S.A.* 95, 8328–8333. doi: 10.1073/PNAS.95.14.8328

Ritter, K., Kuhlencord, A., Thomssen, R., and Bommer, W. (1993). Prolonged haemolytic anaemia in malaria and autoantibodies against triosephosphate isomerase. *Lancet* 342, 1333–1334. doi: 10.1016/0140-6736(93)92248-r

Rivera-Correa, J., Conroy, A. L., Opoka, R. O., Batte, A., Namazzi, R., Ouma, B., et al. (2019b). Autoantibody levels are associated with acute kidney injury, anemia and post-discharge morbidity and mortality in Ugandan children with severe malaria. *Sci. Rep.* 9:14840. doi: 10.1038/s41598-019-51426-z

Rivera-Correa, J., Guthmiller, J. J., Vijay, R., Fernandez-Arias, C., Pardo-Ruge, M. A., Gonzalez, S., et al. (2017). *Plasmodium* DNA-mediated TLR9 activation of T-bet^{+} B cells contributes to autoimmune anaemia during malaria. *Nat. Commun.* 8:1282. doi: 10.1038/s41467-017-01476-6

Rivera-Correa, J., Mackroth, M. S., Jacobs, T., Schulze Zur Wiesch, J., Rolling, T., and Rodriguez, A. (2019a). Atypical memory B-cells are associated with *Plasmodium falciparum* anemia through anti-phosphatidylserine antibodies. *Elife* 8:e48309. doi: 10.7554/eLife.48309

Rivera-Correa, J., and Rodriguez, A. (2019). Autoimmune anemia in malaria. *Trends Parasitol.* 36, 91–97. doi: 10.1016/j.pt.2019.12.002

Rosenberg, E. B., Strickland, G. T., Yang, S. L., and Whalen, G. E. (1973). IgM antibodies to red cells and autoimmune anemia in patients with malaria. *Am. J. Trop. Med. Hyg.* 22, 146–152. doi: 10.4269/ajtmh.1973.22.146

Rosenberg, Y. J. (1978). Autoimmune and polyclonal B cell responses during murine malaria. *Nature* 264, 170–172. doi: 10.1038/274170a0

Seydel, K. B., Milner, D. A., Kamiza, S. B., Molyneux, M. E., and Taylor, T. E. (2006). The distribution and intensity of parasite sequestration in comatose Malawian children. *J. Infect. Dis.* 194, 208–205. doi: 10.1086/505078

Shimada, T., Fournier, A. E., and Yamagat, K. (2013). Neuroprotective function of 14-3-3 proteins in neurodegeneration. *Biomed. Res. Int.* 2013:564534. doi: 10.1155/2013/564534

Sypniewska, P., Duda, J. F., Locatelli, I., Althaus, C. R., Althaus, F., Genton, B. (2017). Clinical and laboratory predictors of death in African children with features of severe malaria: a systematic review and meta-analysis. *BMC Med.* 15:147. doi: 10.1186/s12916-017-0906-5

Taylor, T. E., Fu, W. J., Carr, R. A., Whitten, R. O., Mueller, J. S., Fosiko, N. G., et al. (2004). Differentiating the pathologies of cerebral malaria by postmortem parasite counts. *Nat. Med.* 10, 143–145. doi: 10.1038/nm986

Teasdale, G., and Jennett, B. (1974). Assessment of coma and impaired consciousness. *a practical scale. Lancet* 2, 81–84. doi: 10.1016/s0140-6736(74)91639-0

Teo, A., Feng, G., Brown, G. V., Beeson, J. G., and Rogerson, S. J. (2016). Functional antibodies and protection against blood-stage malaria. *Trends Parasitol.* 32, 867–898. doi: 10.1016/j.pt.2016.07.003

Tischfield, M. A., Baris, H. N., Wu, C., Rudolph, G., Van Maldergem, L., He, W., et al. (2010). Human TUBB3 mutations perturb microtubule dynamics, kinesin

interactions, and axon guidance. *Cell* 140, 74–87. doi: 10.1016/j.cell.2009.12.011

van Velthuysen, M. L. F., and Florquin, S. (2000). Glomerulopathy associated with parasitic infections. *Clin. Microbiol. Rev.* 13, 55–66. doi: 10.1128/cmr.13.1.55-66.2000

Vanderlugt, C. L., and Miller, S. D. (2002). Epitope spreading in immune-mediated diseases: implications fior immunotherapy. *Nat. Rev. Immunol.* 2, 85–95. doi: 10.1038/nri724

Ventura, A. M. R. S., Fernandes, A. A. M., Zanini, G. M., Pratt-Riccio, L. R., Sequeira, C. G., do Monte, C. R. S., et al. (2018). Clinical and immunological profiles of anaemia in children and adolescentes with *Plasmodium vivax* malaria in the Pará state. Brazilian Amazon. *Acta Trop.* 181, 122–131. doi: 10.1016/j.actatropica.2018.01.022

von Seidlein, L., Olaosebikan, R., Hendriksen, I. C. E., Lee, S. J., Adedoyin, O. T., Agbenyega, T., et al. (2012). Predicting the clinical outcome of severe falciparum malaria in African children: findings from a large randomized trial. *Clin. Infect. Dis.* 54, 1080–1090. doi: 10.1093/cid/cis034

Ward, P. A., and Kibuka-Musoke, J. W. (1969). Evidence for soluble immune complexes in the pathogenesis of the glomerulonephritis of quartan malaria. *Lancet* 1, 283–285.

White, N. J. (2018). Anaemia and malaria. *Malar. J.* 17:371. doi: 10.1186/s12936-018-2509-9

WHO | World Malaria Report (2019). *WHO. Available online at: https://www.who.int/publications-detail/world-malaria-report-2019 (accessed on January* 02, 2020).

Wozencraft, A. O., Lloyd, C. M., Staines, N. A., and Griffiths, V. J. (1990). Role of DNA-binding antibodies in kidney pathology associated with murine malaria infections. *Infect Immun.* 58, 2156–2164.

Conflict of Interest: The authors declare that the research was conducted in the absence of any commercial or financial relationships that could be construed as a potential conflict of interest.

frontiers in Cellular and Infection Microbiology

ORIGINAL RESEARCH
published: 12 June 2020
doi: 10.3389/fcimb.2020.00247

DH82 Canine and RAW264.7 Murine Macrophage Cell Lines Display Distinct Activation Profiles Upon Interaction With *Leishmania infantum and Leishmania amazonensis*

Natalia Rocha Nadaes[1†], Leandro Silva da Costa[2†], Raissa Couto Santana[1†], Isabel Ferreira LaRocque-de-Freitas[3], Áislan de Carvalho Vivarini[3], Deivid Costa Soares[4], Amanda Brito Wardini[1], Ulisses Gazos Lopes[3], Elvira M. Saraiva[4], Celio Geraldo Freire-de-Lima[3], Debora Decote-Ricardo[1] and Lucia Helena Pinto-da-Silva[1]*

[1] *Instituto de Veterinária, Universidade Federal Rural Do Rio de Janeiro, Seropédica, Brazil,* [2] *Instituto de Bioquímica Médica Leopoldo De Meis, Universidade Federal Do Rio de Janeiro, Rio de Janeiro, Brazil,* [3] *Instituto de Biofísica Carlos Chagas Filho, Universidade Federal Do Rio de Janeiro, Rio de Janeiro, Brazil,* [4] *Instituto de Microbiologia Paulo de Góes, Universidade Federal Do Rio de Janeiro, Rio de Janeiro, Brazil*

Leishmaniasis is an anthropozoonotic disease, and dogs are considered the main urban reservoir of the parasite. Macrophages, the target cells of *Leishmania sp*., play an important role during infection. Although dogs have a major importance in the epidemiology of the disease, the majority of the current knowledge about *Leishmania*–macrophage interaction comes from murine experimental models. To assess whether the canine macrophage strain DH82 is an accurate model for the study of *Leishmania* interaction, we compared its infection by two species of *Leishmania* (*Leishmania infantum* and *L. amazonensis*) with the murine macrophage cell line (RAW264.7). Our results demonstrated that *L. amazonensis* survival was around 40% at 24 h of infection inside both macrophage cell lines; however, a reduction of 4.3 times in *L. amazonensis* infection at 48 h post-infection in RAW 264.7 macrophages was observed. The survival index of *L. infantum* in DH82 canine macrophages was around 3 times higher than that in RAW264.7 murine cells at 24 and 48 h post-infection; however, at 48 h a reduction in both macrophages was observed. Surprisingly at 24 h post-infection, NO and ROS production by DH82 canine cells stimulated with LPS or menadione or during *Leishmania* infection was minor compared to murine RAW264.7. However, basal arginase activity was higher in DH82 cells when compared to murine RAW264.7 cells. Analysis of the cytokines showed that these macrophages present a different response profile. *L. infantum* induced IL-12, and *L. amazonensis* induced IL-10 in both cell lines. However, *L. infantum and L. amazonensis* also induced TGF-β in RAW 264.7. CD86 and MHC expression showed

OPEN ACCESS

Edited by:
Albert Descoteaux, Institut National de la Recherche Scientifique (INRS), Canada

Reviewed by:
Sandra Marcia Muxel, University of São Paulo, Brazil
Fernando Real, INSERM U1016 Institut Cochin, France
Fernando Silveira, University of the Republic, Uruguay
Maria Fernanda Laranjeira-Silva, University of São Paulo, Brazil

***Correspondence:**
Lucia Helena Pinto-da-Silva
lpintosilva@gmail.com

[†] These authors have contributed equally to this work

Specialty section:
This article was submitted to Microbes and Innate Immunity, a section of the journal Frontiers in Cellular and Infection Microbiology

Received: *24 December 2019*
Accepted: *29 April 2020*
Published: *12 June 2020*

Citation:
Nadaes NR, Silva da Costa L, Santana RC, LaRocque-de-Freitas IF, Vivarini ÁC, Soares DC, Wardini AB, Gazos Lopes U, Saraiva EM, Freire-de-Lima CG, Decote-Ricardo D and Pinto-da-Silva LH (2020) DH82 Canine and RAW264.7 Murine Macrophage Cell Lines Display Distinct Activation Profiles Upon Interaction With Leishmania infantum and Leishmania amazonensis. Front. Cell. Infect. Microbiol. 10:247. doi: 10.3389/fcimb.2020.00247

that *L. amazonensis* modulated them in both cell lines. Conversely, the parasite load profile did not show significant difference between both macrophage cell lines after 48 h of infection, which suggests that other mechanisms of *Leishmania* control could be involved in DH82 cells.

Keywords: DH82 canine, RAW 264.7 murine, macrophages, Leishmania infection, oxidative burst, cytokines, arginase activity

INTRODUCTION

Leishmaniasis is an anthropozoonotic disease transmitted by sandflies, presenting a wide array of clinical symptoms, ranging from cutaneous to visceral manifestations. Dogs are considered the main reservoir of the disease, which is present in different countries of the Old and New World, in urban and periurban areas (Dantas-Torres et al., 2012). Canine leishmaniasis is a complex disease with variable clinical signs and different degrees of susceptibility caused mainly by *Leishmania infantum*. It is considered a serious public health problem since *L. infantum* is the causative agent of human visceral leishmaniasis, the more severe form of this disease. However, other species have also been reported in dogs, such as *L. amazonensis, L. mexicana*, and *L. braziliensis* (Gontijo and De Carvalho, 2003; Castro et al., 2007; Valdivia et al., 2017; Paz et al., 2018).

Macrophages are important innate immune cells in the defense against intracellular microorganisms and play an important role in *Leishmania* infection, since they are the target cells infected by the parasite. Superoxide anion (O_2^-) and nitric oxide (NO) are critical molecules in controlling *Leishmania* infection and are produced by macrophages in response to *Leishmania* phagocytosis and after the activation of macrophages by interferon (IFN)-γ and tumor necrosis factor (TNF)-α (Channon et al., 1984; Gantt et al., 2001; Horta et al., 2012).

The majority of the current knowledge about *Leishmania*–macrophage interaction comes from murine experimental models using different macrophage sources, such as peritoneal, bone marrow-derived, or murine cell lineages (Mosser and Rosenthal, 1993; Handman and Bullen, 2002; Naderer and McConville, 2008). The use of a canine macrophage cell line to study the early aspects of *Leishmania* interaction is easier and more practical compared to macrophages obtained from the bone marrow or purified from peripheral blood from dogs. Added to that, the use of a cell line from an animal species that is the parasite reservoir can contribute for a better understanding about infection and cell response differences among murine and canine experimental models.

Some works have reported the use of DH82, a canine macrophage cell line, as a model to study infection by different microorganisms like virus, bacteria, and protozoa (Howerth et al., 2004; Maia et al., 2007; Ponnusamy and Clinkenbeard, 2012; Mendonça et al., 2017). In this study, we evaluated the interaction of DH82 canine macrophages by *L. amazonensis*, the causative agent of a cutaneous and diffuse cutaneous disease, and *L. infantum*, the causative agent of visceral disease, analyzing ROS and NO production, cytokine profile, arginase activity, and surface molecule expression in comparison to RAW264.7 murine macrophages, a cell line widely used in experimental studies. Our results show that DH82 cells have different characteristics in relation to the immune response to *Leishmania* compared to RAW264.7 ones.

MATERIALS AND METHODS

Parasites

Leishmania infantum (MCAN/BR/2008/OP46) isolated from an infected dog from Governador Valadares, Minas Gerais State, Brazil, characterized by molecular techniques and hamster infection (Moreira et al., 2012, 2016), and *Leishmania amazonensis* (MHOM/BR/75/Josefa) were maintained at 26°C in Schneider's insect medium (Sigma) supplemented with 10% heat-inactivated fetal calf serum (Cripion), 10% human urine, and 40 μg mL^{-1} gentamicin (Sigma). In all assays, promastigotes in the stationary phase of growth (5–6 days) were washed twice in phosphate-buffered saline (PBS) pH 7.2) at 2,700 × *g* for 13 min at 22°C, resuspended in PBS, and used throughout.

Macrophages

Murine RAW264.7 macrophages were maintained in RPMI 1640 medium (Sigma) supplemented with 10% FBS (Cripion) at 37°C 5% CO_2. Canine DH82 macrophages, kindly supplied by Prof. Marcelo Bahia Labruna (Faculdade de Medicina Veterinária e Zootecnia, Universidade de São Paulo, SP, Brazil), were cultured in DMEM (Sigma) supplemented with 10% FBS (Cripion) at 37°C 5% CO_2.

Macrophage Interaction Assays

Macrophages (2×10^5/well) adhered to coverslips (Vision Glass) in 24-well plates (Corning, USA) were incubated for 2 h at 37°C 5% CO_2 and then infected with *Leishmania* promastigotes in the ratio of 5 parasites: 1 macrophage. Macrophages interacting with *L. amazonensis* were maintained at 34°C 5% CO_2, whereas cells interacting with *L. infantum* were maintained at 37°C 5% CO_2. After 2 h of infection, some cultures were washed twice with PBS, fixed, and stained using Diff-Quick (Laborclin) and the association index (uptake) evaluated. To determine the infection index, the cultures were kept in culture for 16 h. After rinsing with PBS twice, the cultures were maintained for an additional 24 and 48 h in the same conditions as above. Then, the cells were washed twice in PBS, fixed, and stained as described above. The association (2 h post-infection) and survival (24 or 48 h post-infection) indexes were assessed by multiplying the percentage of infected macrophages by the number of parasites

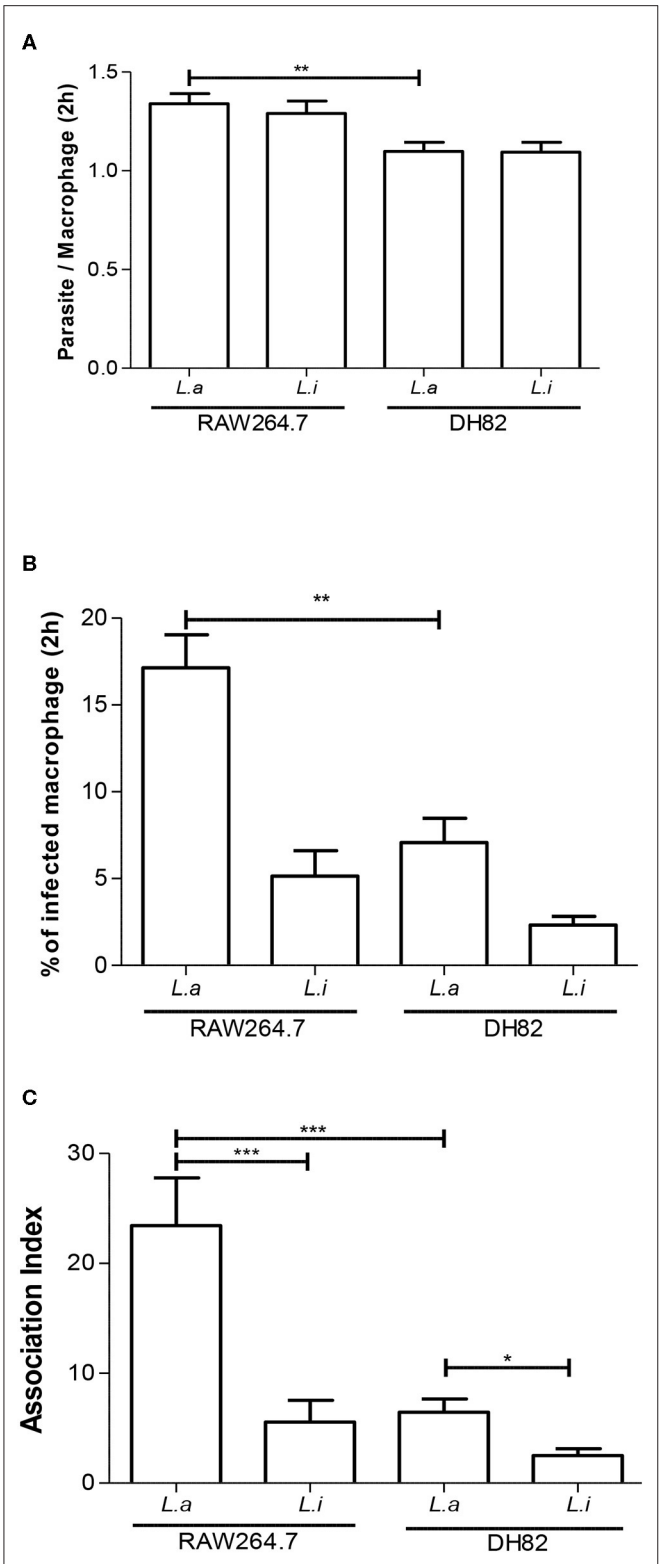

FIGURE 1 | Association index of *Leishmania* in macrophages. Parasite per macrophages **(A)**, % infected macrophages **(B)**, and association index **(C)** in canine DH82 and murine RAW264.7. Macrophages were incubated with *L. amazonensis* (L.a) and *L. infantum* (L.i) promastigotes (5 parasites: 1 macrophage) for 2 h. The data represent mean ± SEM of three independent experiments done in triplicates. $^{***}p < 0.0001$; $^{**}p = 0.0093$; $^{*}p = 0.005$.

per macrophage through randomly counting at least 200 cells in each of triplicate coverslips.

Parasite Load

After 48 h of infection, macrophage cell monolayers were washed and incubated with 0.01% SDS (Sigma) for 10 min to allow lysis of macrophages and the release of amastigotes. Then, cultures were fed with 1 mL of Schneider's medium, supplemented with 10% FCS, and kept at 27°C for an additional 2 days. The relative intracellular load of *L. amazonensis* and *L. infantum* amastigotes was measured by assessing the number of extracellular motile promastigotes transformed (Gomes et al., 2000; Ribeiro-Gomes et al., 2006, 2007).

Detection of Nitric Oxide and ROS Production in DH82 Canine and RAW264.7 Murine Macrophages

The amount of intracellular nitric oxide (NO), total reactive oxygen species (tROS), and mitochondrial ROS (mitROS) was assessed through fluorescent probes. Macrophages (10^6) were plated in 6-well tissue culture plates, stimulated or not with LPS (1 μg/mL) or menadione (0.05 mM) (positive controls) or infected with *L. amazonensis* or *L. infantum* (5 parasites: 1 macrophage). The cultures were maintained for 24 h at 34°C or 37°C/5% CO_2 according to the parasite species. Then, the cells were washed to remove free parasites and were labeled with 1 μM DAF-FM (Molecular Probes), 0.5 μM H_2DCFDA (Thermo Fisher), or 0.25 μM MITOsox (Thermo Fisher). After 45 min in the dark at 37°C, the cells were washed and incubated for more 15 min under the same conditions. Cells were then mechanically released using cell scraper and resuspended in 400 μL of PBS. Stained cells (without any stimuli) were used as negative control to normalize the data in relation to stimulated or infected cells. The percentages of DAF-, DCF-, or MITOsox-positive cells were analyzed by flow cytometry (FACSCalibur) after acquiring 10,000 events. The analyses were performed on the CellQuest program. The gating strategy used in the cytometry evaluation was only to identify a homogeneous macrophages population, since we are working with a culture cell line (**Figure S1**).

Quantitative Real-Time RT-PCR

Total RNA of RAW264.7 and DH82 cells (1×10^6 cells) was extracted with RNeasy Plus Mini Kit (Qiagen 74134, Germany), and 1 μg aliquot was reverse transcribed to first-strand cDNA with ImProm-II (Promega) and oligo(dT) primer according to the manufacturer's instructions. The DNA sequences of the primers used were IL-12-F (mouse): 5′-TCAAGAGCAGTA GCAGTTCCCCTG-3′, IL-12-R (mouse): 5′-GGTCCAGTGTGA CCTTCTCTGCA-3′, IL-12-F (dog): 5′-GCGTCTTCCCTCATG ACC-3′, IL-12-R (dog): 5′-GGGTGCCAGTCCAACTCTAC-3′, IL-10-F (mouse): 5′-CCCAGAAATCAAGGAGCATT-3′, IL-10-R (mouse): 5′-TCACTCTTCACCTGCTCCAC-3′, IL-10-F (dog): 5′-GGTTGCCAGCCCTGTCGG-3′ IL-10-R (dog): 5′-GCGTCGCAGCCTCAGTCTCA-3′, IL-6-F (dog): 5′-GGGA AAGCAGTAGCCATCAC-3′, IL-6-R (dog): 5′-CAGGACCC CAGCTATGAACT-3′, TGF-β-F (mouse): 5′-GTGGCTGA

ACCAAGGAGACGG-3′, TGF-β-R (mouse): 5′-GGCTGATC CCGTTGATTTCCACG-3′, TGF-β-F (dog): 5′-CGAAGCCC TCGACTCC-3′, TGF-β-R (dog): 5′-TGGCTGYCCTTTGATG TCAC-3′, GAPDH-F: 5′-TGCACCACCAACTGCTTAGC-3′ and GAPDH-R: 5′-GGCATGGACTGTGGTCATGAG-3′. qRT-PCR data from the experiments were normalized using Gapdh primers as an endogenous control. Amplicon specificity was carefully verified by the presence of a single melting temperature peak in dissociation curves run after real-time RT-PCR. Real-time quantitative RT-PCR (qRT-PCR) was performed via the Applied Biosystems StepOne™ detection system (Applied Biosystems) using GoTaq® qPCR Master Mix (Promega Corp., Madison, WI, USA). All expression ratios were computed via the analysis of relative gene expression ΔΔCt method through the StepOne software version 2.0 (Applied Biosystems).

Arginase Activity

Uninfected or infected macrophage cell lines stimulated or not with 40 ng/mL of murine interleukin-4 (IL-4, eBioscience) for 24 h were lysed to determine the arginase activity. The macrophage lysates were obtained from 2.5×10^5 cells treated with 100 μL of 0.1% Triton X-100 for 30 min, followed by the addition of 100 μL of a buffer containing 25 mM Tris–HCl (pH 7.4) and 10 μL of 10 mM $MnSO_4$. The enzyme was then activated by heating for 10 min at 56°C, and arginine hydrolysis was carried out by incubating 100 μL of the activated lysate with 100 μL of 0.1 M arginine (pH 9.7) at 37°C for 1 h. The reaction was stopped with 800 μL of H_2SO_4-H_3PO_4-H_2O (1:3:7 [vol/vol/vol]) and 40 μL of 10% α-isonitrosopropiophenone in 100% methanol and heated to 100°C for 30 min. The urea concentration was measured at 540 nm. One unit of enzyme activity was defined as the amount that catalyzed the formation of 1 μmol of urea per min.

MHC and CD86 Expression

The cells were infected or not with *L. infantum and L. amazonensis* and were activated or not by LPS (500 ng/mL). After 24 h post-infection, the cells were detached, washed, adjusted to a concentration of 5.0×10^5 cells/tube, and incubated with blocking buffer (CD16/CD32 Fc Block—eBioscience) for 15 min on ice to prevent non-specific antibody binding to Fc receptors. Cells were stained with anti-dog MHC class II-FITC (Serotech), anti-mouse MHC class II-FITC, and anti-mouse CD86-PECy5 (eBioscience). All washing steps were performed with PBS containing 3% FCS and 0.02% sodium azide. Data were acquired (10,000 events), evaluated on FACSCalibur™ cytometer and analyzed using CellQuest® software (BD Biosciences, Heidelberg, Germany).

Statistical Analysis

Data were analyzed using Student's *t*-test for comparison of two groups or ANOVA for more than three groups with Tukey post-test. Analyses were performed using the GraphPad Prism 5.0 software. The *p*-value was considered significant when equal to or <0.05.

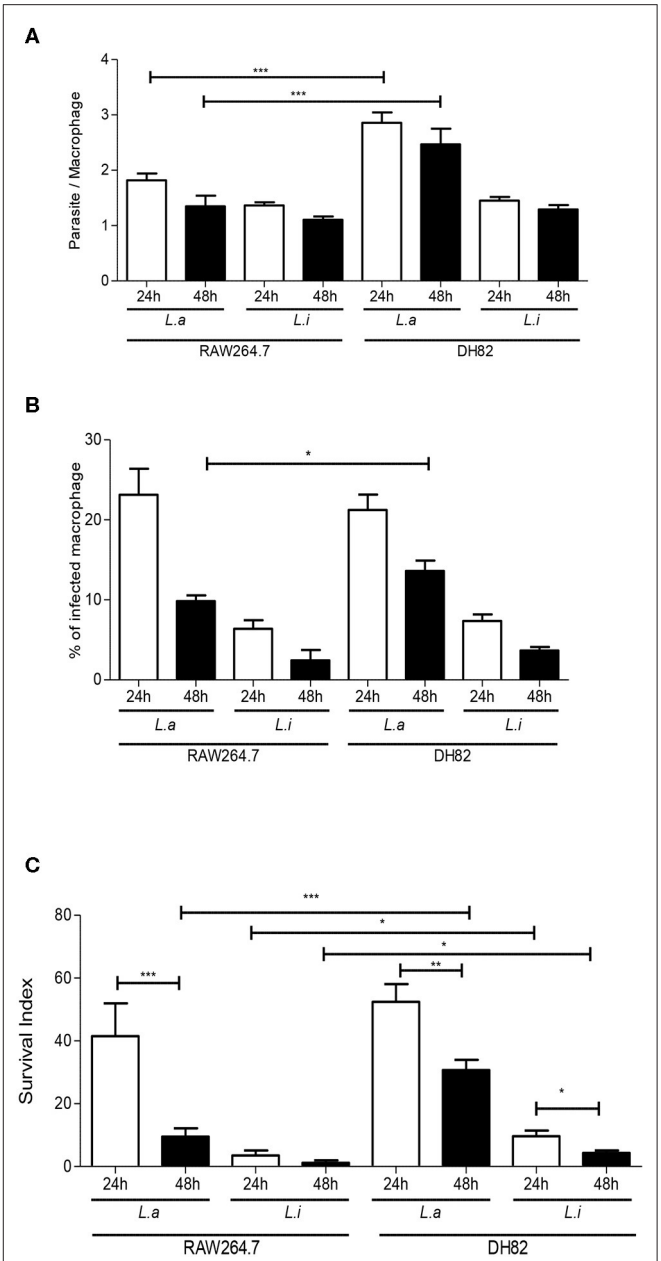

FIGURE 2 | *Leishmania* interaction with macrophages. Parasite per macrophages **(A)**, % infected-macrophages **(B)**, and survival index **(C)** in canine DH82 and murine RAW264.7. Macrophages were infected with *L. amazonensis* (L.a) and *L. infantum* (L.i) promastigotes (5 parasites: 1 macrophage) for 24 and 48 h. The data represent mean ± SEM of six independent experiments done in triplicates. $^{**}p < 0.008$; $^{*}p < 0.05$; $^{***}p < 0.0001$.

RESULTS

First, we incubated DH82 canine and RAW264.7 murine macrophages with *L. amazonensis* or *L. infantum* promastigotes for 2 h, and the capacity of both species to interact with these host cells was evaluated. Our results showed that the number

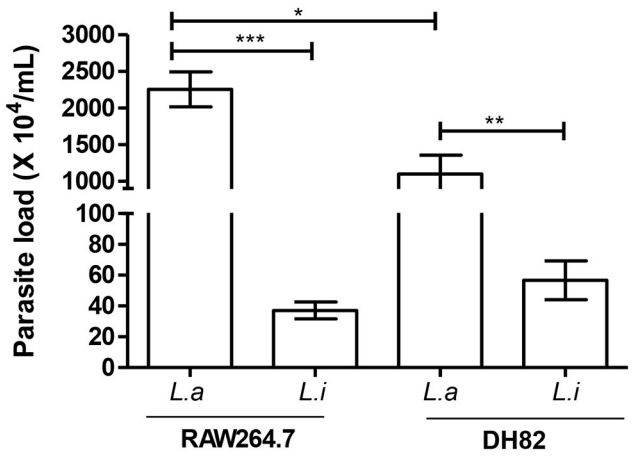

FIGURE 3 | Parasite load in infected macrophages. Canine (DH82) and murine (RAW264.7) macrophages were infected for 48 h at 34°C or 37°C/5% CO_2, according to the *Leishmania* species. Then, the cells were washed, lysed, and fed with Schneider's medium. Macrophage parasite load was evaluated after 2 days in culture at 27°C by extracellular promastigotes production. Results from three independent experiments in triplicate ± SEM. *L. amazonensis* (L.a) and *L. infantum* (L.i). $^{*}p < 0.05$; $^{**}p = 0.0043$; $^{***}p < 0.0009$.

of parasites per cell and the % of infected macrophages was 1.2 and 2.4 times higher in *L. amazonensis* infected RAW264.7 compared to DH82 (**Figures 1A,B**). The association index showed that *L. amazonensis* interacts 2.4 times and 4.2 times more than *L. infantum* promastigotes with DH82 and RAW264.7 macrophages, respectively (**Figure 1C**). Assessing the parasite number per cell of *L. amazonensis* in DH82, there is no significant difference in the number of parasite per macrophages at 24 and 48 h of interaction, although we observed that the parasite number per cell was 1.5 and 1.8 times higher than in RAW264.7 in 24 and 48 h (**Figure 2A**, **Figure S2**). On the other hand, the % of infected DH82 macrophages by *L. amazonensis* was 1.3 times higher at the 48 h than in RAW264.7 (**Figure 2B**). In *L. infantum* survival, no significant difference was observed among DH82 or RAW264.7 macrophages, neither in the percentage of infected macrophages nor in the number of parasites per cell in 24 or 48 h post-infection infection (**Figures 2A,B**). Evaluating *Leishmania* survival in DH82 canine macrophages, we demonstrated that *L. amazonensis* infection decreased 1.6 times 48 h post-infection (**Figure 2C**). Comparing to *L. infantum*, *L. amazonensis* survival was 5 and 7.2 times higher, respectively, at 24 and 48 h post-infection (**Figure 2C**). A decrease of 1.6 and 2.3 times in the parasite survival after 48 h post-infection was observed for *L. amazonensis* and *L. infantum,* respectively.

Comparing parasite survival in RAW264.7 murine macrophages at 24 h post-infection, 42% of *L. amazonensis* survival was observed, similarly to the same time point in the DH82 canine macrophages; however, it decreased 4.3 times at 48 h in RAW264.7 (**Figure 2C**). In RAW264.7 macrophages, *L. infantum* survival did not show significant difference 24 and 48 h post-infection (**Figure 2C**). The interaction of *L. amazonensis* in DH82 canine macrophages was 1.2 and 3.2 times higher than in RAW264.7 murine macrophages at 24 and 48 h post-infection, respectively. A similar difference was observed in the interaction of *L. infantum* that was 3 and 3.5 times lower in RAW264.7 murine macrophages than in DH82 canine macrophages at 24 and 48 h, respectively. *L. infantum* parasite load after 48 h of infection was not statistically different in both macrophages, and *L. amazonensis* parasite load was twice higher in RAW264.7 than in DH82 cells (**Figure 3**).

Then, we compared the ability of both cell lines to produce ROS and NO during *Leishmania* infection. Our results showed that DH82 canine macrophages did not augment the NO expression, when the cells were stimulated with LPS or infected with *L. infantum* or *L. amazonensis* (**Figure 4B**). However, an increase of 14.6, 3.0, and 13.4 times in NO production by RAW264.7 stimulated with LPS, *L. infantum*, and *L. amazonensis*, respectively, was observed (**Figure 4A**).

Total ROS (tROS) analysis showed that RAW264.7 murine macrophages stimulated with LPS augmented tROS production by 10-fold over the control, and after *L. amazonensis* infection, 5 times more tROS production was detected compared with the control; however, a significant increase in tROS production in *L. infantum*–infected cells was not observed (**Figure 5A**). Mitochondrial ROS (mitROS) evaluation showed that RAW264.7 murine macrophages, when stimulated with menadione, induced 42-fold more mitROS compared with the control. In *L. amazonensis*–infected cells, an increase of 8 times in mitROS in relation to unstimulated control was observed. However, although mitROS was increased in *L. infantum*–infected RAW264.7 cells, it was not statistically significant (**Figure 5B**).

Total ROS production by DH82 canine macrophages showed a minor production compared to RAW264.7 murine macrophages. DH82 canine macrophages stimulated with LPS increased 1.7 times tROS production, and in *Leishmania*-stimulated cells, a significant augment in tROS production was not observed (**Figure 5C**). Mitochondrial ROS analysis showed that DH82 canine macrophages stimulated with menadione used as positive control increased 4-fold mitROS production, while *L. infantum* infection augmented 0.73-fold over mitROS in unstimulated control. Even though *L. amazonensis* infection in RAW264.7 macrophages induced an increase in mitROS, a significant induction of mitROS in *L. amazonensis*–infected DH82 cells was not observed (**Figure 5D**).

Next, we determined the cytokine profiles of both macrophages. Our results evidenced that during infection in DH82 cells, *L. infantum* increased 1.4 times IL-12 mRNA expression (**Figure 6A**) and *L. amazonensis* induced 1.8 times more IL-10 mRNA in relation to uninfected control cells (**Figure 6B**). In RAW264.7 macrophages, it was observed that *L. infantum* induced 2.2 times more IL-12 mRNA expression (**Figure 6A**) and both species augmented around 2-fold IL-10 (**Figure 6B**) and TGF-β mRNA expression compared to control uninfected cells (**Figure 6C**). In both macrophage cell lines, LPS stimulation increased the mRNA expression of the three cytokines IL-12, IL-10, and TGF-β, but LPS stimulation induced around 1.5 times more IL-12, TGF-β, and IL-10 mRNA expression in RAW 264.7 macrophages than in DH82 cells (**Figures 6A–C**). IL-6, an important acute phase cytokine, was

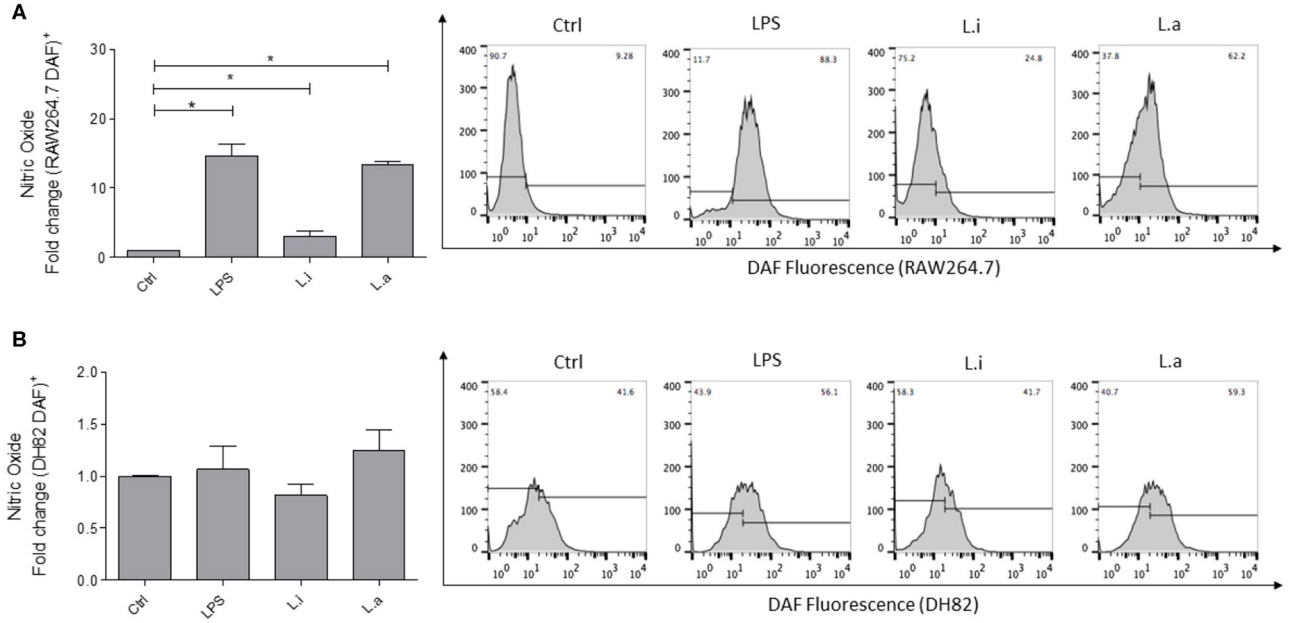

FIGURE 4 | Intracellular nitric oxide (NO) production in murine (RAW264.7) and canine (DH82) macrophages. RAW264.7 **(A)** and DH82 **(B)** macrophages were stimulated with 1 μg/mL LPS or infected with 5p:1 m of *L. infantum* (L.i) or *L. amazonensis* (L.a) and NO production measured using DAF-FM. Data were normalized as fold change in comparison to control cells (unstimulated cells incubate with DAF) and are presented as mean ± SEM of three independent experiments. $^{*}p < 0.05$. Representative histograms of %DAF-FM^{+} cells in unstimulated cells (Ctrl), stimulated with LPS, or infected with *L. infantum* or *L. amazonensis* are shown.

analyzed only in DH82 cells, and an increase in IL-6 mRNA expression during *L. infantum* infection was observed, but not in *L. amazonensis infection* (**Figure S3**).

Arginase activity analysis showed that uninfected DH82 cells produced 12.5-fold higher arginase activity compared to RAW 264.7 cells and that *Leishmania* infection or IL-4 incubation did not modulate arginase activity in DH82 cells. However, in RAW264.7 cells, IL-4 incubation increased 2.2 times the arginase activity compared to control cells, but similar to observed in *Leishmania* infected DH82 both *Leishmania* species did not modulate arginase activity (**Figure 7**).

The evaluation of MHC and CD86 molecules in macrophages during *Leishmania* infection showed that *L. amazonensis* increased 5.6 and 40 times the MHC expression in DH82 and RAW264.7 cells, respectively; however, *L. infantum* did not modulate MHC expression in any of the macrophages (**Figure 8A**). Similarly, LPS stimulation alone or together with *L. infantum* did not increase MHC expression in none of the cells, but it potentiated the MHC expression induced by *L. amazonensis,* which increased 2.2 and 3.1 times in DH82 and RAW264.7 macrophages, respectively (**Figure 8A**). In contrast with *L. infantum*, which did not modulate CD86 expression in DH82 cells, *L. amazonensis* infection increased 15-fold its expression in these macrophages (**Figure 8B**). Interestingly, in RAW264.7 cells although the expression of CD86 doubled in relation to control after both parasites' stimuli, the increase was not significant. Moreover, CD86 expression was not modulated by LPS stimulation of DH82 cells; nevertheless, it augmented 11.7 times CD86 expression in RAW264.7 macrophages. Interestingly, in the presence of *L. amazonensis*, a reduction of 2.4 times in CD86 expression in LPS-stimulated cells was observed (**Figure 8B**).

DISCUSSION

The use of a cell line for studying *in vitro* infections is a useful tool to analyze distinct aspects of *Leishmania* biology. Macrophage cell lines from different origins are favorable to *Leishmania* infection. Thus, the achievement of a canine macrophage–like cell line DH82 prompted us to characterize aspects of the infection with two different species of *Leishmania*. Interestingly, a study comparing the infectivity of different macrophages (mouse, human and dog) by *L. infantum* showed that DH82 canine macrophages, and not the murine macrophages (bone marrow and peritoneal), had a more similar infection when compared to human peripheral blood macrophages (Maia et al., 2007). These reinforce the need to better understand the dynamics and conditions of *Leishmania* infection in a canine cell line, which could be used as experimental model to test drugs, to investigate signaling pathways or modulation of the immune response. Thus, we compared the ability of two different *Leishmania* species to interact with DH82 and RAW264.7 macrophages. It was observed that *L. amazonensis* promastigotes better interacted and were phagocytosed by both canine and murine macrophages, compared to *L. infantum* ones. The ability of DH82 canine macrophages to be infected by a protozoa have been demonstrated using *Trypanosoma cruzi* and *L. infantum* (Maia et al., 2007; Mendonça et al., 2017).

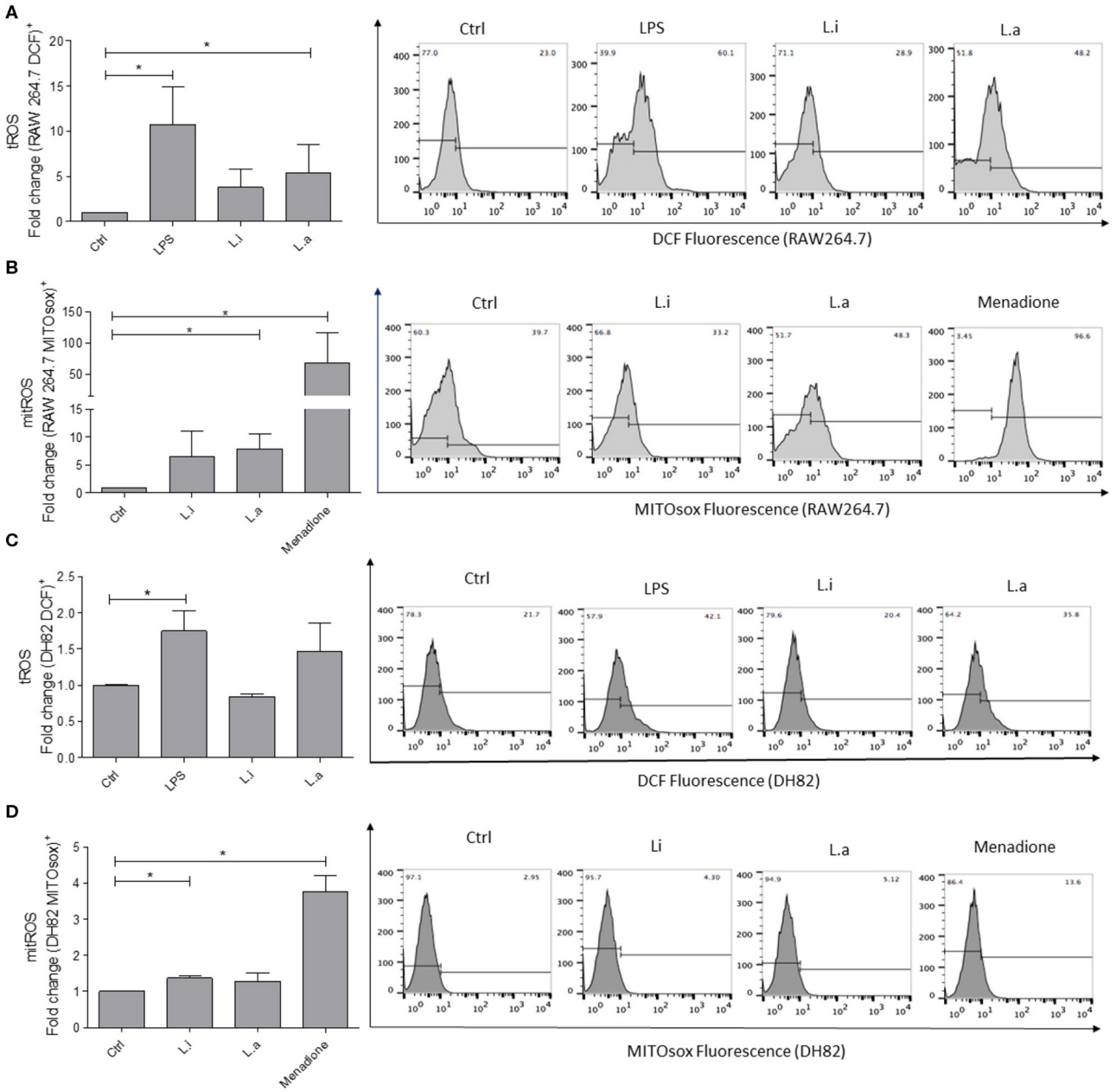

FIGURE 5 | Intracellular ROS production in RAW264.7 murine and DH82 canine macrophages. RAW264.7 **(A)** or DH82 **(C)** macrophages were stimulated or not with 1 μg/mL of LPS or infected with *L. amazonensis* (L.a) or *L. infantum* (L.i) in a ratio of 5p:1m, and total ROS (tROS) production was detected after 24 h with 0.5 mM DCFH-DA. RAW264.7 **(B)** or DH82 **(D)** macrophages stimulated or not with 0.05 mM menadione or infected with *L. amazonensis* (L.a) or *L. infantum* (L.i) as above and mitROS production detected after 24 h with 1 mM MITOsox. Data were normalized as fold change in comparison to control cells (unstimulated cells incubated with DCF or MITOsox) and are presented as mean ± SEM of three independent experiments. *$p < 0.05$. Representative histograms of %DCF-FM$^+$ and MITOSox$^+$ cells of unstimulated (Ctrl), stimulated with LPS, or infected with *L. infantum* or *L. amazonensis* are shown. Representative histograms of % of fluorescent cells in unstimulated cells (Ctrl) or LPS- or menadione-stimulated; infected with *L. infantum* or *L. amazonensis* are shown.

Another study comparing infection of *Yersinia* pestis bacteria between DH82 and RAW264.7 macrophages showed an infection rate of >90% in both macrophages after 2.5 h p.i. (Ponnusamy and Clinkenbeard, 2012). Our data demonstrated that DH82 macrophages were able to interact with *Leishmania* parasites; however, the uptake rate is lower when compared to RAW264.7 murine macrophages, probably by the difference of molecules involved in parasite recognition presented by these cells. Little is known about the molecules expressed by DH82 canine macrophages, although the presence of Fc receptors, CD44 and

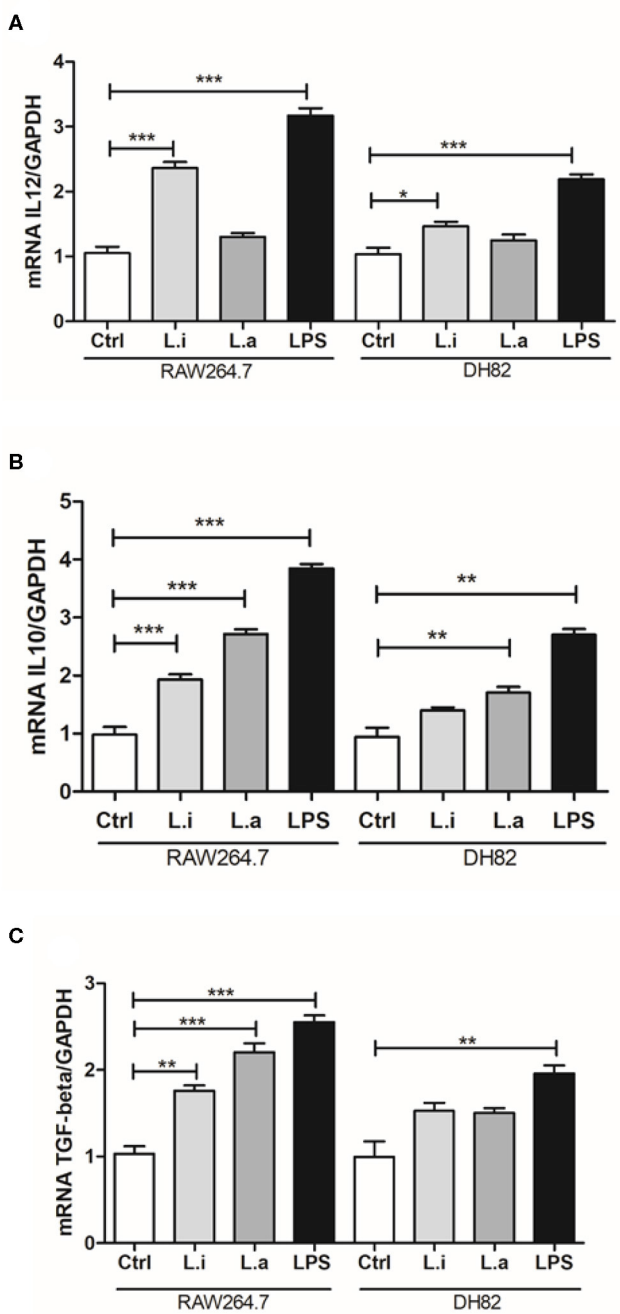

FIGURE 6 | Cytokine profile in *Leishmania*-infected canine (DH82) and murine (RAW264.7) macrophages. Macrophages were stimulated or not (Ctrl) with 1 μg/mL of LPS or infected with *L. amazonensis* or *L. infantum*. After 24 h of infection, the cells were processed and mRNA for the cytokines quantified by qRT-PCR. Data from the experiments were normalized using GADPH primers as an endogenous control. LPS was used as positive control. Data from triplicate are expressed as means ± SEM. $^{*}p < 0.05$; $^{**}p < 0.01$; $^{***}p < 0.001$.

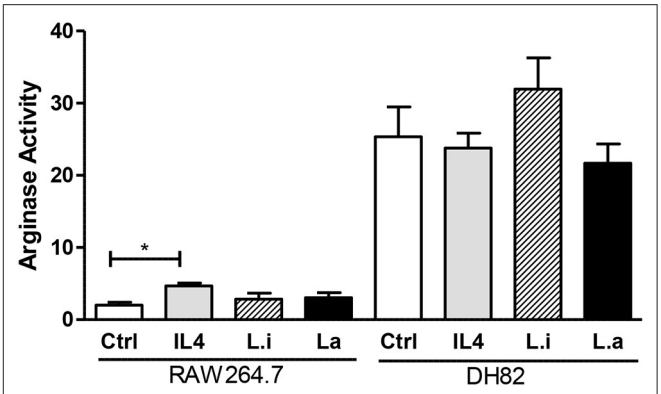

FIGURE 7 | Arginase activity in canine DH82 and murine RAW264.7 macrophages. The cells were infected or not (Ctrl) with *L. infantum* (Li) or *L. amazonensis* (La) (5p:1m) or incubated with 40 ng/mL murine IL-4. After 24 h of infection, the cells were lysed and arginase activity measured by urea concentration at 540 nm. Data from triplicate are expressed as mean ± SEM. $^{*}p < 0.05$.

TLR4, was already detected in these cells (Wellman et al., 1988; Alldinger et al., 1999; Fujimoto et al., 2012); other receptors need to be characterized.

Although the analysis of parasites per cell in 24 and 48 h post-infection showed that the number of parasites in *L. amazonensis*–infected DH82 cells was higher compared with that in RAW264.7 ones, there is no significant difference in the number of parasites per cell in 24 and 48 h in *L. amazonensis*–infected DH82 cells, which suggests that the parasite is not multiplying. The same is observed in RAW 264.7. On the other hand, when we observed the % of infected macrophages, only the point of 48 h was higher in *L. amazonensis*–infected DH82. This may be due to the difference in duplication time of these cells (Barnes et al., 2000; Sakagami et al., 2009; Maeda et al., 2016). Curiously, this difference in % of infected macrophages was not observed in *L. infantum* DH82 interaction compared to RAW264.7 cells. Comparing the data of survival and the parasite load, the different duplication times between these macrophages (Barnes et al., 2000; Sakagami et al., 2009; Maeda et al., 2016) may have influenced the parasite count in stained assays.

The comparison of *L. infantum* survival after 24 h of infection in different macrophages showed that DH82 macrophages and human peripheral blood monocytes infected with *L. infantum* isolated from human and dog samples were less permissive and have a lower number of amastigotes per macrophages compared to mouse bone marrow–derived and mouse peritoneal macrophages (Maia et al., 2007). In our data, the parasite survival analysis of *L. amazonensis* showed a reduction on parasite after 48 h of interaction in both macrophages; however, this reduction was minor in DH82 macrophages compared to RAW264.7 ones. The same was observed in *Leishmania infantum* survival inside both macrophages. No difference in the number of parasites per cell was observed in both macrophages in 24 or 48 h, indicating that the parasite is not multiplying. A study using canine peritoneal macrophages showed that *L. amazonensis*, *L. braziliensis*, *and L. infantum* infect the cells and after 24 h of infection the difference on the % of infected cells disappeared

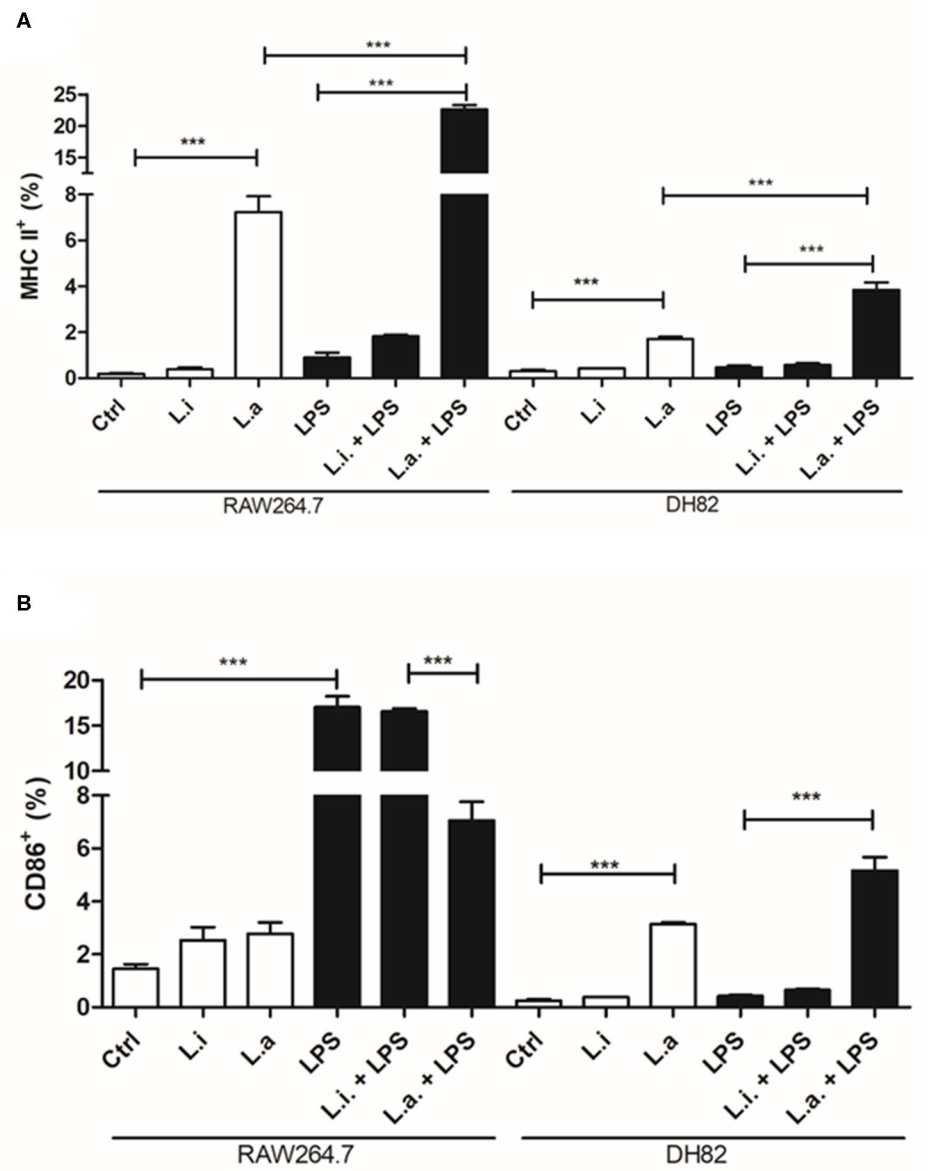

FIGURE 8 | MHC and CD86 expression in canine DH82 and murine RAW264.7 macrophages. The cells (5×10^5/mL) infected or not with (Li.) *L. infantum* or (La.) *L. amazonensis* (5p:1m) were activated or not (Ctrl) with LPS [500 ng/mL] and maintained at 34 or 37°C/5% CO_2. After 24 h post-infection, the cells were detached, stained for MHC **(A)** and CD86 **(B)** and analyzed by flow cytometry. Data from duplicate are expressed as mean ± SEM. ***$p < 0.0001$.

(Madeira et al., 1999). Although *L. infantum* is implicated in canine leishmaniasis, the detection of other species of *Leishmania* in naturally infected dogs has been reported (Sanches et al., 2016; Valdivia et al., 2017; Alves Souza et al., 2019).

It has long been described that macrophages produce reactive species, such as superoxide (O_2^-) anion, hydrogen peroxide (H_2O_2), and also nitric oxide (NO) in high quantities as an efficient mechanism to control intracellular pathogens (Gantt et al., 2001; Piacenza et al., 2019). NO production analysis showed that DH82 macrophages failed to increase the number of DAF^+ macrophages after any stimuli used, such as LPS, *L. amazonensis*, or *L. infantum*. Similarly, the production of NO was also evaluated in DH82 macrophages during *Trypanosoma cruzi* infection, and an increase in this mediator was also not observed after infection or stimulus with LPS and IFN-γ (Mendonça et al., 2017). Curiously, Wasserman et al. (2012) showed that unstimulated DH82 canine cells presented around 90 μM of nitrite detected by the Griess reaction, but the cells failed to respond when it was stimulated with LPS from 0.1 to 10 μg/mL. On the other hand, RAW264.7 murine macrophages augmented NO production, when stimulated by LPS and during *L. amazonensis* and *L. infantum* infection, reaching

up to 60% of the cell population expressing NO during *L. amazonensis* infection.

The same profile was observed in ROS production by both cells. *L. amazonensis* infection induced tROS production by RAW264.7, but not by DH82 cells. On the other hand, *L. infantum* infection did not induce ROS production by none of the two macrophages tested, and yet the tROS as well as mitROS quantity observed in DH82 cells was lower than in RAW264.7 ones. Recently, the involvement of ROS production in inducing inflammasome activation and restricting *L. amazonensis* infection was demonstrated in murine bone marrow–derived macrophages (Lima-Junior et al., 2013, 2017). A study about IL-1 maturation showed that RAW264.7 murine macrophages did not have apoptotic speck-like protein with a caspase-activating recruiting domain for an efficient inflammasome activation (Pelegrin et al., 2008). It is not known if DH82 canine macrophages have all the proteins to assemble an efficient inflammasome, and further studies should be done to clarify this issue.

The balance of arginase and NO synthase in the control of *Leishmania* growth is well-established (Green et al., 1990; Gantt et al., 2001; Iniesta et al., 2001; Van Assche et al., 2011). Interestingly, when we analyzed arginase activity in both macrophages, it was observed that uninfected or unstimulated DH82 canine macrophages have higher arginase activity compared to RAW264.7 cells and their stimulation with IL-4 or *Leishmania* infection did not increase it. On the contrary, RAW264.7 murine macrophages have lower arginase activity which was increased after IL-4 incubation; however, *Leishmania* did not modulate it. The importance of arginase activity in the proliferation of *Leishmania* has been demonstrated (Iniesta et al., 2001), since its inhibition augments *Leishmania* killing by macrophages.

The difference in NO and ROS production and arginase activity between DH82 and RAW264.7 macrophages may explain the infection rates observed. Although the initial association rate (2 h) of *L. amazonensis* with both macrophages was similar, the infection rate at 48 h in RAW264.7 cells was significantly lower than in DH82 ones. Nevertheless, when we evaluated the parasite load after 48 h of infection, it was similar in both macrophages suggesting that other mechanisms should be involved in this latter phenomenon, which still needs to be investigated.

Cytokines are key mediators for determining the modulation of the immune response; thus, it is essential to characterize cytokines produced by macrophages during *Leishmania* infection. Few works demonstrated cytokine profile in *Leishmania*-infected RAW264.7 murine macrophages. The production of IL-10 in the supernatant of *L. amazonensis*–infected RAW264.7 cells was observed after 72 h of infection and the use of an antibody to abrogate it, preventing *L. amazonensis* proliferation (Pereira et al., 2010). In *L. infantum*–infected RAW 264.7 cells, the presence of IL-10 in culture supernatants at 24 h post-infection was also reported (Figueiredo et al., 2017). Our results corroborated that, since we observed IL-10 RNAm expression in RAW264.7 murine macrophages infected by both species. Besides, *L. infantum* infection also induced TGF-β and IL-12 mRNA expression. In the murine model of infection, an inhibition of IL-6 production in *L. amazonensis*–infected macrophages was observed (Craig et al., 2017). Our data showed that *L. infantum* induced IL-6 mRNA expression in canine DH82 macrophages, although it is a cytokine of acute phase produced by different cell types; this cytokine is involved in Th2 differentiation, which could influence the arginase activity (Diehl and Rincón, 2002).

For the first time, our work evaluated the expression of cytokines in *Leishmania*-infected DH82 canine macrophages, and similarly to *L. amazonensis*–infected RAW264.7 cells we also observed an increase in the expression of IL-10 mRNA in canine DH82 macrophages; however, *L. infantum*–infected DH82 cells induced IL-12 mRNA. None of the *Leishmania* species we tested induced TGF-β in DH82 canine macrophages in a significant manner, although an upward trend was observed. The cytokine profile in *T. cruzi*–infected DH82 cells showed the presence of IL-10, TGF-β, and TNF-α (Mendonça et al., 2017). The induction of IL-10 during *L. amazonensis* infection could explain the high amount of parasite observed at 48 h post-infection in comparison to *L. infantum*.

MHC and co-stimulatory molecules are important signals required by T cells to be activated, and down-modulation of these molecules is an escape mechanism of the immune response. Actually, it was already shown that *L. amazonensis* and *L. mexicana* amastigotes inside the parasitophorous vacuole degrade MHC class II molecules (De Souza Leao et al., 1995; Antoine et al., 1999; Costa et al., 2018), without affecting CD86 expression (Costa et al., 2018). Nevertheless, a study in canine peripheral blood monocyte–derived macrophages showed an upregulation of MHC molecules in cells infected with *L. infantum* in the presence of T cells *in vitro* (Diaz et al., 2012). Here we did not observe induction of MHC or CD86 expression in none of the cell lines during *L. infantum* infection. Meanwhile, *L. amazonensis* induced MHC expression in both cell lines. Interestingly, *L. amazonensis* downregulated CD86 expression induced by LPS in RAW264.7 cells. Interestingly, ROS and NO production is also not stimulated in DH82 by LPS, showing a low responsiveness to this stimulant by these cells in relation to RAW264.7 cells. Synergism and higher MHC expression were obtained after stimulation of both cell lines by LPS and *L. amazonensis* compared to each of the isolated stimuli. Remarkably, increased MHC and CD80 expression in DH82 cells was obtained upon stimulation with LPS plus IFN-γ (Mendonça et al., 2017). Recently, it was shown that the DH82 cell line is able to differentiate in the M2a subtype upon IL-4 and IL-13 human cytokine stimulation. The cells did not augment CD206 expression, but express FCεRI independent of stimuli, and upregulated CD163 and IL-10 gene expression. Our results showed that these cells express low levels of CD86 and MHC after LPS and/or *Leishmania* infection compared to RAW264.7 murine cells. Besides having high arginase activity, all this configures that this cell line could be an M2 subtype macrophage model to study *Leishmania* infection.

Taken together, our results show that although DH82 canine and RAW264.7 murine macrophages present different infection profiles after the initial *Leishmania* infection and differently modulate the macrophage response, after 48 h of infection, the

parasite load profile is similar. Further studies are necessary in order to elucidate other possible mechanisms involved in *Leishmania* immunomodulation of these macrophage lines.

DATA AVAILABILITY STATEMENT

All datasets generated for this study are included in the article/**Supplementary Material**.

AUTHOR CONTRIBUTIONS

NN, LS, AW, DD-R, CF, UG, ES, and LP conceived and designed the experiments. NN, LS, RS, IL, DS, ÁV, AW, and LP performed the experiments. NN, RS, LS, IL, ÁV, DD-R, ES, CF, and LP analyzed the data. LP and NN wrote the paper.

FUNDING

We thank the support of Conselho Nacional de Desenvolvimento Científico e Tecnológico (CNPq), Fundação Carlos Chagas Filho de Amparo à Pesquisa do Estado do Rio de Janeiro (FAPERJ) and Coordenação de Aperfeiçoamento de Pessoal de Nível Superior (CAPES) Finance Code 001 for the fellowships to PhD student Raíssa Couto Santana of Programa de Pós-Graduação em Ciências Veterinárias da UFRRJ.

SUPPLEMENTARY MATERIAL

The Supplementary Material for this article can be found online at: https://www.frontiersin.org/articles/10.3389/fcimb.2020.00247/full#supplementary-material

Figure S1 | Representative dotplots of macrophages. Dot plots of DH82 **(A)** and RAW264.7 **(B)** macrophages showing the gates used to acquire and analyze the macrophages populations. Data representative of three independent experiments.

Figure S2 | Optical microscopy DH82 canine macrophages infected with *L. amazonensis* **(A,C)** and *L. infantum* **(B,D)** for 24 and 48 h post-infection Giemsa stained.

Figure S3 | IL-6 detection in *Leishmania* infected-DH82 macrophages. Macrophages were stimulated or not (Ctrl) with 1 μg/mL of LPS or infected with *L. amazonensis* or *L. infantum* in a ratio of 5p:1m. After 24 h of infection, the cells were processed and mRNA quantification by qRT-PCR. Data were normalized using GADPH primers as an endogenous control, and LPS was used as positive control. Data are expressed as means ± SEM of triplicate. $^{***}p < 0.001$.

REFERENCES

Alldinger, S., Baumgärtner, W., Kremmer, E., and Fonfara, S. (1999). Characterization of a canine CD44 specific monoclonal antibody. *Transbound. Emerg. Dis.* 46, 19–32. doi: 10.1046/j.1439-0442.1999.00184.x

Alves Souza, N., Souza Leite, R., de Oliveira Silva, S., Groenner Penna, M., Figueiredo Felicori Vilela, L., Melo, M. N., et al. (2019). Detection of mixed Leishmania infections in dogs from an endemic area in southeastern Brazil. *Acta Tropica*.193:12–17. doi: 10.1016/j.actatropica.2019.02.016

Antoine, J. C., Lang, T., Prina, E., Courret,. N., and Hellio, R. (1999). H-2M molecules, like MHC class II molecules, are targeted to parasitophorous vacuoles of Leishmania-infected macrophages and internalized by amastigotes of *L. amazonensis* and *L. mexicana*. *J Cell Sci.* 112, 2559–2570.

Barnes, A., Bee, A., Bell, S., Gilmore, W., Mee, A., Morris, R., et al. (2000). Immunological and inflammatory characterisation of three canine cell lines: K1, K6 and DH82. *Vet. Immunol. Immunopathol.* 30, 9–25. doi: 10.1016/S0165-24270000184-7

Castro, E. A., Thomaz-Soccol, V., Augur, C., and Luz, E. (2007). Leishmania (Viannia) Braziliensis: epidemiology of canine cutaneous Leishmaniasis in the State of Paraná (Brazil). *Exp. Parasitol.* 11, 13–21. doi: 10.1016/j.exppara.2007.03.003

Channon, J. Y., Roberts, M. B., and Blackwell, J. M. (1984). A study of the differential respiratory burst activity elicited by promastigotes and amastigotes of *Leishmania donovani* in murine resident peritoneal macrophages. *Immunol.* 53, 345–355.

Costa, S. S., Fornazim, M. C., Nowill, A. E., and Giorgio, S. (2018). Leishmania amazonensis induces modulation of costimulatory and surface marker. *Parasit. Immunol.* 40:e12519. doi: 10.1111/pim.12519

Craig, E., Huyghues-Despointes, C. E., Yu, C., Handy, E. L., Sello, J. K., and Kima, P. E. (2017). Structurally optimized analogs of the retrograde trafficking inhibitor Retro-2cycl limit Leishmania infections. *PLoS. Negl. Trop. Dis.* 11:e0005556. doi: 10.1371/journal.pntd.0005556

Dantas-Torres, F., Solano-Gallego, L., Baneth, G., Ribeiro, V.M., dePaiva-Cavalcanti, M., and Otranto, D. (2012). Canine leishmaniasis in the old and new worlds: unveiled similarities and differences. *Trends Parasitol.* 28, 531–538. doi: 10.1016/j.pt.2012.08.007

De Souza Leao, S., Lang, T., Prina, E., Hellio, R., and Antoine, J. C. (1995). Intracellular Leishmania amazonensis amastigotes internalize and degrade MHC class II molecules of their host cells. *J. Cell Sci.* 108, 3219–3231.

Diaz, S., da Fonseca, I. P., Rodrigues, A., Martins, C., Cartaxeiro, C., Silva, M. J., et al. (2012). Canine leishmaniosis. Modulation of macrophage/lymphocyte interactions by *L. infantum*. *Vet. Parasitol.* 189, 137–144. doi: 10.1016/j.vetpar.2012.05.004

Diehl, S., and Rincón, M. (2002). The two faces of IL-6 on Th1/Th2 differentiation. *Mol Immunol.* 39, 531–536. doi: 10.1016/S0161-5890(02)00210-9

Figueiredo, W. M. E., Viana, S. M., Alves, D. T., Guerra, P. V., Coêlho, Z. C. B., Barbosa, H. S., et al. (2017). Protection mediated by chemokine CXCL10 in BALB/c mice infected by *Leishmania infantum*. *Mem. Inst. Oswaldo Cruz.* 112, 561–568. doi: 10.1590/0074-02760160529

Fujimoto, Y., Nakatani, N., Kubo, T., Semi, Y., Yoshida, N., Nakajima, H., et al. (2012). Adenosine and ATP affect LPS-induced cytokine production in canine macrophage cell line DH82 cells. *J. Vet. Med. Sci.* 74, 27–34. doi: 10.1292/jvms.11-0228

Gantt, K. R., Goldman, T. L., McCormick, M. L., Miller, M. A., Jeronimo, S. M., Nascimento, E. T., et al. (2001). Oxidative responses of human and murine macrophages during phagocytosis of *Leishmania chagasi*. *J. Immunol.* 167, 893–901. doi: 10.4049/jimmunol.167.2.893

Gomes, N. A., Gattass, C. R., Barreto-De-Souza, V., Wilson, M. E., and DosReis, G. A. (2000). TGF-beta mediates CTLA-4 suppression of cellular immunity in murine Kalaazar. *J. Immunol.* 164, 2001–2008. doi: 10.4049/jimmunol.164.4.2001

Gontijo, B., and De Carvalho, M. L. R. (2003). Leishmaniose Tegumentar Americana. *Rev. Soc. Bras. Med. Trop.* 36, 71–80. doi: 10.1590/S0037-86822003000100011

Green, S. J., Meltzer, M. S., and Hibbs, J. B. Jr., Nacy, C. A. (1990). Activated macrophages destroy intracellularLeishmania major amastigotes by an L-arginine-dependent killing mechanism. *J. Immunol.* 144, 278–283.

Handman, E., and Bullen, D. V. (2002). Interaction of Leishmania with the host macrophage. *Trends Parasit.* 8, 332–334. doi: 10.1016/S1471-4922(02)02352-8

Horta, M. F., Mendes, B. P., Roma, E. H., Noronha, F. S. M., Macedo, J. P., Oliveira, L. S., et al. (2012). Reactive oxygen species and nitric oxide in cutaneous Leishmaniasis. *J. Parasitol. Res.* 2012:203818. doi: 10.1155/2012/203818

Howerth, E. W., Parlavantzas, G. S., and Stallknecht, D. E. (2004). Replication of epizootic haemorrhagic disease and bluetongue viruses in DH82 cells. *Vet. Ital.* 40, 520–524.

Iniesta, V., Gómez-Nieto, L. C., Corraliza, I. (2001). The inhibition of arginase by N(omega)-hydroxy-l-arginine controls the growth of Leishmania

inside macrophages. *J. Exp. Med.* 193, 777–784. doi: 10.1084/jem.193.6.777

Lima-Junior, D. S., Costa, D. L., Carregaro, V., Cunha, L. D., Silva, A. L., Mineo, T. W., et al. (2013). Inflammasome-derived IL-1β production induces nitric oxide-mediated resistance to Leishmania. *Nat. Med.* 19, 909–915. doi: 10.1038/nm.3221

Lima-Junior, D. S., Mineo, T. W. P., Calich, V. L. G., and Zamboni, D. S. (2017). Dectin-1 Activation during *Leishmania amazonensis* phagocytosis prompts Syk-dependent reactive oxygen species production to trigger inflammasome assembly and restriction of parasite replication. *J. Immunol.* 199, 2055–2068. doi: 10.4049/jimmunol.1700258

Madeira, M., Barbosa-Santos, E., and Marzochi, M. (1999). Experimental infection of canine peritoneal macrophages with visceral and dermotropic Leishmania strains. *Mem. Inst. Oswaldo. Cruz.* 94, 645–648. doi: 10.1590/s0074-02761999000500015

Maeda, J., Froning, C. E., Brents, C. A., Rose, B. J., Thamm, D. H., and Kato, T. A. (2016). Intrinsic radiosensitivity and cellular characterization of 27 canine cancer cell lines. *PLoS ONE.* 11:e0156689. doi: 10.1371/journal.pone.0156689

Maia, C., Rolão, N., Nunes, M., Gonçalves, L., and Campino, L. (2007). Infectivity of five different types of macrophages by *Leishmania infantum*. *Acta Tropica* 103, 150–155. doi: 10.1016/j.actatropica.2007.06.001

Mendonça, P. H. B., da Rocha, R. F. D. B., Moraes,. J. B. de B., LaRocque-de-Freitas, I. F., Logullo, J., Morrot, A., et al. (2017). Canine macrophage DH82 cell line as a model to study susceptibility to *Trypanosoma cruzi* infection. *Front. Immunol.* 8:604. doi: 10.3389/fimmu.2017.00604

Moreira, N. das D., Vitoriano-Souza, J., Roatt, B.M., Vieira, P.M. de A Ker H.G, Cardoso, J.M. de O., Giunchetti, R.C., et al. (2012). Parasite burden in hamsters infected with two different strains of Leishmania (Leishmania) infantum: "Leishman Donovan units" versus real-time PCR. *PloS One* 7:e47907. doi: 10.1371/journal.pone.0047907

Moreira, N. das D., Vitoriano-Souza, J., Roatt, B. M., Vieira, P. M. de A., Coura-Vital, W., Cardoso, J. M. de O., et al. (2016). Clinical, hematological and biochemical alterations in hamster (*Mesocricetus auratus*) experimentally infected with *Leishmania infantum* through different routes of inoculation. *Parasit. Vectors* 9:181. doi: 10.1186/s13071-016-1464-y

Mosser, D. M., and Rosenthal, L. A. (1993). Leishmania-macrophage interactions: multiple receptors, multiple ligands and diverse cellular responses. *Semin. Cell Biol.* 4, 315–322. doi: 10.1006/scel.1993.1038

Naderer, T., and McConville, M. J. (2008). The Leishmania-macrophage interaction: a metabolic perspective. *Cell. Microbiol.* 10, 301–308. doi: 10.1111/j.1462-5822.2007.01096.x

Paz, G. F., Rugani, J. M. N., Marcelino, A. P., and Gontijo, C. M. F. (2018). Implications of the use of serological and molecular methods to detect infection by *Leishmania* spp. in urban pet dogs. *Acta Tropica* 182, 198–201. doi: 10.1016/j.actatropica.2018.03.018

Pelegrin, P., Barroso-Gutierrez, C., and Surprenant, A. (2008). P2X7 receptor differentially couples to distinct release pathways for IL-1beta in mouse macrophage. *J. Immunol.* 180, 7147–7157. doi: 10.4049/jimmunol.180.11.7147

Pereira, R. M., Teixeira, K. L., Barreto de Souza, V., Calegari-Silva, T. C., De-Melo, L. D., Soares, D. C., et al. (2010). Novel role for the double-stranded RNA-activated protein kinase PKR: modulation of macrophage infection by the protozoan parasite Leishmania. *FASEB J.* 24, 617–626. doi: 10.1096/fj.09-140053

Piacenza, L., Trujillo, M., and Radi, R. (2019). Reactive species and pathogen antioxidant networks during phagocytosis. *J. Exp. Med.* 216, 501–516. doi: 10.1084/jem.20181886

Ponnusamy, D., and Clinkenbeard, K. D. (2012). Yersinia pestis intracellular parasitism of macrophages from hosts exhibiting high and low severity of plague. *PLoS ONE* 7:e42211. doi: 10.1371/journal.pone.0042211

Ribeiro-Gomes, F. L., Moniz-de-Souza, M. C. A, Alexandre-Moreira, M. S., Dias, W. B., Lopes, M. F., Nunes, M. P., et al. (2007). Neutrophils activate macrophages for intracellular killing of Leishmania major through recruitment of TLR4 by neutrophil elastase. *J. Immunol.* 179, 3988–3994. doi: 10.4049/jimmunol.179.6.3988

Ribeiro-Gomes, F. L., Silva, M. T., and Dosreis, G. A. (2006). Neutrophils, apoptosis and phagocytic clearance: an innate sequence of cellular responses regulating intramacrophagic parasite infections. *Parasitology* 132, S61–S68. doi: 10.1017/S0031182006000862

Sakagami, H., Kishimo, K., Amano, O., Kanda, Y., Kuni, S., Yokote, Y., et al. (2009). Cell death induced by nutritional starvation in mouse macrophage-like RAW 264.7 cells. *Anticancer Res.* 29, 343–348.

Sanches, L. D., Martini, C. C., Nakamura, A. A., Santiago, M. E., Dolabela de Lima, B., and Lima, V. M. (2016). Natural canine infection by Leishmania infantum and Leishmania amazonensis and their implications for disease control. *Rev. Bras. Parasitol. Vet.* 25, 465–469. doi: 10.1590/s1984-29612016071

Valdivia, H. O., Almeida, L. V., Roatt, B. M., Reis-Cunha, J. L., Pereira, A. A. S., Gontijo, C., et al. (2017). Comparative genomics of canine-isolated *Leishmania* (Leishmania) *amazonensis* from an endemic focus of visceral Leishmaniasis in Governador Valadares, Southeastern Brazil. *Sci. Rep.* 7:40804. doi: 10.1038/srep40804

Van Assche, T., Deschacht, M., da Luz, R. A., Maes, L., and Cos, P. (2011). Leishmania-macrophage interactions: insights into the redox biology. *Free Radic. Biol. Med.* 51, 337–351. doi: 10.1016/j.freeradbiomed.2011.05.011

Wasserman, J., Diese, L., VanGundy, Z., London, C., Carson, W. E., and Papenfuss, T. L. (2012). Suppression of canine myeloid cells by soluble factors from cultured canine Tumor cells. *Vet. Immunol. Immunopathol.* 145, 420–430. doi: 10.1016/j.vetimm.2011.12.018

Wellman, M. L., Krakowka, S., Jacobs, R. M., and Kociba, G. J. (1988). A macrophage-monocyte cell line from a dog with malignant histiocytosis. *In Vitro Cell. Dev. Biol. J. Tiss. Cult. Assoc.* 24, 223–229. doi: 10.1007/BF02623551

Conflict of Interest: The authors declare that the research was conducted in the absence of any commercial or financial relationships that could be construed as a potential conflict of interest.

frontiers in Cellular and Infection Microbiology

ORIGINAL RESEARCH
published: 17 July 2020
doi: 10.3389/fcimb.2020.00363

The NAD$^+$ Responsive Transcription Factor ERM-BP Functions Downstream of Cellular Aggregation and Is an Early Regulator of Development and Heat Shock Response in *Entamoeba*

Dipak Manna[1], *Daniela Lozano-Amado*[1], *Gretchen Ehrenkaufer*[1] *and Upinder Singh*[1,2]*

[1] *Division of Infectious Diseases, Stanford University School of Medicine, Stanford, CA, United States,* [2] *Department of Microbiology and Immunology, Stanford University School of Medicine, Stanford, CA, United States*

OPEN ACCESS

Edited by:
Albert Descoteaux, Institut National de la Recherche Scientifique (INRS), Canada

Reviewed by:
Kai Yang, Indiana University School of Medicine-Lafayette, United States
Patricia Sampaio Tavares Veras, Gonçalo Moniz Institute (IGM), Brazil

***Correspondence:**
Upinder Singh
usingh@stanford.edu

Specialty section:
This article was submitted to Microbes and Innate Immunity, a section of the journal Frontiers in Cellular and Infection Microbiology

Received: *09 January 2020*
Accepted: *11 June 2020*
Published: *17 July 2020*

Citation:
Manna D, Lozano-Amado D, Ehrenkaufer G and Singh U (2020) The NAD$^+$ Responsive Transcription Factor ERM-BP Functions Downstream of Cellular Aggregation and Is an Early Regulator of Development and Heat Shock Response in Entamoeba. Front. Cell. Infect. Microbiol. 10:363. doi: 10.3389/fcimb.2020.00363

Entamoeba histolytica is a protozoan parasite and a major cause of dysentery and diarrheal disease in developing countries. Disease transmission from one host to another occurs via cysts which can survive in environmental extremes and are transmitted through contaminated food and water. Recent studies in our lab identified a novel transcription factor, Encystation Regulatory Motif- Binding Protein (ERM-BP), which is responsive to NAD$^+$ and has an important role in encystation. The key residues important for ERM-BP function were demonstrated *in vitro* using recombinant protein. In this study we demonstrate the *in vivo* functional consequences of mutations in key domains and their impact on *Entamoeba* encystation. Our results show that mutations in the DNA binding domain (ERM-BP-DBM) and in the nicotinamidase domain (ERM-BP-C198A) lead to protein mis-localization in both trophozoites and cysts and significantly reduce encystation efficiency. Additionally, we showed that silencing of ERM-BP significantly decreased the size and number of multi-nucleated giant cells (MGC) that form during encystation, indicating that ERM-BP functions upstream of the cellular aggregation that precedes stage conversion. Dissection of epistatic interactions between ERM-BP and a second encystation-related transcription factor, NF-Y revealed that ERM-BP is upstream of NF-Y in controlling the developmental cascade and appears to be one of the earliest regulators of development identified to date in *Entamoeba*. We also demonstrated that ERM-BP is upregulated during heat stress in *Entamoeba*, another condition which increases intracellular NAD$^+$ levels and that overexpression of ERM-BP makes *E. histolytica* and *E. invadens* parasites more resistant to heat stress. Overexpression of ERM-BP in *E. histolytica* also induced the formation of cyst-like quadrinucleated cells and formation of MGCs. Overall, our work has identified an important role of ERM-BP in *Entamoeba* stress response and links an NAD$^+$-responsive transcription factor to both development and heat shock response. Characterization of stress and developmental cascades are important avenues to investigate for *Entamoeba*, an important human parasitic pathogen.

Keywords: *Entamoeba*, transcription factor, encystation, heat-shock, multinucleated giant cells

INTRODUCTION

The protozoan parasite *Entamoeba histolytica* causes an estimated 50 million cases of invasive disease annually and is the second leading parasitic cause of death worldwide (Haque et al., 2003; Lozano et al., 2012). The life cycle of the parasite involves inter-conversion between trophozoites, a stage which invades tissue and causes clinical disease and cysts, a stage which transmits disease in contaminated food or water (McConnachie, 1969). However, the molecular controls of the developmental life cycle of this parasite are poorly studied, and the triggers that initiate stage conversion are not well-delineated. Most developmental studies have been done in a closely related reptilian parasite, *E. invadens*, which can be encysted *in vitro* using glucose depletion and osmotic stress (Avron et al., 1986) and excysted from cysts to trophozoites using media supplemented with glucose, bile salt, sodium bicarbonate and serum (Mitra and Krishna Murti, 1978). Using this model of *Entamoeba* development, a number of triggers of encystation including catecholamine, gal-terminated ligands, cyclic AMP (cAMP), cholesteryl sulfate, NAD^+, Ca^{2+} signaling, and phospholipase-D (PLD) have been identified (Chayen et al., 1985; Cho and Eichinger, 1998; Eichinger, 2001; Makioka et al., 2001; Coppi et al., 2002; Frederick and Eichinger, 2004; Ehrenkaufer et al., 2013; Martinez-Higuera et al., 2015; Mi-ichi et al., 2015; Manna et al., 2018; Manna and Singh, 2019). Furthermore, a number of molecules, e.g., galactose, N-acetylglucosamine, and short chain fatty acids, have been shown to inhibit encystation (Coppi and Eichinger, 1999; Byers et al., 2005). It has also recently been noted that multinucleated giant cells (MGC), which originate from cell aggregates due to fusion of multiple trophozoites, develop during encystation (Krishnan and Ghosh, 2018) indicating that *Entamoeba* encystation and MGC formation are induced by similar physiological conditions and key regulators, and may share similar control pathways.

In the human pathogen *E. histolytica*, *in vitro* regulated encystation has not been accomplished to date. Reports of cyst-like structures from *E. histolytica* exposed to stress conditions have been reported, but these are not mature cysts as they lack a thick chitinous cyst walls and there are no evidence that these can excyst to trophozoites; instead most likely, these are parasites attempting to encyst (Barron-Gonzalez et al., 2008; Aguilar-Diaz et al., 2010). Using parasites isolated from patients and maintained in xenic conditions, low-level, continuous encystation and excystation has been noted (Ehrenkaufer et al., 2007). In these conditions, mature quadrinucleated cysts and thick cyst walls were produced, but with low efficiency. Heat shock stress has been noted to have some overlap with encystation as genes involved in cyst wall formation (e.g., Chitinase and Jacob) are noted to be upregulated in both conditions (Field et al., 2000).

Three transcription factors with important roles in *Entamoeba* encystation have been identified. Two of these transcription factors - a developmentally regulated Myb protein (drMyb), which binds a hexanucleotide promoter motif CCCCCC, and an Encystation Regulatory Motif-Binding Protein (ERM-BP), which binds a hepta-nucleotide promoter motif, CAACAAA- appear at early time point (24 h) of encystation (Ehrenkaufer et al., 2009; Manna et al., 2018). The third transcription factor, a nuclear factor complex (NF-Y) is composed of three subunits NF-YA, NF-YB, and NF-YC, which bind to a pentanucleotide motif CCAAT and appears at a later time point of encystation (48 h) (Manna and Singh, 2019). Silencing of ERM-BP results in a significantly reduced encystation efficiency and abnormal cysts with defective cyst walls which have reduced viability under excystation conditions (Manna et al., 2018). The function of ERM-BP is regulated by direct binding of the metabolic cofactor NAD^+; binding to NAD^+ changes protein conformation and facilitates ERM-BP binding to the DNA motif. ERM-BP is also capable of nicotinamide catalysis. Biochemical studies using ERM-BP recombinant protein revealed key residues and domains important for NAD^+ binding, DNA binding, and nicotinamide catalysis. A five amino acid cluster at the N-terminus of ERM-BP (S_AR_LTKR) except "A" and "L" as shown in subscripts is a DNA-binding domain which is crucial for DNA binding and a cysteine residue at the C-terminal nicotinamidase domain (C198) is crucial for NAD^+ binding (Manna et al., 2018).

In this study we evaluated the functions of ERM-BP domains *in vivo* by overexpressing mutant versions of the protein in *Entamoeba* parasites and assessing phenotypic outcomes. Our results show that mutations in the DNA binding domain (ERM-BP-DBM) and a single amino acid change in the nicotinamidase domain (ERM-BP-C198A) lead to mis-localization of the mutant protein in both trophozoites and cysts and significantly reduce encystation efficiency. Our study also revealed a role for ERM-BP in formation of multi-nucleated giant cells (MGC) during encystation. We showed that silencing of ERM-BP significantly decreased the number of giant cells formed indicating that encystation and giant cell formation may share similar signaling pathway which is affected by loss of function of ERM-BP. Furthermore, we showed that in heat stress, another condition in which NAD^+ levels increase, ERM-BP is upregulated in both *E. invadens* and in *E. histolytica*. Nuclear extracts from heat stressed parasites specifically bind to ERM, and overexpression of ERM-BP makes parasites more resistant to heat stress. Overexpression of ERM-BP in *E. histolytica* produces quadrinucleate cyst-like structures, and multinucleated giant cells also observed due to heat stress, supporting the concept that heat-stress response and encystation are related. Overall, our work identified an important role of ERM-BP which functions downstream of cellular aggregation and is an early regulator of development and heat shock response in *Entamoeba*.

MATERIALS AND METHODS

Parasite Culture, Transfection, and Induction of Stage Conversion

E. invadens (strain IP-1) was axenically maintained as described earlier (Clark and Diamond, 2002). To make stable transgenic cell lines, parasites were transfected with plasmid DNA by electroporation (Ehrenkaufer and Singh, 2012). Stable cell lines were maintained at G418 concentration of 80 μg/mL

unless otherwise stated. To induce encystation, *E. invadens* trophozoites were incubated in 47% LYI-LG (supplemented with 7% adult bovine serum). Encystation efficiency was determined by counting the number of cells before and after sarkosyl treatment. Data are represented as mean with standard deviation and the *t*-test was performed from well-distributed data set ($n = 3$) of each cell line. Trophozoites of *E. histolytica* strain HM-1:IMSS were grown under axenic conditions in TYI-S-33 medium (Diamond et al., 1978). EhERM-BP (EHI_146360) cell line constitutively overexpressing N-terminally Myc-tagged EhERM-BP was made by using the plasmid pKT-3M as a backbone and maintained at G418 concentration of 12 μg/mL.

Immunostaining

E. invadens trophozoites and cysts expressing myc-tagged WT and mutant versions of ERM-BP were fixed with acetone/methanol (1:1) and permeabilized with 0.1% Triton X-100 as described earlier (Manna et al., 2018). Cells were incubated with 3% bovine serum albumin (BSA) for blocking followed by mouse monoclonal anti-myc antibody (1:500, Cell signaling). Heat-shocked and control *E. histolytica* trophozoites expressing myc-tagged ERM-BP fixed with acetone/methanol (1:1) and permeabilized with 0.1% Triton X-100. Slides were prepared using Vectashield mounting medium with DAPI (Vector Laboratories, Inc) and visualized using a Leica CTR6000 microscope, using a BD CARVII confocal unit. Images were analyzed using Leica LAS-AF software.

Live Cell Imaging

E. invadens cells were encysted for 72 h and stained with cell permeable Cyto11 (stains DNA) and calcofluor white (stains cyst wall) in a 96-well plate. Cells were continuously visualized under 20× objective using three channels (Bright Field, FITC, and DAPI) in a Leica CTR6000 microscope and time-lapse images were captured at 1 s intervals for the indicated time periods. Images were analyzed using Leica LAS-AF software. The movie represents all the channels as merged and 3 frames per second (.mov file).

Electrophoretic Mobility Shift Assays (EMSA)

EMSA was performed as previously described (Pearson et al., 2013). The oligonucleotides used in EMSA are listed in **Supplementary Table 1**. Each motif had an additional 12-nt at 5′ and 8-nt at 3′, which creates a 5′-overhang after annealing and was utilized for radiolabeling using Klenow (Hackney et al., 2007). In brief, complementary overlapping ERM-probes were annealed and labeled using [^{32}P] α-ATP and Klenow fragment (Invitrogen). Binding reaction was set in a total volume of 20 μl, which included 2 μl 10× EMSA binding buffer (10 mM Tris-HCl, pH 7.9, 50 mM NaCl, 1 mM EDTA, 3% glycerol, 0.05% milk powder, and 0.05 mg of bromophenol blue), 5 μg of nuclear extract form control and heat-shocked trophozoites, 2 μg of poly (dI-dC), and 50 fmol of labeled probe. The binding reaction mixes were loaded onto a 9% non-denaturing polyacrylamide gel and run for 3 h. The gel was fixed, dried, and exposed to a phosphor screen. Gels were imaged using Personal Molecular Imager (PMI) system with Quantity One software, Bio-Rad.

RNA Extraction and RT-PCR

Total RNA was extracted from trophozoites using TRIzol method (Life Technologies). RNA was subjected to DNase treatment (DNase kit; Invitrogen) and reverse transcribed using oligo (dT) primers (Invitrogen). The resultant cDNA (3 μl) was used in subsequent PCRs (25 μl total volume). The number of PCR cycles was set to 30, and 10 μl of PCR products was run on a 1.5% agarose gel. The negative control (minus reverse transcriptase [RT]) was split away before the addition of Superscript RT (Invitrogen) and otherwise treated like the other samples. The primers used in RT-PCR are listed in **Supplementary Table 1.**

Plasmid Construction

To overexpress the protein in *Entamoeba* the full-length coding region of ERM-BP gene (EIN_083100) was cloned into the AvrII and SacII sites in the pEi-CKII-myc plasmid as previously described (Manna et al., 2014, 2018). For the mutants, PCR was done from pGEX-2T1 clones (ERM-BP-D12A, ERM-BP-DBM, ERM-BP-K150A, and ERM-BP-C198A) as described earlier and cloned in the pEi-CKII-myc backbone plasmid at AvrII and SacII sites. For the cloning of *E. histolytica* homolog of ERM-BP (EHI_146360) the full-length coding region of EHI_146360 was cloned into pKT-3M backbone as described earlier (Zhang et al., 2008). The primers used in cloning are listed in **Supplementary Table 1**. The constructs were confirmed by sequencing before transfecting into *Entamoeba.*

Measurement of Intracellular NAD^+/NADH

Intracellular NAD^+ and NADH were determined as per the manufacturer's protocol (NAD^+/NADH Assay Kit, Cat No: ab65348, Abcam) and as described earlier (Manna et al., 2018). Briefly 2×10^6 control or heat-shocked cells were lysed in NAD^+/NADH extraction buffer by sonication (five pulses at 15 amp for 15 s). The lysate was centrifuged at 14,000 rpm and the supernatant containing NAD^+/NADH was filtered through a 10 kDa spin column to get rid of enzymes, which may consume NADH rapidly. To detect the NADH in the sample, a decomposition step was performed by heating the samples at 60°C for 30 min; under this condition, all the NAD^+ will be decomposed while NADH will be still intact. 100 μl reaction mix was prepared for each standard and samples were plated in duplicates in a clear bottom 96 well plate (Corning, Catalog # CLS3603). The plate was incubated at room temperature for 5 min to convert NAD^+ to NADH followed by addition of 10 μl NADH developer into each well and incubated at room temperature for 2 h. OD was measured at 450 nm using a plate reader (BioTek Cytation3).

Induction of Heat Stress and Viability Assay

For *E. histolytica,* heat shock was induced in a 42°C water bath for different time points (1, 2, 3, and 8 h). For *E. invadens*, heat shock was induced in a 37°C water bath for different time points (1, 2, 3, and 8 h). RNA expression by RT-PCR was performed at the time point as indicated. Viability assay was performed by

Fluorescein diacetate (FDA) hydrolysis assay. Cells were pelleted and resuspended in PBS containing 10 μg/ml FDA. Cells were incubating at room temperature for 5 min followed by wash with 1× PBS. The cells were then observed under a fluorescence microscope for the fluorescence produced by live cells.

Statistical Analysis

Student's *t*-test was performed for all experiments where two conditions or genotypes were compared. A *p*-value of <0.05 in each independent experiment was considered significant.

RESULTS

Dominant Negative Effect of ERM-BP Mutants on Encystation Efficiency

Transcription factors play a crucial role in controlling different life cycle stages in many organisms. Recent studies in *Entamoeba* identified a novel developmentally regulated transcription factor ERM-BP which has important roles in the encystation process (Manna et al., 2018). Silencing of ERM-BP significantly reduces the encystation efficiency and produces ghost-like cysts, which fail to undergo excystation to trophozoites (Manna et al., 2018). Biochemical studies with recombinant proteins identified distinctive roles of its two domains, an N-terminal DNA-binding domain (DBD) and a C-terminal nicotinamidase domain (Manna et al., 2018). A single amino acid mutation at the Cysteine residue at position 198 to Alanine (C198A) in the nicotinamidase domain (ERM-BP-C198A) impairs both NAD^+ and DNA binding activity. On the other hand, mutation in a five amino acid cluster (S_AR_LTKR) in the DNA-binding domain (ERM-BP-DBM) significantly affects DNA binding properties; however, this mutant can bind NAD^+. Two other mutants, ERM-BP-D12A and ERM-BP-K150A, retain both NAD^+ and DNA binding properties but have reduced enzymatic activity for conversion of nicotinamide to nicotinic acid (Manna et al., 2018).

The above studies were done with recombinant protein in the absence of other amebic cellular factors or proteins. In the current study, we characterized the function of the ERM-BP mutants in *E. invadens* parasites by overexpressing WT and mutant proteins and assessing the phenotypes of the parasites in development. All the mutants and WT-constructs were generated in an *E. invadens* expression vector under CK-promoter and myc-tagged at the N-terminus as described earlier (Ehrenkaufer and Singh, 2012). **Figure 1A** is a schematic of ERM-BP-WT and various mutants with the position of the mutation being indicated by the arrow. All the constructs were transfected into *E. invadens* and stable cell lines were generated. The expression of proteins was tested by western blot analysis using anti-myc antibody. To determine intracellular localization, immunostaining was performed with α-myc antibody in trophozoites and 24 h cysts. Overexpression of mutant ERM-BP-D12A and ERM-BP-K150A showed nuclear and cytoplasmic localization in trophozoites similar to ERM-BP-WT (**Figure 1B**); this is consistent with the *in vitro* results where recombinant ERM-BP-D12A and ERM-BP-K150A retain the ability to bind DNA. However, ERM-BP-C198A and ERM-BP-DBM showed only cytoplasmic localization in trophozoites. ERM-BP-DBM showed intense puncta like structure throughout the cytoplasm and ERM-BP-C198A show localization at the pseudopod (**Figure 1B**). A similar pattern of localization was seen in cysts where ERM-BP-D12A and ERM-BP-K150A localized to the nucleus and ERM-BP-C198A and ERM-BP-DBM mutants showed disintegrated localization in the cytoplasm (**Figure 1C**). Consistent with the altered localization in trophozoites and cysts, overexpression of both ERM-BP-C198A and ERM-BP-DBM mutants significantly reduced encystation efficiency, indicating that these mutants exerted dominant negative effects on the efficiency of stage conversion (**Figure 1D**).

Silencing of ERM-BP Affects Formation of Multi-Nucleated Giant Cells

Cell fusion can lead to formation of giant cells with multiple nuclei in many systems (Milde et al., 2015; Miron and Bosshardt, 2018). Formation of multi-nucleated giant cells (MGC) can increase in response to an infection, such as tuberculosis, herpes, HIV, or other foreign body (Anderson, 2000; Dargent et al., 2000; Brodbeck and Anderson, 2009; McClean and Tobin, 2016). Formation of MGC is also observed in the development of soil-dwelling amoeba *Dictyostelium discoideum* during macrocyst formation (Ishida et al., 2005) and in *E. invadens* during the encystation (Krishnan and Ghosh, 2018). In encystation media *Entamoeba* form aggregates and multiple cells go through cytofusion and transform into giant cells (**Figure 2A**). MGC nuclei are smaller compared to trophozoites suggesting that MGC underwent nuclear division similar to that seen in cysts (Krishnan and Ghosh, 2018) and meiotic genes were reported which expressed during encystation (Ehrenkaufer et al., 2013). These tiny nuclei inside the MGC are mostly clustered and can go through nuclear fusion to make a polyploid nucleus. The mechanisms and signaling responsible for MGC formation are not yet known.

Interestingly, we observed that the silencing of ERM-BP significantly restricts the formation of MGC compare to control parasites. The MGC were observed at a very low frequency in WT-cells (1 in 10^4 cells) and the size of MGC increases with time of incubation of cells in encysting medium due to continuous fusions of cells. Similar to published data, our analysis identified increasing frequency and size of MGC with prolonged exposure in encystation conditions. By 72 h of encystation, in control cell lines the giant cells are very large and most of the giant cells contain over 50 nuclei (**Figure 2B** and **Supplementary Movies 1, 2**). Parasites in which ERM-BP is disrupted (silenced ERM-BP, ERM-BP-C198A, and ERM-BP-DBM) had decreased formation of MGC number and those MGC that were formed were significantly smaller (**Figure 2C**). However, there was no significant difference in the formation of cellular aggregates, suggesting that the MGC formation is downstream of aggregate formation and dependent on ERM-BP function. Silencing of another transcription factor, NF-YC, which appears later in encystation (48 h) showed a moderate effect on MGC formation (**Figure 2C**). In the MGC observed where ERM-BP function is disrupted (ERM-BP silenced, ERM-BP-C198A, and ERM-BP-DBM) the number of nuclei is predominantly between 1 and 10. On the contrary, the nuclei number in control parasites and parasites with silenced-NF-YC ranges between 51 and 100, and in few MGC it's even more than 200 (**Figure 2D**). Our results indicate that encystation pathway and formation of

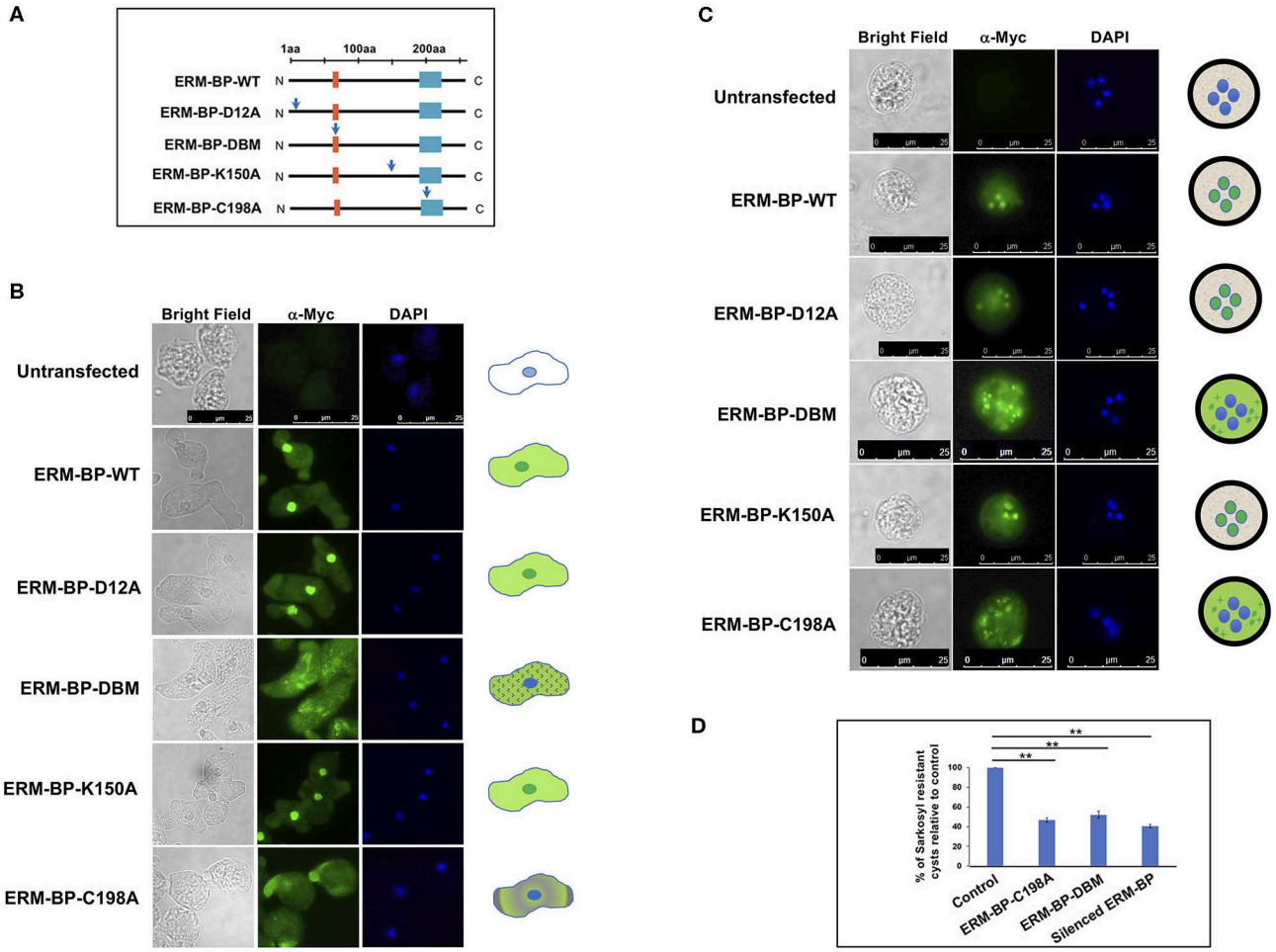

FIGURE 1 | Functional characterization of ERM-BP-WT and mutants and dominant negative effects of C198A and ERM-BP-DBM. **(A)** Different constructs expressing WT and mutant versions of ERM-BP and with Myc-tagged at the N-terminal end are generated by changing each relevant residue into an Alanine as pointed by the blue arrows. Orange box at the N-terminus indicates location of the predicted DNA binding domain (S_AR_LTKR) and cyan-box at the C-terminus indicates the nicotinamidase domain which is important for NAD binding. The mutants are ERM-BP-D12A, ERM-BP-C198A, ERM-BP-K150A and a DNA binding mutant (ERM-BP-DBM) in which five amino acids cluster (S_AR_LTKR) except "A" and "L" as shown in subscripts in the orange-box were changed into Alanine. All the constructs were transfected into *E. invadens* and stable cell lines were generated. Immunostaining with α-myc antibody in **(B)** trophozoites, and **(C)** 24 h cysts were performed in ERM-BP-WT and mutant cells (Green). DNA was stained with DAPI (Blue). The pattern of localization in both trophozoites and cysts are shown in schematic on the right. Scale bars for both trophozoites and cysts are 25 μm. **(D)** Data represents the percentage of sarkosyl resistant cysts relative to control after 72 h of encystation. Data are mean ± s.d. ($n = 3$) Student's *t*-test; $^{**}P < 0.01$.

MGC may share similar signaling pathway(s); both formation of MGC and encystation are affected by ERM-BP function.

NAD^+ Increases With Heat Shock and Overexpression of ERM-BP Makes Parasites More Resistant to Heat Stress

It has previously been shown that stress response important for encystation appears to overlap with that of with heat stress (Field et al., 2000). Thus, we looked to determine whether ERM-BP expression is only specific for encystation or also has correlation with other stress response. RT-PCR revealed that expression of ERM-BP is upregulated in heat stress in *E. histolytica* trophozoites (**Supplementary Figure 1**). However, expression of ERM-BP was not affected by H_2O_2 stress (data not shown). In order to determine if NAD^+ levels changed during heat shock, we measured NAD^+/NADH levels in control and heat-shocked *E. histolytica* trophozoites. Our results demonstrated that intracellular NAD^+ levels goes up significantly in heat stressed parasites (**Figure 3A**). This level of increase is similar to what we noted in *E. invadens* encysting parasites (Manna et al., 2018). Additionally, we tested nuclear extracts from heat-shocked *E. histolytica* trophozoites, which showed specific binding to ERM compared to control parasites where no binding was noted (**Figure 3B**).

In order to define a phenotype with ERM-BP and heat shock response, we overexpressed ERM-BP in both *E. invadens* and *E. histolytica* and exposed the parasites to heat shock

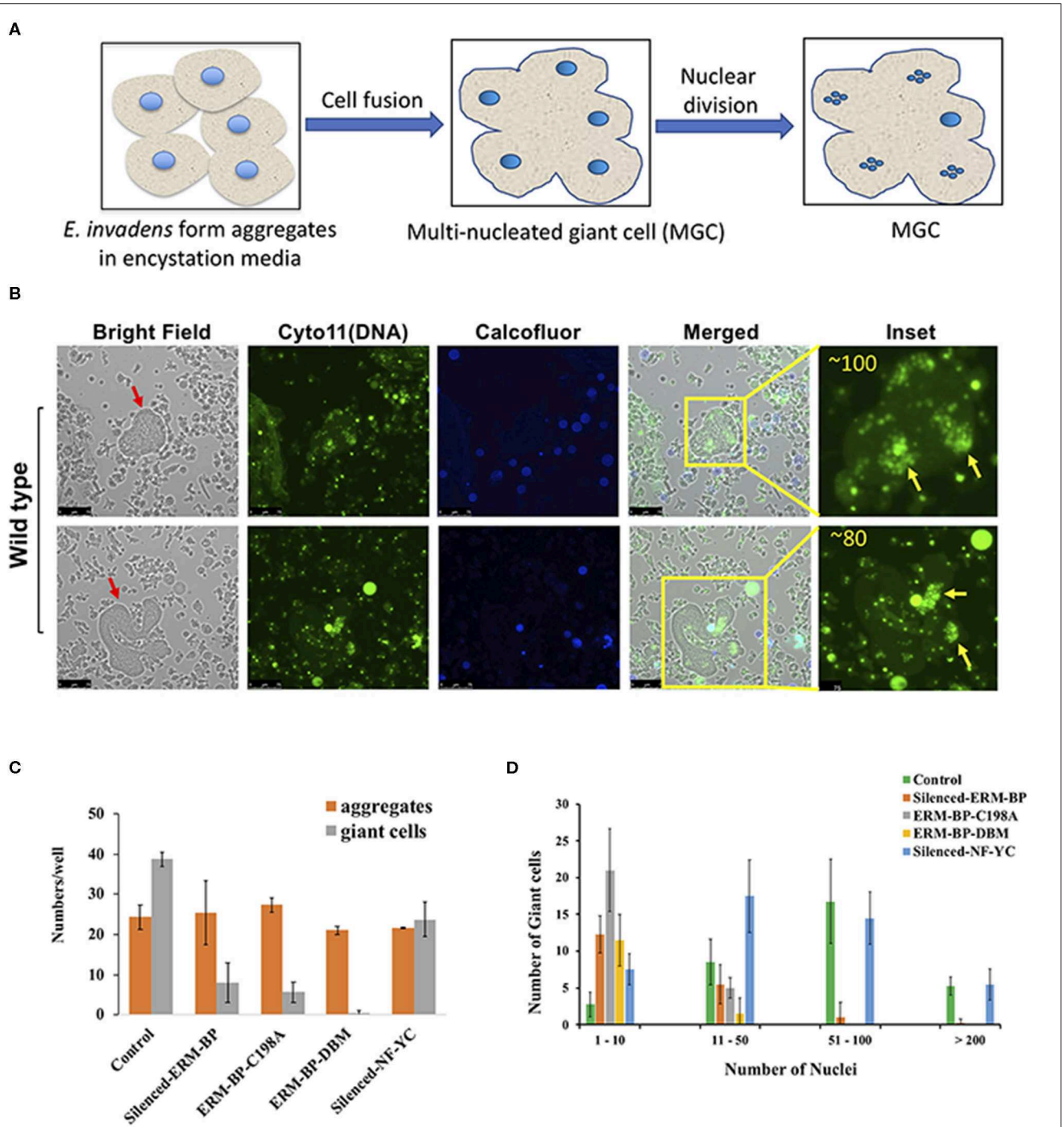

FIGURE 2 | *E. invadens* form Multi-nucleated Giant Cells (MGC) during encystation and silencing of ERM-BP and mutants restrict the formation of MGC during encystation. **(A)** Schematic depicts the formation of giant cells during encystation. Amoeba form aggregates after inoculation into encystation media. Multiple cells can fuse together to make a giant cell. The polyploid entamoeba nucleus undergoes miotic division to make quadrinucleate haploid nuclei and remain as clustered. **(B)** Staining of 72 h encysted cells with cell permeable Cyto11 (in green for DNA) and calcofluor white (in blue for cyst wall) are shown in two representative fields. Red arrow indicates the giant cells. In the inset, nuclear staining observed at higher magnification and the number of nuclei in each giant cell is shown. Yellow arrows indicate the clusters of nuclei in those giant cells. Scale bars are 25 μm. **(C)** Control, silenced-ERM-BP, two other mutants ERM-BP-C198A, ERM-BP-DBM, and silenced-NF-YC were encysted in 96-well plates in six replicates per plate for 72 h. The number of aggregates and number of giant cells per well were represented. **(D)** The number of giant cells and their corresponding number of nuclei content (nuclei numbers: 1–10, 11–50, 51–100, and >200) are shown in control, silenced-ERM-BP, ERM-BP-C198A, ERM-BP-DBM, and silenced-NF-YC. Data are mean ± s.d. ($n = 3$).

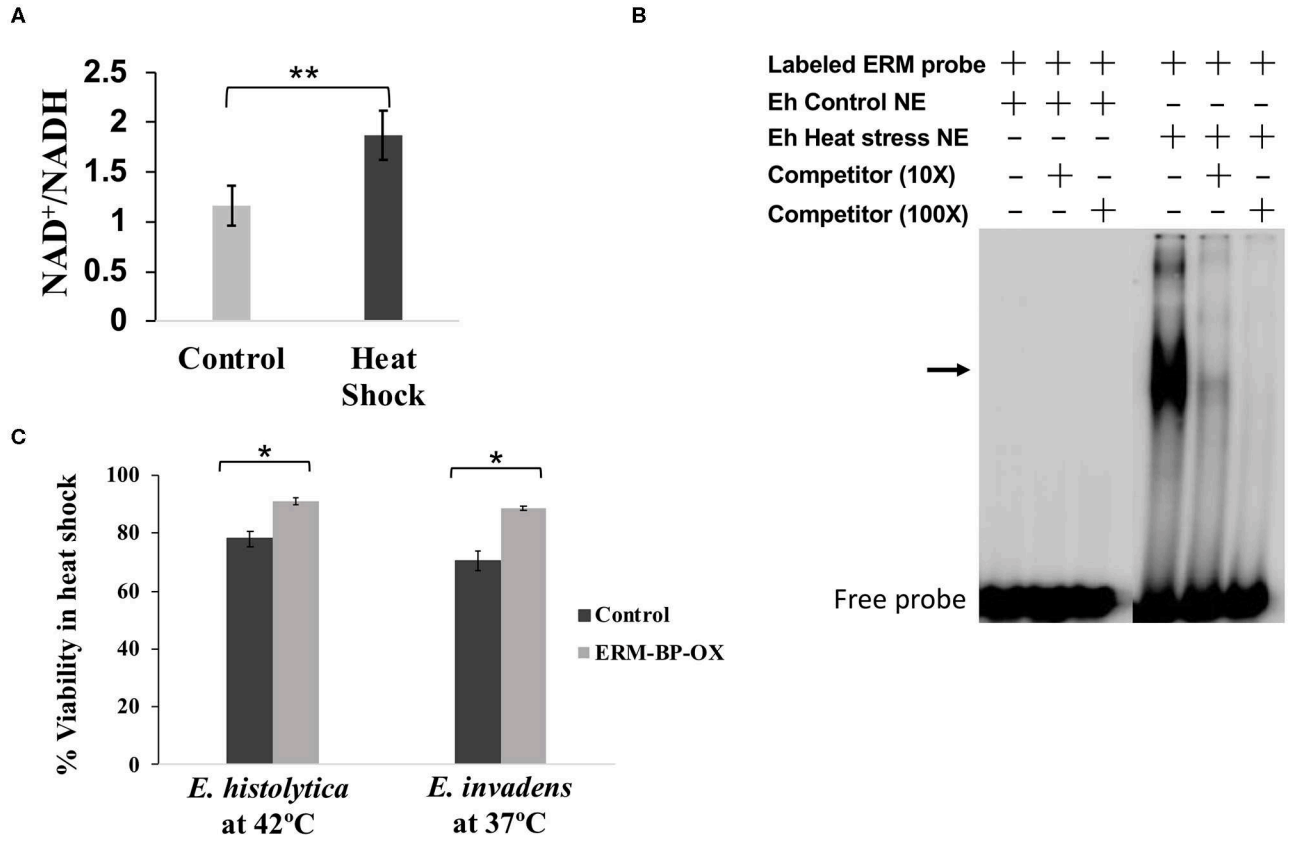

FIGURE 3 | Intracellular NAD^+/NADH elevated due to heat-stress, nuclear protein from heat shock parasites binds specifically to ERM and overexpression of ERM-BP makes parasites more resistant to heat stress. **(A)** Measurement of intracellular NAD^+/NADH in heat-shock and untreated *E. histolytica*. Data are mean ±s.d. ($n = 3$) Student's *t*-test; $^{**}p < 0.01$. **(B)** EMSA was performed using crude nuclear extracts from control and heat-stressed *E. histolytica* cells. EMSA results are shown in the presence and absence of different components marked as "+" and "–," respectively. Radiolabeled ERM probe was used in each reaction. Unlabeled ERM probe at 10× and 100× was used as a specific competitor as indicated. The arrow indicates the major specific band in the gel shift assay; free probe is at the bottom. **(C)** Viability assay of control and overexpressed-ERM-BP cells from both *E. histolytica* and *E. invadens* were performed by FDA hydrolysis assay. Data are mean ± s.d. ($n = 2$) Student's *t*-test; $^{*}P < 0.05$.

for different time points (0, 1, 2, 3, 8 h). For heat stress, *E. invadens* cells were incubated at 37°C and *E. histolytica* at 42°C and cellular viability was determined at different time points (**Supplementary Figure 2**). We observed that overexpression of ERM-BP makes both *E. invadens* and *E. histolytica* more resistant to heat stress after 8 h of incubation (**Figure 3C**). Thus, it appears that ERM-BP has a dual role in *E. invadens* – for regulating both encystation and heat shock response. In *E. histolytica*, ERM-BP is important in mediating heat shock stress response; encystation in *E. histolytica* cannot be assessed.

Heat Stress and Overexpression of ERM-BP Induce the Formation of Quadrinucleated Cyst-Like Structures and MGC

Overexpression of ERM-BP in *E. invadens* enhanced encystation efficiency and addition of NAD^+ had an additive effect and further enhanced encystation in ERM-BP-OX cells (Manna et al., 2018). However, when we overexpressed ERM-BP in *E. histolytica* we did not observe calcofluor stained cysts in glucose deprived and osmotic stress condition, even with the addition of excess NAD^+; instead most of the cells rounded up and died within 16 h of incubation (data not shown). However, upon analyzing *E. histolytica* trophozoites a small percentage of cells with quadrinucleated structures were observed due to heat stress in both WT and ERM-BP overexpressed parasites, suggesting ERM-BP may be transcriptionally active and responsive for the nuclear division in heat stress conditions similar to encystation pathway (**Figure 4A**). We also observed that in heat-shock conditions and when ERM-BP is overexpressed, cell fusion events occur in *E. histolytica*, leading to the formation of bigger cells with multiple nuclei (**Figure 4B**). Multiple blebs throughout the cell surface were observed in those big cells, suggesting that these cells are competent for continuous fusion to making even larger cells. To determine whether these giant cells are viable, FDA hydrolysis assay was performed along with staining the cells with cell permeable Hoechst 33342 to stain DNA and revealed

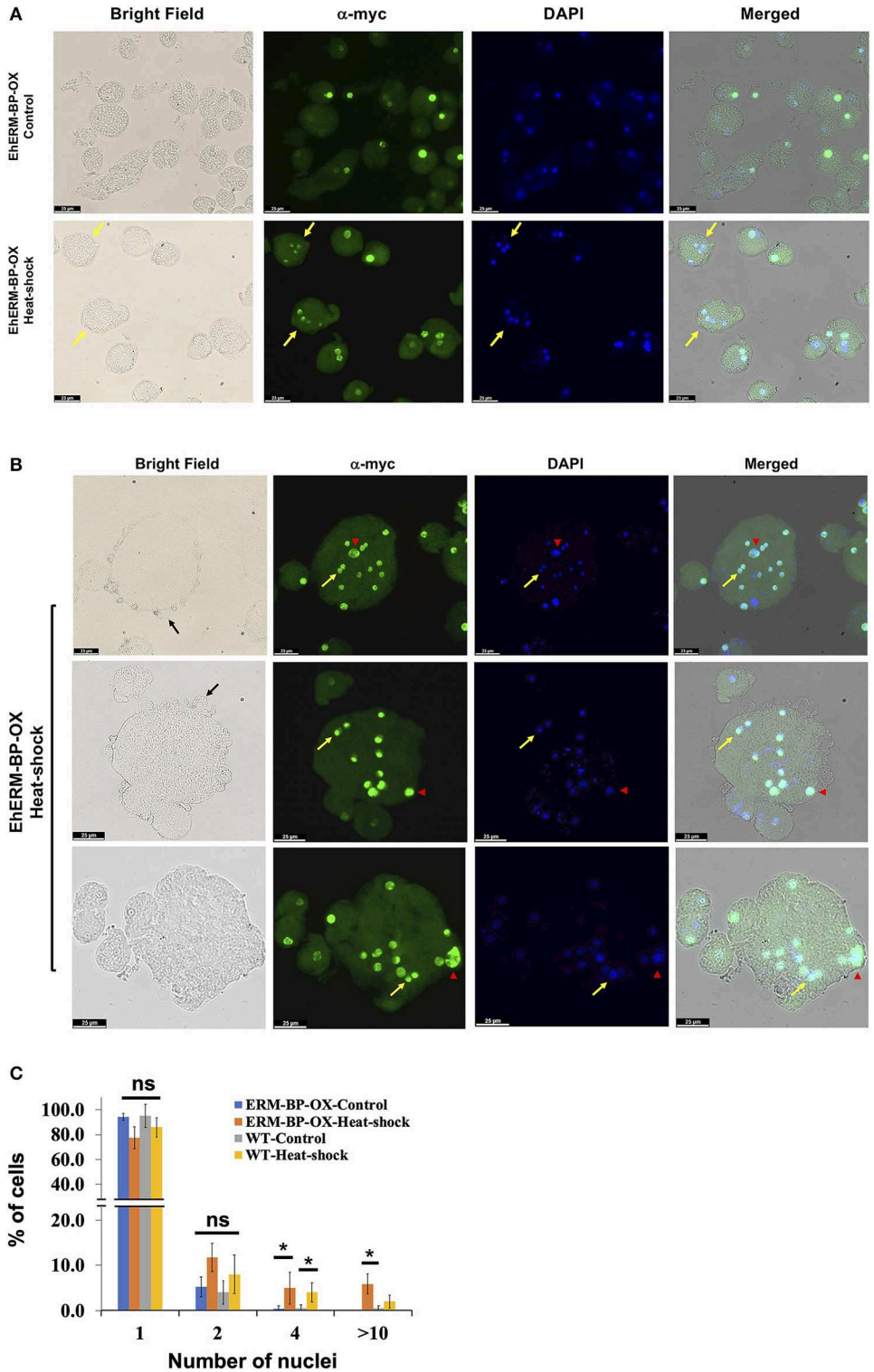

FIGURE 4 | Overexpression of ERM-BP and heat stress induce nuclear division and cell fusion in *E. histolytica*. **(A)** Immunostaining with α-myc antibody in control and heat-shocked ERM-BP-OX cells shown in green. DNA was stained with DAPI (Blue). Yellow arrows indicate the quadri-nucleated cells in heat-shock condition. Scale bars are 25 μm. **(B)** Immunostaining of ERM-BP-OX MGC in heat-shock condition with α-myc antibody shown in green. DNA was stained with DAPI (Blue). Yellow arrow indicates the divided nuclei inside the giant cell and red arrowhead indicates polyploid nuclei. Three fields are shown as representative. Scale bars are 25 μm. **(C)** Percentage of cells with different number of nuclei (1, 2, 4, and >10) in control and heat-shock conditions for both wild type (WT) and ERM-BP-OX are shown. Data are mean ± s.d. ($n = 2$), Student's *t*-test; $^*P < 0.05$. "ns" for not significant.

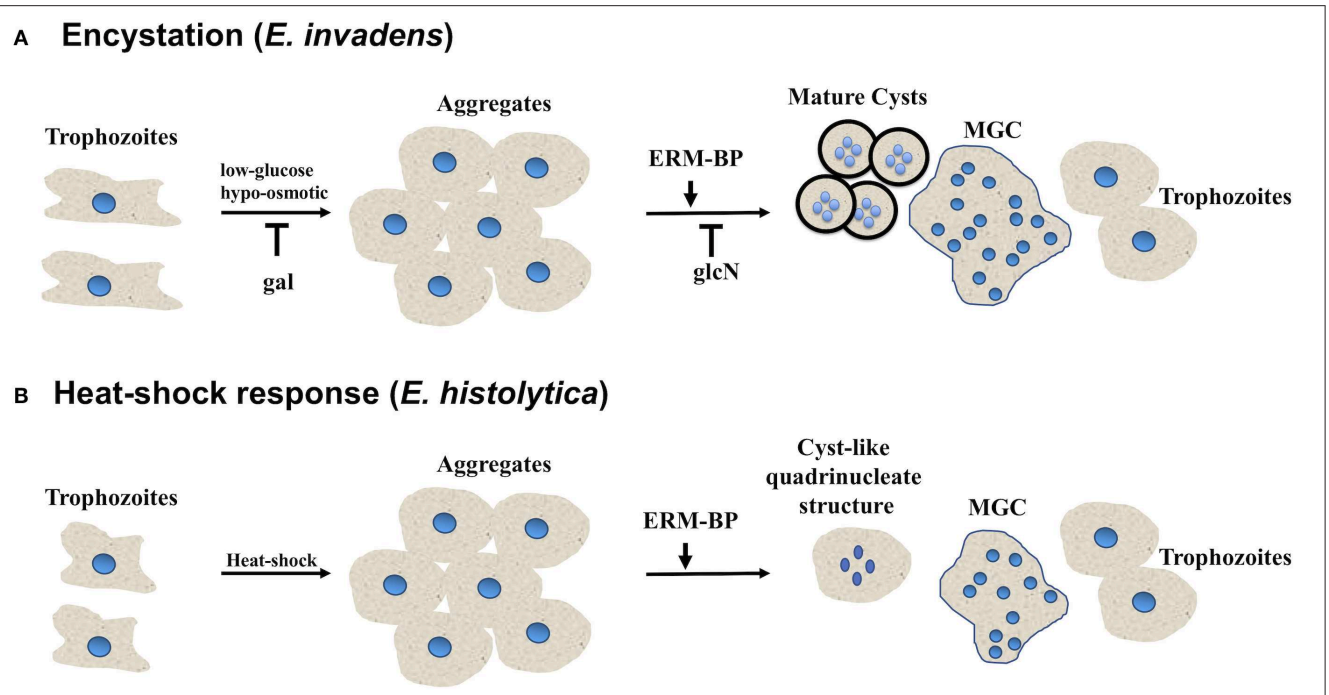

FIGURE 5 | *Entamoeba* encystation and heat-shock response are related. Schematic showing different morphological changes during encystation and heat-shock response in *Entamoeba*. **(A)** *E. invadens* form aggregates in encystation media due to osmotic stress and glucose deprivation. Free galactose (gal) block the multicellular aggregate formation, on the other hand N-acetyl-glucosamine (glcN) does not affect aggregate formation however, it prevents cyst formation. ERM-BP also work downstream of aggregate formation. With the progression of encystation nuclear division take place to make quadrinucleated cyst with thick chitin cyst wall. Cell fusion also take place in encystation conditions, and *Entamoeba* can transform into multinucleated giant cells which are highly motile under confinement may undergo continuous cytofission to generate daughter cells. **(B)** In heat-shock conditions most of the *Entamoeba* become rounded and form aggregates. Nuclear division occurs and quadrinucleated cyst-like structures are observed. Cell fusion also takes place in heat-shock condition and *Entamoeba* can transform into multinucleated giant cells.

that the giant cells are indeed viable (**Supplementary Figure 3**). Additionally, we analyzed the percentage of ERM-BP-OX cells and wild type cells (WT) containing different numbers of nuclei in control and heat-shock conditions. The data reveals that the number of multi-nucleated cells increase upon heat shock, in both wild-type control cells as well as in ERM-BP overexpressing parasites (**Figure 4C**).

Our results suggest that the giant cells are viable, and EhERM-BP may have a functional role in heat-stress response that is similar to its role in encystation. This result supports the notion of previous findings that heat stress and encystation pathway may have some inter-connection with potential overlap in signaling pathways. Overall our results suggest that the encystation pathway and heat-stress response are related in *Entamoeba*. Previous work from other groups and our recent study depicts the model of *Entamoeba* encystation and heat-shock response pathways and summarizes the key factors which involved in both processes (**Figure 5**). ERM-BP is downstream of cellular aggregation in both encystation and heat-shock response but is upstream of multinucleated giant cell formation and encystation.

DISCUSSION

The transcription factor ERM-BP plays an important role in regulating encystation in *Entamoeba*. We dissected the domain functions of ERM-BP further by overexpressing the WT and mutant proteins in *Entamoeba*. Overexpression of ERM-BP-DBM and ERM-BP-C198A resulted in mis-localization of the protein in both trophozoites and cysts and significantly reduced encystation efficiency. During encystation, a subset of *E. invadens* parasites also transform into multi-nucleated giant cells (MGC). We demonstrate that silencing of ERM-BP reduced the number and size of giant cells, which contain fewer nuclei. Among different stress responses, heat-stress was reported earlier to have commonalities with encystation in *Entamoeba* (Field et al., 2000). Our present studies support that notion and demonstrated that NAD^+ levels increase with heat shock, and that overexpression of ERM-BP protects both *E. histolytica* and *E. invadens* parasites against death by heat shock. Furthermore, in *E. histolytica* heat shock results in cell fusion with formation of giant cells, and also nuclear division which produces cyst-like quadrinucleate parasites. We showed that ERM-BP functions downstream of cellular aggregation and is an early regulator of both development and heat shock response in *Entamoeba*. A model that depicts our understanding of ERM-BP in *Entamoeba* development and heat shock is shown in **Figure 5**.

Previous studies on ERM-BP showed that ERM-BP binds to metabolic cofactor NAD^+ and this binding facilitates its DNA binding activity to control the expression of cyst-specific genes. Silencing of ERM-BP significantly decreases encystation

efficiency and produces ghost like cysts, with defective cyst walls which fail to excyst. *In vitro* studies with recombinant protein from two mutant ERM-BPs identified a DNA binding motif at the N-terminus, in which changing five amino acids (ERM-BP-DBM) affects its DNA binding properties. Additionally, changing a single amino acid (Cys198) in the C-terminus in the nicotinamidase domain (ERM-BP-C198A), affects NAD^+ binding as well as DNA binding properties. We have now confirmed these findings in parasites with both mutants (ERM-BP-DBM and ERM-BP-C198A) resulting in abnormal cellular localization in both trophozoites and cysts and resulting in significant reduction in formation of viable cysts. In contrast, mutations in ERM-BP-D12A and ERM-BP-K150A did not affect protein localization in trophozoites or cysts. These results recapitulate studies with recombinant protein and ERM-BP function and demonstrate functional consequences in parasites.

Formation of a small numbers of multinucleated giant cells have been observed during encystation of *E. invadens*. In *E. invadens*, these MGCs were formed in multicellular aggregates through the cyto-fusion of multiple trophozoites in the encystation culture media due to osmotic stress and glucose depletion; however, other stress responses, such as heat shock or oxidative stress did not induce MGC formation in *E. invadens* as described earlier (Krishnan and Ghosh, 2018). Cell fusion and formation of MGC is a common feature that develops during various inflammatory reactions, such as infection with tuberculosis, herpes, HIV or other foreign body (Dargent et al., 2000; Brodbeck and Anderson, 2009; McClean and Tobin, 2016). MGCs are special class of giant cell formed by the fusion of monocytes or macrophages and predominantly found in human tissues and are presumed to contribute to the removal of debris from the tissues (Milde et al., 2015; Miron and Bosshardt, 2018). Formation of MGC can be induced *in vitro* in other systems through the use of conditioned medium (Abe et al., 1991), several different cytokines (Most et al., 1997), addition of lectins alone or in combination with interferon (IFN-γ) (Chambers, 1977; Takashima et al., 1993) and addition of antibodies or phorbol myristate acetate (PMA) or a combination of both (Hassan et al., 1989).

In *E. invadens* the molecular triggers which induce MGC formation are not well-understood. The commonalities between the formation of cyst and MGC include the fact that both require cell aggregate formation, and it is plausible that the initial signaling associated with encystation and MGC formation may be same. A number of meiotic genes were reported to be upregulated during encystation (Ehrenkaufer et al., 2013) and quadrinucleate cysts contain smaller haploid nuclei compared to the polyploid trophozoite nucleus. In MGC, nuclei undergo division after cell fusion and after 48 h of encystation mainly smaller haploid nuclei are observed in MGC (Krishnan and Ghosh, 2018), suggesting that meiotic genes might be also active in MGC. Multinucleated cells also observed in *E. histolytica* trophozoites due to delinking of S-phase and cytokinesis (Das and Lohia, 2002)However, there is a distinct difference between MGC and multinucleated *E. histolytica* cells in that the latter are not giant in size as observed in *E. invadens*. Previously, treatment with the Myosin II inhibitor, 2,3-butanedione monoxime (BDM), was observed to inhibit the cytofission without stopping the cell fusion, thus the number of MGCs was not affected by BDM (Krishnan and Ghosh, 2018). These observations indicate the possibility of continuous fusion and cytofission occurring inside the cell aggregates and that the MGCs observed in older encystation cultures could be the final product of such cyclic fusion. Aggregate formation in encystation media is crucial for cyst formation, and multiple cells fused together in this aggregate could lead to the formation of MGCs.

It was previously reported that the heat shock and encystation response in *Entamoeba* are related (Field et al., 2000). Earlier studies revealed the involvement of heat shock protein 90 (HSP90) as a negative regulator of *Entamoeba* encystation (Singh et al., 2015) (43). Messenger RNA for chitinase and Jacob are strongly induced in both encystation and heat stress (Field et al., 2000) and expression of Jacob protein is also evident in the secretory vesicles of heat-shocked *E. invadens,* suggesting an important link between encystation and heat-shock responses (Field et al., 2000). Recent studies demonstrated that Topoisomerase II is highly upregulated in both during encystation and in heat-stress response as well as due to oxidative stress (Varghese and Ghosh, 2020). Our data, that NAD^+ increases with heat shock, and that overexpression of ERM-BP protects both *E. histolytica* and *E. invadens* parasites against death by heat shock further supports the functional and regulatory link between heat shock and encystation. Furthermore, as we demonstrated that *E. histolytica* heat shock results in cell fusion with giant cells, and also nuclear division which produces cyst-like quadrinucleate parasites it would appear that ERM-BP functions in a parallel manner in both *E. histolytica* and *E. invadens*.

Overall, our work identified that ERM-BP functions downstream of cellular aggregation and is an early regulator of both development and heat shock response in *Entamoeba*. Future studies to dissect the interacting partners of ERM-BP are planned. Definitive proof that ERM-BP regulates development in *E. histolytica* awaits future efforts and development of a system to generate cysts in *E. histolytica*.

DATA AVAILABILITY STATEMENT

All datasets generated for this study are included in the article/**Supplementary Material**.

AUTHOR CONTRIBUTIONS

DM and DL-A designed and performed the experiments. DM, DL-A, GE, and US analyzed the data and wrote the manuscript. US conceived of the project and aided in manuscript preparation. All authors contributed to the article and approved the submitted version.

FUNDING

This work was supported by a grant from NIAID AI119893-02 to US.

ACKNOWLEDGMENTS

We thank all members of the Singh lab for helpful discussions and critical reading of the manuscript.

SUPPLEMENTARY MATERIAL

The Supplementary Material for this article can be found online at: https://www.frontiersin.org/articles/10.3389/fcimb.2020.00363/full#supplementary-material

Supplementary Figure 1 | Transcription factor ERM-BP is upregulated due to heat shock. RT-PCR to detect the expression of *Eh*ERM-BP (EHI_146360) transcript level in *E. histolytica* (HM-1:IMSS) trophozoites in control and heat-stress condition with a loading control (EHI_199600).

Supplementary Figure 2 | Viability assay of control and overexpressed-ERM-BP cells from both *E. histolytica* and *E. invadens*. Viability assay was performed by Fluorescein Diacetate (FDA) hydrolysis at different time points of heat stress (0, 1, 2, 3, and 8 h). Data are mean ± s.d. ($n = 2$) Student's *t*-test; $^*P < 0.05$.

Supplementary Figure 3 | Fluorescein Diacetate (FDA) showing the heat shock induced giant cells are viable. *E. histolytica* cells were heat shocked for 3 h and stained with FDA for viability and Hoechst 33342 to stain DNA. Three fields are shown as representative, yellow arrow indicates the giant cells and red arrowhead showing the dead cells. Scale bars are 25 μm.

Supplementary Movies 1 and 2 | *E. invadens* cells were encysted for 72 h and stained with cell permeable Cyto11 (in green to stain DNA) and calcofluor white (in blue to stain cyst wall) in a 96 well plate. Cells were continuously visualized using three channels (Bright Field, FITC, and DAPI) using a Leica CTR6000 microscope and time-lapse images were captured at 1 s intervals. Images were analyzed using Leica LAS-AF software. The movie represents all the channels as merged and 3 frames per second (.mov file).

REFERENCES

Abe, E., Ishimi, Y., Jin, C. H., Hong, M. H., Sato, T., and Suda, T. (1991). Granulocyte-macrophage colony-stimulating factor is a major macrophage fusion factor present in conditioned medium of concanavalin A-stimulated spleen cell cultures. *J. Immunol.* 147, 1810–1815.

Aguilar-Diaz, H., Diaz-Gallardo, M., Laclette, J. P., and Carrero, J. C. (2010). *In vitro* induction of entamoeba histolytica cyst-like structures from trophozoites. *PLoS Negl. Trop. Dis.* 4:e607. doi: 10.1371/journal.pntd.0000607

Anderson, J. M. (2000). Multinucleated giant cells. *Curr. Opin. Hematol.* 7, 40–47. doi: 10.1097/00062752-200001000-00008

Avron, B., Stolarsky, T., Chayen, A., and Mirelman, D. (1986). Encystation of entamoeba invadens IP-1 is induced by lowering the osmotic pressure and depletion of nutrients from the medium. *J. Protozool.* 33, 522–525. doi: 10.1111/j.1550-7408.1986.tb05655.x

Barron-Gonzalez, M. P., Villarreal-Trevino, L., Resendez-Perez, D., Mata-Cardenas, B. D., and Morales-Vallarta, M. R. (2008). Entamoeba histolytica: cyst-like structures *in vitro* induction. *Exp. Parasitol.* 118, 600–603. doi: 10.1016/j.exppara.2007.11.002

Brodbeck, W. G., and Anderson, J. M. (2009). Giant cell formation and function. *Curr. Opin. Hematol.* 16, 53–57. doi: 10.1097/MOH.0b013e32831ac52e

Byers, J., Faigle, W., and Eichinger, D. (2005). Colonic short-chain fatty acids inhibit encystation of entamoeba invadens. *Cell. Microbiol.* 7, 269–279. doi: 10.1111/j.1462-5822.2004.00457.x

Chambers, T. J. (1977). Fusion of hamster macrophages induced by lectins. *J. Pathol.* 123, 53–61. doi: 10.1002/path.1711230107

Chayen, A., Avron, B., and Mirelman, D. (1985). Changes in cell surface proteins and glycoproteins during the encystation of entamoeba invadens. *Mol. Biochem. Parasitol.* 15, 83–93. doi: 10.1016/0166-6851(85)90030-1

Cho, J., and Eichinger, D. (1998). Crithidia fasciculata induces encystation of entamoeba invadens in a galactose-dependent manner. *J. Parasitol.* 84, 705–710. doi: 10.2307/3284574

Clark, C. G., and Diamond, L. S. (2002). Methods for cultivation of luminal parasitic protists of clinical importance. *Clin. Microbiol. Rev.* 15, 329–341. doi: 10.1128/CMR.15.3.329-341.2002

Coppi, A., and Eichinger, D. (1999). Regulation of entamoeba invadens encystation and gene expression with galactose and N-acetylglucosamine. *Mol. Biochem. Parasitol.* 102, 67–77. doi: 10.1016/S0166-6851(99)00085-7

Coppi, A., Merali, S., and Eichinger, D. (2002). The enteric parasite entamoeba uses an autocrine catecholamine system during differentiation into the infectious cyst stage. *J. Biol. Chem.* 277, 8083–8090. doi: 10.1074/jbc.M111895200

Dargent, J. L., Lespagnard, L., Kornreich, A., Hermans, P., Clumeck, N., and Verhest, A. (2000). HIV-associated multinucleated giant cells in lymphoid tissue of the waldeyer's ring: a detailed study. *Mod. Pathol.* 13, 1293–1299. doi: 10.1038/modpathol.3880237

Das, S., and Lohia, A. (2002). Delinking of S phase and cytokinesis in the protozoan parasite entamoeba histolytica. *Cell. Microbiol.* 4, 55–60. doi: 10.1046/j.1462-5822.2002.00165.x

Diamond, L. S., Harlow, D. R., and Cunnick, C. C. (1978). A new medium for the axenic cultivation of entamoeba histolytica and other entamoeba. *Trans. R. Soc. Trop. Med. Hyg.* 72, 431–432. doi: 10.1016/0035-9203(78)90144-X

Ehrenkaufer, G. M., Hackney, J. A., and Singh, U. (2009). A developmentally regulated Myb domain protein regulates expression of a subset of stage-specific genes in entamoeba histolytica. *Cell. Microbiol.* 11, 898–910. doi: 10.1111/j.1462-5822.2009.01300.x

Ehrenkaufer, G. M., Haque, R., Hackney, J. A., Eichinger, D. J., and Singh, U. (2007). Identification of developmentally regulated genes in entamoeba histolytica: insights into mechanisms of stage conversion in a protozoan parasite. *Cell. Microbiol.* 9, 1426–1444. doi: 10.1111/j.1462-5822.2006.00882.x

Ehrenkaufer, G. M., and Singh, U. (2012). Transient and stable transfection in the protozoan parasite entamoeba invadens. *Mol. Biochem. Parasitol.* 184, 59–62. doi: 10.1016/j.molbiopara.2012.04.007

Ehrenkaufer, G. M., Weedall, G. D., Williams, D., Lorenzi, H. A., Caler, E., Hall, N., et al. (2013). The genome and transcriptome of the enteric parasite entamoeba invadens, a model for encystation. *Genome. Biol.* 14:R77. doi: 10.1186/gb-2013-14-7-r77

Eichinger, D. (2001). A role for a galactose lectin and its ligands during encystment of entamoeba. *J. Eukaryot. Microbiol.* 48, 17–21. doi: 10.1111/j.1550-7408.2001.tb00411.x

Field, J., Van Dellen, K., Ghosh, S. K., and Samuelson, J. (2000). Responses of entamoeba invadens to heat shock and encystation are related. *J. Eukaryot. Microbiol.* 47, 511–514. doi: 10.1111/j.1550-7408.2000.tb00083.x

Frederick, J., and Eichinger, D. (2004). Entamoeba invadens contains the components of a classical adrenergic signaling system. *Mol. Biochem. Parasitol.* 137, 339–343. doi: 10.1016/j.molbiopara.2004.07.003

Hackney, J. A., Ehrenkaufer, G. M., and Singh, U. (2007). Identification of putative transcriptional regulatory networks in entamoeba histolytica using bayesian inference. *Nucleic Acids Res.* 35, 2141–2152. doi: 10.1093/nar/gkm028

Haque, R., Huston, C. D., Hughes, M., Houpt, E., and Petri, W. A. Jr. (2003). Amebiasis. *N Engl. J. Med.* 348, 1565–1573. doi: 10.1056/NEJMra022710

Hassan, N. F., Kamani, N., Meszaros, M. M., and Douglas, S. D. (1989). Induction of multinucleated giant cell formation from human blood-derived monocytes by phorbol myristate acetate in *in vitro* culture. *J. Immunol.* 143, 2179–2184.

Ishida, K., Hata, T., and Urushihara, H. (2005). Gamete fusion and cytokinesis preceding zygote establishment in the sexual process of dictyostelium discoideum. *Dev. Growth Differ.* 47, 25–35. doi: 10.1111/j.1440-169x.2004.00776.x

Krishnan, D., and Ghosh, S. K. (2018). Cellular events of multinucleated giant cells formation during the encystation of entamoeba invadens. *Front. Cell. Infect. Microbiol.* 8:262. doi: 10.3389/fcimb.2018.00262

Lozano, R., Naghavi, M., Foreman, K., Lim, S., Shibuya, K., Aboyans, V., et al. (2012). Global and regional mortality from 235 causes of death for 20 age groups in 1990 and 2010: a systematic analysis for the global burden of disease study 2010. *Lancet* 380, 2095–2128. doi: 10.1016/S0140-6736(12)61728-0

Makioka, A., Kumagai, M., Ohtomo, H., Kobayashi, S., and Takeuchi, T. (2001). Effect of calcium antagonists, calcium channel blockers and calmodulin

inhibitors on the growth and encystation of entamoeba histolytica and *E. invadens*. *Parasitol. Res.* 87, 833–837. doi: 10.1007/s004360100453

Manna, D., Ehrenkaufer, G. M., and Singh, U. (2014). Regulation of gene expression in the protozoan parasite Entamoeba invadens: identification of core promoter elements and promoters with stage-specific expression patterns. *Int. J. Parasitol.* 44, 837–845. doi: 10.1016/j.ijpara.2014.06.008

Manna, D., Lentz, C. S., Ehrenkaufer, G. M., Suresh, S., Bhat, A., and Singh, U. (2018). An NAD^+-dependent novel transcription factor controls stage conversion in entamoeba. *Elife* 7:e37912. doi: 10.7554/eLife.37912.030

Manna, D., and Singh, U. (2019). Nuclear factor Y (NF-Y) modulates encystation in entamoeba via stage-specific expression of the NF-YB and NF-YC subunits. *mBio* 10:e00737-19. doi: 10.1128/mBio.00737-19

Martinez-Higuera, A., Herrera-Martinez, M., Chavez-Munguia, B., Valle-Solis, M., Muniz-Lino, M. A., Cazares-Apatiga, J., et al. (2015). Entamoeba invadens: identification of a SERCA protein and effect of SERCA inhibitors on encystation. *Microb. Pathog.* 89, 18–26. doi: 10.1016/j.micpath.2015.08.016

McClean, C. M., and Tobin, D. M. (2016). Macrophage form, function, and phenotype in mycobacterial infection: lessons from tuberculosis and other diseases. *Pathog. Dis.* 74:ftw068. doi: 10.1093/femspd/ftw068

McConnachie, E. W. (1969). The morphology, formation and development of cysts of entamoeba. *Parasitology* 59, 41–53. doi: 10.1017/S003118200006981X

Mi-ichi, F., Miyamoto, T., Takao, S., Jeelani, G., Hashimoto, T., Hara, H., et al. (2015). Entamoeba mitosomes play an important role in encystation by association with cholesteryl sulfate synthesis. *Proc. Natl. Acad. Sci. U.S.A.* 112, E2884–2890. doi: 10.1073/pnas.1423718112

Milde, R., Ritter, J., Tennent, G. A., Loesch, A., Martinez, F. O., Gordon, S., et al. (2015). Multinucleated giant cells are specialized for complement-mediated phagocytosis and large target destruction. *Cell. Rep.* 13, 1937–1948. doi: 10.1016/j.celrep.2015.10.065

Miron, R. J., and Bosshardt, D. D. (2018). Multinucleated giant cells: good guys or bad guys? *Tissue Eng. B Rev.* 24, 53–65. doi: 10.1089/ten.teb.2017.0242

Mitra, S., and Krishna Murti, C. R. (1978). Encystation of axenically grown entamoeba histolytica: effect of bacterial endotoxins, starch and epinephrine. *Proc. Indian Acad. Sci. B* 87, 9–23.

Most, J., Spotl, L., Mayr, G., Gasser, A., Sarti, A., and Dierich, M. P. (1997). Formation of multinucleated giant cells *in vitro* is dependent on the stage of monocyte to macrophage maturation. *Blood* 89, 662–671. doi: 10.1182/blood.V89.2.662

Pearson, R. J., Morf, L., and Singh, U. (2013). Regulation of H_2O_2 stress-responsive genes through a novel transcription factor in the protozoan pathogen entamoeba histolytica. *J. Biol. Chem.* 288, 4462–4474. doi: 10.1074/jbc.M112.423467

Singh, M., Sharma, S., Bhattacharya, A., and Tatu, U. (2015). Heat shock protein 90 regulates encystation in entamoeba. *Front. Microbiol.* 6:1125. doi: 10.3389/fmicb.2015.01125

Takashima, T., Ohnishi, K., Tsuyuguchi, I., and Kishimoto, S. (1993). Differential regulation of formation of multinucleated giant cells from concanavalin A-stimulated human blood monocytes by IFN-gamma and IL-4. *J. Immunol.* 150, 3002–3010.

Varghese, S. S., and Ghosh, S. K. (2020). Stress-responsive entamoeba topoisomerase II: a potential antiamoebic target. *FEBS Lett.* 594, 1005–1020. doi: 10.1002/1873-3468.13677

Zhang, H., Ehrenkaufer, G. M., Pompey, J. M., Hackney, J. A., and Singh, U. (2008). Small RNAs with 5′-polyphosphate termini associate with a Piwi-related protein and regulate gene expression in the single-celled eukaryote entamoeba histolytica. *PLoS Pathog.* 4:e1000219. doi: 10.1371/journal.ppat.1000219

Conflict of Interest: The authors declare that the research was conducted in the absence of any commercial or financial relationships that could be construed as a potential conflict of interest.

frontiers in Cellular and Infection Microbiology

BRIEF RESEARCH REPORT
published: 13 August 2020
doi: 10.3389/fcimb.2020.00408

LPG2 Gene Duplication in *Leishmania infantum*: A Case for CRISPR-Cas9 Gene Editing

Flávio Henrique Jesus-Santos[1,2], *Jéssica Lobo-Silva*[1], *Pablo Ivan Pereira Ramos*[3], *Albert Descoteaux*[4], *Jonilson Berlink Lima*[5], *Valéria Matos Borges*[1,2] and *Leonardo Paiva Farias*[1,2]*

[1] Laboratory of Inflammation and Biomarkers, Instituto Gonçalo Moniz, Fundação Oswaldo Cruz (FIOCRUZ), Salvador, Brazil, [2] Faculdade de Medicina da Bahia, Federal University of Bahia (UFBA), Salvador, Brazil, [3] Center for Data and Knowledge Integration for Health (CIDACS), Instituto Gonçalo Moniz, Fundação Oswaldo Cruz, Salvador, Brazil, [4] Institut National de la Recherche Scientifique—Centre Armand-Frappier Santé Biotechnologie, Laval, QC, Canada, [5] Center of Biological Sciences and Health, Federal University of Western of Bahia (UFOB), Barreiras, Brazil

On the surface of the *Leishmania* promastigote, phosphoglycans (PG) such as lipophosphoglycan (LPG), proteophosphoglycan (PPG), free phosphoglycan polymers (PGs), and acid phosphatases (sAP), are dominant and contribute to the invasion and survival of *Leishmania* within the host cell by modulating macrophage signaling and intracellular trafficking. Phosphoglycan synthesis depends on the Golgi GDP-mannose transporter encoded by the *LPG2* gene. Aiming to investigate the role of PG-containing molecules in *Leishmania infantum* infection process, herein we describe the generation and characterization of *L. infantum LPG2*-deficient parasites. This gene was unexpectedly identified as duplicated in the *L. infantum* genome, which impaired gene targeting using the conventional homologous recombination approach. This limitation was circumvented by the use of CRISPR/Cas9 technology. Knockout parasites were selected by agglutination assays using CA7AE antibodies followed by a lectin (RCA 120). Five clones were isolated and molecularly characterized, all revealing the expected edited genome, as well as the complete absence of LPG and PG-containing molecule expression. Finally, the deletion of *LPG2* was found to impair the outcome of infection in human neutrophils, as demonstrated by a pronounced reduction (∼83%) in intracellular load compared to wild-type parasite infection. The results obtained herein reinforce the importance of LPG and other PGs as virulence factors in host-parasite interactions.

Keywords: GDP-mannose transporter, lipophosphoglycan, *Leishmania infantum*, gene targeting, CRISPR/CAS9

OPEN ACCESS

Edited by:
Prajwal Gurung,
The University of Iowa, United States

Reviewed by:
Ciaran Michael Lee,
University College Cork, Ireland
Eva Gluenz,
University of Oxford, United Kingdom

***Correspondence:**
Leonardo Paiva Farias
leonardo.farias@bahia.fiocruz.br

Specialty section:
This article was submitted to Microbes and Innate Immunity, a section of the journal Frontiers in Cellular and Infection Microbiology

Received: *20 December 2019*
Accepted: *02 July 2020*
Published: *13 August 2020*

Citation:
Jesus-Santos FH, Lobo-Silva J, Ramos PIP, Descoteaux A, Lima JB, Borges VM and Farias LP (2020) LPG2 Gene Duplication in Leishmania infantum: A Case for CRISPR-Cas9 Gene Editing. Front. Cell. Infect. Microbiol. 10:408. doi: 10.3389/fcimb.2020.00408

INTRODUCTION

Leishmania promastigotes are coated by a thick glycocalyx consisting of glycoconjugates crucial to parasite pathogenesis. Lipophosphoglycan (LPG), proteophosphoglycan (PPG), and glycophosphatidylinositol lipids (GIPL), as well as the GP63 metalloprotease, comprise the vast majority of these molecules. *Leishmania* also secrete protein-linked phosphoglycans (PG) (e.g., secreted proteophosphoglycan (sPPG) and secreted acid phosphatase (sAP) (reviewed in Guha-Niyogi et al., 2001; Franco et al., 2012; Forestier et al., 2015). In promastigotes, LPG plays an important role in parasite survival inside the sand fly vector, in addition to macrophage infection

(Sacks et al., 2000; Balaraman et al., 2005; Moradin and Descoteaux, 2012). Moreover, intracellular survival and the multiplication of amastigotes in macrophages is enhanced by other PG-containing molecules (e.g., PPG and sAP), which are highly expressed on the surface of amastigotes (Gaur et al., 2009).

LPG is organized into four domains: a conserved 1-O-alkyl-2-lyso-phosphatidyl(myo)inositol membrane anchor, a conserved diphosphoheptasaccharide core structure, a polymer that consists of repeating phosphodisaccharide units (phosphoglycan or PG) and carries species-specific side chains, as well as and variable mannose-rich cap structures (reviewed in McConville et al., 1993; Descoteaux and Turco, 1999). The PPGs comprise a heterogeneous family of cell surface and secreted proteins containing Ser-Thr rich regions to which phosphodisaccharide repeating units (Manα1-PO4 residue) (PG) are covalently linked, similarly to the LPG molecule (reviewed in Ilg, 2000b; de Assis et al., 2012). This type of phosphoglycosylation is the most abundant type of protein glycosylation found in *Leishmania*. Investigations focused on the synthesis of LPG and PG-containing molecules (PPG, PGs, sAP) have attracted considerable interest, and several enzymes and transporters involved in this process have been identified either biochemically, genetically, or both (Ryan et al., 1993; Descoteaux et al., 1995, 1998, 2002).

An enzyme critical for the synthesis of LPG and PG-containing molecules is the Golgi GDP-mannose transporter (encoded by *LPG2*) (Descoteaux et al., 1995), which contains up to nine transmembrane domains and presents a TPT domain, which is found in many transporters with affinity for triose phosphate. In *Leishmania,* this gene is required for the addition of disaccharide-phosphate units to lipophosphoglycan and related glycoconjugates (Ma et al., 1997; Hong et al., 2000; Segawa et al., 2005).

Over the past decades, the development of *Leishmania* mutants deficient in LPG or other PG-containing molecules has provided researchers with powerful tools to analyze the function of these structures/molecules (McNeely et al., 1990; Descoteaux et al., 1995; Butcher et al., 1996). *L. major* and *L. donovani* Δ*lpg2* mutants failed to survive in the midgut of the sand fly vector and were unable to establish infection in macrophages. In an animal infection model, *L. major* parasites were found to exhibit persistence without causing pathological manifestations, with parasites persisting at low levels throughout the life of the infected animals (Spath et al., 2003b). However, whether LPG and PGs are necessary for parasite survival in all *Leishmania* species has been contested based on *L. mexicana* studies. Although Δ*lpg1* and Δ*lpg2* parasites of this species exhibit complement sensitivity, no decreases in infectivity were observed *in vitro* in macrophages or *in vivo* in mice (Ilg, 2000a; Ilg et al., 2001; Gaur et al., 2009). Our group recently generated an LPG-deficient mutant of *L. infantum* through the deletion of the putative galactofuranosyl transferase gene (*LPG1)* involved in the synthesis of the LPG glycan core. Phenotypically, this deletion impaired the outcome of infection in murine bone marrow-derived macrophages, likely due to the activation of the iNOS promoter in an NF-κB-dependent manner (Lazaro-Souza et al., 2018). While these parasites expressed a truncated LPG molecule lacking the PG domain, they were still able to assemble and secrete other PG-containing molecules (e.g., PPG, sAP, and other PGs) (Dermine et al., 2000; Spath et al., 2000).

In an effort to investigate the role of PG-containing molecules in the *Leishmania infantum* infection process, we applied gene targeting by homologous recombination and also CRISPR/Cas9 technology to generate an *L. infantum* mutant lacking the Golgi GDP-mannose transporter gene (Δ*lpg2*). Our results demonstrate both the value and the caveats of using of both systems for genome editing. The generated mutant produced distinct infection outcomes in comparison to WT parasites, and can therefore be usefully applied to investigate the role of *L. infantum* PG-containing molecules in host-parasite interactions.

METHODS

Ethics Statement

This study was approved by the Institutional Review Board of Human Ethical Research Committee of Fundação Oswaldo Cruz-Bahia, under number 100/2006.

Parasite Cultures

Leishmania infantum Ba262 (MCAN/BR/89/BA262) promastigotes were cultured in HOMEM medium supplemented with 10% inactivated Fetal Bovine Serum (FBS), 100 U/mL penicillin, 100 μg/mL streptomycin and 2 mM L-glutamine in 25 cm^2 flasks at 25°C until late log-phase. The number of promastigotes was determined by counting in a Neubauer chamber.

LPG2 Gene Targeting by Homologous Recombination

Initially, we attempted to obtain an *L. infantum* LPG-deficient mutant (Δ*lpg2*) by homologous recombination, using a previously described strategy (Scianimanico et al., 1999) with modifications. Briefly, the gene sequences from the resistance markers Hygromycin and Neomycin were amplified by PCR using specific oligonucleotides (**Supplementary Table 1**) and ligated in the pUC18 vector (Sigma, USA), thusly generating the pUC18-Hyg and pUC18-Neo constructs. Next, the 5' and 3' UTR *LPG2* gene regions, consisting of 838 bp and 858 bp fragments respectively, were amplified by PCR from *L. infantum* Ba262 (MCAN/BR/89/BA262) genomic DNA using a specific oligonucleotide design based on the 19 kb genomic contig (GenBank accession CACT01000040.1), which was predicted to encode the *LPG2* gene (LinJ_34_4290) (**Supplementary Table 1**). The respective fragments were then digested with *Eco*RV/*Kpn*I and *Xba*I/*Hind*III enzymes, and ligated in the pUC18-Hyg and pUC18-Neo constructs. The final constructs were sequenced for confirmation and designated p*LPG2*-Hyg and p*LPG2*-Neo. Log-phase WT *L. infantum* promastigotes were electroporated in two steps with 10 μg of purified fragments (p*LPG2*-Neo and p*LPG2*-Hyg) using 0.4 cm cuvettes in a Gene Pulser II (BIO-RAD) under electroporation conditions based on a previously described high voltage protocol (Robinson and Beverley, 2003). Briefly, two pulses were applied at 10-s intervals (25 μF, 1,500 V). Following electroporation, promastigotes were incubated for 24 h

at 25°C in drug-free medium, and the neo-resistant parasites were subsequently selected in the presence of 70 μg/mL G418 for 22 days at 25°C. The resistant parasites ($lpg2^{+/-}$) were isolated and submitted to a second round of electroporation using the p*LPG2*-Hyg fragment to disrupt the second allele of the *LPG2* gene. Double knockout (KO) Δ*lpg2* parasites were then selected in the presence of both 70 μg/mL G418 and 50 μg/mL Hygromycin B for 22 days at 25°C. The absence of the *LPG2* gene in the resulting double drug-resistant promastigotes was verified by PCR following DNA extraction using "NucleoSpin tissue" kit (Macherey Nagel).

gRNA Design and Cloning Into pLdCN

The present procedures involving the CRISPR/Cas9 system were based on pioneering work previously performed by Zhang and Matlashewski (2015) and Zhang et al. (2017) with minimal modifications. Two gRNA-targeting sequences and the respective oligonucleotide donors (oligodonors) were selected using the gRNA designer tool (http://grna.ctegd.uga.edu/) and then manually inspected (**Supplementary Table 1**). The complementary guide sequence oligonucleotides were first phosphorylated in T4 DNA ligase buffer with T4 polynucleotide kinase and then annealed in a thermocycler (MJ Research: PTC-200, DNA Engine) (program: 95°C for 5 min, ramp to 25°C at a rate of −0.1°C/s). The annealed guide sequence was then cloned into the gRNA and Cas9 coexpression vector (pLdCN) (Addgene plasmid #84290; http://n2t.net/addgene:84290; RRID: Addgene_84290) previously digested with *Bbs*I.

Parasite Transfection (CRISPR/Cas9)

To obtain *L. infantum* parasites expressing Cas9, log-phase WT *L. infantum* promastigotes were electroporated with purified pLdCN (gRNA440 and gRNA516) under the same conditions described in the section above (*LPG2* gene targeting by homologous recombination). After selection with G418 (70 μg/mL), four rounds of transfection were performed using 100 μM single-stranded oligodonors at 3-day intervals (Zhang et al., 2017).

LPG2 Knockout Selection and Limiting Dilution Assay

After transfection with the oligodonors, the putative Δ*lpg2* parasites were selected by consecutive rounds of agglutination with the CA7AE monoclonal IgM antibody (MediMabs) (1:2,000 dilution), which recognizes the Gal(β1,4)Man(α1-PO4) repeating units contained in LPG and PG-containing molecules (Descoteaux et al., 1998). Briefly, parasites were incubated for 2 h with the antibody and then centrifuged at 100 × g for 7 min to remove any agglutinated promastigotes. The supernatant was then transferred to a new tube and centrifuged at 1,300 × g for 7 min to sediment non-agglutinated parasites (theoretically Δ*lpg2*). Subsequently, these non-agglutinated parasites were incubated in fresh culture medium containing CA7AE (1:2,000) for 3 days, followed by five rounds of the above-described agglutination steps. As a further selection step, non-agglutinated parasites were selected with 100 μg/ml of Ricin 120 (Vector Laboratories, USA) as described in King and Turco (1988). After selecting the Δ*lpg2* parasites, the pLdCN vector, as well as Cas9 protein expression, were eliminated by growing parasites in the absence of the G418 marker, which was achieved after 5–6 passages. Finally, a limiting dilution assay was performed for clonal isolation using 96-well plates with culture medium containing 100 μg/mL of ricin, incubated for 3 weeks at 25°C with medium supplementation when necessary. To calculate doubling times, cells were seeded at 10^5 cells/ml and density was measured every 24 h. The average doubling time, from day zero until reaching stationary phase, was calculated by (24/(log2(t2/t1)))/number of days evaluated (Beneke et al., 2019). Subsequently, genomic DNA was extracted from the last dilution in which parasite growth was observed.

Sequencing Analysis

The sequence corresponding to the 5'UTR-Neo/Hyg/*LPG2*-3'UTR genomic DNA region was amplified with specific oligonucleotides (**Supplementary Table 1**) by PCR. The PCR products were purified on agarose gels (Wizard® SV Gel and PCR Clean-Up System) and sequenced using the Gonçalo Moniz Institute sequencing platform.

Western Blotting

Late log-phase promastigotes at a concentration of 2×10^7 cells were centrifuged and resuspended in 100 μl of RIPA Lysis Buffer (150 mM NaCl, 0.5 M EDTA, pH 8.0, 1 M Tris, pH 8.0, 1%NP-40, 1% sodium deoxycholate, 0.1% SDS and dH_2O) containing a protease inhibitor (Sigma, cat. No. P-2,714). The extract was incubated on ice and vortexed for approximately 5 min. The lysated material was separated by SDS-PAGE on a 12% polyacrylamide gel and Western blotting was performed as previously described (Lazaro-Souza et al., 2018).

T7 Endonuclease I Assay

Briefly, genomic DNA from *L. infantum* WT and Δ*lpg* clones was extracted using a "NucleoSpin tissue" kit (Macherey Nagel). The sequences corresponding to the *LPG2* and Δ*lpg2* genes were amplified by PCR with specific oligonucleotides (**Supplementary Table 1**) and purified from agarose gels using the Wizard® SV Gel and PCR Clean-Up System. Subsequently, 200 ng of the purified PCR product was denatured and re-annealed at a final volume of 19 μl in 1 × NEBuffer2 (NEB) using a thermocycler in accordance with the following protocol: 95°C for 5 min; ramp to 85°C at a rate of −2°C/s; ramp to 25°C at a rate of −1°C/s; hold at 4°C. The PCR products were then treated with T7 E1 enzyme (NEB) at 37°C for 15 min at a reaction volume of 20 μl. An aliquot (10 μl) of the reaction was subsequently analyzed on a 1% agarose gel.

Confocal Immunofluorescence Microscopy

Late log-phase promastigotes were adhered on Poly-L-Lysine-coated glass coverslips (BD Biosciences, San Jose, CA) by centrifugation, fixed with 4% paraformaldehyde for 20 min and simultaneously blocked and permeabilized for 20 min using a solution containing 0.1% Triton X-100, 1% BSA, 6% non-fat dry milk, 20% goat serum and 50% FBS. The distribution of LPG and other PGs containing the Gal(β1,4)Man(α1-PO4) repeating

unit epitope was visualized using the CA7AE mouse monoclonal antibody (MediMabs, 1:2,000) after a 2 h incubation period, followed by an additional 30 min incubation with Alexa Fluor 488 goat anti-mouse IgM (Molecular Probes) at 1:500. Parasite nuclei were stained with DAPI (Molecular Probes) at 1:17,000. All steps were performed at room temperature. The coverslips were then mounted in Fluoromount-G (Interscience) and sealed with nail polish. Parasites were observed under a Plan APOCHROMAT 63 × oil-immersion DIC 1.4 NA objective on a Leica SP8 confocal microscope in reflective mode, using a 488 nm laser, with an LP505 filter.

Infection Assay

Human blood was obtained from volunteers at the Bahia Foundation of Hematology and Hemotherapy (HEMOBA). Human neutrophils were isolated by gradient separation in polymorphonuclear medium (PMN) according to the manufacturer's instructions (Axis-ShieldPoc AS, Oslo, Norway). Neutrophils were collected and washed three times with saline at 4°C for 10 min at 300 x g. Neutrophils were plated with RPMI-1640 medium, supplemented with 1% Nutridoma-SP, 2 mM L-glutamine, 100 U/ml penicillin and 100 μg/ml of streptomycin. Cells were infected with stationary WT or Δ*lpg2* promastigotes at an MOI of 10 for 3 h at 37°C under 5% CO_2. The intracellular load of *L. infantum* was then evaluated in neutrophils by assessing parasite viability as previously described (Quintela-Carvalho et al., 2017). Briefly, after 3 h of incubation, infected neutrophils were centrifuged at 300 × g for 10 min at 4°C, the supernatant containing non-internalized promastigotes was discarded and replaced by 250 μl of HOMEM medium. After a final incubation at 23°C for 24 h, the number of viable proliferating extracellular promastigotes was counted in a Neubauer chamber.

Statistical Analysis

Diferences in growth curves were analyzed using Area under the Curve (AUC) analysis. Neutrophil infection assays were performed twice from at least five donors, data are presented as means and SE (standard error) of representative experiments. Wild-type and knockout groups were compared using the Student's *t*-test. Differences were considered statistically significant when $p \leq 0.05$. All figures and statistical analyses were performed using PRISM version 5.02 software (GraphPad, San Diego, CA).

RESULTS

LPG2 Is Duplicated in *L. infantum*

After selection of double drug-resistant (Neo/Hyg) parasites, the absence of the *LPG2* gene was assessed by PCR. Electrophoresis results confirmed the expected occurrence of homologous recombination and the successful integration of the resistance markers (Neo and Hyg). However, surprisingly, the coding region of the *LPG2* gene was still detected following amplification (**Figure 1A**).

This effectively indicated that either homologous recombination did not occur, or that the *LPG2* gene is duplicated in this species. No available evidence suggested the latter possibility, since the *L. infantum* JPCM5 genome assembly published at the time of the initial recombination experiments showed *LPG2* as a single-copy gene located in an unplaced 19 kb contig (GenBank accession CACT01000040.1). However, a more recent resequencing of the JPCM5 genome, which employed a hybrid sequencing approach with PacBio long reads and Illumina short reads, yielded a more robust assembly containing 36 scaffolds accounting for the 36 chromosomes present in this species (Gonzalez-de la Fuente et al., 2017) (EMBL accession GCA_900500625.1). BLAST searches of the 19 kb contig as a query against this novel assembly revealed that the entire contig, including the *LPG2* gene, was duplicated in a tandem array in chromosome 34 of *L. infantum* JPCM5 (**Figure 1B** and **Supplementary Figure 1A**). This finding highlights a limitation associated with the obtainment of knockout parasites using conventional homologous recombination procedures.

Generation of *L. infantum* Expressing Cas9

As a first step to perform *LPG2* gene editing, we developed *L. infantum* parasites expressing the Cas9 enzyme. WT parasites were transfected with the pLdCN plasmid and selected in G418 culture medium to generate the strain constitutively expressing the Cas9 nuclease. The expression of the Cas9 enzyme was confirmed in G418-resistant parasites by Western blotting (**Figure 2A**). The growth curves of promastigotes revealed that the expression of Cas9-gRNAs influenced parasite growth. A delay in the replication capability of the Cas9-gRNA expressing parasites was observed in comparison to WT. In addition, the former reached stationary phase by day 6, with a cell density of $\sim 5 \times 10^7$, while the latter reached this phase 2 days later, with a cell density of $\sim 3 \times 10^7$ (**Figure 2B**). Sequencing data revealed no evidence of *LPG2* gene editing at this initial stage (data not shown). Next, *L infantum* expressing Cas9 were submitted to four rounds of transfection using single-stranded oligodonors to improve *LPG2* gene disruption and knockouts were subsequently selected.

Selection of *L. infantum* Δ*lpg2*

Five rounds of selection using the CA7AE antibody were unexpectedly unsuccessful in completely removing WT parasites by agglutination (**Figure 2C**). This was circumvented through the use of Ricin 120, after which complete depletion of WT *L. infantum* and the selection of Δ*lpg2* was observed (**Figure 2D**).

Characterization of *L. infantum* Δ*lpg2*

To examine the types of mutations created by the CRISPR-Cas9 system at the *LPG2*-targeting sites, genomic DNA was extracted from these non-agglutinating parasites after clonal isolation (clones denominated E3, E4, F1, G2, and G6). PCR was performed with primers designed to amplify the *LPG2* gene, followed by DNA sequencing of the targeted sites (**Supplementary Figure 1B** and **Figure 3A**). All five sequenced clones revealed the expected genome editing with oligodonor insertions, and no random insertions/deletions were

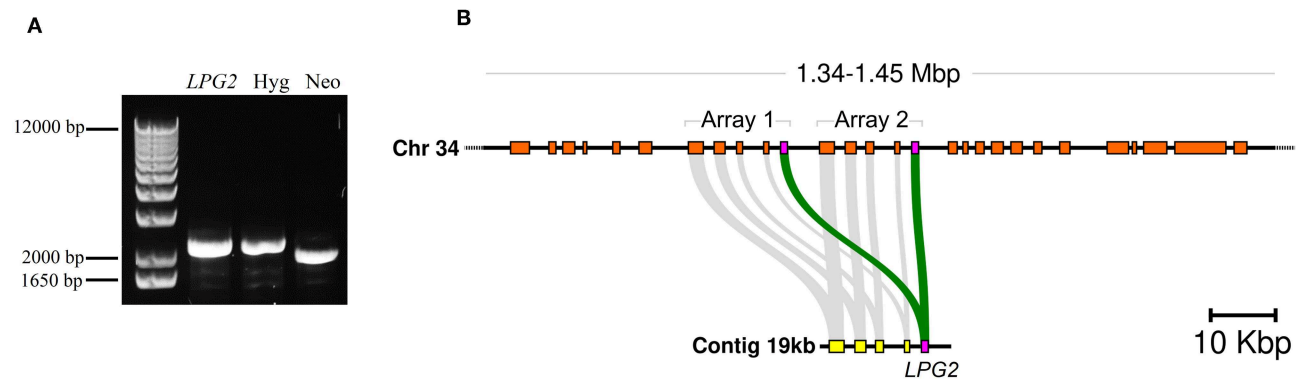

FIGURE 1 | Evidence of *LPG2* duplication in *L. infantum*. **(A)** Genomic DNA from *L. infantum* Hyg/NeoR strain was amplified by PCR using specific oligonucleotides (**Supplementary Table 1**) to verify *LPG2* gene targeting by homologous recombination. **(B)** Comparison of the genomic contexts where *LPG2* (magenta box) was originally located (in an unplaced 19 kbp contig shown at the bottom) to the recent resequencing and reassembly of the *L. infantum* JPCM5 genome (Gonzalez-de la Fuente et al., 2017), where the duplication of the *LPG2* gene array is evidenced in chromosome 34 (top). Gray connecting segments indicate sequence conservation, and the coordinates at the top refer to the novel chromosome 34 assembly.

observed within the sequenced region (nucleotides 15–870, **Supplementary Figure 1C**).

The loss of LPG expression in *L. infantum* Δ*lpg2* was demonstrated in promastigotes of all five isolated clones by Western blot, and by confocal immunofluorescence microscopy for clone G6 (**Figures 3B,C**). To better characterize these five knockout clones, growth curves were constructed and compared to wild-type parasites (**Supplementary Figure 2A**). This assay revealed no apparent differences in the growth profile of the five Δ*lpg2* clones. However, Area Under the Curve (AUC) analysis demonstrated a significant impairment in the growth rate of knockout parasites compared to WT. Our AUC analysis compared the average growth rate of all five knockout clones to WT (**Supplementary Figures 2B,C**), in addition to comparing one specific clone (G6) to WT (**Figures 3D,E**). The doubling time was calculated at 8.1 (G6) and 23.7 (WT). Despite differences in cell densities among Δ*lpg2* parasites, no significant delays were observed in comparison to wild-type parasites with respect to the time needed to reach stationary phase (**Figure 3D** and **Supplementary Figure 2A**). While it appeared that knockout and WT parasites seemed to differentiate into metacyclic forms at similar frequencies, since no apparent morphological differences were observed during growth phase, this warrants further investigation (e.g., through the analysis of ultrastructural and morphometric data or stage-specific gene expression).

Finally, the T7 Endonuclease I assay confirmed the absence of any non-edited versions of *LPG2* in the genomic DNA of clones (G6 and E4) as reveled by the absence of digested products following enzyme incubation (**Supplementary Figure 2D**). After selecting the Δ*lpg2* parasites, Cas9 protein expression was eliminated by removing the selection marker (G418) for the pLdCN vector, which was achieved after 5-6 passages (**Supplementary Figure 2E**). Together, these data indicate that the *LPG2* gene was successfully edited in the Δ*lpg2* mutants, resulting in the generation of a parasite deficient in LPG, as well as PG-containing molecules (e.g., PPGs).

Δ*lpg2* Parasites Exhibit Limited Survival in Neutrophils

To evaluate differences in parasite survival between WT and genome-edited parasites *in vitro*, human neutrophils were experimentally infected and incubated for 3 h. Neutrophils infected with Δ*lpg2* parasites exhibited an ∼83% reduction in intracellular parasite load as estimated by parasite viability determined at 3 h after infection (**Figure 3F**).

DISCUSSION

We recently confirmed the involvement of LPG as a virulence factor in *L. infantum* through the use of parasites that had the *LPG1* gene knocked out (Lazaro-Souza et al., 2018). However, other phosphoglycan-containing molecules (PPGs, PGs and sAPs) may also play a role in parasite survival within host cells (Spath et al., 2003a; Gaur et al., 2009). Here we developed an *L. infantum* species parasite knocked-out for the *LPG2* gene, which did not express LPG or other PG-containing molecules (PPG, PGs, sAP).

Initially, we sought to obtain knockouts using the conventional method of homologous recombination involving resistance marker genes (Cruz et al., 1991). Despite some limitations, this method has been useful for single gene disruption and was shown to successfully knock out the *LPG2* gene in *L. donovani*, *L. Mexicana,* and *L. major* (Scianimanico et al., 1999; Ilg et al., 2001; Spath et al., 2003b). After performing two transformation rounds and selecting for the potential Δ*lpg2* parasites, the presence of an integral allele of the *LPG2* gene was still observed in genomic DNA, suggesting either that the homologous recombination process was inefficient, or that this gene was possibly duplicated in the *L. infantum* genome.

The homologous recombination gene disruption strategy was designed based on information present in an unplaced 19 kb genomic contig of *L. infantum* JPCM5 (GenBank accession

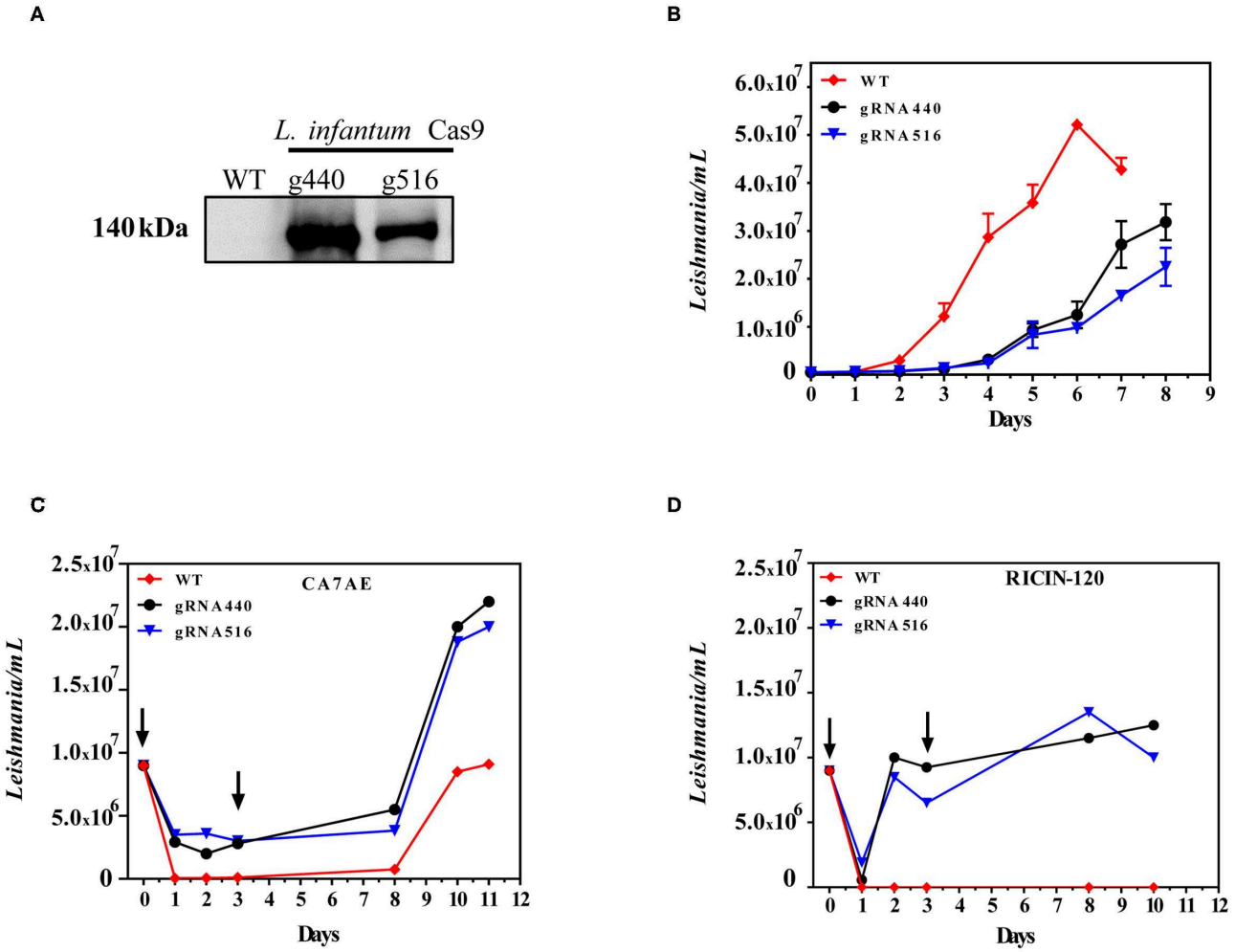

FIGURE 2 | Generation of *LPG2* knockout using CRISPR/Cas9. **(A)** Western blot analysis of *L. infantum* promastigotes expressing Cas9 (gRNA440 and gRNA516). **(B)** Growth curves of *L. infantum* wild-type (WT) and *L. infantum*-Cas9 (gRNA440 and gRNA516) promastigotes. **(C)** Agglutination assay using the CA7AE monoclonal antibody and associated growth curves. **(D)** Agglutination assay using Ricin 120 lectin and associated growth curves, demonstrating the selection of Δ*lpg2*. The arrows indicate the time points where antibody (CA7AE) or lectin (Ricin-120) were added to the cultures, exemplifying the typical agglutination results observed.

CACT01000040.1), in which the *LPG2* gene was originally mapped (LinJ_34_4290). It is important to note that although this contig was described in association with chromosome 34, it was not physically mapped to this chromosome, which raised doubts regarding the consistency of this contig. Subsequent analysis in a new assembly of the *L. infantum* JPCM5 genome (Gonzalez-de la Fuente et al., 2017) indicated that this 19 Kb contig (including the *LPG2* gene) is duplicated in a tandem array located in chromosome 34. This new assembly, performed using PacBio and Illumina technology, was more robust, as evidenced by fewer gaps and increased identification of duplicate regions (tandem arrays). Interestingly, the duplication of the *LPG2* gene in the tandem array was not mentioned by these authors in their list of duplicated genes. More recently the *LPG2* duplication was spotted by a study that performed a comparative genomic and evolutionary analysis of the proteins involved in the biosynthesis of LPG in *Leishmania* (Azevedo et al., 2020).

The fact that the duplication of *LPG2* was not initially identified highlights limitations regarding the way *Leishmania* genomes are traditionally assembled, which usually entails the use of low-coverage whole-genome sequencing using short reads, with subsequent assembly performed using a reference genome obtained from a previously sequenced genome that can even belong to a different *Leishmania* species (Peacock et al., 2007). The presence of two copies of *LPG2* in *L. infantum* limited our ability to perform genetic manipulation via homologous recombination in this parasite species, which emphasizes the need to improve the overall quality of *Leishmania* genomes, i.e., completeness and contiguity, preferentially through the use of recently employed hybrid sequencing strategies (short and long reads) (Gonzalez-de la Fuente et al., 2017, 2019; Lypaczewski

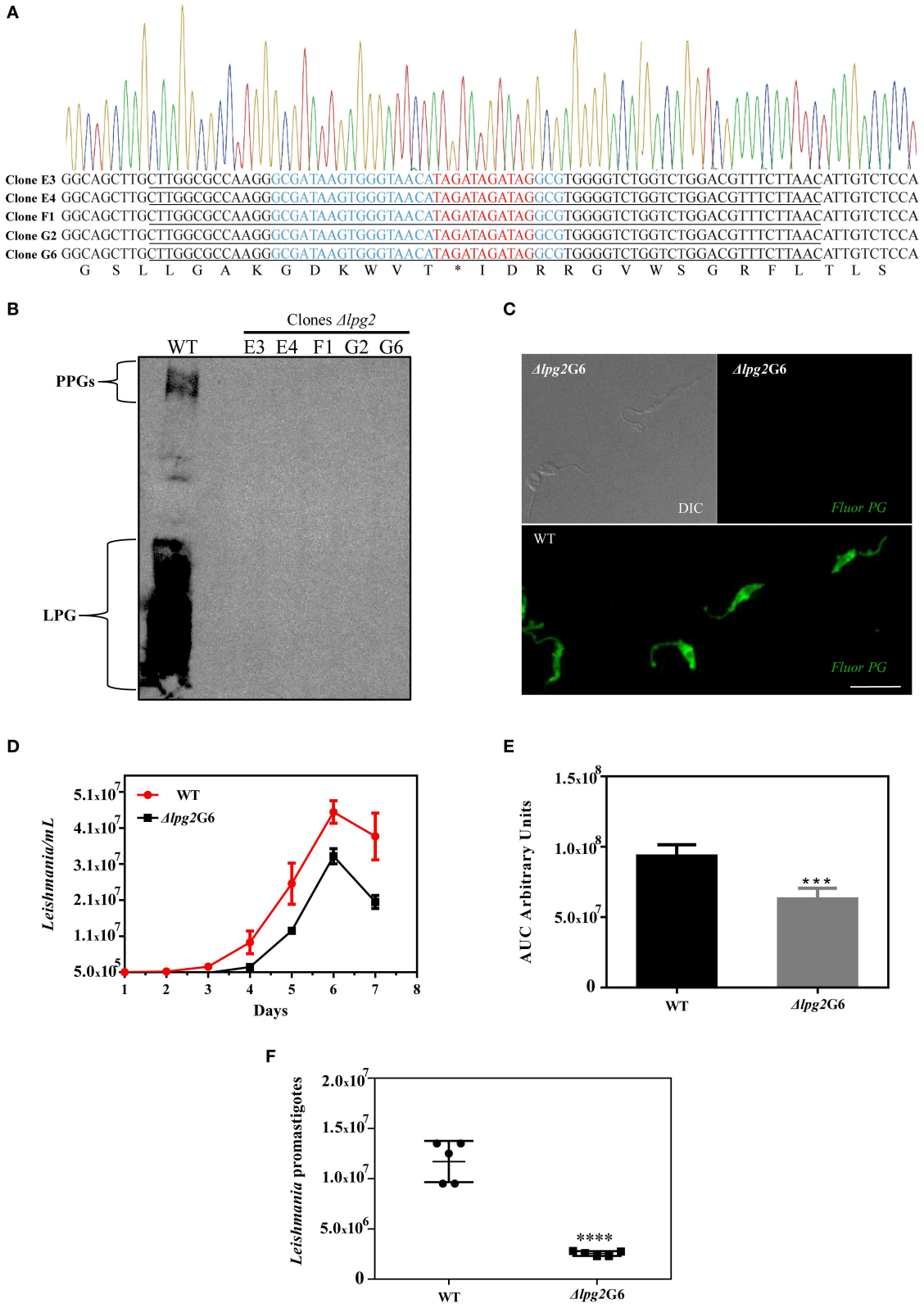

FIGURE 3 | Molecular characterization of Δ*lpg2* and reduced virulence phenotype. **(A)** Chromatogram and translated sequence showing the region of the *LPG2* gene in which the precise insertion of a stop codon (denoted by an *) occurred by homologous recombination at the cleavage site of the Cas9 enzyme (nucleotides in red).

(Continued)

FIGURE 3 | The oligodonor sequence is underlined and the gRNA440 sequence is highlighted in blue. **(B)** Western blot analysis of the expression of LPG and PPGs in *L. infantum* promastigotes WT and Δ*lpg2* clones. **(C)** Confocal immunofluorescence analysis of WT and Δ*lpg2* (clone G6) parasites. Late log-phase promastigotes were adhered on Poly-L-Lysine-coated glass coverslips, fixed and incubated with the CA7AE antibody to visualize LPG and other Gal(β1,4)Man(α1-PO4) repeating unit-containing PGs (green). Differential interference contrast (DIC) for Δ*lpg2* is shown in the upper left panel. Scale bar: 10 μm. **(D)** Axenic growth curves of late log-phase promastigotes of *L. infantum* wild-type (WT) and clone G6 Δ*lpg2,* each point represents mean and SE. Data are representative of at least three independent assays and were collected in triplicate for each experimental condition. **(E)** Area under the curve (AUC) analysis of growth curves presented in **(D)**, $^{***}p < 0.01$. **(F)** Reduced virulence of Δ*lpg2* parasites in human neutrophils. Human neutrophils were infected with *L. infantum* Ba262 wild-type and Δ*lpg2* promastigotes for 3 h. Numbers of viable promastigotes shown after 24 h, with each point on the graph representing the cells from a health donor. Statistical differences were evaluated using the Student *t*-test, $^{****}p < 0.001$.

et al., 2018). In the end, we overcame this limitation through the use of the CRISPR/Cas9 system for genome editing.

The CRISPR/Cas9 system used here proved more flexible in producing *Leishmania* knockouts without the use of genetic resistance markers for selection, thereby allowing for more direct comparisons with WT parasites. In addition, the use of oligodonors containing stop codons permitted more specific editing of the target gene as opposed to random insertions/deletions (Zhang et al., 2017; Zhang and Matlashewski, 2019).

Previous studies found no evidence of Cas9 toxicity in *Leishmania mexicana,* since promastigote forms grew and reached stationary phase at similar rates and densities as wild-type cells (Beneke et al., 2017; Martel et al., 2017). However, others have reported some reduced phenotypic growth in the late stages of culturing (Ishemgulova et al., 2018). The reasons behind these divergent results remain unclear and could rely on the way that this expression is conducted (episomal vs. genomic integration) and also the window of time analyzed, but further study will be necessary.

As the generated *L. infantum* strain expressing Cas9-gRNA presented delayed growth, we speculate that this could be due to the action of Cas9-gRNA and the low efficiency of mechanisms involved in repairing double-strand breaks in *Leishmania*, which may lead to cell cycle arrest and even cell death, as demonstrated by (Zhang and Matlashewski, 2019). Importantly, future studies must address this issue, which remains unclear: Does the expression of Cas9 *per se* negatively affect *Leishmania* growth, or this is a result of Cas9 expression together with a *Leishmania*-DNA-targeting-gRNA?

For the selection and clonal isolation of the Δ*lpg2* parasites, we initially used the CA7AE monoclonal antibody that recognizes the Gal(β1,4)Man(α1-PO4) repeat region of the LPG molecule (Descoteaux et al., 1998). However, after five rounds of agglutination, there was reason to believe that wild-type parasites could still be present in knockout cultures, due to the fact that it was not possible to completely eliminate wild-type parasites in control cultures. These results highlight a limitation associated with the use of this antibody to select Δ*lpg2* parasites in an *L. infantum* model without the additional presence of a resistance gene marker. To overcome this limitation, we chose to employ a lectin (RCA 120), which recognizes terminal β-galactose residues, that was shown to be cytotoxic to wild-type *L. donovani* and *L. major* parasites, but did not affect parasites that do not present LPG and other PG-containing molecules (King and Turco, 1988; Cappai et al., 1994; Opat et al., 1996). After two rounds of agglutination, the use of this lectin resulted in wild-type parasite death and complete elimination. Despite the absence of resistance markers to select knockout parasites, the CRISPR/Cas9 system, coupled to oligodonors, demonstrated high efficiency in target gene editing, as evidenced by the analysis of sequencing data from five of the generated clones, which all presented the expected result at the site of Cas9 cleavage. In addition, Western blotting and confocal microscopy demonstrated the complete elimination of PG-repeating units in both LPG and other PG-containing molecules, which is consistent with the literature (Descoteaux et al., 1995; Dermine et al., 2000; Spath et al., 2003b; Lazaro-Souza et al., 2018). However, it will be important for future experimental design to quantitatively investigate system efficiency by determining how many null mutants are generated as a fraction of oligodonor-transfected parasites.

After selecting the Δ*lpg2* parasites, Cas9 protein expression was eliminated by removing the selection marker (G418) for the pLdCN vector, which was achieved after 5–6 passages (**Supplementary Figure 2E**). No differences in phenotype or growth rates were observed among the five isolated clones, which suggest that, if present, off-target effects had little impact. Although low cell density was observed when the Δ*lpg2* parasites reached stationary phase, the time required to reach this phase was not significantly delayed. This finding stands in contrast to delays seen in achieving stationary phase when knockout parasites are obtained by homologous recombination using resistance markers, which likely occurs due to the presence of antibiotics in culture medium (Lazaro-Souza et al., 2018). In addition, we did not observe any significant morphological or ultrastructural changes, indicating that the deletion of the *LPG2* gene did not interfere with the cellular biology of *L. infantum* promastigotes.

In an attempt to obtain insights regarding the role of LPG and PG-containing molecules in cells present at initial stages of infection, human neutrophils were infected for 3 h with *L. infantum* Δ*lpg2*, revealing a significant reduction in infection rate compared to WT. Neutrophils, essential innate immune system cells, are rapidly recruited to the site of inflammation and have been described as playing a critical role in *Leishmania* infection (Ribeiro-Gomes et al., 2004; Hurrell et al., 2016). In addition, LPG was shown to be important to the induction of autophagy in neutrophils using a model of *L. donovani* infection (Pitale et al., 2019). However, our findings in this cell type must be considered preliminary, as it will be necessary to investigate additional time points and the underling mechanisms. Future studies should also extend the scope of investigation to include macrophages.

In sum, the results presented herein confirm the unexpected duplication of the *LPG2* gene in the *L. infantum* genome. The successful inactivation of both copies of this gene using the CRISPR/Cas9 system highlights the potential of using these KO parasites to assess signal transduction pathways elicited by PG-containing molecules from a variety of *Leishmania* species in different types of immune cells. In addition, the technique demonstrated herein of editing the *LPG2* gene using CRISPR exemplifies the prospects of inactivating other virulence factors sequentially, which could pave the way for new vaccine development.

DATA AVAILABILITY STATEMENT

The datasets generated for this study are available on request to the corresponding author.

ETHICS STATEMENT

The studies involving human participants were reviewed and approved by Institutional Review Board of Human Ethical Research Committee of Fundação Oswaldo Cruz-Bahia. Written informed consent for participation was not required for this study in accordance with the national legislation and the institutional requirements.

AUTHOR CONTRIBUTIONS

FJ-S, PR, AD, JL, VB, and LF conceived and designed the study and contributed to data analysis. FJ-S, JL, JL-S, and LF performed the experiments. FJ-S, JL, PR, AD, JL-S, VB, and LF wrote and critically revised the manuscript. All authors have read and approved the final version of this manuscript.

FUNDING

This work was supported by the Brazilian National Research Council (CNPq) (Grant Number: 431857/2018-0) and the Fundação de Amparo à Pesquisa do Estado da Bahia (FAPESB) (Grant Number: 04/2015) to VB. VB is a senior investigator funded by CNPq. AD holds the Canada Research Chair in Biology of intracellular parasitism. The fellowships received by FJ-S, JL-S, and part of this study was financed by the program: Coordenação de Aperfeiçoamento de Pessoal de Nível Superior—Brasil (CAPES) –Finance Code 001.

ACKNOWLEDGMENTS

The authors would like to thank the Rede de Plataformas Tecnológicas (FIOCRUZ-Bahia) for the use of its DNA Sequencing Platform, Dr. Ricardo Khouri (FIOCRUZ-Bahia) for technical assistance with chemicals and reagents and Astrid Goicochea for her assistance with the neutrophil assays. The authors are also grateful to Andris K. Walter for English language revision and manuscript copyediting assistance (FIOTEC-Programa de Capacitação).

SUPPLEMENTARY MATERIAL

The Supplementary Material for this article can be found online at: https://www.frontiersin.org/articles/10.3389/fcimb.2020.00408/full#supplementary-material

Supplementary Figure 1 | Detail of *LPG2* gene locus indicating gRNA targeting sites. **(A)** Schematic representation of the wild-type alleles of the *LPG2* gene (magenta box) present in a duplicated tandem array. **(B)** Schematic representation showing the insertion of a stop codon in *LPG2* alleles following Cas9 genome editing (white line interrupting the magenta box). **(C)** *LPG2* sequence depicting: gRNA440 sequence in (blue), oligonucleotide donor sequence (underlined) and inserted stop codons (red). Arrows represents primers used for *LPG2* sequence and Δ*lpg2* characterization.

Supplementary Figure 2 | Characterization of Δ*lpg2* clones. **(A)** Growth curve of wild-type (WT) *L. infantum* promastigotes and five different Δ*lpg2* clones. **(B)** Analysis of growth curve of *L. infantum* wild-type (WT) promastigotes and mean growth rates of all five different Δ*lpg2* clones **(C)** Area under the curve (AUC) of growth curve presented in **(B)**. **(D)** T7 Endonuclease I assay using genomic DNA from *L. infantum* wild-type (WT) promastigotes and two clones (E4 and G6) of *L. infantum* Δ*lpg2*. A positive control containing equal amounts of WT and KO DNA demonstrates the presence of two bands following digestion. **(E)** Western blot analysis of *L. infantum* promastigotes (clone G6) demonstrating the loss of the pLdCN vector after 5–6 passages in the absence of the G418 marker.

Supplementary Table 1 | Oligonucleotides sequences used to assemble the fragments pLPG2-Hyg and pLPG2-Neo for gene targeting of LPG2 by homologous recombination and CRISPR/Cas9.

REFERENCES

Azevedo, L. G., de Queiroz, A. T. L., Barral, A., Santos, L. A., and Ramos, P. I. P. (2020). Proteins involved in the biosynthesis of lipophosphoglycan in Leishmania: a comparative genomic and evolutionary analysis. *Parasit. Vectors* 13:44. doi: 10.1186/s13071-020-3914-9

Balaraman, S., Singh, V. K., Tewary, P., and Madhubala, R. (2005). Leishmania lipophosphoglycan activates the transcription factor activating protein 1 in J774A.1 macrophages through the extracellular signal-related kinase (ERK) and p38 mitogen-activated protein kinase. *Mol. Biochem. Parasitol.* 139, 117–127. doi: 10.1016/j.molbiopara.2004.10.006

Beneke, T., Demay, F., Hookway, E., Ashman, N., Jeffery, H., Smith, J., et al. (2019). Genetic dissection of a Leishmania flagellar proteome demonstrates requirement for directional motility in sand fly infections. *PLoS. Pathog.* 15:e1007828. doi: 10.1371/journal.ppat.1007828

Beneke, T., Madden, R., Makin, L., Valli, J., Sunter, J., and Gluenz, E. (2017). A CRISPR Cas9 high-throughput genome editing toolkit for kinetoplastids. *R Soc. Open Sci.* 4:170095. doi: 10.1098/rsos.170095

Butcher, B. A., Turco, S. J., Hilty, B. A., Pimenta, P. F., Panunzio, M., and Sacks, D. L. (1996). Deficiency in beta1,3-galactosyltransferase of a Leishmania major lipophosphoglycan mutant adversely influences the Leishmania-sand fly interaction. *J. Biol. Chem.* 271, 20573–20579. doi: 10.1074/jbc.271.34.20573

Cappai, R., Morris, L., Aebischer, T., Bacic, A., Curtis, J. M., Kelleher, M., et al. (1994). Ricin-resistant mutants of Leishmania major which express modified lipophosphoglycan remain infective for mice. *Parasitology* 108 (Pt 4), 397–405. doi: 10.1017/S0031182000075946

Cruz, A., Coburn, C. M., and Beverley, S. M. (1991). Double targeted gene replacement for creating null mutants. *Proc. Natl. Acad. Sci. U. S. A.* 88, 7170–7174. doi: 10.1073/pnas.88.16.7170

de Assis, R. R., Ibraim, I. C., Nogueira, P. M., Soares, R. P., and Turco, S. J. (2012). Glycoconjugates in New World species of Leishmania: polymorphisms in

lipophosphoglycan and glycoinositolphospholipids and interaction with hosts. *Biochim Biophys. Acta* 1820, 1354–1365. doi: 10.1016/j.bbagen.2011.11.001

Dermine, J. F., Scianimanico, S., Prive, C., Descoteaux, A., and Desjardins, M. (2000). Leishmania promastigotes require lipophosphoglycan to actively modulate the fusion properties of phagosomes at an early step of phagocytosis. *Cell Microbiol.* 2, 115–126. doi: 10.1046/j.1462-5822.2000.00037.x

Descoteaux, A., Avila, H. A., Zhang, K., Turco, S. J., and Beverley, S. M. (2002). Leishmania LPG3 encodes a GRP94 homolog required for phosphoglycan synthesis implicated in parasite virulence but not viability. *EMBO J.* 21, 4458–4469. doi: 10.1093/emboj/cdf447

Descoteaux, A., Luo, Y., Turco, S. J., and Beverley, S. M. (1995). A specialized pathway affecting virulence glycoconjugates of Leishmania. *Science* 269, 1869–1872. doi: 10.1126/science.7569927

Descoteaux, A., Mengeling, B. J., Beverley, S. M., and Turco, S. J. (1998). Leishmania donovani has distinct mannosylphosphoryltransferases for the initiation and elongation phases of lipophosphoglycan repeating unit biosynthesis. *Mol. Biochem. Parasitol.* 94, 27–40. doi: 10.1016/S0166-6851(98)00047-4

Descoteaux, A., and Turco, S. J. (1999). Glycoconjugates in Leishmania infectivity. *Biochim Biophys. Acta* 1455, 341–352. doi: 10.1016/S0925-4439(99)00065-4

Forestier, C. L., Gao, Q., and Boons, G. J. (2015). Leishmania lipophosphoglycan: how to establish structure-activity relationships for this highly complex and multifunctional glycoconjugate? *Front. Cell. Infect. Microbiol.* 4:193. doi: 10.3389/fcimb.2014.00193

Franco, L. H., Beverley, S. M., and Zamboni, D. S. (2012). Innate immune activation and subversion of Mammalian functions by leishmania lipophosphoglycan. *J. Parasitol. Res.* 2012:165126. doi: 10.1155/2012/165126

Gaur, U., Showalter, M., Hickerson, S., Dalvi, R., Turco, S. J., Wilson, M. E., et al. (2009). Leishmania donovani lacking the Golgi GDP-Man transporter LPG2 exhibit attenuated virulence in mammalian hosts. *Exp. Parasitol.* 122, 182–191. doi: 10.1016/j.exppara.2009.03.014

Gonzalez-de la Fuente, S., Camacho, E., Peiro-Pastor, R., Rastrojo, A., Carrasco-Ramiro, F., Aguado, B., et al. (2019). Complete and de novo assembly of the Leishmania braziliensis (M2904) genome. *Mem. Inst. Oswaldo Cruz* 114:e180438. doi: 10.1590/0074-02760180438

Gonzalez-de la Fuente, S., Peiro-Pastor, R., Rastrojo, A., Moreno, J., Carrasco-Ramiro, F., Requena, J. M., et al. (2017). Resequencing of the Leishmania infantum (strain JPCM5) genome and de novo assembly into 36 contigs. *Sci Rep*. 7:18050. doi: 10.1038/s41598-017-18374-y

Guha-Niyogi, A., Sullivan, D. R., and Turco, S. J. (2001). Glycoconjugate structures of parasitic protozoa. *Glycobiology* 11(4), 45R-59R. doi: 10.1093/glycob/11.4.45R

Hong, K., Ma, D., Beverley, S. M., and Turco, S. J. (2000). The Leishmania GDP-mannose transporter is an autonomous, multi-specific, hexameric complex of LPG2 subunits. *Biochemistry* 39, 2013–2022. doi: 10.1021/bi992363l

Hurrell, B. P., Regli, I. B., and Tacchini-Cottier, F. (2016). Different Leishmania Species Drive Distinct Neutrophil Functions. *Trends Parasitol.* 32, 392–401. doi: 10.1016/j.pt.2016.02.003

Ilg, T. (2000a). Lipophosphoglycan is not required for infection of macrophages or mice by Leishmania mexicana. *EMBO J* 19, 1953–1962. doi: 10.1093/emboj/19.9.1953

Ilg, T. (2000b). Proteophosphoglycans of Leishmania. *Parasitol. Today* 16, 489–497. doi: 10.1016/S0169-4758(00)01791-9

Ilg, T., Demar, M., and Harbecke, D. (2001). Phosphoglycan repeat-deficient Leishmania mexicana parasites remain infectious to macrophages and mice. *J Biol. Chem.* 276, 4988–4997. doi: 10.1074/jbc.M008030200

Ishemgulova, A., Hlavacova, J., Majerova, K., Butenko, A., Lukes, J., Votypka, J., et al. (2018). CRISPR/Cas9 in Leishmania mexicana: A case study of LmxBTN1. *PLoS One* 13:e0192723. doi: 10.1371/journal.pone.0192723

King, D. L., and Turco, S. J. (1988). A ricin agglutinin-resistant clone of Leishmania donovani deficient in lipophosphoglycan. *Mol. Biochem. Parasitol.* 28, 285–293. doi: 10.1016/0166-6851(88)90013-8

Lazaro-Souza, M., Matte, C., Lima, J. B., Arango Duque, G., Quintela-Carvalho, G., de Carvalho Vivarini, A., et al. (2018). Leishmania infantum Lipophosphoglycan-Deficient Mutants: A Tool to Study Host Cell-Parasite Interplay. *Front. Microbiol.* 9:626. doi: 10.3389/fmicb.2018.00626

Lypaczewski, P., Hoshizaki, J., Zhang, W. W., McCall, L. I., Torcivia-Rodriguez, J., Simonyan, V., et al. (2018). A complete Leishmania donovani reference genome identifies novel genetic variations associated with virulence. *Sci. Rep*. 8:16549. doi: 10.1038/s41598-018-34812-x

Ma, D., Russell, D. G., Beverley, S. M., and Turco, S. J. (1997). Golgi GDP-mannose uptake requires Leishmania LPG2. *A member of a eukaryotic family of putative nucleotide-sugar transporters. J. Biol. Chem.* 272, 3799–3805. doi: 10.1074/jbc.272.6.3799

Martel, D., Beneke, T., Gluenz, E., Spath, G. F., and Rachidi, N. (2017). Characterisation of Casein Kinase 1.1 in Leishmania donovani Using the CRISPR Cas9 Toolkit. *Biomed. Res. Int.* 2017:4635605. doi: 10.1155/2017/4635605

McConville, M. J., Collidge, T. A., Ferguson, M. A., and Schneider, P. (1993). The glycoinositol phospholipids of Leishmania mexicana promastigotes. *Evidence for the presence of three distinct pathways of glycolipid biosynthesis. J. Biol. Chem.* 268, 15595–15604.

McNeely, T. B., Tolson, D. L., Pearson, T. W., and Turco, S. J. (1990). Characterization of Leishmania donovani variant clones using anti-lipophosphoglycan monoclonal antibodies. *Glycobiology* 1, 63–69. doi: 10.1093/glycob/1.1.63

Moradin, N., and Descoteaux, A. (2012). Leishmania promastigotes: building a safe niche within macrophages. *Front. Cell. Infect. Microbiol.* 2:121. doi: 10.3389/fcimb.2012.00121

Opat, A., Ng, K., Currie, G., Handman, E., and Bacic, A. (1996). Characterization of lipophosphoglycan from a ricin-resistant mutant of Leishmania major. *Glycobiology* 6, 387–397. doi: 10.1093/glycob/6.4.387

Peacock, C. S., Seeger, K., Harris, D., Murphy, L., Ruiz, J. C., Quail, M. A., et al. (2007). Comparative genomic analysis of three Leishmania species that cause diverse human disease. *Nat. Genet.* 39, 839–847. doi: 10.1038/ng2053

Pitale, D. M., Gendalur, N. S., Descoteaux, A., and Shaha, C. (2019). Leishmania donovani Induces Autophagy in Human Blood-Derived Neutrophils. *J. Immunol.* 202, 1163–1175. doi: 10.4049/jimmunol.1801053

Quintela-Carvalho, G., Luz, N. F., Celes, F. S., Zanette, D. L., Andrade, D., Menezes, D., et al. (2017). Heme Drives Oxidative Stress-Associated Cell Death in Human Neutrophils Infected with Leishmania infantum. *Front. Immunol.* 8:1620. doi: 10.3389/fimmu.2017.01620

Ribeiro-Gomes, F. L., Otero, A. C., Gomes, N. A., Moniz-De-Souza, M. C., Cysne-Finkelstein, L., Arnholdt, A. C., et al. (2004). Macrophage interactions with neutrophils regulate Leishmania major infection. *J. Immunol.* 172, 4454–4462. doi: 10.4049/jimmunol.172.7.4454

Robinson, K. A., and Beverley, S. M. (2003). Improvements in transfection efficiency and tests of RNA interference (RNAi) approaches in the protozoan parasite Leishmania. *Mol. Biochem. Parasitol.* 128, 217–228. doi: 10.1016/S0166-6851(03)00079-3

Ryan, K. A., Garraway, L. A., Descoteaux, A., Turco, S. J., and Beverley, S. M. (1993). Isolation of virulence genes directing surface glycosyl-phosphatidylinositol synthesis by functional complementation of Leishmania. *Proc. Natl. Acad. Sci. U. S. A.* 90, 8609–8613. doi: 10.1073/pnas.90.18.8609

Sacks, D. L., Modi, G., Rowton, E., Spath, G., Epstein, L., Turco, S. J., et al. (2000). The role of phosphoglycans in Leishmania-sand fly interactions. *Proc. Natl. Acad. Sci. U. S. A.* 97, 406–411. doi: 10.1073/pnas.97.1.406

Scianimanico, S., Desrosiers, M., Dermine, J. F., Meresse, S., Descoteaux, A., and Desjardins, M. (1999). Impaired recruitment of the small GTPase rab7 correlates with the inhibition of phagosome maturation by Leishmania donovani promastigotes. *Cell Microbiol.* 1, 19–32. doi: 10.1046/j.1462-5822.1999.00002.x

Segawa, H., Soares, R. P., Kawakita, M., Beverley, S. M., and Turco, S. J. (2005). Reconstitution of GDP-mannose transport activity with purified Leishmania LPG2 protein in liposomes. *J. Biol. Chem.* 280, 2028–2035. doi: 10.1074/jbc.M404915200

Spath, G. F., Epstein, L., Leader, B., Singer, S. M., Avila, H. A., Turco, S. J., et al. (2000). Lipophosphoglycan is a virulence factor distinct from related glycoconjugates in the protozoan parasite Leishmania major. *Proc. Natl. Acad. Sci. U. S. A.* 97, 9258–9263. doi: 10.1073/pnas.160257897

Spath, G. F., Garraway, L. A., Turco, S. J., and Beverley, S. M. (2003a). The role(s) of lipophosphoglycan (LPG) in the establishment of Leishmania major infections in mammalian hosts. *Proc. Natl. Acad. Sci. U. S. A.* 100, 9536–9541. doi: 10.1073/pnas.1530604100

Spath, G. F., Lye, L. F., Segawa, H., Sacks, D. L., Turco, S. J., and Beverley, S. M. (2003b). Persistence without pathology in phosphoglycan-deficient

Leishmania major. *Science* 301, 1241–1243. doi: 10.1126/science.1087499

Zhang, W. W., Lypaczewski, P., and Matlashewski, G. (2017). Optimized CRISPR-Cas9 Genome Editing for Leishmania and Its Use To Target a Multigene Family, Induce Chromosomal Translocation, and Study DNA Break Repair Mechanisms. *mSphere* 2, e00340-16 doi: 10.1128/mSphere.00340-16

Zhang, W. W., and Matlashewski, G. (2015). CRISPR-Cas9-Mediated Genome Editing in Leishmania donovani. *mBio* 6, e00861. doi: 10.1128/mBio.00861-15

Zhang, W. W., and Matlashewski, G. (2019). Single-Strand Annealing Plays a Major Role in Double-Strand DNA Break Repair following CRISPR-Cas9 Cleavage in Leishmania. *mSphere* 4, e00408-19. doi: 10.1128/mSphere.00408-19

Conflict of Interest: The authors declare that the research was conducted in the absence of any commercial or financial relationships that could be construed as a potential conflict of interest.

frontiers in Cellular and Infection Microbiology

BRIEF RESEARCH REPORT
published: 09 September 2020
doi: 10.3389/fcimb.2020.00488

Infection by the Protozoan Parasite *Toxoplasma gondii* Inhibits Host MNK1/2-eIF4E Axis to Promote Its Survival

Louis-Philippe Leroux, Visnu Chaparro and Maritza Jaramillo**

Institut National de la Recherche Scientifique (INRS)-Centre Armand-Frappier Santé Biotechnologie (CAFSB), Laval, QC, Canada

The obligate intracellular parasite *Toxoplasma gondii* reprograms host gene expression through multiple mechanisms that promote infection, including the up-regulation of mTOR-dependent host mRNA translation. In addition to the mTOR-4E-BP1/2 axis, MAPK-interacting kinases 1 and 2 (MNK1/2) control the activity of the mRNA cap-binding protein eIF4E. Herein, we show that *T. gondii* inhibits the phosphorylation of MNK1/2 and their downstream target eIF4E in murine and human macrophages. Exposure to soluble *T. gondii* antigens (STAg) failed to fully recapitulate this phenotype indicating the requirement of live infection. Treatment with okadaic acid, a potent phosphatase inhibitor, restored phosphorylation of MNK1/2 and eIF4E regardless of infection. *T. gondii* replication was higher in macrophages isolated from mice mutated at the residue where eIF4E is phosphorylated (eIF4E S209A knock-in) than in wild-type (WT) control cells despite no differences in infection rates. Similarly, parasitemia in the mesenteric lymph nodes and spleen, as well as brain cyst burden were significantly augmented in infected eIF4E S209A knock-in mice compared to their WT counterparts. Of note, mutant mice were more susceptible to acute toxoplasmosis and displayed exacerbated levels of IFNγ. In all, these data suggest that the MNK1/2-eIF4E axis is required to control *T. gondii* infection and that its inactivation represents a strategy exploited by the parasite to promote its survival.

Keywords: *Toxoplasma gondii*, MNK1/2, eIF4E phosphorylation, p38 MAPK, macrophages, IFNγ, inflammation

OPEN ACCESS

Edited by:
Nicolas Blanchard, INSERM U1043 Centre de Physiopathologie de Toulouse Purpan, France

Reviewed by:
Antonio Barragan, Stockholm University, Sweden
Eric Denkers, University of New Mexico, United States

****Correspondence:***
Louis-Philippe Leroux
louis-philippe.leroux@inrs.ca
Maritza Jaramillo
maritza.jaramillo@inrs.ca

Specialty section:
This article was submitted to Parasite and Host, a section of the journal Frontiers in Cellular and Infection Microbiology

Received: *29 April 2020*
Accepted: *06 August 2020*
Published: *09 September 2020*

Citation:
Leroux L-P, Chaparro V and Jaramillo M (2020) Infection by the Protozoan Parasite Toxoplasma gondii Inhibits Host MNK1/2-eIF4E Axis to Promote Its Survival. Front. Cell. Infect. Microbiol. 10:488. doi: 10.3389/fcimb.2020.00488

INTRODUCTION

Toxoplasma gondii (*T. gondii*), the etiologic agent of toxoplasmosis, is an intracellular protozoan parasite that infects a wide variety of vertebrate hosts, including humans and mice (Innes et al., 2019). It is estimated that about 30–50% of the world population is seropositive for *T. gondii* (Montazeri et al., 2017). Toxoplasmosis is generally asymptomatic yet reactivation of encysted parasites can lead to life-threatening consequences in immuno-compromised individuals (Luft and Remington, 1992), or cause abortions or birth defects if contracted during pregnancy (Montoya and Remington, 2008). *T. gondii* is able to invade any nucleated cell and usurps host cell organelles and nutrients in order to replicate within its parasitophorous vacuole (Clough and Frickel, 2017). The parasite targets signaling pathways and host gene expression to subvert immune responses and establish a favorable

environment (Hakimi et al., 2017; Blume and Seeber, 2018; Delgado Betancourt et al., 2019). Among the different strategies employed by the parasite, it was shown that *T. gondii* is able to fine-tune host gene expression post-transcriptionally in part through perturbations in translational efficiency of host mRNAs (Leroux et al., 2018).

Translational control enables cells to rapidly adapt their proteome to respond to stress or other metabolic cues without *de novo* mRNA synthesis (Gebauer and Hentze, 2004; Sonenberg and Hinnebusch, 2009). Changes in translational efficiency represent a fundamental mechanism in normal biological processes including cell differentiation, growth, metabolism, and proliferation (Gebauer and Hentze, 2004; Hershey et al., 2012). Translational control is also required for balanced immune functions (Piccirillo et al., 2014) and is observed during infectious diseases (Alain et al., 2010; Mohr and Sonenberg, 2012; Walsh et al., 2013; Nehdi et al., 2014; Leroux et al., 2018; Hoang et al., 2019; Chaparro et al., 2020). In eukaryotic cells, translational efficiency is mainly regulated at the initiation step during which ribosomes are recruited to the mRNA, a process facilitated by recognition of the mRNA 5′-m^7G-cap structure by eukaryotic initiation factor 4E (eIF4E), which, together with scaffold protein eIF4G and RNA helicase eIF4A, form the eIF4F complex (Jackson et al., 2010). Assembly of the eIF4F complex is precluded by eIF4E-binding proteins (4E-BPs), which block eIF4E:eIF4G interaction and eIF4F formation (Pause et al., 1994; Lin and Lawrence, 1996). Hyper-phosphorylation of 4E-BPs by mechanistic target of rapamycin (mTOR) complex 1 (mTORC1) lowers 4E-BPs' affinity to eIF4E, thus favoring eIF4E:eIF4G interaction and initiation of translation (Gingras et al., 2001). Phosphorylation of eIF4E at residue S209 is an additional regulatory mechanism of translation initiation (Pelletier et al., 2015), and is mediated by MAP kinase-interacting serine/threonine-protein kinase 1 and 2 (MNK1/2) (Ueda et al., 2004). MNK1/2 are phosphorylated by upstream kinases, specifically p38 MAPK and ERK1/2, following various stimuli (ex: growth factors, cytokines, etc.) (Waskiewicz et al., 1997).

Some studies have reported an increase in translation upon eIF4E phosphorylation (Furic et al., 2010; Robichaud et al., 2015). In contrast, others have suggested that phosphorylation of eIF4E lowers its affinity for the mRNA cap structure (Scheper et al., 2002; Zuberek et al., 2003, 2004; Slepenkov et al., 2006). These seemingly contradictory observations could be reconciled by the possibility that reduced cap affinity favors eIF4E recycling and thus increases translation initiation rates (Scheper and Proud, 2002). Translation of transcripts with highly structured 5′ UTRs is facilitated through eIF4E activity, and RNA regulons controlling cell proliferation and survival are tightly regulated themselves by eIF4E (Volpon et al., 2019). In addition to its role in translation initiation, eIF4E carries out other functions including mRNA nuclear export, stability, and sequestration (Volpon et al., 2019). However, aberrant eIF4E activity is a determining factor in the development of various pathologies. Dysregulated MNK1/2 activity as well as elevated phosphorylated and total levels of eIF4E have been shown to promote oncogenesis and tumor growth (Proud, 2015). Phosphorylation of eIF4E was reported to increase translational efficiency of the mRNA encoding the NF-κB inhibitor IκBα. Hence, mice mutated at the residue where eIF4E is phosphorylated (S209A) were less susceptible to viral infections by virtue of enhanced NF-κB activity and type I interferon production (Herdy et al., 2012). In macrophages, efficient translation of HES-1 (Su et al., 2015), a transcriptional repressor of inflammatory genes, and IRF8 (Xu et al., 2012), a transcription factor that promotes M1 polarization, was shown to require MNK-mediated phosphorylation of eIF4E.

Modulation of eIF4E phosphorylation has been associated with enhanced viral replication (Kleijn et al., 1996; Walsh and Mohr, 2004). However, the role of the MNK1/2-eIF4E axis during infections by protozoan parasites has yet to be investigated. Here, we report that *T. gondii* reduces MNK1/2 and eIF4E phosphorylation levels and disrupts upstream signaling in infected macrophages. Importantly, we demonstrate that genetic ablation of eIF4E phosphorylation dramatically increases parasite replication *in vitro* as well as parasitemia and host susceptibility in an experimental toxoplasmosis model. These results highlight a central role for the MNK1/2-eIF4E axis in mitigating disease outcome during *T. gondii* infection.

MATERIALS AND METHODS

Reagents

Culture media and supplements were purchased from Wisent; okadaic acid (*Prorocentrum* sp.) and phorbol-12-myristate-13-acetate (PMA) were acquired from Calbiochem; CellTracker Green (CMFDA) and DAPI were purchased from Invitrogen; Zombie Violet was supplied by BioLegend; resazurin sodium salt was acquired through Alfa Aesar; High Pure PCR Template Preparation Kit, and cOmplete EDTA-free protease inhibitor and PhosSTOP phosphatase inhibitor tablets were purchased from Roche; antibodies were acquired from Cell Signaling Technologies, R&D Systems, Sigma-Aldrich, and BD Biosciences.

Differentiation of Murine Bone Marrow-Derived Macrophages

Bone marrow-derived macrophages (BMDMs) were generated from 6 to 8 week-old female C57BL/6 mice (Jackson Laboratory), as previously described (Leroux et al., 2018; Zakaria et al., 2018; Chaparro et al., 2020). Briefly, marrow was extracted from bones of the hind legs, red blood cells were lysed, and progenitor cells were resuspended in BMDM culture medium supplemented with 15% L929 fibroblast-conditioned culture medium (LCCM). Non-adherent cells were collected the following day and were cultured for 7 days in BMDM culture medium supplemented with 30% LCCM with fresh medium replenishment at day 3 of incubation.

THP-1 Culture and Differentiation

The human monocytic cell line THP-1 (ATCC TIB-202) was maintained in suspension (DMEM, 10% heat-inactivated FBS, 2 mM L-glutamate, 1 mM sodium pyruvate, 100 U/mL penicillin, 100 μg/mL streptomycin, 20 mM HEPES, 55 μM β-mercaptoethanol). Cells were differentiated into macrophages by adding 20 ng/mL PMA for 24 h. The following day, spent medium was removed and fresh medium without PMA was

added, and cells were allowed to rest for another 24 h prior to infection.

Parasite Maintenance and Harvest

T. gondii cultures (RH and ME49 strains) were maintained by serial passages in Vero cells, as previously described (Leroux et al., 2018). For experimental infections, freshly egressed tachyzoites were harvested from Vero cultures, pelleted by centrifugation (1,300 × *g*, 7 min, 4°C), resuspended in ice-cold PBS (pH 7.2–7.4), and passed through a syringe fitted with a 27 G needle. Large cellular debris and intact host cells were pelleted by low-speed centrifugation (200 × *g*, 3 min, 4°C), and the supernatant containing parasites was filtered with a 3 μm-polycarbonate filter (Millipore). Tachyzoites were then washed twice in PBS and finally resuspended in the appropriate culture medium, according to the experiment.

Soluble *T. gondii* Antigens (STAg)

STAg were prepared from freshly egressed tachyzoites, as previously described (Leroux et al., 2015a). Briefly, parasites were resuspended in ice-cold PBS, subjected to three 5-min cycles of freezing/thawing using liquid nitrogen and a 37°C water bath, then sonicated on ice for 5 min (1 s on/off pulses, 30% duty cycle) using a Sonic Dismembrator FB505 (ThermoFisher). Lysates were cleared by centrifugation (21,000 × *g*, 15 min, 4°C), and soluble material containing STAg was used for downstream experiments.

Infection and Treatments of BMDM and THP-1 Cultures

Macrophages were plated 1 day before infection and allowed to adhere O/N at 37°C, 5% CO_2. Cultures were serum-starved for 2 h and then inoculated with *T. gondii* (MOI 6:1; unless otherwise specified), treated with 50 μg/mL STAg (where applicable), or left uninfected in fresh medium with 1% FBS. Any remaining extracellular parasites were rinsed away with warm PBS (pH 7.2–7.4) 1 h following inoculation, and fresh medium was added. Cells were treated with 10 nM okadaic acid or DMSO 1 h after infection (where applicable).

Western Blot Analysis

Cells were lysed in RIPA buffer supplemented with protease and phosphatase inhibitors, and samples were prepared for western blotting as described (Leroux et al., 2018; William et al., 2019). Primary antibodies anti-phospho-p38 (T180/Y182; #9216), anti-p38 (#8690), anti-phospho-ERK1/2 (T202/Y204; #9106), anti-ERK1/2 (#9102), anti-phospho-MNK1/2 (T197/202; #2111), anti-MNK1/2 (#2195), anti-phospho-eIF4E (S209; #9741), and anti-β-actin (#3700) were purchased from Cell Signaling Technologies; anti-eIF4E (#610269) was obtained from BD Biosciences; and anti-*T. gondii* profilin (#AF3860) was acquired from R&D Systems. Horseradish peroxidase (HRP)-linked goat anti-rabbit (#A0545) and goat anti-mouse IgG (#A4416) secondary antibodies were purchased from Sigma-Aldrich, and rabbit anti-goat (#HAF017) was acquired from R&D Systems. Densitometric analyses were performed with FIJI software.

Experimental Toxoplasmosis

Tachyzoites were harvested as described above and resuspended in sterile PBS. WT and eIF4E S209A KI mice in the C57BL/6 background (Furic et al., 2010) were infected intraperitoneally with either 10^2 RH or 10^3 ME49 *T. gondii*, or mock infected with PBS. Serum, mesenteric lymph nodes (MLN), and spleens were collected 8 days post-infection (acute), while brains were harvested after 21 days (chronic) for downstream analyses. Mouse health status was monitored up to 21 days post-infection. At least 5 mice per genotype were monitored in each infection trial.

Measurement of *in vitro* Parasite Replication, *in vivo* Parasitemia, and Cyst Burden by qPCR

In vitro parasite replication was evaluated by epifluorescence microscopy. Briefly, infected BMDM cultures were fixed at the indicated times with PBS with 3.7% PFA (15 min, RT). Cells were permeabilized with PBS with 0.2% Triton X-100 (5 min, RT), stained with DAPI (5 min, RT), then mounted onto slides. The number of parasites in at least 50 vacuoles in different fields for each genotype and time point was counted by microscopy using a 60X oil-immersion objective. The observer was blinded as to which sample was being evaluated to avoid bias during enumeration of the parasites. *In vivo* parasitemia and cyst burden were quantified by amplification of the *T. gondii B1* gene, as previously described (Leroux et al., 2015b, 2018). Genomic DNA (gDNA) was extracted from MLN, spleen, and brain tissues using High Pure PCR Template Preparation Kit (Roche) as per manufacturer's guidelines. *T. gondii B1* gene was amplified by qPCR using the PowerUP SYBR Green PCR Master Mix (Applied Biosystems) with the following primers: forward (5′-TCCCC TCTGCTGGCGAAAAGT-3′) and reverse (5′-AGCGTTCGTG GTCAACTATCGATTG-3′) (Integrated DNA Technologies). Reaction was carried out in a QuantStudio 3 Real-Time PCR System (Applied Biosciences). Values were normalized using the mouse *β-actin* gene amplified with forward (5′-CACCCACACT GTGCCCATCTACGA-3′) and reverse (5′- CAGCGGAACC GCTCATTGCCAATGG-3′) primers. Analysis was carried out by relative quantification using the Comparative C_t method ($2^{-\Delta\Delta Ct}$) (Livak and Schmittgen, 2001).

ELISA

Serum from acutely infected mice and mock-injected control mice was collected 8 days post-infection. IFNγ levels were measured by sandwich ELISA using a Mouse IFN-γ ELISA MAX Deluxe kit (Biolegend; #430804).

Statistical Analyses

Where applicable, data are presented as mean [SD]. Statistical significance was determined using unpaired *T*-test followed by Welch's correction or paired *T*-test (for *in vitro* replication assay); calculations were performed using Prism Software (GraphPad). For survival curves, log-rank test (Mantel-Cox) was used to determine significance. Differences were considered significant when $^{*}P < 0.05$, $^{**}P < 0.01$, $^{***}P < 0.001$.

RESULTS

T. gondii Inhibits Host MNK1/2 and eIF4E Phosphorylation and Disrupts Upstream Signaling in Infected Macrophages

As we and others have previously demonstrated, infection by *T. gondii* increases host mTOR signaling (Wang et al., 2010; Al-Bajalan et al., 2017) and mTOR-dependent mRNA translation (Leroux et al., 2018). In addition to the mTOR-4E-BP1/2 axis, MAPK-interacting kinases 1 and 2 (MNK1/2) control the activity of the mRNA cap-binding protein eIF4E (Proud, 2015). We therefore sought to determine if the cap-binding initiation factor eIF4E and its upstream signaling intermediates were activated upon infection by monitoring their phosphorylation status. Of note, parasite extracts (i.e., devoid of any host cell; "*Tg* only") were probed in parallel to rule out the possibility that any observed changes in signaling were due to cross-reactivity of the antibodies against *T. gondii* proteins. We first assayed the phosphorylation status of the upstream kinases of MNK1/2, specifically p38 MAPK and ERK1/2 (Waskiewicz et al., 1997). Phosphorylation of p38 MAPK (T180/Y182) was severely compromised in infected BMDMs by both parasite strains (**Figures 1A,B**). As for ERK1/2, phosphorylation at residues T202/Y204 gradually increased over time in cells infected by ME49 only, revealing a strain-dependent modulation. Regardless of ERK1/2 activation, phosphorylation of MNK1/2 (T197/202) was reduced in BMDMs infected with either strain compared to uninfected control cells. Consistently, phosphorylation levels of eIF4E (S209) were readily abrogated and remained as such in infected BMDM cultures. The induction of ERK1/2 phosphorylation by ME49, and the inhibition of MNK1/2 and eIF4E phosphorylation by both RH and ME49 followed an MOI-dependent trend whereby the respective phenotypes were increasingly pronounced as the parasite-to-host ratio increased (**Supplementary Figure 1**). On the other hand, an MOI of 1:1 was enough to lead to the inhibition of p38 phosphorylation by both *T. gondii* strains. In addition, MNK1/2 and eIF4E phosphorylation levels were reduced in infected human THP-1 macrophages (**Figures 1C,D**). In summary, *T. gondii* infection inhibits the MNK1/2-eIF4E signaling axis in both murine and human macrophages.

Live Parasites and Phosphatase Activity Are Required for Inhibition of the MNK1/2-eIF4E Axis During *T. gondii* Infection in Macrophages

We next sought to determine if live infection was required to disrupt the activation of the MNK1/2-eIF4E pathway. Unlike infection with live parasites, treatment of BMDM cultures with soluble *T. gondii* antigens (STAg) failed to inhibit eIF4E phosphorylation (**Figures 2A,B**). To begin deciphering the molecular mechanisms involved in the inhibition of MNK1/2-eIF4E phosphorylation, we first infected BMDM cultures and 1 h later treated them with 10 nM okadaic acid, a potent protein phosphatase type 1 and 2A inhibitor (Li et al., 2010). This approach helped avoid any effects of the inhibitor on the parasite's ability to infect host cells. Treatment with okadaic acid restored phosphorylation of MNK1/2 and eIF4E regardless of infection by *T. gondii* (**Figures 2C,D**). However, p38 phosphorylation levels remained markedly inhibited in infected cells suggesting that different mechanisms are responsible for the dephosphorylation of p38 and MNK1/2-eIF4E observed upon infection. Of note, treatment with 10 to 50 nM okadaic acid did not affect the viability of BMDM cultures and extracellular *T. gondii* parasites up to 12 and 24 h, respectively (**Supplementary Figures 2A,B**). Taking together, these results indicate a complex repression of the MNK1/2-eIF4E axis by *T. gondii* that is independent of p38 inactivation but implicates parasite- and/or host-derived phosphatases that remain to be identified.

Parasite Replication Within eIF4E S209A KI BMDMs Is Increased While 4E KI Mice Are More Susceptible to Toxoplasmosis

To begin evaluating the impact of eIF4E phosphorylation on *T. gondii* replication, we infected BMDM cultures generated from WT mice or mutated at the residue where eIF4E is phosphorylated (eIF4E S209A knock-in [KI]; 4E KI) (Furic et al., 2010). *In vitro* parasite replication was enhanced in eIF4E S209A KI BMDMs compared to WT cells as measured by microscopic analyses (**Figure 3A**). The average number of parasite per vacuole appeared to increase at a slightly higher rate for both RH and ME49 in the mutant host cells at 16 h post-infection, a phenotype was statistically significant at 24 h and on following infection. These data suggest that the inhibition of eIF4E phosphorylation in BMDMs represents a strategy that favors *T. gondii*. Importantly, the rate of infection (i.e., number of infected cells) did not differ between WT and 4E KI BMDM cultures (**Supplementary Figures 3A,B**). Furthermore, up-regulation of ERK1/2 phosphorylation, and inhibition of p38 and MNK1/2 phosphorylation by *T. gondii* were similar in WT and mutant macrophages (**Supplementary Figures 3C,D**).

To further extent our *in vitro* observations and to determine the impact of eIF4E phosphorylation on the outcome of toxoplasmosis, we infected and compared WT and eIF4E S209A KI mice. We first measured parasitemia levels in the mesenteric lymph nodes (MLN) and spleens 8 days post-inoculation (i.e., acute phase). Analyses by qPCR revealed a substantial increase in parasite loads in both MLN and spleen tissues in 4E KI mice compared to WT counterparts (**Figure 3B**). Inflammation appeared to be exacerbated in the former group as revealed by a ∼4-fold increase in serum IFNγ concentration (**Figure 3C**). The observed phenotype in 4E KI mice did not appear to be due to an underlying basal inflammatory state since IFNγ was not detectable in mock-injected animals. In light of these results, we then compared survival rates between 4E KI and WT mice. While most WT animals survived past the acute phase into the chronic phase, 4E KI mice were significantly more susceptible to acute toxoplasmosis with a majority of mortality (∼77%) occurring within 2 weeks post-infection (**Figure 4A**). This heighten susceptibility was reflected by a larger increase in the *T. gondii* cyst burden in the brain of 4E KI mice that survived until the chronic phase of infection in comparison to

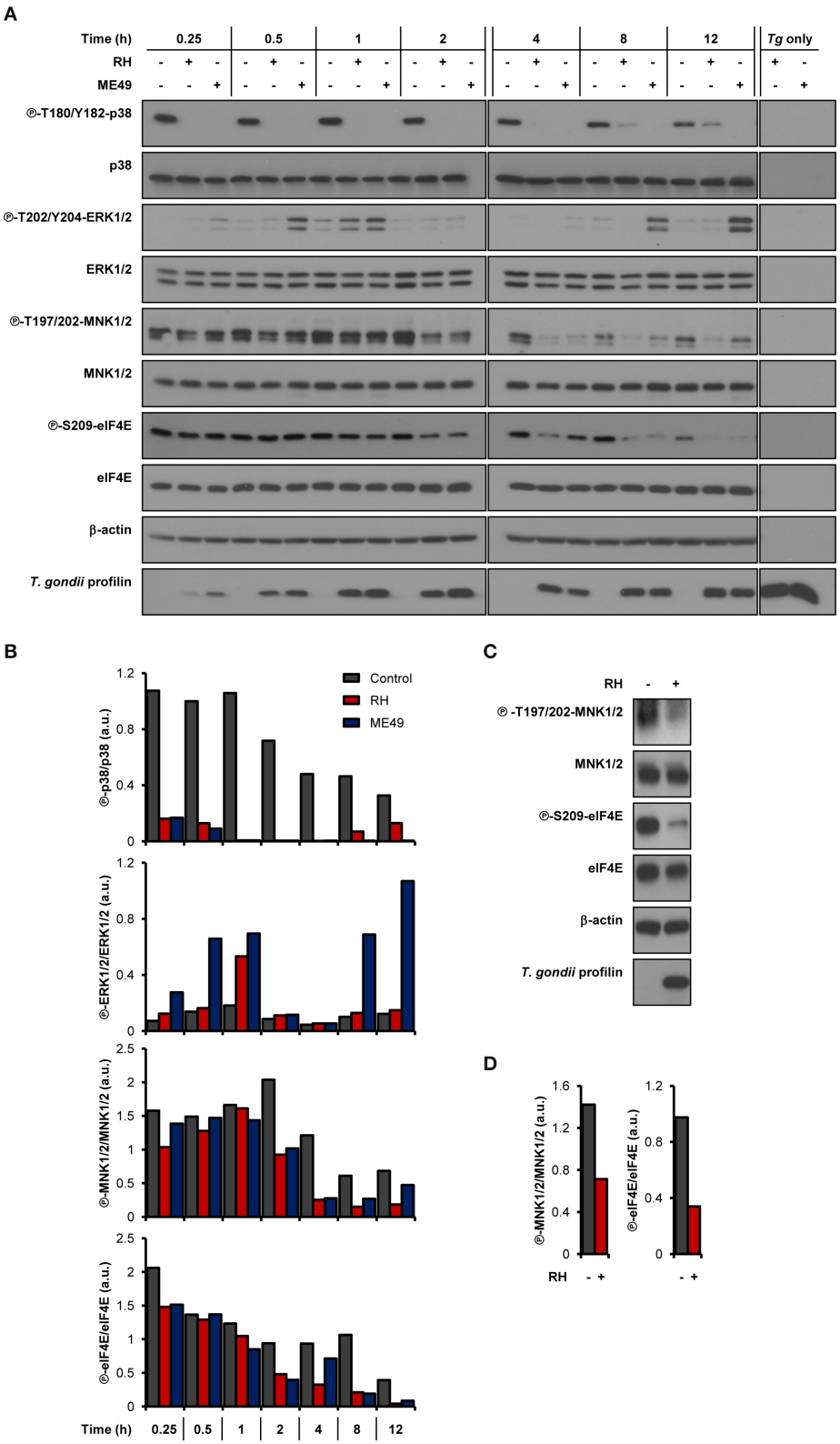

FIGURE 1 | *T. gondii* represses MNK1/2-eIF4E signaling pathway in macrophages. **(A,B)** BMDM cultures were infected with either RH or ME49 for the indicated times or left uninfected. **(C,D)** PMA-differentiated THP-1 cells were infected with RH strain for 8 h or left uninfected. **(A,C)** Phosphorylation and expression levels of indicated

(Continued)

FIGURE 1 | proteins were monitored by western blotting. Total amounts of β-actin were used as a loading control and an antibody against *T. gondii* profilin-like protein was employed to assess the infection of the BMDM cultures. Total protein extracts from extracellular tachyzoites (RH and ME49) (*Tg* only) were used to control for any cross-reactivity of the antibodies against *T. gondii* proteins. **(B,D)** Densitometric analysis of the phosphorylation status of indicated proteins in uninfected control cultures and infected cells using the FIJI software. Data and data analyses are representative of at least two biological replicates.

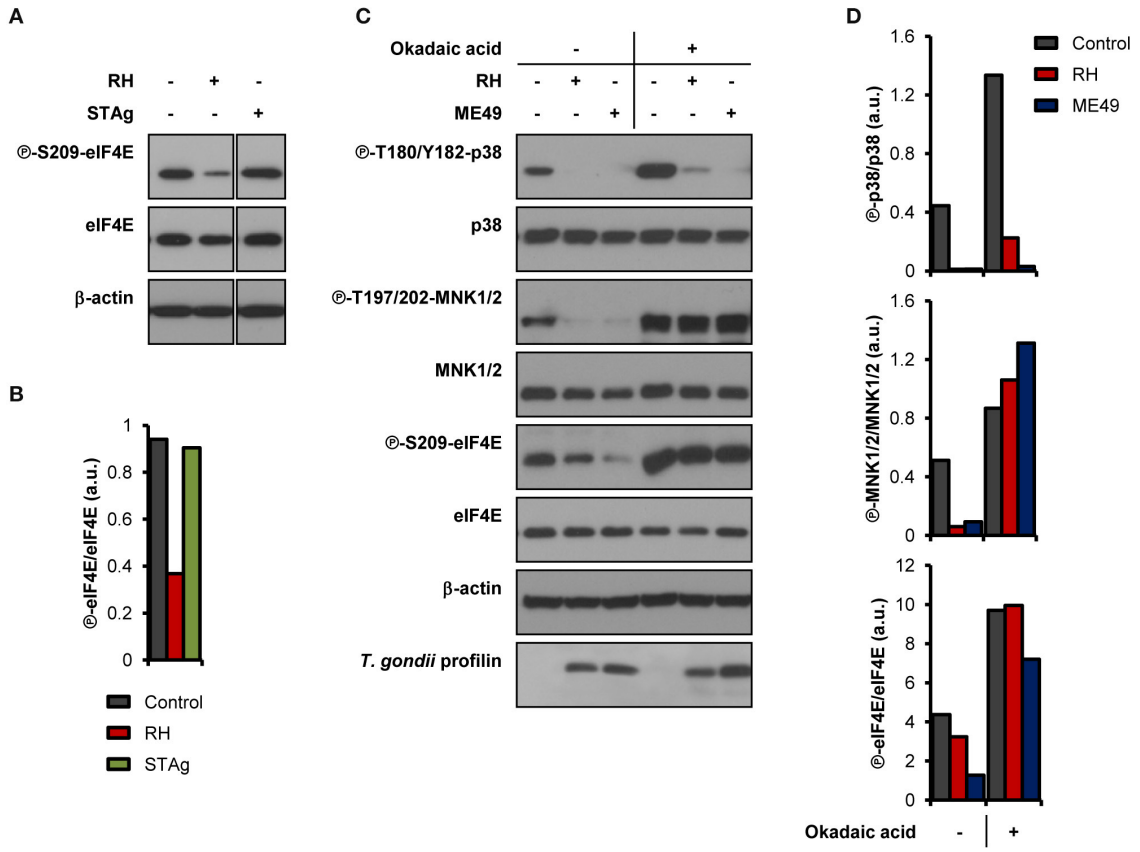

FIGURE 2 | *T. gondii*-derived soluble antigens do not fully recapitulate inhibitory effects of live infection, while okadaic acid restores phosphorylation levels of MNK1/2-eIF4E. BMDM cultures were infected with **(A,B)** RH strain or treated with 50 μg/mL of STAg, or **(C,D)** infected with either RH or ME49 strains then treated with DMSO (vehicle) or 10 nM okadaic acid for 8 h. In all cases, uninfected cultures were collected in parallel. **(A,C)** Phosphorylation and expression levels of indicated proteins were monitored by western blotting. Total amounts of β-actin were used as a loading control and an antibody against *T. gondii* profilin-like protein was employed to assess the infection of the BMDM cultures. **(B,D)** Densitometric analysis of the phosphorylation status of indicated proteins in uninfected control cultures and infected cells using the FIJI software. Data and data analyses are representative of two biological replicates.

WT counterparts (**Figure 4B**). In summary, the absence of eIF4E phosphorylation appears to compromise host resistance against toxoplasmosis despite increased IFNγ production.

DISCUSSION

Disruption of host signaling pathways and gene expression through altered translation is a strategy employed by diverse pathogens (Mohr and Sonenberg, 2012; Walsh et al., 2013). In this study, our results suggest that *T. gondii* targets and disrupts the host MNK1/2-eIF4E signaling axis, an important translational control node. Both type I and II strains markedly inhibit p38, MNK1/2, and eIF4E phosphorylation in infected macrophages. Interestingly, we have observed a marked difference in the induction of ERK1/2 phosphorylation between the two parasite strains. ERK1/2 phosphorylation increased transiently 1 h after infection by both strains and decreased afterwards. At later time points, however, infection by ME49 led to a gradually increased and sustained phosphorylation of ERK1/2, an observation in line with a recent study that reported a similar trend in bone marrow-derived dendritic cells infected with Prugniaud, another type II strain (Olafsson et al., 2020). Meanwhile, phospho-ERK1/2 levels in RH-infected cells remained low and comparable to basal levels seen in uninfected cultures. Chemical inhibition of phosphatases PP1 and PP2A with okadaic acid restores MNK1/2 and eIF4E phosphorylation but not p38, revealing a disconnection between these signaling

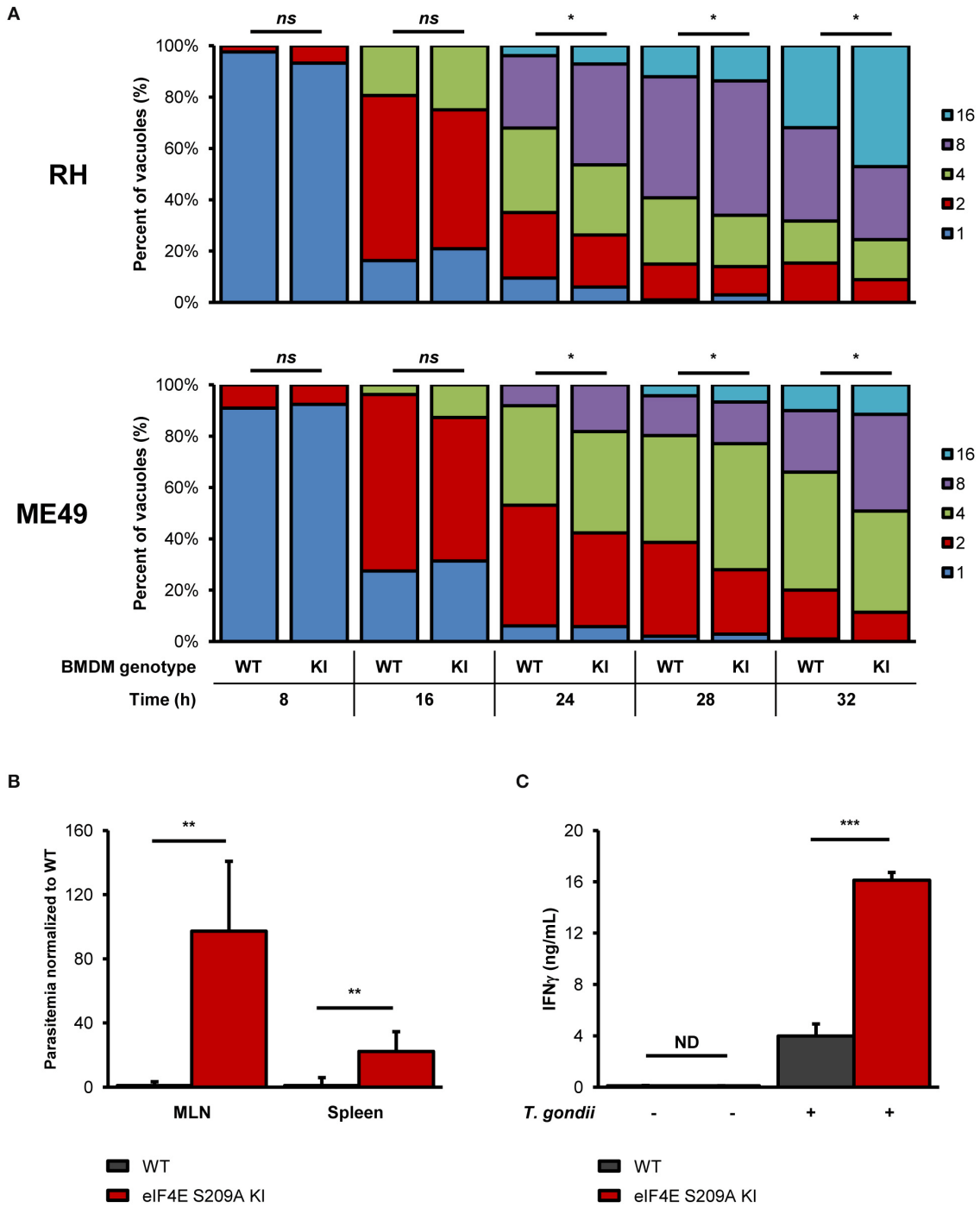

FIGURE 3 | Genetic inhibition of eIF4E phosphorylation increases *in vitro* parasite replication, and exacerbates parasite burden and inflammation during experimental toxoplasmosis. **(A)** BMDM differentiated from WT or eIF4E S209A KI mice were infected with RH tachyzoites for the indicated time, fixed, stained with DAPI, and mounted onto slides. The number of parasites in at least 50 vacuoles in different fields for each genotype and time point was counted by epifluorescence microscopy. Data are representative of two biological replicates; "*ns*" refers to "not significant." **(B,C)** WT and eIF4E S209A KI mice were inoculated intraperitoneally (IP) with 10^2 RH tachyzoites or PBS (mock) and euthanized 8 days post-infection. **(B)** Parasitemia in the MLN and spleen was determined by qPCR by amplification of the *T. gondii B1* gene. Ct values were normalized to the mouse *β-actin* gene, and values are expressed as fold-change compared to WT mice. **(C)** Serum IFNγ levels were measured by sandwich ELISA. Results are presented as mean [SD] calculated from values obtained from infected mice (two independent experiments; at least 5 mice per group); all samples were analyzed in technical triplicates; "ND" refers to "not detected". $^*P < 0.05$, $^{**}P < 0.01$, $^{***}P < 0.001$.

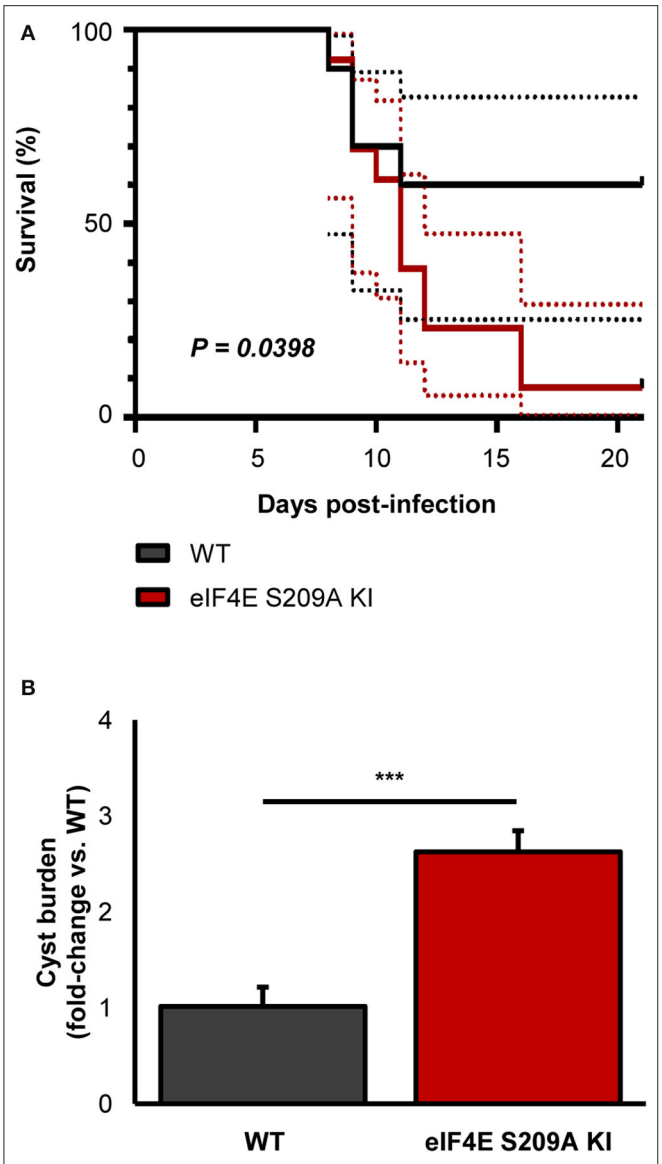

FIGURE 4 | Deficiency in eIF4E phosphorylation confers higher susceptibility to experimental toxoplasmosis and higher brain cyst burdens. Mice were infected IP with 10^3 ME49 tachyzoites. **(A)** Survival was monitored up to 21 days post-infection. Dashed lines represent 95% confidence intervals. **(B)** Brain cyst burden was measured by qPCR. Results are presented as mean [SD] calculated from values obtained from infected mice (two independent experiments; at least 5 mice per group; all samples were analyzed in technical triplicates. ***$P < 0.001$.

mediators following *T. gondii* infection. Seemingly conflicting reports about the regulation of p38 by *T. gondii* are found in the literature. A study by Kim et al. had reported a transient phosphorylation of p38 in BMDMs between 10 to 20 min (RH) and 10 to 60 min (ME49) following infection, after which phospho-p38 levels return to levels comparable to uninfected controls (Kim et al., 2006). It has also been shown that dense granule protein 24 (GRA24) directly interacts with and activates p38 through autophosphorylation (Braun et al., 2013). As the authors of the latter study pointed out, GRA24 presents several alternative splice variants. Thus, under certain growth conditions (e.g., host cell type and/or species, high vs. reduced nutrient availability, time of infection, etc.), *T. gondii* may turn off GRA24-dependent p38 autophosphorylation by synthesizing different GRA24 isoforms (Braun et al., 2013). In contrast, ROP18 is predicted to bind to p38 and cause its degradation (Yang et al., 2017). In our model, we have consistently observed a rapid (i.e., within 15 min after inoculation) and robust inhibition of phosphorylation of p38 by both RH and ME49 strains in both WT and eIF4E S209A KI macrophages. Thus, the reasons for the disparities among the different reports regarding this signaling molecule remain unclear at this point.

The data we obtained with okadaic acid treatment suggest that either parasite-derived phosphatases (devoid of function-altering strain polymorphisms) and/or host phosphatases are implicated in inactivation of the MNK1/2-eIF4E axis by *T. gondii*. To date, the mammalian PP2A phosphatase is the only enzyme shown to dephosphorylate both MNK1/2 and eIF4E (Li et al., 2010). Intriguingly, *T. gondii* GRA16 forms a complex with host PP2A and Herpesvirus-associated ubiquitin-specific protease (HAUSP) (Bougdour et al., 2013). Also, GRA18 binds to host GSK3/PP2A-B56 and to affect β-catenin-mediated gene expression (He et al., 2018). Whether these GRA16- and GRA18-containing complexes display phosphatase activity toward host MNK1/2 and eIF4E or that other host-parasite chimeric complexes are formed remains to be determined. For example, TgWIP, a rhoptry protein, interacts with host SHP2 phosphatase (Sangare et al., 2019). There are 52 predicted phosphatase genes in the *T. gondii* genome of which two encode for the PP2A catalytic subunits, referred to as PP2A1 and PP2A2 (Yang and Arrizabalaga, 2017). The PP2A1 protein sequence contains a signal peptide which raises the possibility that it is secreted into the host cells and targets host MNK1/2 and eIF4E. The fact that STAg failed to recapitulate the effects of live infection does not exclude that soluble factors are linked to MNK1/2-eIF4E dephosphorylation but rather that certain events are required for these factors to mediate their effects within the host cell (e.g., formation and presence of the parasitophorous vacuole membrane, specific route of entry of these molecules, etc.).

The increased replication rate *in vitro*, and parasitemia and virulence in eIF4E S209A KI mice suggest that preventing eIF4E phosphorylation favors *T. gondii* persistence within its host. We observed a substantial increase in serum IFNγ levels 8 days post-infection in 4E KI mice compared to their WT counterparts. Although IFNγ has long been identified as a critical cytokine to control toxoplasmosis (Denkers and Gazzinelli, 1998), it is possible that exacerbated inflammation leads to detrimental effects. Also, it is conceivable that complete absence of eIF4E phosphorylation in infected but also in uninfected 4E KI cells and mice precludes an appropriate immune response to develop against toxoplasmosis. Coincidentally, excessive inflammation has been linked to changes in eIF4E phosphorylation levels in other conditions. In a study by Amorim et al., it was shown that LPS treatment leads to a greater production of inflammatory cytokines IL-2, TNFα, and IFNγ in the brain of 4E KI mice

compared to WT animals (Amorim et al., 2018). Similarly, decreased synthesis of the NF-κB inhibitor IκBα has been reported in 4E KI fibroblasts infected with vesicular stomatitis virus (VSV), which leads to increased production of IFNβ (Herdy et al., 2012), and in the brain of 4E KI mice (Aguilar-Valles et al., 2018). Another recent study reported heighten levels of TNFα and IL-1β in 4E KI in old and young mice, respectively (Mody et al., 2020). Thus, higher IFNγ levels in 4E KI mice following *T. gondii* infection could be due to increased parasite burden and/or genetic predisposition to exacerbated inflammation in these mutant mice, which, according to our model, appears to be detrimental to the host. Future studies will be necessary to fully understand the underlying mechanisms linked to the increased susceptibility of 4E KI mice to toxoplasmosis.

It has been reported that phosphorylation of eIF4E regulates translation of a subset of mRNAs including several containing a gamma interferon-activated inhibition of translation (GAIT) element in their 3′ UTR (Amorim et al., 2018), or a 5′-terminal cap and a hairpin structure (Korneeva et al., 2016). It remains to be determined if the translational efficiency of specific subsets of host transcripts is affected by the reduction of phosphorylated eIF4E levels in *T. gondii*-infected cells. Functions of eIF4E beyond translation initiation *per se* are yet to be investigated in the context of parasitic infections. Furthermore, eIF4E-independent effects mediated by MNK1/2 could also play a role during *T. gondii* infection. Other MNK1/2 substrates identified to date include hnRNP A1, PSF, Sprouty2, and cPLA2 (Xie et al., 2019). One study showed that phosphorylation of hnRNP A1 by MNK1/2 decreases its affinity for *Tnfa* mRNA which, in turn, increases translation and synthesis of TNFα by T cells (Buxade et al., 2005). This evidence brings forth the possibility that immune responses mediated by MNK1/2 and its substrates could be dysregulated upon *T. gondii* and warrant future investigation.

In summary, our study identifies the MNK1/2-eIF4E axis as another regulatory node targeted by *T. gondii* to subvert host cell functions and promote its replication. Future studies will allow identification of host- and parasite-derived factors linked to this molecular rewiring and will provide a better understanding of its biological consequences during toxoplasmosis.

DATA AVAILABILITY STATEMENT

The original contributions presented in the study are included in the article/supplementary material, further inquiries can be directed to the corresponding author/s.

ETHICS STATEMENT

The animal study was reviewed and approved by Comité Institutionnel de Protection des Animaux (CIPA) of the INRS-CAFSB (CIPA 1502-03 and 1611-10).

AUTHOR CONTRIBUTIONS

L-PL and MJ conceived and designed the experiments and wrote the manuscript. L-PL, VC, and MJ analyzed the data. L-PL performed the experiments. All authors reviewed and edited the manuscript.

FUNDING

This work was supported by a Natural Sciences and Engineering Council (NSERC) Discovery Grant to MJ (RGPIN-2019-06671). MJ was supported by a salary award *Chercheur-boursier Junior 2* from the Fonds de Recherche du Québec en Santé (FRQS). VC was supported by a Ph.D. scholarship from FRQS. The Funders had no role in the study design, data collection and analysis, decision to publish, or preparation of the manuscript.

ACKNOWLEDGMENTS

We wish to thank Dr. Nahum Sonenberg (McGill University, Montreal, QC, Canada) for providing C57BL/6 eIF4E S209A KI mice. We are grateful to Jessie Tremblay for assistance with flow cytometry and epifluorescence microscopy experiments.

SUPPLEMENTARY MATERIAL

The Supplementary Material for this article can be found online at: https://www.frontiersin.org/articles/10.3389/fcimb.2020.00488/full#supplementary-material

REFERENCES

Aguilar-Valles, A., Haji, N., De Gregorio, D., Matta-Camacho, E., Eslamizade, M. J., Popic, J., et al. (2018). Translational control of depression-like behavior via phosphorylation of eukaryotic translation initiation factor 4E. *Nat. Commun.* 9:2459. doi: 10.1038/s41467-018-04883-5

Alain, T., Lun, X., Martineau, Y., Sean, P., Pulendran, B., Petroulakis, E., et al. (2010). Vesicular stomatitis virus oncolysis is potentiated by impairing mTORC1-dependent type I IFN production. *Proc. Natl. Acad. Sci. U.S.A.* 107, 1576–1581. doi: 10.1073/pnas.0912344107

Al-Bajalan, M. M. M., Xia, D., Armstrong, S., Randle, N., and Wastling, J. M. (2017). *Toxoplasma gondii* and *Neospora caninum* induce different host cell responses at proteome-wide phosphorylation events; a step forward for uncovering the biological differences between these closely related parasites. *Parasitol. Res.* 116, 2707–2719. doi: 10.1007/s00436-017-5579-7

Amorim, I. S., Kedia, S., Kouloulia, S., Simbriger, K., Gantois, I., Jafarnejad, S. M., et al. (2018). Loss of eIF4E phosphorylation engenders depression-like behaviors via selective mRNA translation. *J. Neurosci.* 38, 2118–2133. doi: 10.1523/JNEUROSCI.2673-17.2018

Blume, M., and Seeber, F. (2018). Metabolic interactions between *Toxoplasma gondii* and its host. *F1000Res* 7:F1000 Faculty Rev-1719. doi: 10.12688/f1000research.16021.1

Bougdour, A., Durandau, E., Brenier-Pinchart, M. P., Ortet, P., Barakat, M., Kieffer, S., et al. (2013). Host cell subversion by *Toxoplasma* GRA16, an exported dense granule protein that targets the host cell nucleus and alters gene expression. *Cell Host Microbe* 13, 489–500. doi: 10.1016/j.chom.2013.03.002

Braun, L., Brenier-Pinchart, M. P., Yogavel, M., Curt-Varesano, A., Curt-Bertini, R. L., Hussain, T., et al. (2013). A *Toxoplasma* dense granule protein, GRA24, modulates the early immune response to infection by promoting a direct

and sustained host p38 MAPK activation. *J. Exp. Med.* 210, 2071–2086. doi: 10.1084/jem.20130103

Buxade, M., Parra, J. L., Rousseau, S., Shpiro, N., Marquez, R., Morrice, N., et al. (2005). The Mnks are novel components in the control of TNF alpha biosynthesis and phosphorylate and regulate hnRNP A1. *Immunity* 23, 177–189. doi: 10.1016/j.immuni.2005.06.009

Chaparro, V., Leroux, L. P., Masvidal, L., Lorent, J., Graber, T. E., Zimmermann, A., et al. (2020). Translational profiling of macrophages infected with *Leishmania donovani* identifies mTOR- and eIF4A-sensitive immune-related transcripts. *PLoS Pathog.* 16:e1008291. doi: 10.1371/journal.ppat.1008291

Clough, B., and Frickel, E. M. (2017). The *Toxoplasma* parasitophorous vacuole: an evolving host-parasite frontier. *Trends Parasitol.* 33, 473–488. doi: 10.1016/j.pt.2017.02.007

Delgado Betancourt, E., Hamid, B., Fabian, B. T., Klotz, C., Hartmann, S., and Seeber, F. (2019). From entry to early dissemination-*Toxoplasma gondii*'s initial encounter with its host. *Front. Cell. Infect. Microbiol.* 9:46. doi: 10.3389/fcimb.2019.00046

Denkers, E. Y., and Gazzinelli, R. T. (1998). Regulation and function of T-cell-mediated immunity during *Toxoplasma gondii* infection. *Clin. Microbiol. Rev.* 11, 569–588. doi: 10.1128/CMR.11.4.569

Furic, L., Rong, L., Larsson, O., Koumakpayi, I. H., Yoshida, K., Brueschke, A., et al. (2010). eIF4E phosphorylation promotes tumorigenesis and is associated with prostate cancer progression. *Proc. Natl. Acad. Sci. U.S.A.* 107, 14134–14139. doi: 10.1073/pnas.1005320107

Gebauer, F., and Hentze, M. W. (2004). Molecular mechanisms of translational control. *Nat. Rev. Mol. Cell Biol.* 5, 827–835. doi: 10.1038/nrm1488

Gingras, A. C., Raught, B., Gygi, S. P., Niedzwiecka, A., Miron, M., Burley, S. K., et al. (2001). Hierarchical phosphorylation of the translation inhibitor 4E-BP1. *Genes Dev.* 15, 2852–2864. doi: 10.1101/gad.912401

Hakimi, M. A., Olias, P., and Sibley, L. D. (2017). *Toxoplasma* effectors targeting host signaling and transcription. *Clin. Microbiol. Rev.* 30, 615–645. doi: 10.1128/CMR.00005-17

He, H., Brenier-Pinchart, M. P., Braun, L., Kraut, A., Touquet, B., Coute, Y., et al. (2018). Characterization of a *Toxoplasma* effector uncovers an alternative GSK3/beta-catenin-regulatory pathway of inflammation. *Elife* 7:e39887. doi: 10.7554/eLife.39887.027

Herdy, B., Jaramillo, M., Svitkin, Y. V., Rosenfeld, A. B., Kobayashi, M., Walsh, D., et al. (2012). Translational control of the activation of transcription factor NF-kappaB and production of type I interferon by phosphorylation of the translation factor eIF4E. *Nat. Immunol.* 13, 543–550. doi: 10.1038/ni.2291

Hershey, J. W., Sonenberg, N., and Mathews, M. B. (2012). Principles of translational control: an overview. *Cold Spring Harb. Perspect. Biol.* 4:a011528. doi: 10.1101/cshperspect.a011528

Hoang, H. D., Graber, T. E., Jia, J. J., Vaidya, N., Gilchrist, V. H., Xiang, X., et al. (2019). Induction of an alternative mRNA 5′ leader enhances translation of the ciliopathy gene Inpp5e and resistance to oncolytic virus infection. *Cell Rep.* 29, 4010–4023.e5. doi: 10.1016/j.celrep.2019.11.072

Innes, E. A., Hamilton, C., Garcia, J. L., Chryssafidis, A., and Smith, D. (2019). A one health approach to vaccines against *Toxoplasma gondii*. *Food Waterborne Parasitol.* 15:e00053. doi: 10.1016/j.fawpar.2019.e00053

Jackson, R. J., Hellen, C. U., and Pestova, T. V. (2010). The mechanism of eukaryotic translation initiation and principles of its regulation. *Nat. Rev. Mol. Cell Biol.* 11, 113–127. doi: 10.1038/nrm2838

Kim, L., Butcher, B. A., Lee, C. W., Uematsu, S., Akira, S., and Denkers, E. Y. (2006). *Toxoplasma gondii* genotype determines MyD88-dependent signaling in infected macrophages. *J. Immunol.* 177, 2584–2591. doi: 10.4049/jimmunol.177.4.2584

Kleijn, M., Vrins, C. L., Voorma, H. O., and Thomas, A. A. (1996). Phosphorylation state of the cap-binding protein eIF4E during viral infection. *Virology* 217, 486–494. doi: 10.1006/viro.1996.0143

Korneeva, N. L., Song, A., Gram, H., Edens, M. A., and Rhoads, R. E. (2016). Inhibition of mitogen-activated protein kinase (MAPK)-interacting kinase (MNK) preferentially affects translation of mRNAs containing both a 5′-terminal cap and hairpin. *J. Biol. Chem.* 291, 3455–3467. doi: 10.1074/jbc.M115.694190

Leroux, L. P., Dasanayake, D., Rommereim, L. M., Fox, B. A., Bzik, D. J., Jardim, A., et al. (2015a). Secreted *Toxoplasma gondii* molecules interfere with expression of MHC-II in interferon gamma-activated macrophages. *Int. J. Parasitol.* 45, 319–332. doi: 10.1016/j.ijpara.2015.01.003

Leroux, L. P., Lorent, J., Graber, T. E., Chaparro, V., Masvidal, L., Aguirre, M., et al. (2018). The protozoan parasite *Toxoplasma gondii* selectively reprograms the host cell translatome. *Infect. Immun.* 86:e00244-18. doi: 10.1128/IAI.00244-18

Leroux, L. P., Nishi, M., El-Hage, S., Fox, B. A., Bzik, D. J., and Dzierszinski, F. S. (2015b). Parasite manipulation of the invariant chain and the peptide editor H2-DM affects major histocompatibility complex class II antigen presentation during *Toxoplasma gondii* infection. *Infect. Immun.* 83, 3865–3880. doi: 10.1128/IAI.00415-15

Li, Y., Yue, P., Deng, X., Ueda, T., Fukunaga, R., Khuri, F. R., et al. (2010). Protein phosphatase 2A negatively regulates eukaryotic initiation factor 4E phosphorylation and eIF4F assembly through direct dephosphorylation of Mnk and eIF4E. *Neoplasia* 12, 848–855. doi: 10.1593/neo.10704

Lin, T. A., and Lawrence, J. C. Jr. (1996). Control of the translational regulators PHAS-I and PHAS-II by insulin and cAMP in 3T3-L1 adipocytes. *J. Biol. Chem.* 271, 30199–30204. doi: 10.1074/jbc.271.47.30199

Livak, K. J., and Schmittgen, T. D. (2001). Analysis of relative gene expression data using real-time quantitative PCR and the 2(-Delta Delta C(T)) method. *Methods* 25, 402–408. doi: 10.1006/meth.2001.1262

Luft, B. J., and Remington, J. S. (1992). Toxoplasmic encephalitis in AIDS. *Clin. Infect. Dis.* 15, 211–222. doi: 10.1093/clinids/15.2.211

Mody, P. H., Dos Santos, N. L., Barron, L. R., Price, T. J., and Burton, M. D. (2020). eIF4E phosphorylation modulates pain and neuroinflammation in the aged. *Geroscience*. doi: 10.1007/s11357-020-00220-1. [Epub ahead of print].

Mohr, I., and Sonenberg, N. (2012). Host translation at the nexus of infection and immunity. *Cell Host Microbe* 12, 470–483. doi: 10.1016/j.chom.2012.09.006

Montazeri, M., Sharif, M., Sarvi, S., Mehrzadi, S., Ahmadpour, E., and Daryani, A. (2017). A systematic review of *in vitro* and *in vivo* activities of anti-*Toxoplasma* drugs and compounds (2006-2016). *Front. Microbiol.* 8:25. doi: 10.3389/fmicb.2017.00025

Montoya, J. G., and Remington, J. S. (2008). Management of *Toxoplasma gondii* infection during pregnancy. *Clin. Infect. Dis.* 47, 554–566. doi: 10.1086/590149

Nehdi, A., Sean, P., Linares, I., Colina, R., Jaramillo, M., and Alain, T. (2014). Deficiency in either 4E-BP1 or 4E-BP2 augments innate antiviral immune responses. *PLoS ONE* 9:e114854. doi: 10.1371/journal.pone.0114854

Olafsson, E. B., Ten Hoeve, A. L., Li-Wang, X., Westermark, L., Varas-Godoy, M., and Barragan, A. (2020). Convergent Met and voltage-gated Ca(2+) channel signaling drives hypermigration of *Toxoplasma*-infected dendritic cells. *J. Cell Sci.* 134:jcs.241752. doi: 10.1242/jcs.241752

Pause, A., Belsham, G. J., Gingras, A. C., Donze, O., Lin, T. A., Lawrence, J. C. Jr., et al. (1994). Insulin-dependent stimulation of protein synthesis by phosphorylation of a regulator of 5′-cap function. *Nature* 371, 762–767. doi: 10.1038/371762a0

Pelletier, J., Graff, J., Ruggero, D., and Sonenberg, N. (2015). Targeting the eIF4F translation initiation complex: a critical nexus for cancer development. *Cancer Res.* 75, 250–263. doi: 10.1158/0008-5472.CAN-14-2789

Piccirillo, C. A., Bjur, E., Topisirovic, I., Sonenberg, N., and Larsson, O. (2014). Translational control of immune responses: from transcripts to translatomes. *Nat. Immunol.* 15, 503–511. doi: 10.1038/ni.2891

Proud, C. G. (2015). Mnks, eIF4E phosphorylation and cancer. *Biochim. Biophys. Acta* 1849, 766–773. doi: 10.1016/j.bbagrm.2014.10.003

Robichaud, N., del Rincon, S. V., Huor, B., Alain, T., Petruccelli, L. A., Hearnden, J., et al. (2015). Phosphorylation of eIF4E promotes EMT and metastasis via translational control of SNAIL and MMP-3. *Oncogene* 34, 2032–2042. doi: 10.1038/onc.2014.146

Sangare, L. O., Olafsson, E. B., Wang, Y., Yang, N., Julien, L., Camejo, A., et al. (2019). *In vivo* CRISPR screen identifies TgWIP as a *Toxoplasma* modulator of dendritic cell migration. *Cell Host Microbe* 26, 478–492 e478. doi: 10.1016/j.chom.2019.09.008

Scheper, G. C., and Proud, C. G. (2002). Does phosphorylation of the cap-binding protein eIF4E play a role in translation initiation? *Eur. J. Biochem.* 269, 5350–5359. doi: 10.1046/j.1432-1033.2002.03291.x

Scheper, G. C., van Kollenburg, B., Hu, J., Luo, Y., Goss, D. J., and Proud, C. G. (2002). Phosphorylation of eukaryotic initiation factor 4E markedly reduces its affinity for capped mRNA. *J. Biol. Chem.* 277, 3303–3309. doi: 10.1074/jbc.M103607200

Slepenkov, S. V., Darzynkiewicz, E., and Rhoads, R. E. (2006). Stopped-flow kinetic analysis of eIF4E and phosphorylated eIF4E binding to cap analogs and capped oligoribonucleotides: evidence for a one-step binding mechanism. *J. Biol. Chem.* 281, 14927–14938. doi: 10.1074/jbc.M601653200

Sonenberg, N., and Hinnebusch, A. G. (2009). Regulation of translation initiation in eukaryotes: mechanisms and biological targets. *Cell* 136, 731–745. doi: 10.1016/j.cell.2009.01.042

Su, X., Yu, Y., Zhong, Y., Giannopoulou, E. G., Hu, X., Liu, H., et al. (2015). Interferon-gamma regulates cellular metabolism and mRNA translation to potentiate macrophage activation. *Nat. Immunol.* 16, 838–849. doi: 10.1038/ni.3205

Ueda, T., Watanabe-Fukunaga, R., Fukuyama, H., Nagata, S., and Fukunaga, R. (2004). Mnk2 and Mnk1 are essential for constitutive and inducible phosphorylation of eukaryotic initiation factor 4E but not for cell growth or development. *Mol. Cell. Biol.* 24, 6539–6549. doi: 10.1128/MCB.24.15.6539-6549.2004

Volpon, L., Osborne, M. J., and Borden, K. L. B. (2019). Biochemical and structural insights into the eukaryotic translation initiation factor eIF4E. *Curr. Prot. Pept. Sci.* 20:525–535. doi: 10.2174/1389203720666190110142438

Walsh, D., Mathews, M. B., and Mohr, I. (2013). Tinkering with translation: protein synthesis in virus-infected cells. *Cold Spring Harb. Perspect. Biol.* 5:a012351. doi: 10.1101/cshperspect.a012351

Walsh, D., and Mohr, I. (2004). Phosphorylation of eIF4E by Mnk-1 enhances HSV-1 translation and replication in quiescent cells. *Genes Dev.* 18, 660–672. doi: 10.1101/gad.1185304

Wang, Y., Weiss, L. M., and Orlofsky, A. (2010). Coordinate control of host centrosome position, organelle distribution, and migratory response by *Toxoplasma gondii* via host mTORC2. *J. Biol. Chem.* 285, 15611–15618. doi: 10.1074/jbc.M109.095778

Waskiewicz, A. J., Flynn, A., Proud, C. G., and Cooper, J. A. (1997). Mitogen-activated protein kinases activate the serine/threonine kinases Mnk1 and Mnk2. *EMBO J.* 16, 1909–1920. doi: 10.1093/emboj/16.8.1909

William, M., Leroux, L. P., Chaparro, V., Graber, T. E., Alain, T., and Jaramillo, M. (2019). Translational repression of *Ccl5* and *Cxcl10* by 4E-BP1 and 4E-BP2 restrains the ability of mouse macrophages to induce migration of activated T cells. *Eur. J. Immunol.* 49, 1200–1212. doi: 10.1002/eji.201847857

Xie, J., Merrett, J. E., Jensen, K. B., and Proud, C. G. (2019). The MAP kinase-interacting kinases (MNKs) as targets in oncology. *Expert Opin. Ther. Targets* 23, 187–199. doi: 10.1080/14728222.2019.1571043

Xu, H., Zhu, J., Smith, S., Foldi, J., Zhao, B., Chung, A. Y., et al. (2012). Notch-RBP-J signaling regulates the transcription factor IRF8 to promote inflammatory macrophage polarization. *Nat. Immunol.* 13, 642–650. doi: 10.1038/ni.2304

Yang, C., and Arrizabalaga, G. (2017). The serine/threonine phosphatases of apicomplexan parasites. *Mol. Microbiol.* 106, 1–21. doi: 10.1111/mmi.13715

Yang, Z., Hou, Y., Hao, T., Rho, H. S., Wan, J., Luan, Y., et al. (2017). A human proteome array approach to identifying key host proteins targeted by *Toxoplasma* kinase ROP18. *Mol. Cell. Proteomics* 16, 469–484. doi: 10.1074/mcp.M116.063602

Zakaria, C., Sean, P., Hoang, H. D., Leroux, L. P., Watson, M., Workenhe, S. T., et al. (2018). Active-site mTOR inhibitors augment HSV1-dICP0 infection in cancer cells via dysregulated eIF4E/4E-BP axis. *PLoS Pathog.* 14:e1007264. doi: 10.1371/journal.ppat.1007264

Zuberek, J., Jemielity, J., Jablonowska, A., Stepinski, J., Dadlez, M., Stolarski, R., et al. (2004). Influence of electric charge variation at residues 209 and 159 on the interaction of eIF4E with the mRNA 5′ terminus. *Biochemistry* 43, 5370–5379. doi: 10.1021/bi030266t

Zuberek, J., Wyslouch-Cieszynska, A., Niedzwiecka, A., Dadlez, M., Stepinski, J., Augustyniak, W., et al. (2003). Phosphorylation of eIF4E attenuates its interaction with mRNA 5′ cap analogs by electrostatic repulsion: intein-mediated protein ligation strategy to obtain phosphorylated protein. *RNA* 9, 52–61. doi: 10.1261/rna.2133403

Conflict of Interest: The authors declare that the research was conducted in the absence of any commercial or financial relationships that could be construed as a potential conflict of interest.

frontiers in Cellular and Infection Microbiology

BRIEF RESEARCH REPORT
published: 29 October 2020
doi: 10.3389/fcimb.2020.536985

Endocytic Rabs Are Recruited to the *Trypanosoma cruzi* Parasitophorous Vacuole and Contribute to the Process of Infection in Non-professional Phagocytic Cells

Betiana Nebaí Salassa[1,2], *Juan Agustín Cueto*[1,3], *Julián Gambarte Tudela*[4] and *Patricia Silvia Romano*[1,5]*

[1] Laboratorio de Biología de Trypanosoma cruzi la célula hospedadora, Instituto de Histología y Embriología, Consejo Nacional de Investigaciones Científicas y Técnicas (IHEM-CONICET), Universidad Nacional de Cuyo, Mendoza, Argentina, [2] Facultad de Odontología, Universidad Nacional de Cuyo, Mendoza, Argentina, [3] Instituto de Fisiología, Facultad de Ciencias Médicas, Universidad Nacional de Cuyo, Mendoza, Argentina, [4] Instituto de Bioquímica y Biotecnología, Facultad de Ciencias Médicas, Universidad Nacional de Cuyo, Mendoza, Argentina, [5] Facultad de Ciencias Médicas, Universidad Nacional de Cuyo, Mendoza, Argentina

OPEN ACCESS

Edited by:
Juliana Perrone Bezerra De Menezes, Gonçalo Moniz Institute (IGM), Brazil

Reviewed by:
Danilo Ciccone Miguel, Campinas State University, Brazil
Luciana Oliveira Andrade, Federal University of Minas Gerais, Brazil

***Correspondence:**
Patricia Silvia Romano
promano@fcm.uncu.edu.ar

Specialty section:
This article was submitted to Microbes and Innate Immunity, a section of the journal Frontiers in Cellular and Infection Microbiology

Received: 21 February 2020
Accepted: 17 September 2020
Published: 29 October 2020

Citation:
Salassa BN, Cueto JA, Gambarte Tudela J and Romano PS (2020) Endocytic Rabs Are Recruited to the Trypanosoma cruzi Parasitophorous Vacuole and Contribute to the Process of Infection in Non-professional Phagocytic Cells. Front. Cell. Infect. Microbiol. 10:536985. doi: 10.3389/fcimb.2020.536985

Trypanosoma cruzi is the parasite causative of Chagas disease, a highly disseminated illness endemic in Latin-American countries. *T. cruzi* has a complex life cycle that involves mammalian hosts and insect vectors both of which exhibits different parasitic forms. Trypomastigotes are the infective forms capable to invade several types of host cells from mammals. *T. cruzi* infection process comprises two sequential steps, the formation and the maturation of the *Trypanosoma cruzi* parasitophorous vacuole. Host Rab GTPases are proteins that control the intracellular vesicular traffic by regulating budding, transport, docking, and tethering of vesicles. From over 70 Rab GTPases identified in mammalian cells only two, Rab5 and Rab7 have been found in the *T. cruzi* vacuole to date. In this work, we have characterized the role of the endocytic, recycling, and secretory routes in the *T. cruzi* infection process in CHO cells, by studying the most representative Rabs of these pathways. We found that endocytic Rabs are selectively recruited to the vacuole of *T. cruzi*, among them Rab22a, Rab5, and Rab21 right away after the infection followed by Rab7 and Rab39a at later times. However, neither recycling nor secretory Rabs were present in the vacuole membrane at the times studied. Interestingly loss of function of endocytic Rabs by the use of their dominant-negative mutant forms significantly decreases *T. cruzi* infection. These data highlight the contribution of these proteins and the endosomal route in the process of *T. cruzi* infection.

Keywords: *Trypanosoma cruzi*, host cell infection, endocytosis, Rab proteins, *T. cruzi* parasitophorous vacuole

INTRODUCTION

The Ras-associated binding proteins, Rabs, are small GTP–binding proteins that control the budding, transport, docking, and tethering of vesicles from a donor to an acceptor compartment. Early endocytosis is regulated by Rab5 subfamily of GTPases mainly composed by Rab5, Rab22a, and Rab21 (Li, 2012). Rab5, the first characterized protein and the prototype of this subfamily,

is located in the cytoplasmic side of plasma membrane, endocytic vesicles and early endosomes (EE) and regulates the formation, uncoating, and transport of endocytic vesicles and fusion with early endosomes (Chavrier et al., 1990; Gorvel et al., 1991). Rab22a and Rab21 have similar distribution than Rab5 and promote, with it, the sorting to late endosomes (LE)/lysosomes due to interaction with similar effectors and regulators. Interestingly, the effector of Rab22a, Rabex-5, is a GEF of Rab5 and Rab21, indicating that these Rabs can also cooperate to produce the Rab22a-Rab5/Rab21 cascade (Zhu et al., 2009), which allow the sorting to LE. Moreover, the class C VPS/HOPS complex (Rieder and Emr, 1997; Seals et al., 2000), is a Rab5 effector that promotes the arrival of Rab7 and the sorting of endocytosed ligands from early to late endosomes which, in turn, will mature into lysosomes, the degradative compartment of the cell (Rink et al., 2005). Besides Rab7, other Rabs participate in the late endocytic transport. Rab39a is a poorly characterized Rab located in endocytic compartments that regulates transport and fusion of vesicles from the Golgi complex to LE/multivesicular bodies (Chen et al., 2003; Gambarte Tudela et al., 2019). In contrast, the so-called anterograde transport to plasma membrane is regulated by another subset of Rabs. Rab1 and Rab2 participate in the transport of secretory proteins throughout the endoplasmic reticulum and Golgi complex, while Rab3 is associated with the fusion of secretory vesicles to the plasma membrane, especially synaptic vesicles (Schlüter et al., 2004). In addition, the recycling of cargo from endosomes to plasma membrane is regulated by Rab4 and Rab11, which promote the rapid or the slow recycling of endocytic components, respectively (Grant and Donaldson, 2009). Due to antibodies against Rab proteins have low sensitivity, the most important tool used to study these proteins has been the expression of mutant proteins defective in the binding (dominant-negative mutants) or in the hydrolysis (dominant-positive mutants) of GTP. These mutants fused to GFP have been widely used to localize and to describe the function of a particular Rab in a particular traffic (Tisdale et al., 1992; Zerial and Stenmark, 1993).

Trypanosoma cruzi, the causal agent of Chagas disease, is an obligate intracellular parasite in mammalian hosts. The infective forms of *T. cruzi* are metacyclic or blood trypomastigotes, according to their origin from the feces of the insect vector or in the blood of mammalian hosts, respectively. After the invasion, trypomastigotes temporally reside in a membrane-bound compartment called the *T. cruzi* parasitophorous vacuole (TcPV). Inside the TcPV, trypomastigotes start the differentiation to amastigotes and the process ends in the cytoplasm. Amastigotes then actively replicate and when they are in high number, differentiate back to trypomastigotes which exit the cell to infect new cells and to continue the parasite cycle. Target cells are preferentially muscle cells like smooth muscle digestive tract and cardiac tissue, both places where *T. cruzi* develops the pathology.

Invasion of *T. cruzi* and transit in the TcPV is a key step during the *T. cruzi* intracellular cycle. Like other successful intracellular microorganisms, *T. cruzi* manipulates the host cell machinery to enter and persist within the host cell. Two main processes of invasion of trypomastigotes in non-professional phagocytes have been described up to date. In the well-described lysosomal-dependent model, *T. cruzi* exploits the plasma membrane damage repair response to invade the host cells. Trypomastigotes induce small injuries in the host cell membrane leading to a cytosolic calcium increase that in turn, elicits the exocytosis of lysosomes and entry of parasites (Tardieux et al., 1992; Rodríguez et al., 1996; Andrade and Andrews, 2005). However, in the lysosomal-independent model, trypomastigotes enter to the host cells by invagination of the plasma membrane and formation of a vacuole initially enriched in plasma membrane markers that later interact with lysosomes (Woolsey et al., 2003). Further studies from the same authors showed that a fraction of the nascent vacuole acquired EEA-1, a Rab-5 effector involved in the fusion of vesicles to early endosomes (Christoforidis et al., 1999). They postulated that this resultant vacuole gradually maturates until fusion with lysosomes (Woolsey and Burleigh, 2004).

It is widely accepted that fusion of TcPV with lysosomes is a key step to retain the parasite inside the cell (Andrade and Andrews, 2004). In a previous work from our lab we demonstrated the involvement of the SNARE VAMP7 in this process (Cueto et al., 2017). Eventhough the molecular components that regulate the transit of the initial vacuole until the fusion with lysosomes were not completely known up to date. Indeed, despite evidences that showed the presence of Rab5 and Rab7 in the TcPV (Wilkowsky et al., 2002; Maganto-Garcia et al., 2008; Barrias et al., 2010), the functional role of them in the *T. cruzi* infection still remains not understood. In this work we explored the possible participation of the main vesicular pathways that would contribute to the control of the early events during *T. cruzi* infection, mainly focusing in the mechanisms that promote vacuole maturation and lysosomal fusion.

METHODS

Reagents

Minimal essential medium (α-MEM) and Dulbecco–modified minimal essential medium (D–MEM) were obtained from Gibco Laboratories (Buenos Aires, Argentina). Fetal bovine serum (FBS) was purchased from Natocor S.A. (Córdoba, Argentina). Rabbit anti–*T. cruzi* polyclonal antibody was kindly provided by Dr. Catalina Alba (Instituto de Investigaciones en Microbiología y Parasitología Médica, Buenos Aires, Argentina). The secondary Cy3 conjugated anti–rabbit antibody was purchased from Life Technologies (Buenos Aires, Argentina).

Plasmids

pEGFPC3 encoding GFP–VAMP3 and GFP–VAMP7 were previously characterized by Dr. Thierry Galli (The École des Neurosciences de Paris Île-de-France, Paris, France) (Martinez-Arca et al., 2000a,b) and are available at Addgene. pEGFP-Rab1 WT, pEGFP-Rab3a WT, pEGFP-Rab4 WT, pEGFP-Rab6 WT, pEGFP-Rab25 WT, pEGFP-Rab22a WT, and pEGFP-Rab22a S22N were kindly provided by Dr. Javier Magadán (Instituto de Histología y Embriología de Mendoza "Dr. Mario Burgos," Mendoza, Argentina) (Magadán et al., 2006). Plasmids encoding enhanced GFP (EGFP)-Rab7 and its mutants were kindly provided by Bo van Deurs (University of Copenhagen,

Copenhagen, Denmark) and the plasmid encoding enhanced GFP (EGFP)-Rab5wt was kindly provided by Dr. Philip D. Stahl (Washington University). The pEGFP-Rab29 was gently provided by Drs. Jorge Galán and Stefania Spano (Yale University School of Medicine, New Haven). The pEGFPRab11 plasmid was used as previously described (Savina et al., 2002). pcDNA.DEST47-GFP-Rab39a WT and pcDNA.DEST47-GFP-Rab39a S22N were a generous gift from Bruno Goud (Curie Institute, Paris, France). pEGFP-Rab21 WT and pEGFP-Rab21 T31N were gifted by Dr. Thierry Galli (The École des Neurosciences de Paris Île-de-France, Paris, France).

Cell Culture

Vero cells, a monkey epithelial cell line (obtained from ABAC, Asociación Banco Argentino de Células, Buenos Aires, Argentina) were grown in D–MEM supplemented with 10% FBS and antibiotics at 37°C in an atmosphere of 95% air and 5% CO_2. CHO cells (ABAC), were maintained in α-MEM supplemented with 10% FBS and antibiotics at 37°C in an atmosphere of 95% air and 5% CO_2.

Propagation of *T. cruzi* Trypomastigotes

Y strain of *T. cruzi* was provided by Dr. Wanderley De Souza (Instituto de Biofísica Carlos Chagas Filho, Universidade Federal do Rio de Janeiro, Brasil) and handled in a biosafety level II facility. Tissue cell trypomastigotes (TCT) was prepared as follows. Vero cells (5×10^5 cells/ml) were plated in T25 flasks and maintained at 37°C in D–MEM supplemented with 3% FBS and antibiotics (infection medium). Cells were infected with TCT suspensions (5×10^6 cells/ml) for 3 days in infection medium at 37 °C in an atmosphere of 95% air and 5% CO_2. After 4 to 6 days, intracellular TCT lysed the cells and reached the medium. Medium containing parasites was harvested and centrifuged at 600 g for 15 min at room temperature. The supernatant was discarded, and the pellet, containing TCT and amastigotes, was covered with 1 ml of fresh medium and incubated for 3 h at 37°C to allow TCT to swim up. Supernatant enriched in TCTs was harvested, and parasites were counted in a Neubauer chamber and used for infection experiments. All procedures involved live *T. cruzi* were made under a biosafety level II and approved by the institutional biosecurity committee.

Cell Transfections

The previous day, CHO cells were plated on 13 mm round coverslips distributed in 24 well-plates in α-MEM supplemented with 10% FBS and antibiotics. Then cells 90% of confluence (about 1,50,000 cells), were transfected with plasmids (1 μg/μl) using the Lipofectamine 2000 reagent (Thermo Fisher Scientific) according to the instructions of the manufacturer. Transfected cells were incubated for 24 h in an appropriate medium before being exposed to parasites. After that, cells were infected as follow.

Infection of Cells With Trypomastigotes

CHO cells attached to coverslips in 24 well-plates were washed three times with PBS. Then a TCT–enriched suspension was added at a multiplicity of infection of 20. To favor parasite–cell interaction, plates were subsequently centrifuged for 5 min at 4°C. Infection was carried out for 1 h at 37°C (or 15 min in a one-time point in kinetic experiments). Afterward, extracellular parasites were removed by washing several times, and cells were subjected to IF.

Immunofluorescence

Cells were fixed with 4% paraformaldehyde solution in PBS for 20 min at room temperature and subsequently quenched by incubating with 50 mM NH_4Cl in PBS. Then, cells were permeabilized with 0.1% saponin in PBS containing 0.2% BSA and incubated with primary antibodies for 2 h. Intracellular parasites were detected with a rabbit anti–*T. cruzi* polyclonal antibody (1:200). Next, cells were incubated for 2 h with Cy3 anti–rabbit (1:500). Additionally, cells were treated with Hoechst for DNA staining, mounted onto glass slides with Mowiol and analyzed with an Olympus Confocal Microscope FV1000–EVA (Olympus), with the FV10–ASW (version 01.07.00.16) software. In some experiments we control the immunofluorescence by performing a double detection prior and after permeabilization using the same primary antibody and two secondary antibodies labeled with different fluorescent markers. After the analysis of images, we confirmed that only the intracellular parasites were stained after permeabilization whereas extracellular parasites exhibit double-labeling.

Analysis of Protein Recruitment to TcPV

The recruitment of Rabs to TcPV was confirmed by studying the fluoresce profile in the site where the *T. cruzi* vacuole is located. In the confocal image depicting the infected cell, a straight line was drawn through the vacuole and fluorescence intensity across this line were visualized in a graphic. If the protein was recruited, it can be seen how the fluorescence intensity of the green channel (Rab protein) on the surface of TcPV is several times greater than the fluorescence intensity of cytoplasm (background). Recruitment was considered positive when the fluorescence intensity of the area of interest was at least three times greater than the surrounding fluorescence. The TcPV can be localized by the increase in the intensity of red fluorescence that correspond to parasite detection and also by the blue fluorescence that labeled the parasite nucleus. When the protein under study was not recruited to the vacuole membrane, the green peaks around the parasite were not observed in the graphic. After analysis of recruitment, the percentage of vacuoles with positive recruitment were calculated for each Rab protein and compared with the vector.

RESULTS

Rab Proteins From Early and Late Endocytic Pathway Are Recruited to the TcPV

In a previous work we studied the recruitment of the SNARE proteins VAMP3 and VAMP7 to the parasitophorous vacuole of *T. cruzi* CL Brener strain at different times after infection. In that work we established that formation of the

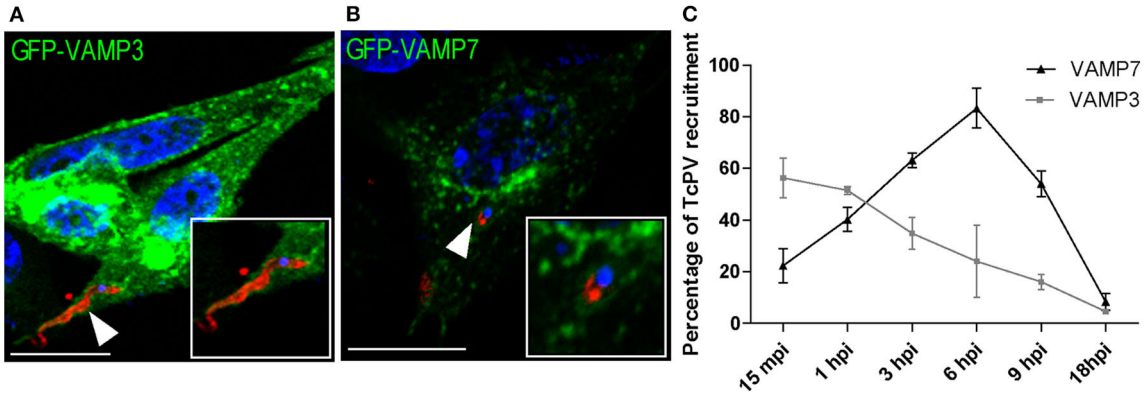

FIGURE 1 | Kinetics of the recruitment of VAMP3 and VAMP7 on the *T. cruzi* parasitophorous vacuole. **(A,B)** CHO cells overexpressing GFP-VAMP3 or GFP-VAMP7 were infected with TCT (MOI 20) for 15 min or 6 h, respectively. The parasites were detected by indirect immunofluorescence using a specific antibody anti-*T. cruzi* followed by a secondary antibody labeled with Cy3 (red). The DNA of nuclei and kinetoplasts were detected with Hoechst (blue). Confocal images are representative for each condition and the magnifications are delimited in the original photo. Scale bar: 10 μm. **(C)** The percentage of the recruitment of VAMPs to TcPV were quantified from the images obtained by confocal microscopy at the indicated times after infection from 15 min to 18 h. Data are representative of three independent experiments.

TABLE 1 | Analysis of the recruitment of Rab proteins to TcPV.

TcPV recruitment	1 hpi
Rab1	–
Rab3a	–
Rab4	–
Rab5	+ (***)
Rab6	–
Rab7	+ (***)
Rab11	–
Rab21	+ (***)
Rab22a	+ (***)
Rab25	–
Rab29	–
Rab39a	+ (**)

*CHO cells overexpressing GFP-Rabs were infected by 1 h (1hpi), fixed and subjected to indirect immunofluorescence to detect parasites before confocal microscopy analysis. The number of parasites that showed recruitment of GFP-proteins to the parasitophorous vacuole was detected. The + and – signs represents the Rab proteins that were significantly or not significantly recruited to TcPV compared to GFP-Vector respectively. Data are representative of three independent experiments. (***P < 0.001, **P < 0.01, two-way ANOVA and Bonferroni's multiple comparison test).*

vacuole is extended up to 1 h after infection followed by vacuole maturation which was characterized by the arrival and fusion of VAMP7 and Lamp1-positive vesicles and vacuole acidification from 1 h to around 6 h after infection (Cueto et al., 2017). In this work we used the *T. cruzi* Y strain, we studied the recruitment of these SNAREs and confirmed their presence in the vacuole membrane (**Figures 1A,B**). We also observed a similar kinetics of association displayed by these proteins although the transit in the vacuole was slower than the previously observed for CL Brener strain showing the peak of VAMP7 recruitment at 6 h after infection (**Figure 1C**). To characterize the possible participation of endocytic, secretory and recycling pathways in the *T. cruzi* entry, we studied the presence of different Rabs, representative of these routes, at 1 h after infection (1 hpi) which is, according to our data, the time between formation and maturation of the vacuole. To asses this, different Rab proteins fused with GFP were overexpressed in CHO cells before infection with TCT. At 1 hpi, cells were fixed and parasites were detected by indirect immunofluorescence followed by confocal microscopy analysis. We studied the recruitment of Rab5, Rab22a, and Rab21 representative of early endocytic transport and Rab7 and Rab39a from the late endosomes and lysosomes. Recycling pathways were analyzed by the presence of Rab4, Rab11, and Rab25 and exocytic/secretory route by Rab1, Rab3, Rab6, and Rab29 (Wandinger-Ness and Zerial, 2014). From the 12 Rabs analyzed, only five, Rab22a, Rab5, Rab21, Rab7, and Rab39a were significantly recruited to the vacuole membrane at this time (**Table 1**). These data showed that early and late endocytic compartments interact with the TcPV during its transit. In contrast, neither recycling nor secretory vesicles reach the vacuole at this time (**Table 1**; **Supplementary Figure 1A**).

The TcPV Transit Is Characterized by the Sequential Acquisition of Endosomal Rabs

To extend our characterization we next studied the kinetic of recruitment of the Rabs found in the TcPV. We performed infection experiments on cells expressing GFP-Rabs at different times from 15 min to 12 h and quantified the percentage of TcPVs surrounded by these proteins. We also used cells transfected with the GFP protein alone (GFP-Vector) as a control. Our data confirmed the presence of all Rabs found previously in the vacuole with some interesting qualitative and quantitative differences between them. Association of GFP-Rab5 to the vacuole membrane was discontinuous whereas the other Rabs

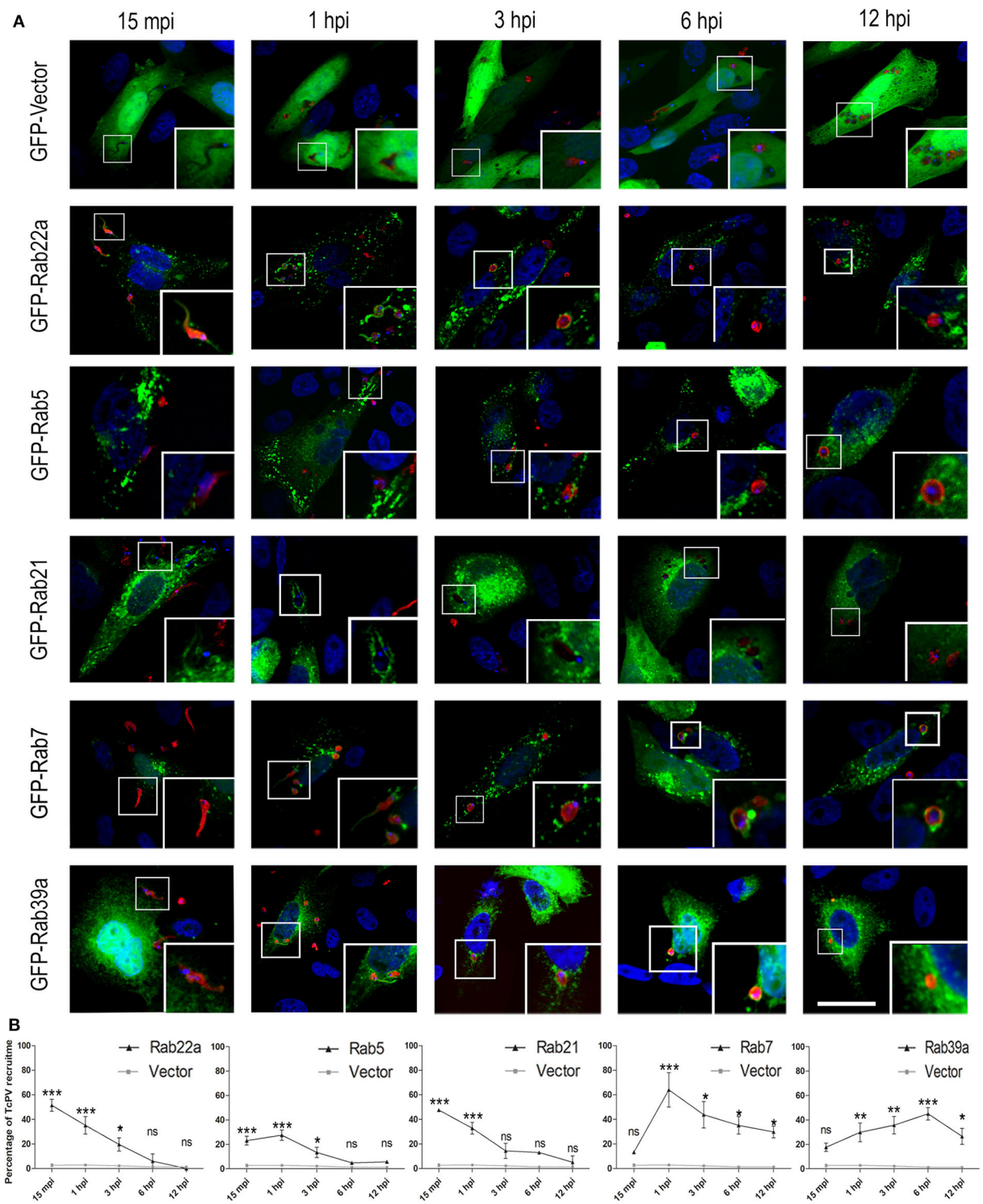

FIGURE 2 | Recruitment kinetics of Rab proteins to *T. cruzi* parasitophorous vacuole. **(A)** Recruitment of Rab to TcPV were examined at the indicated time–points. CHO cells overexpressing GFP-Rabs were infected for 15 min (15 mpi), 1, 3, 6, or 12 h (hpi) with TCT (MOI 20). The parasites were detected by indirect immunofluorescence using a specific antibody anti-*T. cruzi* followed by a secondary antibody labeled with Cy3 (red). The DNA of nuclei and kinetoplasts were detected with Hoechst (blue). Images are representative for each condition and the magnifications are delimited in the original photo. Scale bar: 10 μm. **(B)** Kinetic graphs represent the recruitment of GFP-Rabs to TcPV. Data are representative of two independent experiments. (***$P < 0.001$, **$P < 0.01$, *$P < 0.05$, two-way ANOVA and Bonferroni's multiple comparison test).

displayed a uniform pattern around the parasite at the times of significant recruitment (**Figure 2A**). For early endocytic Rabs, the recruitment to TcPV was statistically significant at the early times mainly 15 min and 1 h and reached values around 50% of vacuoles for GFP-Rab22 and GFP-Rab21 in comparison with cells that overexpressed the vector (GFP alone) that never overcame ≈5% of vacuoles at any time studied. In contrast, Rab7 and Rab39a were significantly acquired at later times from 1 h up to even 12 h displaying a peak at 1 and 6 h, respectively (**Figure 2B**). Since the acquisition of VAMP7 indicates the arrival of lysosomes to the TcPV (Cueto et al., 2017), and considering that our data showed the presence of Rab7 prior to VAMP7 (compare **Figure 1B** with **Figure 2B**), this could indicate a key role of Rab7 in the docking and fusion of lysosomes, as was demonstrated previously (Bucci et al., 2000). We also analyzed the kinetic of recruitment of GFP-Rab11 and GFP-Rab6, representative of recycling and secretory routes, respectively, and obtained very low percentage of recruitments, similar to controls at all times (**Supplementary Figures 1B,C**). Therefore, these pathways displayed low (or null) interaction with the *T. cruzi*-containing vacuoles in the early stages of the infection.

Endocytic Rabs Are Required for *T. cruzi* Infection

To disclose the possible effect of endocytic Rabs on the process of *T. cruzi* infection, we transfected cells with the dominant-negative forms of these Rabs to prevent the normal function of the proteins and compare the level of infection obtained at 1 h after infection, with cells transfected with the GFP plasmid alone (GFP-Vector) and also with cells that overexpress the wild-type forms of these Rabs (GFP-Rab WT). Before infection assays, we tested the viability of dominant-negative transfected cells by the trypan blue dye exclusion staining and confirmed that these cells displayed the same viability than the controls (data not shown). Remarkably, in the infection experiments, we observed that in contrast to Rabs WT, the dominant-negative mutants of these proteins were not recruited to the TcPV membrane, therefore confirming their lack of activity (**Figure 3A**, arrowheads). Furthermore, with the exception of Rab21 mutant, the reduction of Rab function decreased the percentage of infected cells being this value significantly minor for Rab22a S19N, Rab5 S34N, and Rab39a S22N while the WT forms exhibit similar levels of infection in comparison with the GFP-Vector transfected cells (**Figure 3B**). We also quantified the percentage of mutant cells that contained 1, 2, or 3 (or more) parasites/cell and observed that the percentage of cells with 3 or more parasites was reduced to half (or even less) with the concomitantly increase in the percentage of cells with 1 or 2 parasites (**Figure 3C**). Unexpectedly, Rab21 T31N displayed an opposite result which could be explained by the different features of this mutant previously reported (Simpson et al., 2004; Egami and Araki, 2009). In summary these data confirmed that *T. cruzi* infection is partially regulated by the recruitment of endocytic Rabs to the TcPV which follows a maturation process until the arrival of lysosomes.

DISCUSSION

In previous works Woolsey and coworkers proposed that *T. cruzi* invasion initiated by a common step involving signaling, actin disassembly and plasma membrane invagination. This process culminated with the formation of a plasma membrane-derived vacuole that can directly fuse with lysosomes or pass through an early endosomal intermediate before lysosomal fusion (Woolsey et al., 2003; Woolsey and Burleigh, 2004). In agreement to these observations, our data confirmed the existence of this endosomal intermediate that follow a maturation process characterized by the sequential acquisition of endocytic Rabs. Rab22a, Rab5, and Rab21 were mainly recruited to vacuole at early stages (15 min-1 h) followed by Rab39a and Rab7 at later times. According to this model, the initial step of *T. cruzi* invasion takes very few minutes and involves the events that culminate with the formation of the nascent vacuole containing plasma-membrane components such as PI(4,5)P2. Interestingly, the work of Fernandes et al. demonstrated that *T. cruzi* induces the arrival of lysosomes containing sphingomyelinase that repairs the plasma membrane and generates a ceramide-enriched endosome that contains the recently internalized parasites (Fernandes et al., 2011).

In the second step, the initial vacuole will mature by the direct fusion with lysosomes or with endosomes which in turn will reach to lysosomes too. Why *T. cruzi* employs two different routes that finally converge in lysosomes is an open question to date. Due to in the steady state, many cells usually contain a relatively low number of lysosomes (Xu and Ren, 2015), and considering that lack of lysosomal fusion to vacuole leads to the previously described reversal infection (Andrade and Andrews, 2004), it is likely that the alternative endosomal route was an adaptation of parasites which could modify the membrane of their vacuole with endosomal proteins to prevent a new fusion with the plasma membrane and the exit of trypomastigotes from the cell. In agreement to this, our previous work demonstrated a significant increase on the infection produced by the expansion of the lysosomal compartment induced in pre-starved cells (Romano et al., 2009). The interaction with endosomes previous to lysosomes could also benefit some *T. cruzi* strains by conferring an additional time to be ready for the lytic lysosomal environment. Interestingly, a previous work showed that interaction of *T. cruzi* with cardiomyocytes leads to a reduction of Rab7 expression and impairment of the fusion between endocytic compartments (Batista et al., 2006). This response could be induced by soluble factors secreted from the parasite in an attempt to delay the fusion with lysosomes, a strategy displayed by several intracellular pathogens (Kumar and Valdivia, 2009).

Chronological acquisition of Rabs in the TcPV observed in our kinetic studies, could be related to the existence of a Rab cascade, described in other types of transports (Rink et al., 2005; Rivera-Molina and Novick, 2009). According to our kinetics experiments, it is possible that Rab22a, which is highly recruited at 15 min, allow the recruitment of Rab5 and/or Rab21 that in turn, by the action of specific effectors, recruits Rab7 that will promote the fusion with lysosomes. Fusion with early endosomes confer to TcPV some differential properties compared to the

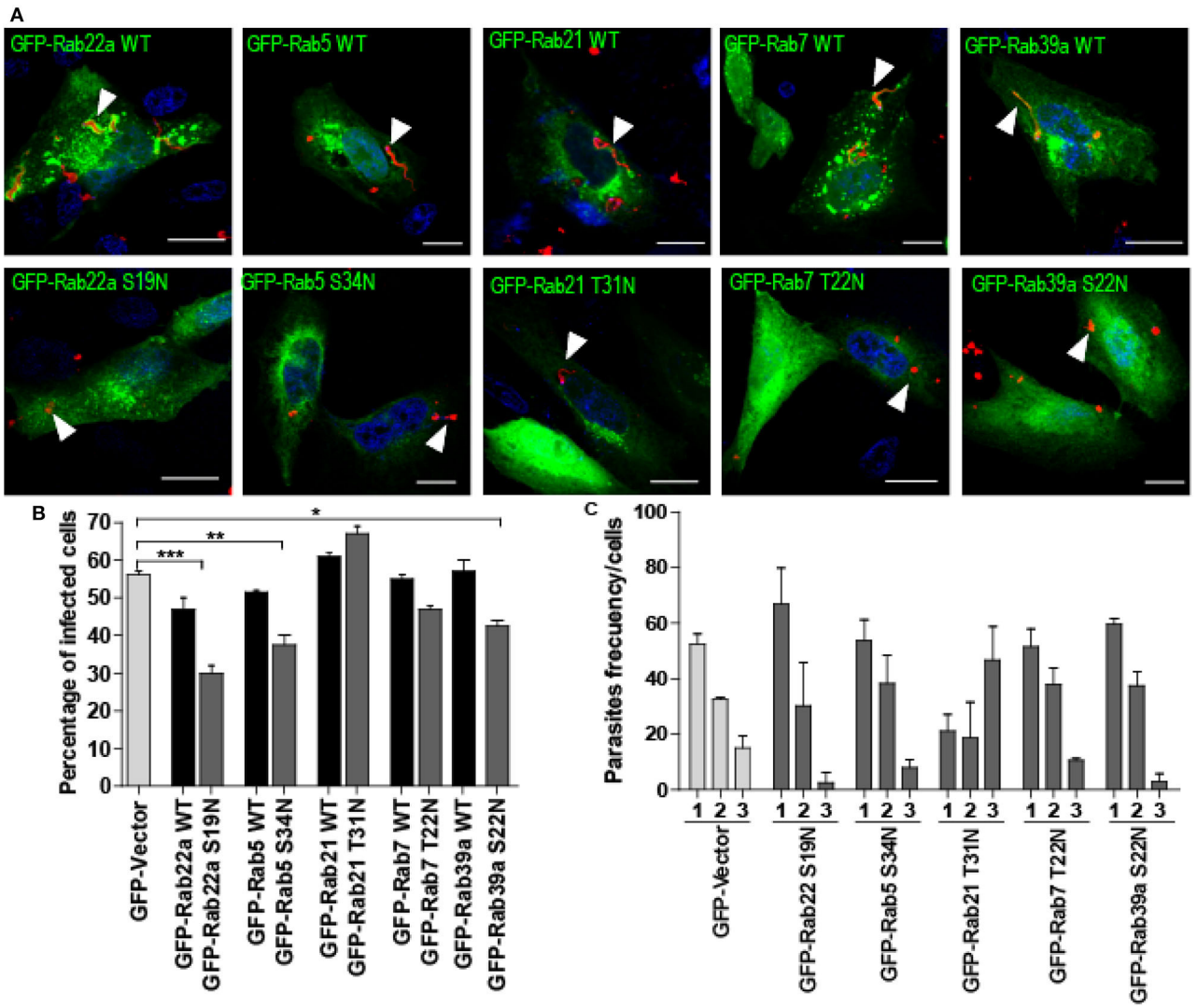

FIGURE 3 | Effect of dominant-negative Rab-proteins on *T. cruzi* infection. **(A)** CHO cells overexpressing GFP-Rabs wild type (WT) or dominant-negative mutants were infected with TCT (MOI 20) for 1 h. After fixation, the parasites were detected by indirect immunofluorescence using a specific antibody anti-*T. cruzi* followed by a secondary antibody labeled with Cy3 (red). The DNA of nuclei and kinetoplasts were detected with Hoechst. Arrowheads indicate the localization of parasites. Scale bar: 10 μm. **(B)** Bar graph represents the percentage of infected cells at 1-h post-infection. For this experiment at least 120 cells were quantified. Data are representative of two independent experiments. (***$P < 0.001$, **$P < 0.01$, *$P < 0.05$, one-way ANOVA and Bonferroni's multiple comparison test). **(C)** Bar Graph represents the percentage of cells that contained 1, 2, or 3 or more parasites/cell at 1-h post-infection. For this experiment at least 120 cells were quantified. Data are representative of two independent experiments. (**$P < 0.01$, one-way ANOVA and Bonferroni's multiple comparison test).

extracellular site where the parasites come from. Acidification of TcPV is crucial to the action of the Tc-Tox, the *T. cruzi* toxin that will allow the exit to the vacuole (Ley et al., 1990). Fusion of the TcPV with early endosomes could explain the mechanism of this acidification through the arrival of subunits of the V-ATPase, which pumps protons from cytosol to the lumen of endocytic compartments. Further interaction with late endosomes through Rab7 and Rab39a would favor the final assembly of the pump (Lafourcade et al., 2008) and the fusion with lysosomes. Vacuole maturation is also characterized by the change in the *T. cruzi* form from the slender trypomastigote to the round-shaped intermediate form indicative that parasite differentiation from trypomastigotes to amastigotes, a process also induced by a reduced pH (Frevert et al., 1995; Romano et al., 2009), is starting inside the vacuole and requires the arrival of late endosomes and lysosomes.

Interestingly, Rabs from the secretory and recycling pathways are absent in the TcPV indicating that these routes do not interact with the *T. cruzi* vacuole at least in the times studied by us. Other authors also showed the absence of Golgi-proteins on nascent parasitophorous vacuoles (Fernandes et al., 2015). In contrast to other pathogens like *C. trachomatis* or

L. pneumophila that interact with Golgi-derived vesicles to get nutrients for replication (Rejman Lipinski et al., 2009; Schoebel et al., 2009), our data showed that *T. cruzi* do not require components derived from these routes, probably because in the vacuolar stage, *T. cruzi* undergoes the initial steps of differentiation to amastigotes and do not require high quantity of nutrients. In fact, metacyclogenesis, the differentiation of epimastigotes to metacyclic trypomastigotes, performed in the insect stage of the *T. cruzi* cycle, is carried out under nutrient deprivation which activates parasite autophagy, a process required for this differentiation (Vanrell et al., 2017).

The participation of endocytic Rabs on the *T. cruzi* infection was confirmed by the reduction of the infection observed in cells that express the dominant-negative mutants of these Rabs. Although these proteins usually displayed overlapped functions (Zhen and Stenmark, 2015), the impairment of the activity of one of them separately was sufficient to affect the infection. This effect is likely produced by the reduction of functional Rabs available to allow the fusion of endosomes to the nascent vacuoles, which eventually could fuse with the plasma membrane and release the parasites out of cells, in a similar way to the minor infection observed when the lysosomal fusion is impaired (Andrade and Andrews, 2004). Other authors also showed that inhibition of endocytosis processes, when cells are treated with the dynamin inhibitor, dynasore (Barrias et al., 2010) or in the case of LAMP-2 lacking cells where caveolin-dependent endocytosis is impaired (Couto et al., 2017), leads to a reduction on the infection.

In conclusion, this work demonstrated that endocytic Rabs are sequentially acquired by the TcPV and regulate the transit of the vacuole up to the fusion with lysosomes. The impairment of these Rabs affected the fraction of vacuoles that interacts with endosomes and decreased the infection. These data added new molecular regulators on the complex process of *T. cruzi* invasion and contributed to understand the big versatility displayed by *T. cruzi* to parasitize the different types of host cells.

DATA AVAILABILITY STATEMENT

All datasets generated for this study are included in the article/**Supplementary Material**.

AUTHOR CONTRIBUTIONS

BS, JC, and JG contributed conception and design of experiments, made figures, and performed the statistical analysis. BS and PR contributed conception and design of the study. PR wrote the first draft of the manuscript. BS wrote sections of the manuscript. All authors contributed to manuscript revision, read and approved the submitted version.

FUNDING

This work has been supported by grants from Consejo Nacional de Investigaciones Científicas y Tecnológicas (CONICET-PIP 2014-2016), Secretaría de Investigación, Internacionales y Posgrado (SIIP, Universidad Nacional de Cuyo, Proyectos Bienales 2019–2021) and Agencia Nacional de Promoción Científica y Tecnológica (PICT# 2017-1456) to PR.

SUPPLEMENTARY MATERIAL

The Supplementary Material for this article can be found online at: https://www.frontiersin.org/articles/10.3389/fcimb.2020.536985/full#supplementary-material

Supplementary Figure 1 | Recycling and secretory Rabs are not recruited to TcPV. **(A)** CHO cells overexpressing GFP-Rabs (green) were infected 1 h (1hpi) with TCT (MOI 20). After fixation, parasites were detected by indirect immunofluorescence using a specific antibody anti-*T. cruzi* followed by a secondary antibody labeled with Cy3 (red). The DNA of nuclei and kinetoplasts were detected with Hoechst (blue). **(B)** CHO cells overexpressing GFP-Rab6 and GFP-Rab11 were infected for 15 min (15 mpi), 1 or 6 h (hpi) with TCT (MOI 20) and processed as indicated above. The Images are representative for each condition and the magnifications are delimited in the original photo. Scale bar: 10 μm. **(C)** Kinetic graphs represent the recruitment of GFP-Rab6 and GFP-Rab11 to TcPV.

REFERENCES

Andrade, L. O., and Andrews, N. W. (2004). Lysosomal fusion is essential for the retention of *Trypanosoma cruzi* inside host cells. *J. Exp. Med*. 200, 1135–1143. doi: 10.1084/jem.20041408

Andrade, L. O., and Andrews, N. W. (2005). The *Trypanosoma cruzi*–host-cell interplay: location, invasion, retention. *Nat. Rev. Microbiol*. 3, 819–823. doi: 10.1038/nrmicro1249

Barrias, E. S., Reignault, L. C., De Souza, W., and Carvalho, T. M. U. (2010). Dynasore, a dynamin inhibitor, inhibits *Trypanosoma cruzi* entry into peritoneal macrophages. *PLoS ONE* 5:e7764. doi: 10.1371/journal.pone.0007764

Batista, D. G. J., Silva, C. F., Mota, R. A., Costa, L. C., Meirelles, M. N. L., Meuser-Batista, M., et al. (2006). *Trypanosoma cruzi* modulates the expression of rabs and alters the endocytosis in mouse cardiomyocytes *in vitro*. *J. Histochem. Cytochem*. 54, 605–614. doi: 10.1369/jhc.5A6654.2005

Bucci, C., Thomsen, P., Nicoziani, P., McCarthy, J., and Van Deurs, B. (2000). Rab7: a key to lysosome biogenesis. *Mol. Biol. Cell* 11, 467–480. doi: 10.1091/mbc.11.2.467

Chavrier, P., Parton, R. G., Hauri, H. P., Simons, K., and Zerial, M. (1990). Localization of low molecular weight GTP binding proteins to exocytic and endocytic compartments. *Cell* 62, 317–329. doi: 10.1016/0092-8674(90)90369-P

Chen, T., Han, Y., Yang, M., Zhang, W., Li, N., Wan, T., et al. (2003). Rab39, a novel Golgi-associated Rab GTPase from human dendritic cells involved in cellular endocytosis. *Biochem. Biophys. Res. Commun*. 303, 1114–1120. doi: 10.1016/S0006-291X(03)00482-0

Christoforidis, S., McBride, H. M., Burgoyne, R. D., and Zerial, M. (1999). The rab5 effector EEA1 is a core component of endosome docking. *Nature* 397, 621–625. doi: 10.1038/17618

Couto, N. F., Pedersane, D., Rezende, L., Dias, P. P., Corbani, T. L., Bentini, L. C., et al. (2017). LAMP-2 absence interferes with plasma membrane repair and decreases *T. cruzi* host cell invasion. *PLoS Negl. Trop. Dis*. 11:e0005657. doi: 10.1371/journal.pntd.0005657

Cueto, J. A., Vanrell, M. C., Salassa, B. N., Nola, S., Galli, T., Colombo, M. I., et al. (2017). Soluble N-ethylmaleimide-sensitive factor attachment protein receptors required during *Trypanosoma cruzi* parasitophorous vacuole development. *Cell. Microbiol*. 19, 2–6. doi: 10.1111/cmi.12713

Egami, Y., and Araki, N. (2009). Dynamic changes in the spatiotemporal localization of Rab21 in live RAW264 cells during macropinocytosis. *PLoS ONE* 4:e6689. doi: 10.1371/journal.pone.0006689

Fernandes, M. C., Corrotte, M., Miguel, D. C., Tam, C., and Andrews, N. W. (2015). The exocyst is required for trypanosome invasion and the repair of mechanical plasma membrane wounds. *J. Cell Sci.* 128, 27–32. doi: 10.1242/jcs.150573

Fernandes, M. C., Cortez, M., Flannery, A. R., Tam, C., Mortara, R. A., and Andrews, N. W. (2011). *Trypanosoma cruzi* subverts the sphingomyelinase-mediated plasma membrane repair pathway for cell invasion. *J. Exp. Med.* 208, 909–921. doi: 10.1084/jem.20102518

Frevert, U., Vandekerckhove, F., and Nussenzweig, V. (1995). The induction of *Trypanosoma cruzi* trypomastigote to amastigote transformation by low pH. *Parasitology* 110, 547–554. doi: 10.1017/S0031182000065264

Gambarte Tudela, J., Buonfigli, J., Luján, A., Alonso Bivou, M., Cebrián, I., Capmany, A., et al. (2019). Rab39a and Rab39b display different intracellular distribution and function in sphingolipids and phospholipids transport. *Int. J. Mol. Sci.* 20:1688. doi: 10.3390/ijms20071688

Gorvel, J. P., Chavrier, P., Zerial, M., and Gruenberg, J. (1991). rab5 controls early endosome fusion *in vitro*. *Cell* 64, 915–925. doi: 10.1016/0092-8674(91)90316-Q

Grant, B. D., and Donaldson, J. G. (2009). Pathways and mechanisms of endocytic recycling. *Nat. Rev. Mol. Cell Biol.* 10, 597–608. doi: 10.1038/nrm2755

Kumar, Y., and Valdivia, R. H. (2009). Leading a sheltered life: intracellular pathogens and maintenance of vacuolar compartments. *Cell Host Microbe* 5, 593–601. doi: 10.1016/j.chom.2009.05.014

Lafourcade, C., Sobo, K., Kieffer-Jaquinod, S., Garin, J., and van der Goot, F. G. (2008). Regulation of the V-ATPase along the endocytic pathway occurs through reversible subunit association and membrane localization. *PLoS ONE* 3:e2758. doi: 10.1371/journal.pone.0002758

Ley, V., Robbins, E. S., Nussenzweig, V., and Andrews, N. W. (1990). The exit of *Trypanosoma cruzi* from the phagosome is inhibited by raising the pH of acidic compartments. *J. Exp. Med.* 171, 401–413. doi: 10.1084/jem.171.2.401

Li, G. (2012). "Early endocytosis: Rab5, rab21, and rab22," in *Rab GTPases and Membrane Trafficking*, eds G. Li, and N. Segev (Sharjah: Bentham Science Publishers Ltd), 93–107.

Magadán, J. G., Barbieri, M. A., Mesa, R., Stahl, P. D., and Mayorga, L. S. (2006). Rab22a regulates the sorting of transferrin to recycling endosomes. *Mol. Cell Biol.* 26, 2595–2614. doi: 10.1128/MCB.26.7.2595-2614.2006

Maganto-Garcia, E., Punzon, C., Terhorst, C., and Fresno, M. (2008). Rab5 activation by toll-like receptor 2 is required for *trypanosoma cruzi* internalization and replication in macrophages. *Traffic* 9, 1299–1315. doi: 10.1111/j.1600-0854.2008.00760.x

Martinez-Arca, S., Alberts, P., and Galli, T. (2000a). Clostridial neurotoxin-insensitive vesicular SNAREs in exocytosis and endocytosis. *Biol. Cell* 92, 449–453. doi: 10.1016/S0248-4900(00)01096-0

Martinez-Arca, S., Alberts, P., Zahraoui, A., Louvard, D., and Galli, T. (2000b). Role of tetanus neurotoxin insensitive vesicle-associated membrane protein (TI-VAMP) in vesicular transport mediating neurite outgrowth. *J. Cell Biol.* 149, 889–899. doi: 10.1083/jcb.149.4.889

Rejman Lipinski, A., Heymann, J., Meissner, C., Karlas, A., Brinkmann, V., Meyer, T. F., et al. (2009). Rab6 and Rab11 regulate *Chlamydia trachomatis* development and golgin-84-dependent Golgi fragmentation. *PLoS Pathog.* 5:e1000615. doi: 10.1371/journal.ppat.1000615

Rieder, S. E., and Emr, S. D. (1997). A novel RING finger protein complex essential for a late step in protein transport to the yeast vacuole. *Mol. Biol. Cell* 8, 2307–2327. doi: 10.1091/mbc.8.11.2307

Rink, J., Ghigo, E., Kalaidzidis, Y., and Zerial, M. (2005). Rab conversion as a mechanism of progression from early to late endosomes. *Cell* 122, 735–749. doi: 10.1016/j.cell.2005.06.043

Rivera-Molina, F. E., and Novick, P. J. (2009). A Rab GAP cascade defines the boundary between two Rab GTPases on the secretory pathway. *Proc. Natl. Acad. Sci. U.S. A.* 106, 14408–14413. doi: 10.1073/pnas.0906536106

Rodríguez, A., Samoff, E., Rioult, M. G., Chung, A., and Andrews, N. W. (1996). Host cell invasion by trypanosomes requires lysosomes and microtubule/kinesin-mediated transport. *J. Cell Biol.* 134, 349–362. doi: 10.1083/jcb.134.2.349

Romano, P. S., Arboit, M. A., Vázquez, C. L., and Colombo, M. I. (2009). The autophagic pathway is a key component in the lysosomal dependent entry of *Trypanosoma cruzi* into the host cell. *Autophagy* 5, 6–18. doi: 10.4161/auto.5.1.7160

Savina, A., Vidal, M., and Colombo, M. I. (2002). The exosome pathway in K562 cells is regulated by Rab11. *J. Cell Sci.* 115 (Pt. 12), 2505–2515.

Schlüter, O. M., Schmitz, F., Jahn, R., Rosenmund, C., and Südhof, T. C. (2004). A complete genetic analysis of neuronal Rab3 function. *J. Neurosci.* 24, 6629–6637. doi: 10.1523/JNEUROSCI.1610-04.2004

Schoebel, S., Oesterlin, L. K., Blankenfeldt, W., Goody, R. S., and Itzen, A. (2009). RabGDI displacement by DrrA from legionella is a consequence of its guanine nucleotide exchange activity. *Mol. Cell* 36, 1060–1072. doi: 10.1016/j.molcel.2009.11.014

Seals, D. F., Eitzen, G., Margolis, N., Wickner, W. T., and Price, A. (2000). A Ypt/Rab effector complex containing the Sec1 homolog Vps33p is required for homotypic vacuole fusion. *Proc. Natl. Acad. Sci. U.S.A.* 97, 9402–9407. doi: 10.1073/pnas.97.17.9402

Simpson, J. C., Griffiths, G., Wessling-Resnick, M., Fransen, J. A. M., Bennett, H., and Jones, A. T. (2004). A role for the small GTPase Rab21 in the early endocytic pathway. *J. Cell Sci.* 117, 6297–6311. doi: 10.1242/jcs.01560

Tardieux, I., Webster, P., Ravesloot, J., Boron, W., Lunn, J. A., Heuser, J. E., et al. (1992). Lysosome recruitment and fusion are early events required for trypanosome invasion of mammalian cells. *Cell* 71, 1117–1130. doi: 10.1016/S0092-8674(05)80061-3

Tisdale, E. J., Bourne, J. R., Khosravi-Far, R., Der, C. J., and Balch, W. E. (1992). GTP-binding mutants of Rab1 and Rab2 are potent inhibitors of vesicular transport from the endoplasmic reticulum to the golgi complex. *J. Cell Biol.* 119, 749–761. doi: 10.1083/jcb.119.4.749

Vanrell, M. C., Losinno, A. D., Cueto, J. A., Balcazar, D., Fraccaroli, L. V., Carrillo, C., et al. (2017). The regulation of autophagy differentially affects *Trypanosoma cruzi* metacyclogenesis. *PLoS Negl. Trop. Dis.* 11:e0006049. doi: 10.1371/journal.pntd.0006049

Wandinger-Ness, A., and Zerial, M. (2014). Rab proteins and the compartmentalization of the endosomal system. *Cold Spring Harb. Perspect. Biol.* 6:a022616. doi: 10.1101/cshperspect.a022616

Wilkowsky, S. E., Barbieri, M. A., Stahl, P. D., and Isola, E. L. D. (2002). Regulation of *Trypanosoma cruzi* invasion of nonphagocytic cells by the endocytically active GTPases dynamin, Rab5, and Rab7. *Biochem. Biophys. Res. Commun.* 291, 516–521. doi: 10.1006/bbrc.2002.6474

Woolsey, A. M., and Burleigh, B. A. (2004). Host cell actin polymerization is required for cellular retention of *Trypanosoma cruzi* and early association with endosomal/lysosomal compartments. *Cell Microbiol.* 6, 829–838. doi: 10.1111/j.1462-5822.2004.00405.x

Woolsey, A. M., Sunwoo, L., Petersen, C. A., Brachmann, S. M., Cantley, L. C., and Burleigh, B. A. (2003). Novel PI 3-kinase-dependent mechanisms of trypanosome invasion and vacuole maturation. *J. Cell Sci.* 116, 3611–3622. doi: 10.1242/jcs.00666

Xu, H., and Ren, D. (2015). Lysosomal physiology. *Annu. Rev. Physiol.* 77, 57–80. doi: 10.1146/annurev-physiol-021014-071649

Zerial, M., and Stenmark, H. (1993). Rab GTPases in vesicular transport. *Curr. Opin. Cell Biol.* 5, 613–620. doi: 10.1016/0955-0674(93)90130-I

Zhen, Y., and Stenmark, H. (2015). Cellular functions of Rab GTPases at a glance. *J. Cell Sci.* 128, 3171–3176. doi: 10.1242/jcs.166074

Zhu, H., Liang, Z., and Li, G. (2009). Rabex-5 is a rab22 effector and mediates a rab22-rab5 signaling cascade in endocytosis. *Mol. Biol. Cell* 20, 4720–4729. doi: 10.1091/mbc.e09-06-0453

Conflict of Interest: The authors declare that the research was conducted in the absence of any commercial or financial relationships that could be construed as a potential conflict of interest.

frontiers in Cellular and Infection Microbiology

ORIGINAL RESEARCH
published: 05 January 2021
doi: 10.3389/fcimb.2020.526997

TLR4 Deficiency Exacerbates Biliary Injuries and Peribiliary Fibrosis Caused by *Clonorchis sinensis* in a Resistant Mouse Strain

Chao Yan[1,2†], Jing Wu[1,3†], Na Xu[1], Jing Li[1], Qian-Yang Zhou[1], Hui-Min Yang[1], Xiao-Dan Cheng[1], Ji-Xin Liu[1], Xin Dong[1], Stephane Koda[1], Bei-Bei Zhang[1,2], Qian Yu[1,2], Jia-Xu Chen[4], Ren-Xian Tang[1,2] and Kui-Yang Zheng[1,2*]*

[1] Jiangsu Key Laboratory of Immunity and Metabolism, Laboratory of Infection and Immunity, Department of Pathogenic Biology and Immunology, Xuzhou Medical University, Xuzhou, China, [2] National Experimental Demonstration Center for Basic Medicine Education, Department of Clinical Medicine, Xuzhou Medical University, Xuzhou, China, [3] Huai'an Center for Disease Control and Prevention, Huai'an, China, [4] National Institute of Parasitic Diseases, Chinese Center for Disease Control and Prevention, Key Laboratory of Parasite and Vector Biology, Ministry of Health, WHO Collaborating Center of Malaria, Schistosomiasis and Filariasis, Shanghai, China

OPEN ACCESS

Edited by:
Patricia Sampaio Tavares Veras, Gonçalo Moniz Institute (IGM), Brazil

Reviewed by:
Sharon DeMorrow, University of Texas at Austin, United States
Lindsey Kennedy, Texas A&M University, United States

***Correspondence:**
Chao Yan
yanchao6957@xzhmu.edu.cn
Kui-Yang Zheng
zky@xzhmu.edu.cn

[†]These authors have contributed equally to this work

Specialty section:
This article was submitted to Parasite and Host, a section of the journal Frontiers in Cellular and Infection Microbiology

Received: 15 January 2020
Accepted: 13 November 2020
Published: 05 January 2021

Citation:
Yan C, Wu J, Xu N, Li J, Zhou Q-Y, Yang H-M, Cheng X-D, Liu J-X, Dong X, Koda S, Zhang B-B, Yu Q, Chen J-X, Tang R-X and Zheng K-Y (2021) TLR4 Deficiency Exacerbates Biliary Injuries and Peribiliary Fibrosis Caused by Clonorchis sinensis in a Resistant Mouse Strain. Front. Cell. Infect. Microbiol. 10:526997. doi: 10.3389/fcimb.2020.526997

Mice with different genetic backgrounds have various susceptibilities to infection with *Clonorchis sinensis*, although the mechanisms underlying are largely unknown. Toll-like receptor 4 (TLR4) as one of the most important pattern recognition receptors (PPRs) is essential for the invasion, survival, pathogenesis, and elimination of worms. The roles played by TLR4 in *C. sinensis* infection may vary due to the different genetic backgrounds of mice. In the present study, a relatively resistant mouse strain-C57BL/10 to *C. sinensis* was used for investigation on the possible roles of TLR4 in the biliary injuries and peribiliary fibrosis. TLR4 wild type ($TLR4^{wild}$) and TLR4 defective ($TLR4^{def}$) mice were orally infected with 45 metacercariae of *C. sinensis*, and all *C. sinensis*-infected mice and non-infected groups were anesthetized on day 28 post-infection. The liver and serum from each mouse were collected for assessment of the biliary injuries and biliary fibrosis. Meanwhile, hepatic leukocytes were isolated and detected for the activation of M1 or M2 macrophage using flow cytometry. The hepatic type 1 immune response and type 2 immune responses -relative molecules were also evaluated using ELISA and quantitative PCR. The data showed that $TLR4^{def}$ aggravated liver inflammatory cell infiltrations, bile duct proliferation, biliary and hepatocellular injuries, and ECM deposition in *C. sinensis*-infected mice, compared with $TLR4^{wild}$ mice when they were intragastrically administered with the same amounts of *C. sinensis* metacercaria. Furthermore, the M2-like macrophages and type 2 immune responses were significantly predominant induced in $TLR4^{def}$ mice, compared with that of $TLR4^{wild}$ mice following *C. sinensis* infection. But the type 1 immune response were significantly decreased in $TLR4^{def}$ mice, compared with $TLR4^{wild}$ mice after *C. sinensis* infection. These data demonstrate that TLR4 deficiency exacerbates biliary injuries and peribiliary fibrosis caused by *C. sinensis* in C57BL/10 strain mice, which is contributed by augments of type 2 immune responses and decrease pro-inflammatory responses.

Keywords: TLR4, *Clonorchis sinensis*, cholangiocytes, fibrosis, C57BL/10 mice

INTRODUCTION

Clonorchis sinensis is a zoonotic food-borne parasite which infects human or other mammals *via* ingestion of raw or undercooked fresh fish and shrimp containing metacercaria (Tang et al., 2016). The adult worm mainly dwells in the intrahepatic bile duct, common bile duct, or gall bladder, although it can be also accidentally found in the pancreatic duct (Kim, 1999). Infection with *C. sinensis* caused 5,591 deaths every year and 275,370 disability-adjusted Life Year (DALYs) (Sripa, 2012), of which ranges from cholangitis, obstructive jaundice, gallstones to hepatic fibrosis due to its mechanical stimulation and production and secretion antigen (Hong and Fang, 2012; Zheng et al., 2015). In addition, a long-term infection by *C. sinensis* can potently induce bile duct carcinoma and *C. sinensis* is considered as a type I Biological carcinogen (Tyson and El-Serag, 2011; Zheng et al., 2015).

Toll-like receptors (TLRs) are an important family of pattern recognition receptors (PRRs), which play a very important role in the innate immune response as well as adaptive immune responses (Akira et al., 2001). It is widely expressed in immune cells (such as macrophages, dendritic cells, NK cells, lymphocytes, granulocytes) and non-immune cells (such as epithelial cells, endothelial cells, fibroblasts, cancer cells, etc.), and is involved in almost all human disease processes (Ciferska et al., 2020). Among the 13 TLRs in human or 11 TLRs in mice, TLR4 has been the first to be identified and has a relatively broad ligand specificity. TLR4 can interact with LPS, peptidoglycan, glycoprotein, and so on, and ultimately produce pro-inflammatory cytokines and inflammatory chemokines through MyD88 or TRIF adaptor protein to regulate immunity, which play critical roles in fighting against pathogenic insults (Iwasaki and Medzhitov, 2004). For example, upon binding to the ligand, TLR4 can activate nuclear transcription factors NF-κB or MAPK to induce the release of pro-inflammatory cytokines and regulate activation of macrophage by MyD88 dependent signaling pathway and TRIF-dependent signaling pathway (Li and Cherayil, 2003; Jiang et al., 2015; Molteni et al., 2016). However, recent studies also showed that the TLR4-induced signaling pathway participates in the homeostasis of the tissue and orchestrated tissues repair after damages caused by various insults. Studies have confirmed that TLR4 plays an important role in liver injury (Cengiz et al., 2015; Seki and Schwabe, 2015; Gandhi, 2020).

Our previous study also showed that TLR4 promoted peribiliary fibrosis by orchestrating the TGF-β signaling pathway in a susceptible mouse model (C3H/HeN mice) (Yan et al., 2017). However, the roles of TLR4 might vary in the different genetic backgrounds of the mouse following the encounter with different stimuli. In the present study, we used TLR4^{wild} (C57BL/10JNju, TLR4^{wild}) and TLR4^{def} (C57BL/10ScN, TLR4^{def}) mice to explore the roles of TLR4 in the pathogenesis of biliary injury within a resistant strain mice by *C. sinensis*. Surprisingly, different from the roles of TLR4 in a susceptible mouse model demonstrated by our previous study, in the present study, we found that TLR4 ^{def} mice showed an aggravation of the biliary injuries and peribiliary fibrosis caused by *C. sinensis*, which was associated with the increased type 2 immune responses in *C. sinensis*-resistant mice.

MATERIALS AND METHODS

Ethics

Animal care and all experimental perform in this study were strictly conformed to the guidelines of the National Laboratory Animal Center. The main procedures and protocol were reviewed and approved by the Animal Care and Use Committee of Xuzhou Medical University License (2017-SK-05).

Mice

Six- to 8-week-old TLR4^{wild} mice (C57BL/10JNju) and TLR4^{def} mice (C57BL/10ScN, TLR4^{def}) were purchased from the Model Animal Research Center of Nanjing University and maintained under specific non-pathogenic conditions in the model animal research center of Xuzhou Medical University (Xuzhou, Jiangsu, China). The mice were housed in an air-conditioned room at 24° C with a 12-h dark/light cycle and permitted free access to food and water.

Parasites Infection

Metacercariae of *C. sinensis* from *Pseudorasbora parva* were collected by digestion with a pepsin-HCl (0.6%) artificial gastric juice (Yan et al., 2015). In each infected group, 45 metacercariae were intragastrically administrated to the individual, and the irrigating solution was observed under the microscope to ensure that all the metacercariae were completely intragastrically administrated; the mice of the non-infected received the same volume of normal saline. On day 28th post-infection all the mice were sacrificed and the serum and liver tissues were collected for further study.

Liver Function Test

The activities of alanine aminotransferase (ALT), aspartate aminotransferase (AST), total bilirubin (TBIL), alkaline phosphatase (ALP), total bile acid (TBA) were assayed in the Department of Laboratory Medicine, Affiliated Hospital of Xuzhou Medical University, China to indicate for hepatocellular and biliary injuries in infected mice and uninfected mice.

Hematoxylin and Eosin Staining

Partial liver tissue (about 10 mm × 10 mm × 1 mm) was immersed in 4% paraformaldehyde for 48 h. The embedded tissue wax blocks were serially sectioned at 4 μm for hematoxylin and eosin (H&E) staining according to the manufacturer's instructions (Jiangsu Beyotime biotechnology research institute, China). After sealing the slides with neutral adhesive, the pathological changes of stained histological sections were observed by microscope (Olympus, Japan).

Masson's Trichrome Staining

Four percent paraformaldehyde was used to fix the liver tissue from each strain of mice, then the liver was embedded in paraffin.

Three- to 4-μm thick sections were prepared and stained with Masson's trichrome according to the manufacturer's instructions (Jiancheng, Nanjing, Jiangsu, China). The sections were observed under the microscope and digitized using an imaging system (Olympus, Japan). Five high-power visual fields (×400 magnifications, Olympus, Japan) were randomly selected from the staining sections of each mouse, and Image Pro Plus6.0 software was used to calculate the Integral optical density (IOD) of fibrous tissue. A higher IOD value means stronger positive expression.

Immunohistochemistry Staining

Three- to 4-μm serial thick sections of embedded tissue from each mouse were used for immunohistochemical staining of cytokeratin 19 (CK-19), ki67, alpha-smooth muscle Actin (α-SMA). The liver tissue was deparaffinized, hydrated, and heated in citric acid buffer at 95°C for 10 min and then blocked with 5% BSA for 30 min. The slides were then incubated overnight with primary Anti-Cytokeratin 19(1:500, ab52625, Abcam, Cambridge, US), ki67 (1:400, ab15580, Abcam, Cambridge, US), alpha-smooth muscle Actin (α-SMA) (1:400, ab124964, Abcam, Cambridge, US). After washing with PBS, DAB (1:200, ZSGB–BIO, Beijing, China) as an enzyme-substrate was added. Five high-power fields (×100 magnifications, Olympus, Japan) were randomly selected from each mouse staining section. CK19, ki67, α-SMA positive expression was calculated by the software of Image J (NIH, Bethesda, USA).

Flow Cytometry Analysis

Intrahepatic leukocytes were obtained as descript elsewhere with minor modification (Blom et al., 2009). Partial liver tissue from each mouse was minced and grinded gently through a 40 μm-gauge nylon strainer using a sterile syringe plunger, the preparation was then centrifuged at 1,500 rpm for 10 min, the cells were resuspended using 4 ml 40% Percoll (GE Healthcare, catalog number: 17-0891-01) and then transferred into a new tube containing 5 ml 80% Percoll slowly. Subsequently, the gradient solution was centrifuged at 2,500 rpm for 25 min, the leukocytes were obtained from the interphase between 40% Percoll and 80% Percoll. Red blood cells in cell pellets were removed using ACK Lysis Buffer (BD Biosciences, catalog number: 555899, USA). Approximate 10^7 cells were subjected to cell surface phenotyping by flow cytometry. A panel of antibodies used as markers for detection as follows: anti-CD45 was labeled with PE, anti-CD11b was labeled with PerCP-Cy5.5, anti-CD86 was labeled with PE-Cy^{TM}7, anti-CD206 was labeled with Alexa Fluor 647 (all antibodies from BD PharMingen, San Diego, CA, USA). The cells were incubated with antibodies directed toward various cell surface antigens and in the dark on ice for 30 min, following the manufacturer's recommendations (BD PharMingen, San Diego, CA, USA). Subsequently, the cells were washed by centrifugation at 1500 rpm for 10 min, resuspended in 400 μl FACS buffer, and analyzed utilizing FACSCantoII flow cytometer (Becton Dickinson, San Jose, CA, USA).

Enzyme-Linked Immunosorbent Assay

Serum and mouse liver homogenate from each mouse was immediately subjected to evaluate the concentration of IgE, IL-4, IL-6, IL-10, IL-13, MCP-1, and TNF-α by commercial Enzyme-linked Immunosorbent Assay (ELISA) Kits (Thermo Scientific, US). All procedures were performed according to the instructions provided by the kit. Concentrations of cytokine in the sera were calculated using standard curves as references.

Quantitative Real-Time Fluorescence PCR

Total RNA was isolated from the liver by the use of Trizol (Vazyme, Nanjing, China). According to the manufacturer's instruction, RNA was reverse transcribed into cDNA by use of the FastQuant RT First Kit With gDNase (TIANGEN, Beijing, China). Primers for mouse: *NOS2* F: GGCAGCCTCTTGTCTTTGACC; R: GGGAATC TTGGAGCGAGTTGT; *Tnfa* F: CTCCTCCACTTGGT GGTTTGT; R: GGTGCCTATGTCTCAGCCTCT; *Arg1* F: GTCAGTCCCTGGCTTATGGTT; R: CAGCAGAGG AGGTGAAGAGTA; *Ym1* F: GGATGGCTACACTGGAGAAA; R: AGAAGGGTCACTCAGGATAA; *Fizzl* F: CCCTCCACT GTAACGAAG; R: GTGGTCCAGTCAACGAGTAA; *ILIb* F: TGTGTTTTCCTCCTTGCCTCTGAT; R: TGCTGCCTAATG TCCCCTTGAAT; *IL6* F: TCACAGAAGGAGTGGCT AAGGACC; R: ACGCACTAGGTTTGCCGAGTAGAT; *Tgfb* F: CCACCTGCAAGACCATCGAC; R: CTGGCGAGCC TTAGTTTGGAC;*Col-1a* F: CAGGGTATTGCTGGACAACGTG; R: GGACCTTGTTTGCCAGGTTCA

The real-time quantitative PCR was performed using a Roche 480 detection system using SYBR Green PCR master mix solution (Roche Diagnostics Ltd, Shanghai, China). Fold changes of each gene to that of control mice were calculated using the formula of $2^{-\Delta\Delta Ct}$, which was normalized by β-actin. The specificity of each PCR was monitored by Roche 480 detection system with melt-curve analysis.

Detection of Hydroxyproline Contents

The hydroxyproline content of the mouse liver were assayed to indicate for collagen deposition of liver in the infected mice and uninfected mice using a commercial kit (Nanjing JianCheng Technology Co. LTD, China). The assay was performed according to the instructions provided in the kit.

Statistical Analysis

All values were expressed as mean ± SEM. The data were analyzed by SPSS19.0 software (SPSS Inc, Chicago, IL, USA). The student *t*-test was used for comparison between the two groups. One-way ANOVA with Tukey's *post hoc* test was used for comparison for more than two groups. If the test level was α=0.05, the difference was statistically significant when $P< 0.05$.

RESULTS

TLR4^{def} Accelerate Hepatic Damages in *C. sinensis*-Infected Mice

There were no obvious changes in the liver between TLR4^{wild} and TLR4^{def} mice without infection of *C. sinensis* (**Figure 1A**). However, following *C. sinensis* infection, gross changes of the liver in TLR4 wild-type infected mice were scarce. In contrast, the liver of TLR4^{def} mice infected by *C. sinensis* had a dark color, tough texture, and uneven edges. Multiple white sesame-sized

nodules were visible and most of them were lesions distributed on the left lobe of the liver (**Figure 1A**). Histological changes of the liver collected from each mouse were observed by H&E staining (**Figure 1B**). HE staining showed that the hepatocytes in the normal group were arranged neatly, the hepatic lobule structure was complete, and there was no inflammatory cell infiltration in the portal area, bile duct expansion, or hyperplasia (**Figure 1B**). Following *C. sinensis* infection, the histological analysis of the liver of wild-type infected mice showed an infiltration of inflammatory cells, with thickened bile duct hyperplasia and a small amount of fibrous tissue hyperplasia (**Figure 1B**). However, the overall hepatic lobule structure was orderly, the damaged area was relatively limited, and the hepatocytes were orderly arranged. Worm bodies in the bile ducts were not observed within the staining of liver tissues. However, TLR4^{def} infected mice had very serious liver damage: a large number of inflammatory cells were infiltrated around the bile duct, the bile duct epithelium was disrupted, the hepatic lobule structure was damaged, and the liver cells were arranged in disorder (**Figure 1B**, as indicated by arrows). Liver inflammation was increased as indicated by the mHAI score (**Figure 1B**, $P<0.05$). For the bile duct, it could be seen that the bile duct had a complete structure with single-layer epithelium in the non-infected groups of mice. However, when the mice were infected by *C. sinensis*, TLR4^{wild} mice showed an irregular bile duct and mild proliferation of BECs accompanied by only a few inflammatory cells infiltrated. Compared with TLR4^{wild} mice infected by *C. sinensis*, TLR4^{def} infected mice showed that the bile duct was more severe and irregular in shape, where mature worms bodies could be observed (indicated as triangle, **Figure 1B**). Furthermore, we evaluated hepatic damages as indicated by the activities of ALT and AST. It was found that the levels of ALT and AST in TLR4^{def} infected mice were significantly higher than those of TLR4^{def} uninfected mice. Meanwhile, compared with TLR4^{wild} infection group, the activities of ALT and AST were significantly increased in TLR4^{def} infection group (**Figures 1C, D**, $P<0.05$).

It has been reported that the increased production of IgE during the worms infection is related to tissue damages (Hamid et al., 2015). The data showed that the serum IgE secretion by TLR4^{wild} infected mice was slightly higher than that of TLR4^{wild} non-infected mice (**Figure 1E**, $P<0.05$). However, the serum IgE secretion in TLR4^{def} infected mice was higher than that of the non-infected group, as well as that of TLR4^{wild} infected mice (**Figure 1E**, $P<0.001$).

TLR4^{def} Aggravates Liver Fibrosis in Mice Infected by *C. sinensis*

To observe and evaluate the liver fibrosis caused by *C. sinensis*, we used Masson's trichrome staining and the expression of α-SMA was used for assessment of the degree of liver fibrosis. Masson staining showed that no obvious collagen deposition was observed in the non-infected groups. However, following *C. sinensis* infection, the hyperplasia of fibrous tissue in TLR4^{wild} infected mice was mainly deposited around the bile duct, although the overall damage was relatively limited. In contrast, TLR4^{def} infected mice had a large amount of fibrous tissue hyperplasia around the diseased bile duct (indicated as arrows, **Figure 2A**). The depositions of collagen in TLR4^{def} infected mice were increased compared with the non-infected group (**Figure 2A**, $P<0.05$), whereas the mice in the TLR4^{def} infected group had more fibrosis than those in the TLR4^{wild} infected group (**Figure 2A**, $P<0.05$). IHC showed that the expression of α-SMA was slightly increased after *C. sinensis*-infected TLR4^{wild}mice, compared with non-infected mice (**Figure 2B**). However, the expression of α-SMA was significantly increased in *C. sinensis*-

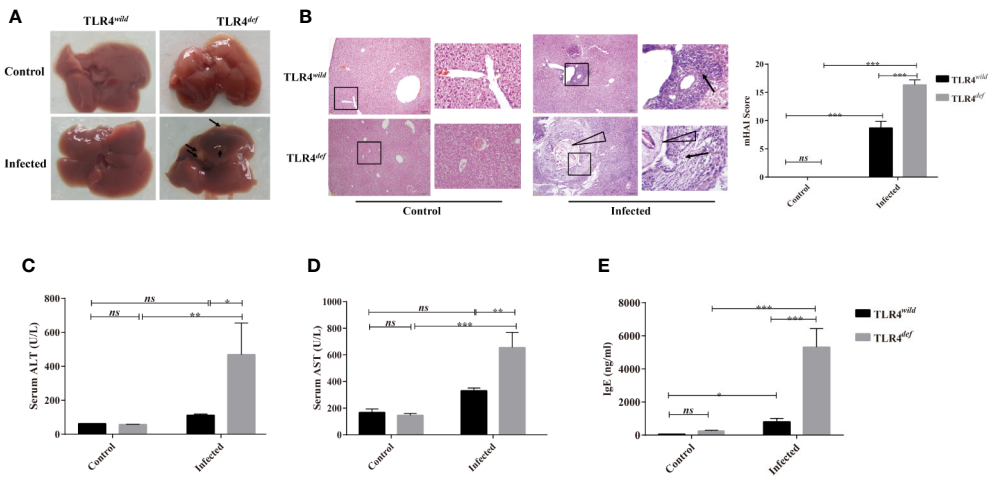

FIGURE 1 | Toll-like receptor 4 (TLR4) deficiency aggravated liver injuries in C57BL/10 mice infected by *Clonorchis sinensis*. **(A)** Gross lesions in liver tissue of TLR4^{wild} and TLR4^{def} mice infected with *C. sinensis*. The arrow indicates the lesion nodule. **(B)** Histological changes of liver in TLR4^{wild} and TLR4^{def} mice infected with *C. sinensis* under 100× and 400× microscope were indicated by HE staining and liver histopathological changes were assessed by the mHAI score. An arrow indicates the infiltrated immune cells; triangle indicates worm bodies in the bile ducts. **(C)** The activities of alanine aminotransferase (ALT) and **(D)** aspartate aminotransferase (AST) were assessed in the sera of TLR4^{wild} and TLR4^{def} mice infected with *C. sinensis*. **(E)** The secretion of IgE in sera of TLR4^{wild} and TLR4^{def} mice infected with *C. sinensis* were determined using ELISA. The values were expressed as mean ± SEM. Compared with indicated groups, $^{*}P < 0.05$, $^{**}P < 0.01$, $^{***}P < 0.001$.

infected TLR4^{def} mice and there were statistical differences in the expression of α-SMA between TLR4^{wild} and TLR4^{def} mice that were infected with the same amount of *C. sinensis* (positive areas indicated as arrows, **Figure 2B**, $P<0.05$). Furthermore, the concentrations of hydroxyproline in TLR4^{def} infected mice was increased compared with the non-infected group (**Figure 2C**, $P<0.001$), and the mice in the TLR4^{def} infected group had more fibrosis than those in the TLR4^{wild} infected group (**Figure 2C**, $P<0.001$). We further detected the relative hepatic expression of *Tgfb* and *Col1a* transcripts in the livers of TLR4^{wild} as well as TLR4^{def} mice infected by *C. sinensis* by qRT-PCR. It was found that the expression of *Tgfb and Col1a* mRNA transcripts in the liver of TLR4^{def} mice were significantly increased compared with TLR4^{wild} mice after *C. sinensis* infection (**Figures 2D, E**, $P<0.001$). Taken together, our data suggested that TLR4 deficiency aggravated hepatic fibrosis in C57BL/10 mice infected by *C. sinensis*.

TLR4^{def} Exacerbates Bile Duct Hyperplasia and Biliary Injuries Caused by *C. sinensis*

In the present study, we detected CK19 and ki67 as indicators of the hyperplasia of biliary epithelium cells (BECs) and the morphology of the bile duct by immunohistochemistry. For semi-quantitative analysis for CK19 and Ki67 expression, compared with non-infection and TLR4^{wild}-infected mice, TLR4^{def} infected mice showed higher expression of CK19 and Ki67 (as indicated by arrow), suggesting that TLR4^{def} infected mice had more bile duct hyperplasia than TLR4^{wild} infected mice (**Figure 3A** for CK19, and **Figure 3B** for Ki67, $P<0.01$). In addition, we also detected the serum activities of ALP, TBIL, and TBA which also indicated biliary injuries. The data showed that the levels of these indicators in TLR4^{def} mice infected by *C. sinensis* were significantly increased, compared with those in TLR4^{wild} mice when they were infected with the same dose of *C. sinensis* (**Figures 3C–E**, $P<0.001$). Taken together, our data indicated that TLR4 deficiency in mice with the C57BL/10 genetic background exacerbated hyperplasia and injuries of cholangiocytes caused by *C. sinensis*.

TLR4^{def} Promotes the Activation of M2-Like Macrophages in *C. sinensis*-Infected Mice

To investigate the possible mechanisms that may contribute to the deteriorative clonorchiasis in TLR4^{def} mice, we detected hepatic M1/M2-like macrophages in mice after *C. sinensis* infection. It was found that there were no significantly increased in percentages of

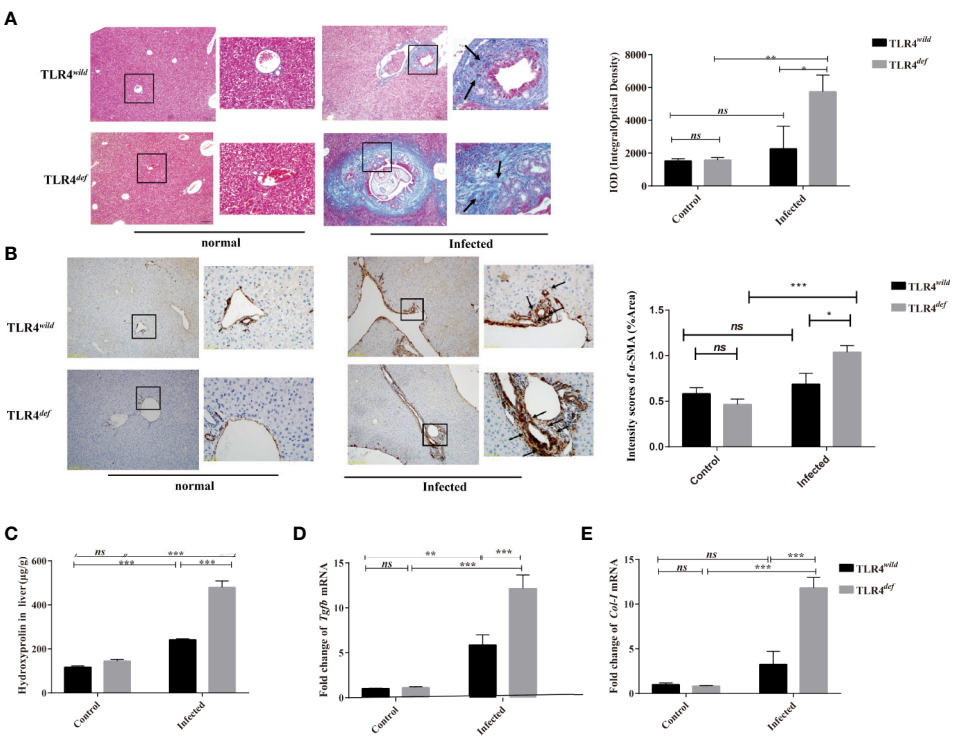

FIGURE 2 | TLR4^{def} led to an increased *Clonorchis sinensis*-caused pathogen-associated liver fibrosis in C57BL/10 mice. **(A)** Masson's staining showed collagen depositions of the liver in TLR4^{wild} and TLR4^{def} mice infected with *C. sinensis* under 100× and 400× microscope. The integral optical density (IOD) of collagen fibers indicated by Masson's trichrome staining was digitized and quantitated in the liver of non-infected and infected mice by on Image-Pro Plus software. **(B)** The expression of α-SMA of the liver in mice infected with *C. sinensis* under 100× and 400× microscope. Arrow indicates the positive cells. The positive areas in the liver of non-infected and infected mice were quantitated by Image J. **(C)** Detection of hydroxyproline in mice liver after *C. sinensis* infection. **(D, E)** Fold expression of fibrotic related molecules in *Tgfb* **(D)**, *Col1a* **(E)** in the liver of mice infected with *C. sinensis*. The values were expressed as mean ± SEM. Compared with indicated groups, $^{*}P < 0.05$, $^{**}P < 0.01$, $^{***}P < 0.001$.

$CD86^+$ in $CD11b^+F4/80^+$ macrophages (M1-like macrophage) in $TLR4^{def}$ mice, compared with $TLR4^{wild}$ mice when they were infected with the same amounts of *C. sinensis* (**Figure 4B**, $P>0.05$), but the proportion of $CD206^+$ in $CD11b^+F4/80^+$ macrophages (M2-like macrophage) in *C. sinensis*-infected $TLR4^{def}$ was significantly higher than that in $TLR4^{wild}$ mice infected by *C. sinensis* (**Figure 4C**, $P<0.05$).

Loss of TLR4 Increases Type 2 Immune Responses but Decreases Type 1 Responses in *C. sinensis*-Infected Mice

We next detected the levels of type 1 immune responses and type 2 immune responses of $TLR4^{wild}$ and $TLR4^{def}$ mice after *C. sinensis* infection. The data showed that there were significantly increases in IL-4, IL-10, and IL-13 cytokines in $TLR4^{def}$ mice, compared with $TLR4^{wild}$ mice when they were infected by the same amounts of *C. sinensis* (**Figures 5A–C**, $P<0.05$). Furthermore, we detected another type 2 immune molecules such as *Arg1*, *Ym1* and *Fizz1* using qPCR, it was found that the relative expression of *Arg1*, *Ym1* and *Fizz1* in the livers of *C. sinensis*-infected $TLR4^{def}$ mice were significantly higher than those in mice in *C. sinensis*-infected $TLR4^{wild}$ mice (**Figures 5D–F**, $P<0.001$).

For type 1 immune responses, it was found that the secretion of MCP-1 and TNF-α in the liver of *C. sinensis*-infected $TLR4^{def}$ was significantly lower than that in $TLR4^{wild}$ mice infected by *C. sinensis* (**Figures 6A, B**, $P<0.05$). And the qPCR data showed that the transcripts of *NOS2, Tnfa*, and *IL1b* in the liver of $TLR4^{def}$ mice were significantly depressed, compared with $TLR4^{wild}$ mice after *C. sinensis* infection (**Figures 6C–F**, $P<0.05$). These data together suggested that $TLR4^{def}$ mice induced an augment of type 2 immune responses and decrease type 1 response, which might result in the exacerbation of biliary injuries and peribiliary fibrosis caused by *C. sinensis* in a resistant mice strain.

DISCUSSION

Mice are widely used to mimic pathogenesis in human-caused by *C. sinensis* since they have gall-bladder and the genetic background is clear enough and many reagents are commercially available. However, other and our previous studies demonstrated that mice with different genetic backgrounds showed distinct susceptibility to *C. sinensis*. For example, liver damage of C3H/HeN (with the normal function of TLR4), BALB/c and FVB mice infected mice were characterized by massive hyperplasia and disordered arrangement of bile duct epithelial cells, as well as deposition of extracellular matrix (Yoon et al., 2001; Zhang et al., 2017).

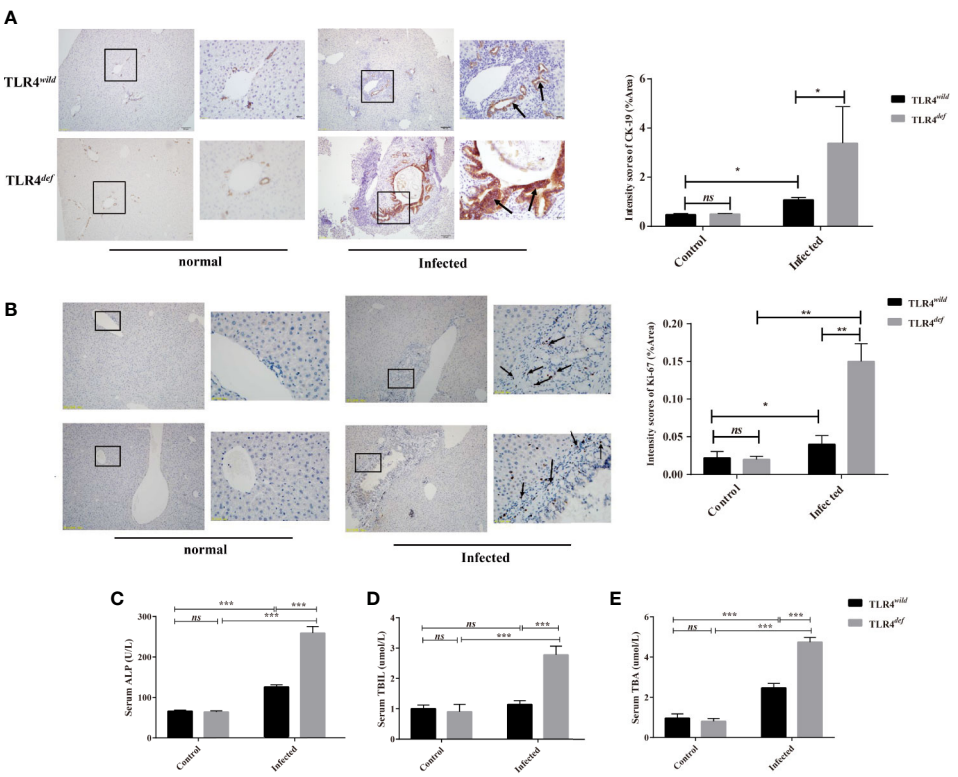

FIGURE 3 | $TLR4^{def}$ promoted bile duct hyperplasia and biliary injuries in a resistant mouse strain of *Clonorchis sinensis* infection. **(A, B)** Hyperplasia of intrahepatic bile duct epithelial cells in mice with *C. sinensis* was indicated by immunohistochemical staining of CK19 **(A)** and ki67 **(B)**, an arrow indicates the positive cells. **(C–E)** The activities of ALP **(C)**, TBIL **(D)**, and TBA **(E)** in the sera of $TLR4^{wild}$ and $TLR4^{def}$ mice were assessed for biliary injuries. The values were expressed as mean ± SEM. Compared with indicated groups, $^*P < 0.05$, $^{**}P < 0.01$, $^{***}P < 0.001$.

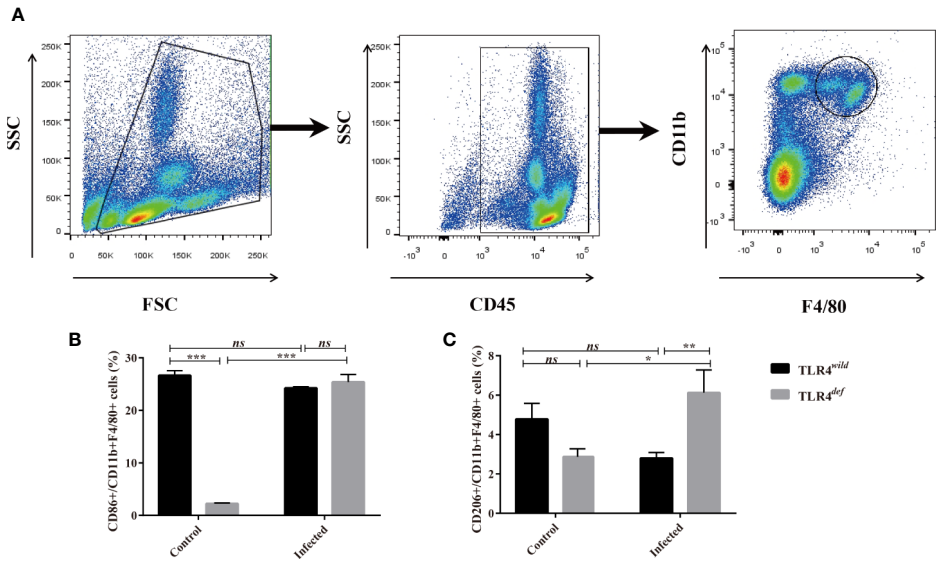

FIGURE 4 | TLR4^{def} mice infected with *Clonorchis sinensis* induced an predominant M2-like macrophage. **(A)** The strategies of gating hepatic macrophages. Hepatic leukocytes were isolated from TLR4^{def} and TLR4^{wild} mice, these cells were gated by CD45, and further gating for CD11b^{+}F4/80^{+} cells using flow cytometer. **(B)** The percentages of CD86^{+}cells in CD11b^{+}F4/80^{+} cells from all the mice were calculated. **(C)** The percentages of CD206^{+}cells in CD11b^{+}F4/80^{+} cells from all the mice were calculated. The values were expressed as mean ± SEM. Compared with indicated groups, $^{*}P < 0.05$, $^{**}P < 0.01$, $^{***}P < 0.001$.

Furthermore, adult worm bodies can be found in the bile ducts of these strains of mice. In contrast, Uddin et al. found that C57BL/6 mice had the lowest worm recovery at 4 weeks after infection and the worms were less developed, which induced mild histological changes in the liver (Uddin et al., 2012). The lesions of C57BL/10 or C57BL/6 infected mice were very limited, with only a small amount of inflammatory cell infiltration in the lesions when they were subjected to the same amount of *C. sinensis* (Zhang et al., 2017). In addition, mild fibrosis lesions indicating by Masson staining and hydroxyproline assay were also found in *C. sinensis*-infected C57BL/10 and C57BL/6, which further suggested that the susceptibility of different strains of mice to *C. sinensis* was different (Robey et al., 2015). The mechanisms accounting for these may be very complex and largely unknown. In our present study, in contrast with TLR4 wild-type mice, we found that the loss of TLR4 in C57BL/10 mice showed exacerbated biliary injuries and

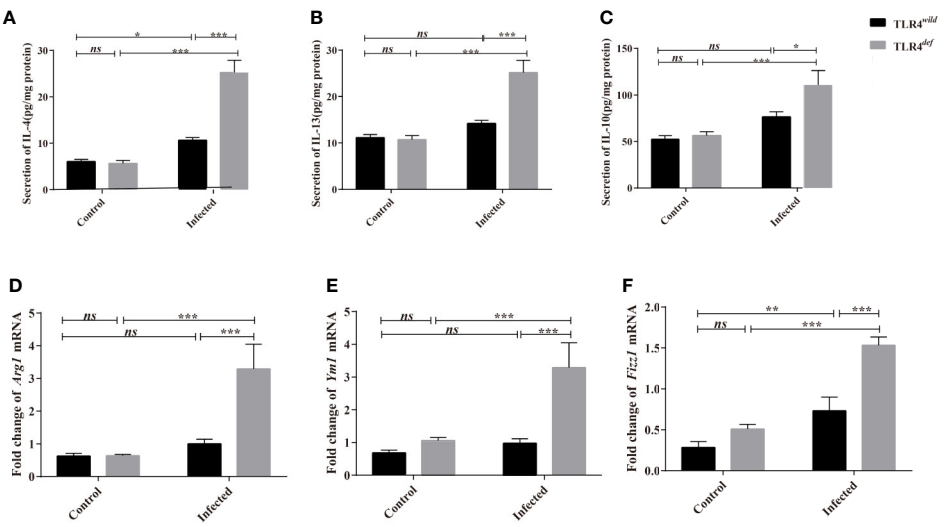

FIGURE 5 | TLR4^{def} enhanced type 2 immune response in C57BL/10 mice infected by *Clonorchis sinensis*. **(A~C)** The hepatic concentrations of IL-4 **(A)**, IL-13 **(B)**, and IL-10 **(C)** in the TLR4^{wild} and TLR4^{def} mice infected with *C. sinensis* were detected using ELISA kits. **(D~F)** The hepatic levels of *Arg1* **(D)**, *Ym1* **(E)**, *Fizz1* **(F)** were determined by qPCR. The values were expressed as mean ± SEM. Compared with indicated groups, $^{*}P < 0.05$, $^{**}P < 0.01$, $^{***}P < 0.001$.

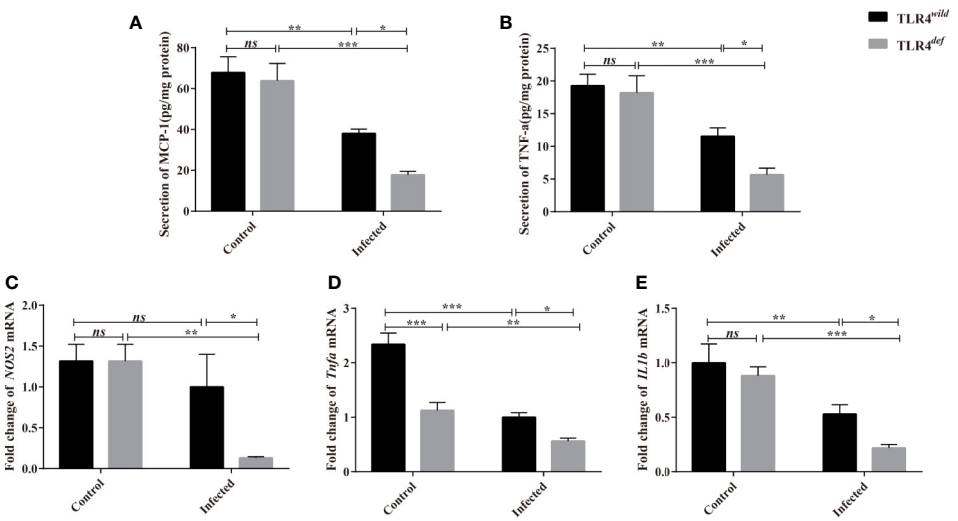

FIGURE 6 | TLR4^{def} decreased type 1 immune responses in C57BL/10 mice infected by *Clonorchis sinensis*. **(A, B)** The hepatic concentrations of MCP-1 **(A)** and TNF-e **(B)** in the TLR4^{wild} and TLR4^{def} mice infected with *C. sinensis* were detected using ELISA kits. **(C, D)** Fold changes of type 1 immunity-related molecules in *NOS2* **(C)**, *Tnfa* **(D)**, *IL1b* **(F)** in the liver of mice infected with *C. sinensis* from each group were determined by qPCR. The values were expressed as mean ± SEM. Compared with indicated groups, $^{*}P < 0.05$, $^{**}P < 0.01$, $^{***}P < 0.01$.

peribiliary fibrosis caused by *C. sinensis*, which may be associated with an increase of type 2 immune responses due to TLR4 deficiency. There were some similarities or disparities of our data from TLR4 deficiency mice with patients infected by *C. sinensis*, for example, TLR4 deficiency mice showed relatively high levels of liver function indexes (such as ALP, ALT, AST, TBIL, and TBA, etc), IgE antibodies subclass as well as type 2 immune responses, which were also elevated in human infected by *C. sinensis* (Cai et al., 2004; Han et al., 2015); however, we did not find an increase of type 1 immune responses in TLR4^{def} mice infected by *C. sinensis* whereas human with *C. sinensis* infection showed high levels pro-inflammatory cytokines such as TNF-α (Yuan et al., 2013).

A high level of IgE production is a hallmark of infection by helminth. It is believed that IgE plays a central role in protective immunity against worm infection although the mechanism underlying it remains unclear (Cooper et al., 2008). It also suggested that IgE induced the activation of mast cells to recruit immune effector cells including Th2 cells, M2 macrophage, and eosinophils and trigger type II cytokines (i.e. IL-4, IL-5, and IL-13), leading to cell hyperplasia and tissue injuries due to the hypersensitivity reactions (Gurish et al., 2004; Kondo et al., 2008). Interestingly, treatment with monoclonal IgE antibody (omalizumab, Xolair) alleviates allergic reactions and airway damages in asthma by blockade of IgE binding with Fc εRI receptor on the mast cells and other effector cells (Corren et al., 2017). In our present study, we found that the relative higher IgE production in TLR4 deficiency mice was induced by *C. sinensis*, compared with TLR4 wild type mice, suggesting that IgE may be involved in the pathogenesis caused by *C. sinensis* in addition to expelling worms.

TLR4, as an ancient and conservative pattern recognition receptor, plays an important role in the invasion, colonization, pathogenesis, and elimination of pathogens, and may display multiple effects at different stages of disease development (Shah et al., 2012; Cheng et al., 2015). Recently, it has been reported that the TLR4-mediated NF-κB signaling pathway which can cross-talk with the TGF-β/samds signaling pathway plays a very important role in the pathogenesis of hepatic fibrosis and cholestatic injuries (Seki et al., 2007). Our previous study has used C3H/HeN (TLR4 wild) and C3H/HeJ (TLR4 mutation) strain mice to establish the *C. sinensis* infection model and found that the biliary fibrosis of TLR4 mutant mice (TLR4^{mut}) was ameliorative, compared with wild-type mice, which suggested that TLR4 promotes liver fibrosis caused by *C. sinensis* (Yan et al., 2017). In contrast, in the present study, TLR4 deficiency in a resistant mouse strain following *C. sinensis* infection deteriorated the biliary injuries and biliary fibrosis, as indicated by CK19 immunohistochemical staining and Masson staining, respectively, which was consistent with previous studies (Yang et al., 2017; Zhang et al., 2017). Furthermore, we also found that the liver function was also damped to some extent as the activities of ALT were significantly increased in the TLR4 deficient mouse infected by *C. sinensis*, compared with TLR4 wild type with the same background. These data suggested that TLR4 might play contradictory roles in pathogenesis caused by *C. sinensis* due to the different genetic backgrounds of mice (Zhang et al., 2018).

Type 1 immune responses are characterized with CD4+Th1, classically activated macrophages (M1 macrophages), group 1 innate lymphoid cells (ILC1s), and cytotoxic T cells, which protect against intracellular microbes and enhance cell-mediated immunity by secretion of cytokines such as TNF-α, IL-6, INF-γ, and MCP-1 and secretion of NO (Annunziato et al., 2015); Type 2 immune responses are mediated by CD4+Th2 cells, group 2 ILCs, eosinophils, basophils, mast cells, M2 macrophages by producing the cytokines IL−4, IL−5, IL−9,

IL−13, and the IgE antibody subclass, which suppress the development of type 1-driven inflammation and contribute to the pathogenesis of allergy and tissue fibrosis (Wynn, 2015). In the healthy animals, the type 1 and 2 immune responses of the host are finely regulated; however, their balance might determine the occurrence, development, and outcome of the disease. For example, during worm infection, Type 2 immune responses were overwhelmed in the chronic infection to protect from such large extra−cellular helminth parasites infection as well as facilitate tissue fibrosis (Wynn, 2015). In our previous study, compared with BALB/c and FVB mice, we found that C57BL/6 mice showed stronger resistance to *C. sinensis* infection and the worm body was not completely developed or retarded and even eliminated (Zhang et al., 2017). It was speculated that these differences might be closely related to the high level of type 2 immune responses in the liver of BALB/c and FVB mice (Zhang et al., 2017). The type 1 immune response was predominant in C57BL/6 mice. For example, macrophages of C57BL/6 mice can effectively eliminate the bacterial infection in the model of cecal ligation and perforated peritonitis by producing high levels of TNF-α, IL-12 and NO, and other types I immune response molecules (Uddin et al., 2012; Pine et al., 2018). However, BALB/c mice have a dominating type II immune response and could not eliminate bacterial infections effectively (Watanabe et al., 2004; Jovicic et al., 2015). Studies also have shown that type 2 immune response can promote the development and progression of liver fibrosis, thereby promoting the activation of HSCs by producing IL-10, Arg-1, Ym1, and Fizz1 (Liu et al., 2004) whereas pro-inflammatory mediators such as iNOS could inhibit the activation or induce the apoptosis of HSCs (Allen and Sutherland, 2014; Pine et al., 2018). In our present study, we focused on the hepatic macrophages which play a critical role in the cholestatic liver injuries including pathogenesis caused by *C. sinensis* (Kim et al., 2017; Guicciardi et al., 2018). To address this issue, we used CD86+CD11b+F4/80 + defining as an activation marker of M1 macrophage whereas CD206+CD11b+F4/80+ were used to assess M2 activation, we found that TLR4 deficiency in C57BL/10 increase M2 macrophage producing the molecules of *Arg-1, Ym1 and Fizz1* to possibly result in severe immunopathological damages (such as liver fibrosis), however, whether the biased type 2 immune responses induced by TLR4 deficiency may affect the development of the worms in the host or not, it remains to be further studied.

In conclusion, the present study found that biliary injuries and peribiliary fibrosis caused by *C. sinensis* had deteriorated when TLR4 was absent, suggesting that TLR4 might be involved in the resistance to *C. sinensis* in C57BL/10 mice. However, further studies on the mechanisms by which TLR4 deficiency in C57BL/10 mice induced pathogenesis of *C. sinensis* should be warranted.

DATA AVAILABILITY STATEMENT

The datasets generated for this study are available on request to the corresponding authors.

ETHICS STATEMENT

The animal study was reviewed and approved by Animal Care and Use Committee of Xuzhou Medical University.

AUTHOR CONTRIBUTIONS

CY and K-YZ conceived and designed the experiments. CY, JW, and NX performed the majority of experiments. JL, Q-YZ, H-MY, X-DC, J-XL, XD, SK, QY, B-BZ, J-XC, and R-XT contributed to the acquisition of data. JW and CY wrote the paper. All authors contributed to the article and approved the submitted version.

FUNDING

This study was supported by National Natural Science Foundation of China (Grant Nos: 81572019 to K-YZ and 81702027 to QY), Natural Science Foundation of Jiangsu Province of China (Grant No. BK20171176 to CY and Grant No. BK20201011 for B-BZ), China Postdoctoral Science Foundation (Grant No. 2018M640525 to CY), Qian Lan Project of Jiangsu Province (to CY), Jiangsu Planned Projects for Postdoctoral Research Funds (No. 2018K053B to CY), the starting grants for young scientist of Xuzhou Medical University (No. D2019040 to B-BZ), Priority Academic Program Development of Jiangsu Higher Education Institutions of China (Grant No. 1506 to K-YZ) and Graduate research project of Jiangsu Province (Grant No. KYCX18-2172 to JW). The funders had no role in study design, data collection and analysis, decision to publish, or preparation of the manuscript.

REFERENCES

Akira, S., Takeda, K., and Kaisho, T. (2001). Toll-like receptors: critical proteins linking innate and acquired immunity. *Nat. Immunol.* 2 (8), 675–680. doi: 10.1038/90609

Allen, J. E., and Sutherland, T. E. (2014). Host protective roles of type 2 immunity: parasite killing and tissue repair, flip sides of the same coin. *Semin. Immunol.* 26 (4), 329–340. doi: 10.1016/j.smim.2014.06.003

Annunziato, F., Romagnani, C., and Romagnani, S. (2015). The 3 major types of innate and adaptive cell-mediated effector immunity. *J. Allergy Clin. Immunol.* 135 (3), 626–635. doi: 10.1016/j.jaci.2014.11.001

Blom, K. G., Qazi, M. R., Matos, J. B., Nelson, B. D., DePierre, J. W., Abedi-Valugerdi, M., et al. (2009). Isolation of murine intrahepatic immune cells employing a modified procedure for mechanical disruption and functional characterization ofT and natural killer T cells obtained. *Clin. Exp. Immunol.* 155 (2), 320–329. doi: 10.1111/j.1365-2249.2008.03815.x

Cai, L. S., Xiao, J. Y., Xin, H., Zhu, L. X., Chen, G., Zhang, T., et al. (2004). Studies on the relationship between the level of cytokine and liver function in patients with clonorchiasis sinensis. *Zhongguo Ji Sheng Chong Xue Yu Ji Sheng Chong Bing Za Zhi* 22 (1), 54–56. doi: 1000-7423(2004)-01-0054-03

Cengiz, M., Ozenirler, S., and Elbeg, S. (2015). Role of serum toll-like receptors 2 and 4 in non-alcoholic steatohepatitis and liver fibrosis. *J. Gastroenterol. Hepatol.* 30 (7), 1190–1196. doi: 10.1111/jgh.12924

Cheng, Y., Zhu, Y., Huang, X., Zhang, W., Han, Z., and Liu, S. (2015). Association between TLR2 and TLR4 Gene Polymorphisms and the Susceptibility to Inflammatory Bowel Disease: A Meta-Analysis. *PloS One* 10 (5), e0126803. doi: 10.1371/journal.pone.0126803

Ciferska, H., Honsova, E., Lodererova, A., Hruskova, Z., Neprasova, M., Vachek, J., et al. (2020). Does the renal expression of Toll-like receptors play a role in patients with IgA nephropathy? *J. Nephrol.* 33(2):307–316. doi: 10.1007/s40620-019-00640-z

Cooper, P. J., Ayre, G., Martin, C., Rizzo, J. A., Ponte, E. V., and Cruz, A. A. (2008). Geohelminth infections: a review of the role of IgE and assessment of potential risks of anti-IgE treatment. *Allergy* 63 (4), 409–417. doi: 10.1111/j.1398-9995.2007.01601.x

Corren, J., Kavati, A., Ortiz, B., Colby, J. A., Ruiz, K., Maiese, B. A., et al. (2017). Efficacy and safety of omalizumab in children and adolescents with moderate-to-severe asthma: A systematic literature review. *Allergy Asthma Proc.* 38 (4), 250–263. doi: 10.2500/aap.2017.38.4067

Gandhi, C. R. (2020). Pro- and Anti-fibrogenic Functions of Gram-Negative Bacterial Lipopolysaccharide in the Liver. *Front. Med. (Lausanne)* 7, 130. doi: 10.3389/fmed.2020.00130

Guicciardi, M. E., Trussoni, C. E., Krishnan, A., Bronk, S. F., Lorenzo Pisarello, M. J., O'Hara, S. P., et al. (2018). Macrophages contribute to the pathogenesis of sclerosing cholangitis in mice. *J. Hepatol.* 69 (3), 676–686. doi: 10.1016/j.jhep.2018.05.018

Gurish, M. F., Bryce, P. J., Tao, H., Kisselgof, A. B., Thornton, E. M., Miller, H. R., et al. (2004). IgE enhances parasite clearance and regulates mast cell responses in mice infected with *Trichinella spiralis*. *J. Immunol.* 172 (2), 1139–1145. doi: 10.4049/jimmunol.172.2.1139

Hamid, F., Amoah, A. S., van Ree, R., and Yazdanbakhsh, M. (2015). Helminth-induced IgE and protection against allergic disorders. *Curr. Top. Microbiol. Immunol.* 388, 91–108. doi: 10.1007/978-3-319-13725-4_5

Han, X., Xu, J. X., Wang, B. L., Sun, T. T., Sun, Z. Y., Dai, Y., et al. (2015). Role of cytokines(IL-6,IL-10,TNF-α) in liver dysfunction patients with *Clonorchis sinensis*. *Chin. J. Microecology* 27 (3), 263–263. doi: 10.13381/j.cnki.cjm.201503005

Hong, S. T., and Fang, Y. (2012). *Clonorchis sinensis* and clonorchiasis, an update. *Parasitol. Int.* 61 (1), 17–24. doi: 10.1016/j.parint.2011.06.007

Iwasaki, A., and Medzhitov, R. (2004). Toll-like receptor control of the adaptive immune responses. *Nat. Immunol.* 5 (10), 987–995. doi: 10.1038/ni1112

Jiang, Q., Yi, M., Guo, Q., Wang, C., Wang, H., Meng, S., et al. (2015). Protective effects of polydatin on lipopolysaccharide-induced acute lung injury through TLR4-MyD88-NF-kappaB pathway. *Int. Immunopharmacol.* 29 (2), 370–376. doi: 10.1016/j.intimp.2015.10.027

Jovicic, N., Jeftic, I., Jovanovic, I., Radosavljevic, G., Arsenijevic, N., Lukic, M. L., et al. (2015). Differential Immunometabolic Phenotype in Th1 and Th2 Dominant Mouse Strains in Response to High-Fat Feeding. *PloS One* 10 (7), e0134089. doi: 10.1371/journal.pone.0134089

Kim, E. M., Kwak, Y. S., Yi, M. H., Kim, J. Y., Sohn, W. M., and Yong, T. S. (2017). *Clonorchis sinensis* antigens alter hepatic macrophage polarization in vitro and in vivo. *PloS Negl. Trop. Dis.* 11 (5), e0005614. doi: 10.1371/journal.pntd.0005614

Kim, Y. H. (1999). Pancreatitis in association with *Clonorchis sinensis* infestation: CT evaluation. *AJR Am. J. Roentgenol.* 172 (5), 1293–1296. doi: 10.2214/ajr.172.5.10227505

Kondo, Y., Yoshimoto, T., Yasuda, K., Futatsugi-Yumikura, S., Morimoto, M., Hayashi, N., et al. (2008). Administration of IL-33 induces airway hyperresponsiveness and goblet cell hyperplasia in the lungs in the absence of adaptive immune system. *Int. Immunol.* 20 (6), 791–800. doi: 10.1093/intimm/dxn037

Li, Q., and Cherayil, B. J. (2003). Role of Toll-like receptor 4 in macrophage activation and tolerance during *Salmonella enterica serovar Typhimurium* infection. *Infect. Immun.* 71 (9), 4873–4882. doi: 10.1128/iai.71.9.4873-4882.2003

Liu, T., Dhanasekaran, S. M., Jin, H., Hu, B., Tomlins, S. A., Chinnaiyan, A. M., et al. (2004). FIZZ1 stimulation of myofibroblast differentiation. *Am. J. Pathol.* 164 (4), 1315–1326. doi: 10.1016/S0002-9440(10)63218-X

Molteni, M., Gemma, S., and Rossetti, C. (2016). The Role of Toll-Like Receptor 4 in Infectious and Noninfectious Inflammation. *Mediators Inflamm.* 2016, 6978936. doi: 10.1155/2016/6978936

Pine, G. M., Batugedara, H. M., and Nair, M. G. (2018). Here, there and everywhere: Resistin-like molecules in infection, inflammation, and metabolic disorders. *Cytokine* 110, 442–451. doi: 10.1016/j.cyto.2018.05.014

Robey, R. B., Weisz, J., Kuemmerle, N. B., Salzberg, A. C., Berg, A., Brown, D. G., et al. (2015). Metabolic reprogramming and dysregulated metabolism: cause, consequence and/or enabler of environmental carcinogenesis? *Carcinogenesis* 36 Suppl 1, S203–S231. doi: 10.1093/carcin/bgv037

Seki, E., and Schwabe, R. F. (2015). Hepatic inflammation and fibrosis: functional links and key pathways. *Hepatology* 61 (3), 1066–1079. doi: 10.1002/hep.27332

Seki, E., De Minicis, S., Osterreicher, C. H., Kluwe, J., Osawa, Y., Brenner, D. A., et al. (2007). TLR4 enhances TGF-beta signaling and hepatic fibrosis. *Nat. Med.* 13 (11), 1324–1332. doi: 10.1038/nm1663

Shah, J. A., Vary, J. C., Chau, T. T., Bang, N. D., Yen, N. T., Farrar, J. J., et al. (2012). Human TOLLIP regulates TLR2 and TLR4 signaling and its polymorphisms are associated with susceptibility to tuberculosis. *J. Immunol.* 189 (4), 1737–1746. doi: 10.4049/jimmunol.1103541

Sripa, B. (2012). Global burden of food-borne trematodiasis. *Lancet Infect. Dis.* 12 (3), 171–172. doi: 10.1016/S1473-3099(11)70321-8

Tang, Z. L., Huang, Y., and Yu, X. B. (2016). Current status and perspectives of *Clonorchis sinensis* and clonorchiasis: epidemiology, pathogenesis, omics, prevention and control. *Infect. Dis. Poverty* 5 (1), 71. doi: 10.1186/s40249-016-0166-1

Tyson, G. L., and El-Serag, H. B. (2011). Risk factors for cholangiocarcinoma. *Hepatology* 54 (1), 173–184. doi: 10.1002/hep.24351

Uddin, M. H., Li, S., Bae, Y. M., Choi, M. H., and Hong, S. T. (2012). Strain variation in the susceptibility and immune response to *Clonorchis sinensis* infection in mice. *Parasitol. Int.* 61 (1), 118–123. doi: 10.1016/j.parint.2011.07.002

Watanabe, H., Numata, K., Ito, T., Takagi, K., and Matsukawa, A. (2004). Innate immune response in Th1- and Th2-dominant mouse strains. *Shock* 22 (5), 460–466. doi: 10.1097/01.shk.0000142249.08135.e9

Wynn, T. A. (2015). Type 2 cytokines: mechanisms and therapeutic strategies. *Nat. Rev. Immunol.* 15 (5), 271–282. doi: 10.1038/nri3831

Yan, C., Wang, L., Li, B., Zhang, B. B., Zhang, B., Wang, Y. H., et al. (2015). The expression dynamics of transforming growth factor-beta/Smad signaling in the liver fibrosis experimentally caused by *Clonorchis sinensis*. *Parasit. Vectors* 8, 70. doi: 10.1186/s13071-015-0675-y

Yan, C., Li, B., Fan, F., Du, Y., Ma, R., Cheng, X. D., et al. (2017). The roles of Toll-like receptor 4 in the pathogenesis of pathogen-associated biliary fibrosis caused by *Clonorchis sinensis*. *Sci. Rep.* 7 (1), 3909. doi: 10.1038/s41598-017-04018-8

Yang, Q. L., Shen, J. Q., Jiang, Z. H., Shi, Y. L., Wan, X. L., and Yang, Y. C. (2017). TLR2 signal influences the iNOS/NO responses and worm development in C57BL/6J mice infected with *Clonorchis sinensis*. *Parasit. Vectors* 10 (1), 379. doi: 10.1186/s13071-017-2318-y

Yoon, B. I., Choi, Y. K., Kim, D. Y., Hyun, B. H., Joo, K. H., Rim, H. J., et al. (2001). Infectivity and pathological changes in murine clonorchiasis: comparison in immunocompetent and immunodeficient mice. *J. Vet. Med. Sci.* 63 (4), 421–425. doi: 10.1292/jvms.63.421

Yuan, J.-f., Yuan, J., and Luo, Y. (2013). Influence of Albendazole Combined with Astragalus Injection on Th1/Th2 Cytokines of Patients Infected with *Clonorchis Sinensis*. *Chin. Gen. Pract.* 33, 119–121. doi: 10.3969/j.issn.1007-9572.2013.09.111

Zhang, B. B., Yan, C., Fang, F., Du, Y., Ma, R., Li, X. Y., et al. (2017). Increased hepatic Th2 and Treg subsets are associated with biliary fibrosis in different strains of mice caused by *Clonorchis sinensis*. *PloS One* 12 (2), e0171005. doi: 10.1371/journal.pone.0171005

Zhang, R., Sun, Q., Chen, Y., Sun, X., Gu, Y., Zhao, Z., et al. (2018). Ts-Hsp70 induces protective immunity against Trichinella spiralis infection in mouse by activating dendritic cells through TLR2 and TLR4. *PloS Negl. Trop. Dis.* 12 (5), e0006502. doi: 10.1371/journal.pntd.0006502

Zheng, M., Hu, K., Liu, W., and Yu, X. (2015). Characterization of a *Clonorchis sinensis* antigen, calmodulin, and its relationship with liver fibrosis. *Nan Fang Yi Ke Da Xue Xue Bao* 35 (5), 659–664. doi: 10.1186/1743-422X-9-89

Conflict of Interest: The authors declare that the research was conducted in the absence of any commercial or financial relationships that could be construed as a potential conflict of interest.

Advantages of publishing in Frontiers

OPEN ACCESS
Articles are free to read for greatest visibility and readership

FAST PUBLICATION
Around 90 days from submission to decision

HIGH QUALITY PEER-REVIEW
Rigorous, collaborative, and constructive peer-review

TRANSPARENT PEER-REVIEW
Editors and reviewers acknowledged by name on published articles

Frontiers
Avenue du Tribunal-Fédéral 34
1005 Lausanne | Switzerland

Visit us: www.frontiersin.org
Contact us: frontiersin.org/about/contact

REPRODUCIBILITY OF RESEARCH
Support open data and methods to enhance research reproducibility

DIGITAL PUBLISHING
Articles designed for optimal readership across devices

FOLLOW US
@frontiersin

IMPACT METRICS
Advanced article metrics track visibility across digital media

EXTENSIVE PROMOTION
Marketing and promotion of impactful research

LOOP RESEARCH NETWORK
Our network increases your article's readership